CONTINUOUS HYDROLOGICAL MODELING USING SOIL MOISTURE ACCOUNTING FOR WATER RESOURCES ASSESSMENT IN KELANI RIVER BASIN, SRI LANKA

Mohammad Najim Nasimi

(179243H)

Degree of Master of Science

Department of Civil Engineering

University of Moratuwa

Sri Lanka

May 2018

CONTINUOUS HYDROLOGICAL MODELING USING SOIL MOISTURE ACCOUNTING FOR WATER RESOURCES ASSESSMENT IN KELANI RIVER BASIN, SRI LANKA

Mohammad Najim Nasimi

(179243H)

Thesis submitted in partial fulfilment of the requirements for the degree of Master of Science in Water Resources Engineering and Management

Supervised by

Dr. R. L. H. L. Rajapakse

UNESCO Madanjeet Singh Centre for
South Asia Water Management (UMCSAWM)

Department of Civil Engineering

University of Moratuwa
Sri Lanka

May 2018

DECLARATION

I declare that this is my own work and this thesis does not incorporate without acknowledgement any material previously submitted for a Degree or Diploma in any other University or institute of higher learning and to the best of my knowledge and belief it does not contain any material previously published or written by another person except where the acknowledgement is made in the text.

Also, I hereby grant to University of Moratuwa the non-exclusive right to reproduce and distribute my thesis, in whole or in part in print, electronic or other medium. I retain the right to use this content in whole or part in future works (such as articles or books).

…….. …….

Mohammad Najim Nasimi Date

The above candidate has carried out research for the Master's thesis under my supervision.

…….. …….

Dr. R. L. H. L. Rajapakse Date

Continuous Hydrological Modelling Using Soil Moisture Accounting for Water Resources Assessment in the Kelani River Basin, Sri Lanka

ABSTRACT

The assessment of water resources in a river basin for fulfilling various needs in the present and future requires a proper estimation of water availability. This is possible through hydrological modelling. The Kelani river basin in Sri Lanka experiences water stress under the current water uses, development, and urbanization effects. It requires a continuous hydrological model for the assessment of its water resources, focusing on impending climate change impacts. Continuous hydrological models, unlike event-based models, simulate longer periods that include both dry and wet conditions. Soil moisture accounting (SMA) model in the Hydrologic Engineering Centre-Hydrologic Modelling System (HEC-HMS) is chosen to simulate the streamflow. However, the SMA loss model requires precise and updated soil and land use data for parameter estimation, which is not available for the study area. In addition, the lumped nature of the model comparing to distributed models is also in question. This research discusses the development, parametrization and calibration methodologies for the 14 parameters of the HEC-HMS model with the SMA algorithm by considering a catchment divided into several sub-catchments. This division is based on the maximum drainage area method to improve the model accuracy in a scarce soil data situation.

The SMA loss model requires 14 parameters to be set. Among these, the impervious percentage is calculated from a land use map; the groundwater 1 and 2 storage as well as the groundwater 1 and 2 coefficients are calculated through the streamflow recession analysis. The maximum infiltration, soil storage, tension storage, and soil percolation rate are calculated from the similar studies; and the groundwater 1 and 2 percolation with four initial parameters are calculated only through a calibration procedure. The model is calibrated using daily data from 2007 to 2012 and validated from 2012 to 2017. The mean ratio of absolute error (MRAE) is used as a primary objective function. The coefficient of determination (R^2), percent volume error (PVE), and Nash-Sutcliffe efficiency (NSE) are also used to compare and evaluate the model performance.

The results indicate that the performance of the rainfall-runoff model significantly improves when the basin is subdivided into three to eight sub-catchments and the optimum result is found with the five sub-catchments. For the calibration period, the performance of the model is adequate with a R^2 of 0.83, a NSE of 0.82, a PVE of 5.3%, and a MRAE = of 0.38. Similarly, adequate results are also retrieved for the validation period, with a R^2 of 0.81, a NSE of 0.80, a PVE of 13.1%, and a MRAE of 0.36. The results of the statistical analysis indicate that the simulated and observed flows are reasonably well correlated. The parameter analysis shows that the soil percolation and tension zone storage rates are the most sensitive and second storage of ground water (GW2) is the least sensitive parameters. Furthermore, for the Kelani river basin up to the Hanwella catchment, the simple surface, simple canopy, ModClark, recession and Muskingum methods are found to be the most suitable methods alongside the SMA model.

The model performance can potentially be improved through further calibration using hourly climatic input data instead of daily data and with using multiple gauging stations instead of single gauge station. In the future, the validated HEC-HMS model can be employed with seasonal climate forecasts under long-range land use and climate projections. Besides, radar-based precipitation data can be used to represent the climatic variability on a grid-based scale.

Keywords: Multi sub-catchment comparison, SMA parameter estimation, soil scarcity situation, watershed subdivision

DEDICATION

Every challenging work needs self-effort as well as the guidance of elders especially those who are very close to our heart.

My humble efforts are dedicated to my sweet and loving

father & mother

whose affection, love, encouragement, and prayers of each day and night allowed me to accomplish this success and honour.

Along with the above, this work is also dedicated to my committed and respected

teachers

ACKNOWLEDGEMENTS

First and above all, I praise Allah, the Almighty for providing me with this opportunity and granting me the capability to proceed successfully.

I want to express my sincere gratitude to my research supervisor, Dr. R.L.H. Lalith Rajapakse for his continuous support of my study, his patience, motivation, and immense knowledge. Without his dedicated supervision and continued guidance, this thesis would not have been in a success. I am truly grateful to him for spending his valuable time with me working towards completing this research. He consistency ensured that this research was my own work by steering me in the right direction whenever I deviated.

I will never hesitate to convey my thanks to the Professor N.T.S. Wijesekera for extending all necessary help. He was kind enough to provide help and support even with his busy schedule. His sincere and consistent encouragement is greatly appreciated.

I take this opportunity to express gratitude to all members of the Department of Civil Engineering for their help and support. I place on record my sincere thanks to the South Asia Foundation for providing me with a scholarship to pursue a master's degree in Water Resources Engineering and Management. I would like to thank my mentor, Mr. H.W. Kumarasinghe, for his kind assistance during my stay in Sri Lanka.

Finally, I must express my very profound gratitude to my parents for providing me with unfailing support and continuous encouragement throughout my years of study and through the process of researching and writing this thesis. This accomplishment would not have been possible without them.

TABLE OF CONTENTS

LIST OF FIGURES

LIST OF TABELS

LIST OF ABBREVIATIONS

Abbreviations	Description
CHM	Continuous Hydrological Modelling
CN	Curve Number
DEM	Digital Elevation Model
E (t)	Evapotranspiration
GIS	Geographic Information Center
GW	Groundwater
HEC-GeoHMS	Hydrologic Engineering Centre – Geospatial Hydrologic Modelling
HEC-HMS	Hydrologic Engineering Centre – Hydrologic Modeling System
MRAE	Mean Ratio of Absolute Error
NRCs	Natural Resources Conservation Service
NSE	Nash-Sutcliffe Efficiency
P (t)	Rainfall
PBIAS	Percent Bias
PRMS	Precipitation-Runoff Modelling System
PVE	Percent Volume Error
Q (t)	Runoff
R^2	Coefficient of Determination
RE	Relative Error
RMSE	Root-Mean-Square Error
SCS	Soil Conservation Service
SMA	Soil Moisture Accounting
USA	United States of America
USACE	United States Army Corps of Engineers
WMO	World Meteorological Organization
ΔS	Change in Storage

LIST OF APPENDICES

1 INTRODUCTION

1.1 General

The assessment of water resources is a primary requisite to formulate long term sustainable management strategies and to combat the present global water scarcity issues. Hydrologic models that comprise the integration of key hydrologic processes are appropriate tools for such assessments. However, the hydrological modelling, which is a simplified representation of a real situation, is a challenging task, particularly for regions with limited available data. Hydrologic models should be well calibrated, and their performance should be evaluated to provide reliable results.

Hydrologic models are used for a variety of purposes, such as streamflow forecasting, flood inundation mapping, infrastructures design, and water supply planning. Many hydrological models, such as those developed by the Natural Resources Conservation Service (NRCS), the curve number-based (CN) model by the US Army Corps of Engineers (USACE), and the Hydrologic Engineering Centre Hydrologic Modelling Software (HEC-HMS), which are widely used today, primarily focus on surface processes but ignore or simplify soil profiles. Soil moisture accounting models exist but are rarely employed due to the challenges of parameter estimation and calibration (Bouvier, Tramblay, & Martin, 2010). There is a need to clarify the soil profile's impact on streamflow to better use it in planning practices.

Rainfall-runoff modelling, or hydrological modelling is a significant component in hydrological studies (Kanchanamala, Herath, & Nandalal, 2016). There are two approaches in rainfall-runoff modelling which are the lumped, and distributed approaches. Lumped models consider the whole catchment as a single unit with similar or homogeneous spatial variability. However, in reality, the process of runoff in a catchment varies so significantly with time and space that it is hard to find even a small catchment with such homogeneous spatial variability. Thus, distributed models represent reality more accurately other than lumped models. Though distributed models are much more precise, simulation is a tedious job that requires more data, time, and effort. Therefore, many modellers prefer using only lumped model.

An application of a distributed models to the Coweeta river basin in the USA reveals that the topography strongly influences a representative elementary area. This study found that the variability of rainfall and soil between sub-catchments increases the variability of runoff generation between sub-catchments (Wood & Sivapalan, 1988). Another study carried out on the Lucky Hills watershed to study the effects of scale in the KINEROS model shows a reducing runoff volume, peak, and sediment yield per unit area when the watershed size increases (Canfield & Goodrich, 1995). The effects of spatial input data resolution on hydrological modelling are investigated using the PCRXAJ distributed hydrological model and indicate that an increase in the grid size causes the loss of important information, which in turn results in a decrease of the model efficiency (Yildiz & Barros, 2009).

The effects of watershed subdivision on the values of calibrated model parameters, hydrological processes, and the subsequent interpretation of water balance components using the HEC-HMS model have been reported by Li, Zhang, and Wang (2013) and Kanchanamala, Herath, and Nandalal (2016). Hydrological modelling has become important in Sri Lanka due to the variety of development activities are affecting water resources. Whether to use lumped or distributed models is of interest to many modellers who are applying the HEC-HMS model, but only vague and ambiguous guidelines are available at present in assessing the efficiency of these models. This research presents an investigation on the possibility of improving the accuracy of lumped hydrological model by dividing moderate and large catchments into several sub-catchments in a soil-data-scarce situation focusing on the Kelani-Ganga river basin up to the Hanwella catchment.

Continuous hydrologic modelling synthesizes hydrologic processes and phenomena (i.e., synthetic responses of the basin to several rain events and their cumulative effects) over a longer period that includes both wet and dry conditions (Chu & Steinman, 2009). Many studies have reported the successful use of the HEC-HMS model to simulate different basins around the world. However, very few studies have reported long-term hydrological simulation using HEC-HMS in Sri Lankan basins. Anticipating the importance of rainfall-runoff modelling for future water resources management, a study needs to be conducted for the modelling of streamflow using a

continuous SMA algorithm in the HEC-HMS conceptual model for the Kelani river basin in Sri Lanka.

Soil moisture accounting exists as one of the loss methods in the HEC-HMS model to simulate rainfall-runoff processes, but due to the wide range of parameters and huge amount of data, it is rarely used by researchers and modellers in the Sri Lankan context (Jayadeera, 2016). The SMA model is suitable for high altitude areas with prolonged series of rainfall events because it shows better results that the widely used SCS curve number method (Haque, Hossain, Hashimoto, & Salehin, 2017). The SCS curve number method is used to simulate flow for upper river basins using of the HEC-HMS models where the underestimation of flows was observed when applied over long simulation periods (Ali, Narzis, & Haque, 2016). A study on the Kalu Ganga river basin in Sri Lanka using the Green and Ampt loss method indicates that the low flow is underestimated. The peak and magnitude do not match either (Jayadeera, 2016). In this research, the SMA loss method was applied for a part of the Kelani Ganga river basin in Sri Lanka to examine the efficiency of this model compare to other available loss methods in the HEC-HMS model.

Understanding the rainfall-runoff process in the Kelani river basin has significant societal and economic benefits for both the commercial capital (Colombo) and as well as the administrative capital (Sri Jayawardenapura Kotte) of Sri Lanka. The Colombo district has a population of 2.2 million concentrated within an area of 642 km^2. According to the census of population and housing in 2001, it has a population density that is approximately 10 times higher than that of the rest parts of the island. Urbanization in the district has contributed to changes in rainfall-runoff and drainage mechanisms in the lower Kelani river basin. Floods have become more frequent in those districts over recent decades, causing significant economic losses to the country and disruptions to the lives of communities along and around the riverbanks. The Kelani river basin is also the primary source of drinking water for the population in the Colombo district. Thus, the simulation of continuous streamflow in the Kelani river is important for water managers and decision makers.

Optimum management of the water resources of this inter-state river basin under changing climatic scenarios is of utmost importance regarding the fact that rapid

urbanization, deforestation, mineral exploitation, industrialization and agricultural expansion are taking place all over the basin. It may further be noted that to the best of our knowledge, there is no work-related, to the calibration and validation of the HEC-HMS with the SMA algorithm regarding the Kelan river basin in Sri Lanka. It is also worth mentioning that the HEC-HMS model has been used successfully by researchers worldwide (Fleming & Neary, 2004; McColl & Aggett, 2007; Yusop, Chan, and Katimon, 2007; Oleyiblo & LI, 2010).

The HEC-HMS model with the SMA algorithm is rarely used around the world, especially in regions with limited soil data. Unlike other models, the SMA model requires the hydraulic properties of soil, which make the job of modelling very difficult. This research tries to discover a methodology for applying the SMA model in a region where soil data is scarce. It tries to show modellers that even without the required soil data, they can use this model for their objectives in any catchment around the word. With the use of the HEC-HMS model for different hydrological purposes by modellers, there is still uncertainty over whether to select lumped or distributed models with an unknown number of sub-catchments to increase the accuracy of results. This research tries to compare a single catchment with multiple sub-catchments to find the best results, especially for water resource assessment and flooding purposes. In the process of different modelling methods were used conjunction with SMA, which helps to model the natural processes. This research will find the best methods for use alongside SMA model to get optimum results.

Parameter estimations for the SMA model along with other methods are a challenging and require deep study of parameter behaviours. Many types of research related to hydrological modelling require parameters that need to be estimated using soil, land use, and climatic data. This research presents an alternative for estimating the parameters required to well simulate the streamflow. This research will open the door of future research regarding the behaviours and estimation of hydrologic parameters in a soil-data-scarce situation.

This research develops a methodology for parameter estimation for a HEC-HMS model with an SMA algorithm in a soil-data-scarce situation. It also compares the lumped model and distributed models which can better simulate streamflow with daily time steps in a part of the Kelani Ganga river basin in Sri Lanka.

1.2 Problem statement

The assessment of water resources in the Kelani Ganga river basin in Sri Lanka is both necessary and difficult. So far, there is no model available for the basin that precisely simulates low and intermediate flows with the high accuracy that would be useful for researchers and water managers. Due to the lack of soil data, most of the researchers avoid modelling of low and intermediate flows of this river. Some models exist for the respective basins for flood study purposes, but intermediate and low flows require a more precise hydrological model. In addition to how to deal with the lack of soil data, determining the number of sub-catchments for accurate modelling is always a matter of research question which this research investigates. The reasons for selecting the Kelani Ganga river basin were the availability of rainfall and streamflow data, the necessity for future infrastructure projects, ongoing urbanization, climate change, the nature of the basin concerning floods, and the existence of multiple water demands.

1.3 Objectives of the study

The objectives of this research are classified into two sections as follows.

1.3.1 Overall objective

The overall objective is to develop, calibrate, and verify the SMA loss model with the HEC-HMS model in a soil-data-scarce situation considering the effect of watershed subdivisions on improving the accuracy of the model for water resource assessment purposes.

1.3.2 Specific objectives

The specific objectives include the following:

1. Development of parametrisation and calibration methodologies for the HEC-HMS model using SMA algorithm in soil-data-scarce situations.
2. Determining of the suitability of the HEC-HMS model with the SMA algorithm in the studied catchment.
3. Investigating the multiple sub-catchment effect on the overall efficiency of the model.
4. Deriving recommendations for better water resource management and future studies.

2 LITERATURE REVIEW

2.1 Hydrological models

Hydrologic models are a simplifications of real-world systems (e.g., surface water, soil water, wetlands, groundwater, and estuaries) that aid their users in understanding, predicting, and managing water resources. Both the quantity and quality of water flows are commonly studied using hydrologic models. In other words, hydrological models are simplified representations of the actual hydrological cycle that are widely used to help in providing sustainable solutions for integrated water resources planning and management.

The application of mathematical, physical, and semi-physical models in water resource planning and forecasting has become increasingly popular during recent decades in Sri Lanka with the introduction of microcomputers. Numerical models in simulations of river flows are used in the planning of water resource projects and real-time flood forecasting (Dharmasena, 1997).

2.2 Type of hydrological models

Hydrologic models can be classified based on their capabilities and limitations. According to Chow, Maidment, and Mays (1988), hydrological models can be divided into two broad categories: physical and abstract (mathematical) models. A physically based model is a mathematically idealised representation of a real phenomenon which includes the physical processes of a catchment (Devi, Ganasri, & Dwarakish, 2015). Physical models can be further divided into two groups: scale models and analog models. A scale model is a physical representation of a real system that maintains relationships between important aspects of the system. Analog models are based on analogous ways to represent the process being studied (i.e., the flow of electricity follows the same fundamental principles as the flow of water).

Models that are developed using logical programming languages and mathematical concepts to explain the land phases of the hydrological cycle in space and time are called abstract (mathematical) models (Jajarmizadeh, Harun, & Salarpour, 2012). According to Chow et al. (1988), a mathematical model can be classified as deterministic and stochastic. In deterministic models, outcomes are determined by

known relationships among states and events without the consideration of random variation. In other words, a deterministic model will always produce the same output for a single input value and does not account for randomness. In a stochastic model, on the other hand, different values of outputs can be produced for a single set of inputs that include some randomness. Cunderlik J. (2003) stated that deterministic models could be divided into three broad categories: lumped, distributed, and semi-distributed. Lumped models consider the catchment as a whole, with state variables that represent averages over the entire basin (Beven, 2001). Distributed models have state variables that represent local averages, in which the catchment is divided into cells or a grid net and flows are passed from one cell (node) to another as water drains through the basin (Xu C.-y. , 2002).

According to Arnold, Srinivasan, Muttiah, and J. (1998), distributed models usually requires an extensive amount of data for parameterization. Further, Geethalakshmi, Umetsu, Palanisamy, and Yatagai (2009) stated that due to a lack of data, a full understanding of hydrological basins is unachievable via fully-distributed models. However, lumped models do not account for land use or the spatial variability of the hydrological process (Ghaffari, 2011). A model that has some of the advantages of both types of spatial representation is called a semi-distributed model. A semi-distributed model partly accounts for variations in space with the division of a catchment into sub-basins. This model is more physical in comparison with the lumped model but requires less data than the fully-distributed model (Jajarmizadeh, Harun, & Salarpour, 2012). This category of model can be further divided into event-based and continuous hydrological models. Event-based models account for a single hydrological event, like a storm, a flood or soil moisture, considering a relatively short period of time. Continuous hydrological models simulate multiple state variables (e.g., soil moisture, surface storage) for a longer period. The classification is shown in Figure 2-1.

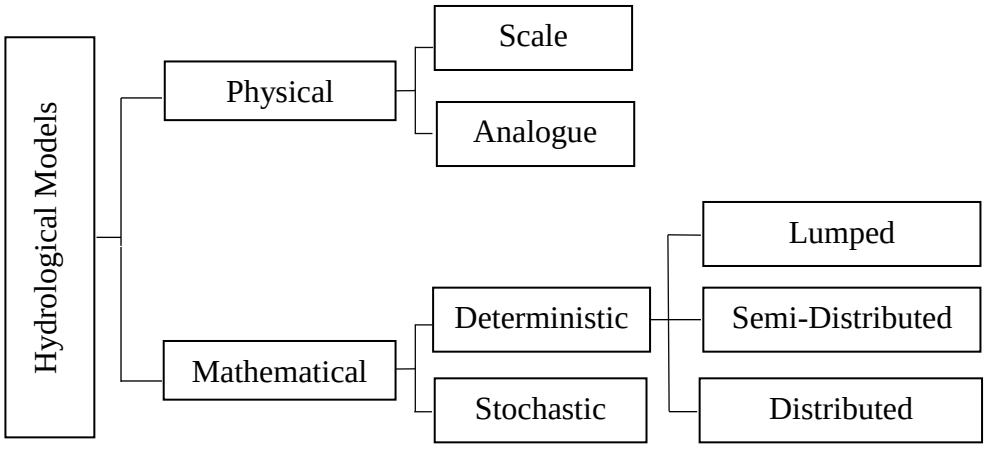

Figure 2-1 Hydrologic model classification

2.3 HEC-HMS with SMA algorithm

The primary distinction in using the SMA model with the HEC-HMS model is the evapotranspiration and groundwater seepage flow that can be ignored in event-based modelling but not in continuous hydrological modelling. Soil moisture has a significant influence on the hydrological response of a watershed. However, it is rarely tracked in simulation models due to the complexity of the model structure and challenges of parameter estimation (Bouvier, Tramblay, and Martin, 2010; Holberg, 2015). In HEC-HMS, the soil moisture accounting algorithm and deficit-constant loss methods are the only loss methods that account for the evapotranspiration process (Samady, 2017).

The Hydrologic Engineering Centre Hydrologic Modelling System, developed by the US Army Corps of Engineers, is a physical and deterministic model, supporting both lumped and distributed models (Madsen, 2000). The HEC-HMS model is used to simulate rainfall-runoff correlation, and due to its capability in short-time simulations, ease of use, and the use of common methods it has become a popular and reliable hydrologic model (Arekhi, 2012). It is intended to simulate the precipitation-runoff process of dendritic watershed systems (USACE, 2016). The HEC-HMS model has been used for studies of water availability, urban drainage, flow forecasting, future urbanization impact, reservoir spillway design, flood damage reduction, flood plain regulation, and systems operation (HEC, 2000).

For estimations of the Kelani river basin streamflow for water resources assessment, the SMA model was used in this research due to the necessity of long period simulation. The results of this model will useful to designers and planners for the assessment of water resources, floods, and drought for future infrastructure projects and for providing continuous drinking water to the Colombo district. The water loss through soil moisture, infiltration, and evaporation cannot be ignored. The HEC-HMS model was used because of its capability and simplicity and because it has been successfully calibrated and verified in many watersheds and river basins around the world. In addition, the free availability of the software that supports the SMA algorithm was a key factor for selecting it in this research.

2.4 Model structure

The model used in this study, HEC-HMS 4.2, was developed by the United States Army Corps of Engineers and designed to simulate the precipitation-runoff processes of dendritic watershed systems (R. Meenu, 2012). The HEC-HMS model setup consists of a basin model, a meteorological model, control specifications, and an input data time series (USACE, 2016).

Four main components that are created for developing an HEC-HMS project are:

- a basin model manager,
- a meteorological model manager,
- a control specifications manager, and
- input data (a time series, paired data, and gridded data).

2.4.1 Basin model

The basin model manager (watershed model) is a representation of a real-world object that describes the different elements of the hydrological system, such as sub-watersheds, reaches, junctions, sources, sinks, reservoirs, and diversions, that have to be included in a model with the help of HEC-GeoHMS, or manually inside the HEC-HMS. Each of these elements needs some parameters to define its interactions in a hydrological system (Bhuiyan, McNairn, Powers, & Merzouki, 2017). These elements are inter-linked to facilitate the flow of water and to create a dendritic network.

2.4.2 Control specifications manager

A Control specifications manager was one of the main components of the project, and is principally used to control the time intervals of the simulation.

2.4.3 Meteorological component

The meteorological component is the first computational element by means of which precipitation input is spatially and temporally distributed over the river basin. Spatiotemporal precipitation distribution is accomplished by the inverse distance and Thiessen methods. Several methods for evapotranspiration computations exist, including the Thornthwaite and Penman-Monteith methods. In addition, it is always possible that several basins with several control specification managers and

meteorological components could be made inside the HEC-HMS model and compared with one another, especially during the simulation procedure.

2.4.4 Input data

A hydrologic model often requires a time-series of precipitation data for estimating average basin rainfall. A time-series of flow data is often called the observed flow or observed discharge. This main component provides the inputs for all the meteorological data such as rainfall, observed discharge, evapotranspiration, wind speed, humidity, and sunshine hours.

2.5 Soil moisture accounting

The SMA loss method is used to investigate soil profile behaviour via downward model development. The SMA in HEC-HMS model conceptually divides the movement of rainfall into soil into five zones. In order to simulate the hydrologic processes of these five zones, which consist of interception, surface depression storage, infiltration, soil storage, percolation, and groundwater storage, 12 parameters need to be estimated. For simulation of the movement of water through the storage zones, the following measures are required for the model: the maximum depths of each storage zone, the percentage that each storage zone is filled at the beginning of the simulation, and the transfer rates, such as the maximum infiltration rate.

In addition to precipitation, the other input for the soil moisture accounting algorithm is the potential evapotranspiration rate (HEC, 2000). The SMA method in the HEC-HMS model is the most flexible and extensive loss method available (Figure 2-2). To fully define these eight storage components of the SMA model, a total of 17 parameters are required. Soil moisture accounting is heavily based on Leavesley's Precipitation-Runoff Modelling System (PRMS). Its basic operations are described below (Ford, Pingel, & DeVries, 2008).

The SMA method in the HEC-HMS model is a one-dimensional, semi-distributed representation of soil processes. One-dimensional hydrologic models only allow water to flow in one direction during a time-step. This works well for many applications but has the potential to decrease model accuracy at large spatial scales. Greater variability in topography and soil type is likely to occur when a large spatial scale is considered.

A one-dimensional model may fail to capture the complex flow behaviour that results from a varied landscape and anisotropic soils. The HEC-HMS attempts to solve these issues through semi-distributed modelling capabilities and multiple storage components in the soil profile. A complete description of the mathematical models can be found in the model's technical manuals, HEC (2000) and Bennett (1998). Soil moisture accounting takes a precipitation hyetograph as its input and routes it through canopy, surface, and soil storages, taking into account groundwater, base flow, and evapotranspiration processes before outputting a streamflow hydrograph.

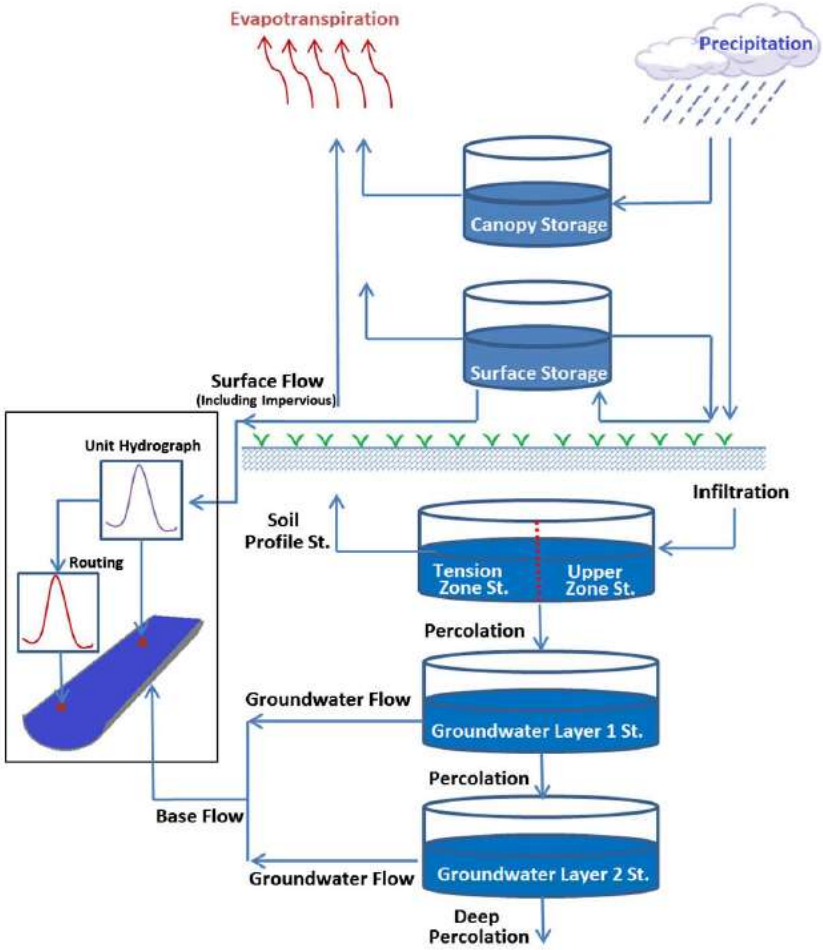

Figure 2-2 Schematic of SMA model (HEC, 2000)

When precipitation occurs, first the canopy storage is filled. The surface storage is next. Once both of these storage components are filled, precipitation has a chance of infiltrating into the ground. If the precipitation intensity is greater than the maximum

infiltration capacity of the soil profile, the excess precipitation will become surface runoff instead of infiltrating.

When precipitation infiltrates into the soil, it fills the tension zone first, and then the upper zone. Precipitation can percolate from the upper zone into the groundwater layer 1 (GW1) storage, but not from the tension zone. Some water in GW1will be routed to the first base flow reservoir while the rest percolates down to groundwater layer 2 (GW2). From GW2, water can be transferred to the second base flow reservoir. Otherwise, it percolates down to a deep aquifer and is considered lost from the system. Water in the base flow reservoirs is transformed to streamflow based on the characteristics of the reservoirs, such as the quantity and flow coefficient.

When precipitation does not occur, evapotranspiration occurs if water is present in the system. The rate of evapotranspiration is dependent upon the weather conditions of the region, but common values for temperate climates are about 170 mm per month during the summer season and 13 mm per month in the winter months (Fleming & Neary, 2004). Evapotranspiration first occurs from the canopy storage, then the surface storage. If sufficient water is not present in the first two storage components to fulfil the evapotranspiration potential, water is first removed from the upper zone storage. When evapotranspiration occurs from one of these three storages, water is lost from the system at the potential evapotranspiration rate. If evapotranspiration is still not satisfied, then water is removed from the tension zone storage. Evapotranspiration from the tension zone storage occurs at a decreased rate based on the current soil storage depth and the maximum storage capacity of the tension zone.

The SMA model was first used by the United States Army Corps of Engineers (USACE) in the Nashville district, which encompasses 46,422 km^2, to evaluate the performance of the HMS model with the SMA algorithm. That study found a methodology for estimating parameter values by selecting the fewest possible parameters to adjust during model calibration and minimizing the uncertainties associated with setting a parameter's initial state (Fleming & Neary, 2004).

The HEC-HMS model is used in flood forecasting in the Sturgeon Creek watershed in Manitoba Canada, with an SMA algorithm. In a study applying event and continuous modelling of the HEC-HMS model, sufficient agreement was confirmed between observed and simulated flows. The results of that study clearly show that the HEC-

HMS model can be an appropriate tool for flood forecasting at the HFC in Manitoba (Bhuiyan, McNairn, Powers, & Merzouki, 2017).

2.6 Continuous hydrological modelling with the SMA algorithm

Continuous hydrologic models, unlike event-based models, account for a watershed's soil moisture balance over a long-term period and are suitable for simulating daily, monthly, and seasonal streamflow (Ponce, 1989).

Fleming and Neary (2004) simulated the streamflow in the Cumberland river basin. They developed a methodology for estimating twelfth SMA parameters. A geographic information system (GIS) was used for estimating seven parameters, and the remaining parameters were estimated via streamflow recession analysis. In order to allow calibration and validation processes inside the watershed, it was divided into five sub-watersheds that each had a gauge on its outlet. For the time that surface runoff was contributing to streamflow, the tension zone depth was adjusted, and emphasis was placed on matching the observed and simulated streamflow peaks. The remaining parameters were adjusted to match simulated and observed peak flows when inter-flow and groundwater flow were the main contributors to the streamflow. Although the results showed reasonable matching, the daily data used in this study as for six years, and the evaporation data was had a monthly scale, which could potentially have affected the model accuracy. Parameter estimation using streamflow recession analysis was used for the Kelani river basin. To improve the accuracy of the model, further calibration and validation was carried out based on the gauged outlet located inside the basin. Emphasize in this model was placed on matching the peak flows in the calibration and validation periods.

A continuous hydrologic model (CHM) with SMA used in the Karkheh river basin (KRB) of Iran for area of more than 50,000 km^2. Manual calibration was performed to ensure the physical relevance of the HEC-HMS model parameter values. Manual parameters calibration begins with an educated estimate of initial parameters to run the model. The KRB model was developed at daily time scales using a 14-years simulation horizon (1987–2000) split between calibration (1994–2000) and validation (1987–1994) periods. Because manual calibration entails changing each parameter value in a

user-defined setting, it is often a time-consuming procedure complicated by a multitude of interacting parameters. To address this setback, an event-based calibration technique (EBCT) was implemented for the KRB and its interior sub-basins. A sensitivity analysis provided insights into the basin's snowfall and melt characteristics, distinguishing antecedent temperature index (ATI), cold rate coefficient, and baseflow recession coefficients as key parameters affecting hydrograph shape and magnitude of the peak flow. Results based on goodness of fit metrics suggests that event-based parameter estimation using seasonal characteristics improved the efficiency and accuracy of the continuous HEC-HMS model (CORRL and NSE 0.78–0.87 and 0.5–0.7, respectively) while facilitating application to a large, data-poor river basin with heterogeneous climatic condition (Rahman Davtalab, et al., 2015).

Continuous hydrological modelling with the SMA algorithm for the loss method was used in the Vamsadhara river basin in India for a 7,921km^2 catchment area. The Clark UH method, and the exponential recession method, and the Muskingum routing method were selected to model rainfall excess transform, baseflow, and reach routing respectively. This model was successfully calibrated and verified from 1984 to 1989 for the calibration period and from 1990 to 1993 for the validation period. The basin was discretized into smaller sub-basins, and semi-distributed models were applied to every sub-basin. For the evaporation period, due to a lack of data, the Thornwaite method was applied. The overall model efficiencies (EFF) given by the Nash Sutcliffe Efficiency criteria were 0.701 and 0.762 for the calibration and validation periods, respectively; indicating a good model fit. A sensitivity analysis of the model reveals that soil storage, soil percolation rate, maximum infiltration rate, percentage impervious area, and tension soil storage are the most sensitive parameters, with the soil storage being the most sensitive and the GW2 percolation rate being the least sensitive. From an overall evaluation, it could be included that the SMA algorithm available in the HEC-HMS model could be used to model streamflow in the Vamsadhara river basin (Rahul Singh & K.Jain, 2015).

A study conducted to apply and HEC-HMS model to predict streamflow in the Stung Sangker catchment, located in Tonlesap Lake basin in Cambodia, showed that the

calibration was acceptable on a monthly basis. In addition, it was found that the most sensitive method is the SMA loss method, which has10 parameters for calibration. The most sensitive parameters in this method are tension storage, groundwater two storage, soil percolation, and the groundwater 1 coefficient. The model performance was evaluated by Nash-Sutcliffe Efficiency criteria, which resulted in values of 0.44 for daily time steps and 0.71 for monthly time steps. The percent biases (PBIASs) for daily and monthly simulation were 4.13% and 3.56% respectively, indicating a satisfactory model fit. The results indicate that the HEC-HMS conceptual model can be used to simulate streamflow in the Stung Sangke catchment on a continuous time scale, particularly on a monthly basis. It also demonstrates that there was clear seasonal variation in monthly water availability, especially during both the wet and dry seasons (Sok & Oeurng, 2016).

2.7 Sensitivity analysis

A study carried out on the Cumberland river basin showed that the maximum infiltration rate, maximum soil depth, and the tension zone depth caused the most variation. There were recognized as the most sensitive parameters (Fleming & Neary, 2004).

Samady (2017) applied the HEC-HMS model with an SMA algorithm to simulate streamflow for studying the effect of drought on the lower Colorado River in Texas. The results of a sensitivity analysis indicate that the maximum soil storage, maximum infiltration rate, tension zone storage, baseflow (GW2) storage, and deep percolation rate had more of an effect on the simulation results compared to other parameters. To minimize the calibration parameters and not overfit, only the interflow storage capacity (GW1) and the deep percolation rate (GW2) parameters were adjusted during the model calibration. The GW2 percolation rate is a conceptual parameter with a high sensitivity.

According to Linseley, Koiuer, M.A., and Paulus (1958) the inflection point on the receding limb of a hydrograph marks where surface flow has stopped contributing to the runoff. The runoff after that is the result of adding the interflow and groundwater. During sensitive analysis, it is important to check the uniformity and non-uniformity

of the contributions of interflow and groundwater flow through the years. In a Cumberland sub-watershed called Byrdstown, the interflow and groundwater flow are did not uniformly contribute to the streamflow. The GW2 percolation rate is a conceptual parameter with a high sensitivity, and thus it is often selected as a calibration parameter (Samady, 2017). when studying the Kelani river basin, the GW2 parameter was be checked in order to verify which parameter is the most sensitive.

2.8 Parameter estimation

Fleming and Neary (2004) estimated the seven parameters (canopy interception storage, surface depression storage, maximum infiltration rate, maximum soil storage, tension zone storage, soil zone percolation rate, and groundwater one percolation rate) of the SMA model. According to their study, 12 parameters were estimated from the landuse, land cover, and soil data by GIS. The surface depression storage was estimated according to Bennett and Peters (2000), as presented in Table 2-1.

Table 2-1 Surface depression storage values

Description	Slope %	Surface storage (mm)
Paved impervious areas	NA	3.2-6.4
Steep, smooth slopes	>30	1.0
Moderate to gentle slope	5-30	12.7 -6.5
Flat, furrowed land	0-5	50.8

Source: Surface storage values from Bennet et al. (2000)

Four of the parameters (groundwater 1, two storage depths, and the storage coefficients) were estimated by the streamflow recession analysis of historic streamflow measurements. The groundwater 2 percolation rate was the only parameter that was not estimated from the methods mentioned above, but it was adjusted during the model calibration.

2.8.1 Parameter estimation using land cover and landuse

The precipitation intercepted by vegetation is called canopy interception. The canopy storage capacity varies with the vegetation structure and meteorological factors. Canopy storage can be calculated using the landuse and land cover classes and canopy interception values provided in Table 2-2, as suggested by Bennett et al. (2000).

Table 2-2 Canopy storage values

Vegetation type	Canopy interception (mm)
General vegetation	1.27
Grasses and deciduous trees	2.032
Trees and coniferous trees	2.54

Source: Fleming (2002) and Bennett (2000)

2.8.2 Initial parameter estimation

The estimated and calibrated parameters obtained from the similar studies Fleming et al. (2004); McEnroe (2010); Gyawali et al. (2013); Holberg (2015) and Samady (2017) suggests that the estimated parameters are generally in the same range, except that the impervious surface values are lower than the values used in other studies because the impervious percentage is defer from place to place. For the Kelani river basin, the initial parameter was used according to the literature review.

2.9 Model calibration

In the HEC-HMS model, two kinds of calibration strategies exist: manual and automated. Both of them has the functionality to minimize the objective functions. Here, both of them are explained.

2.9.1 Automated calibration

The automatic calibration procedure in the HEC-HMS model uses an iterative method to minimize an objective function, such as the sum of the absolute error, the sum of the squared error, the percent error in the peak, and the peak-weighted root means square error (HEC, 2000).

2.9.2 Manual calibration

The default values in the HEC-HMS model do not always produce a reasonable result because the range of each parameter varies a lot. In the case of the storage depths and storage coefficients, these limits are 2.54–1,500.00 mm and 0.1–10,000 hr respectively (Fleming & Neary, 2004). Fleming et al. (2004) applied the HEC-HMS model to the Cumberland river basin. Data for that study included years 1994 to 1999. Out of those years, 1994, 1998, and 1999 were chosen for calibration because they represented

relatively average ratios of runoff to rainfall in the six years of data. Both manual and automated calibration methods were adopted.

In conclusion, manual calibration helps to determine a practical range of parameter values, while automated calibration is used to refine the search for the optimum parameter values. For the Kelani river basin, both manual and automated calibration methods were adopted.

2.10 Model validation

Refsgaard and Knudsen (1996) defined model validation as "the process of demonstrating that a given site-specific model is capable of making accurate predictions for periods outside a calibration period". Model validation is used to determine the effectiveness of parametrization and calibration methodologies. Based on Refsgaard et al. (1996), model validation "involves calibration of a model based on 3–5 years of data and validation for another period of similar length".

A study on the Cumberland river basin by Fleming et al. (2004) was carried out and out of six years' data from 1994 to 1999, only 1995, 1997, and 1996 were selected as the validation periods because they displayed the lowest and highest runoff to rainfall ratios. For the Kelani river basin, the validation period was selected from the years that displayed the lowest and highest runoff to rainfall ratios.

2.11 Evapotranspiration

Evapotranspiration is a combined process of water vaporizations from soil and vegetative surfaces and transpiration through plant canopies. In the SMA model, it is defined as loss of water from canopy interception, surface depressions, and soil profile storage (USACE, 2016). The HEC-HMS model provides seven optional methods for calculating evapotranspiration, including annual and monthly average evapotranspiration, the Priestley-Taylor, the Penman-Monteith method, and evapotranspiration specified for each time step (Samady, 2017).

2.12 Streamflow classification

According to Wijesekera (2018) there is minimal guidance for determining streamflow thresholds systematically in a particular watershed. Monthly flow duration curves

demonstrate an easy way to capture streamflow thresholds compared to daily flow duration curves (Wijesekera S. N., 2018). Flows within the range of 70-99% time exceedance are usually most widely used as low flows (Smakhtin, 2000).

Yilmaz, Gupta, and Wagener (2008) in a diagnostic approach to model evaluation applied to the NWS distributed hydrologic model, divided flow duration curves into three categories based on flow exceedance probabilities with 0-0.02 flow exceedance probabilities for high flows, 0.2-0.7 as the exceedance limits for intermediate flows, and the rest as low flows. According to Cai, Wang, Xu, and Yue (2016) an inexact two-stage stochastic programming model for sustainable utilization of water resource in Dalian city evaluating regional hydrological models used the same thresholds reported by Yilmaz, Gupta, and Wagener (2008). Wijesekera (2018) in the evaluation of streamflow classifications for Kalu Ganga and Gin Ganga, developed duration curves for both watersheds considering the probability of exceedance. In his findings, he mentioned that there should be a consistency in each category relating to the PoR slope curve, but it should be within the ranges proposed by the literature.

2.13 Objective function

Model testing typically includes two steps: calibration and verification. Correspondingly, the whole data set is divided into two parts: a calibration period and a verification period. The primary criteria to test the performance of the model, both in the calibration and verification periods is the objective functions that determine the level of confidence of the model to be used in practice (Guo & Wang, 2002). For evaluating the simulated and observed streamflows, different objective functions are used by researchers. Fleming et al. (2004) which compared between observed and simulated streamflows through the objective function shown in Table 2-3.

Table 2-3 List of statistics used to compare model output and observed data

Statistic	Equation
Mean hourly flow (m^3/s)	$(1/n)\sum Q$
Standard deviation (m^3/s)	$\sqrt{(1/n)\sum(Q-\bar{Q})^2}$
Mean absolute error (m^3/s)	$(1/n)\sum\lvert Q_o - Q_s\rvert$
Root mean square error (m^3/s)	$\sqrt{[\sum\lvert Q_o - Q_s\rvert^2]/n}$
Baseline-adjusted coefficient of efficiency	$1.0 - [\sum\lvert Q_o - Q_s\rvert]/[\sum\lvert Q_o - \overline{Q`}\rvert]$
Error in volume (%)	$[(V_o - V_s)/V_o] * 100$
The average error in time to peaks (h)	$(1/n)\sum\lvert T_s - T_0\rvert$
The average error in magnitude of peaks (%)	$[(1/n)\sum\lvert(Q_o - Q_s)/Q_o\rvert] * 100$

Source: Fleming et al. (2004)

In the above table (Table 2-3), $Q = \text{hourly streamflow}$, $\bar{Q} = \text{average streamflow}$ Q_o= observed hourly streamflow, Q_s = hourly simulated streamflow, $\overline{Q`}$ =baseline streamflow, V_o= observed streamflow volume, V_s = simulated streamflow volume, T_s= simulated hour of peak flow, and T_0=observed hour of peak flow.

Samady (2017) applied HEC-HMS with an SMA algorithm to the Colorado river basin in Texas. The model was calibrated from 2004 to 2012 and validated from 2012 to 2017. To evaluate the model performance, the present streamflow volume error (PVE), coefficient of determination (R^2), percent bias (PBIAS), and Nash-Sutcliffe Efficiency coefficients were used. Later on, the same objective functions were used by Gyawal (2013).

2.13.1 Percent streamflow volume error (PVE) or percent bias (PBIAS)

PBIAS or PVE indicates the overall agreement between the observed flow and simulated flow over a specified time interval (Samady, 2017). The PVE is used as a primary metric for the objective function in most hydrologic models (Jain & Singh, 2003).

$$\text{PVE}\% = \frac{Q_{obs} - Q_{sim}}{Q_{obs}} * 100, \qquad (2.1)$$

In this equation, Q_{obs} is the observed streamflow (m^3/sec) and Q_{sim} is the simulated streamflow (m^3/sec) at the watershed outlet. Percent bias compares the average

tendency of the simulated flows to be larger or smaller than the observed flow values (Gupta, Sorooshian, & Yapo, 1999). It measures the bias of model performance. The optimal value is 0, which means that the model has an unbiased flow simulation. Positive values indicate a tendency towards overestimation; negative values indicate a tendency towards underestimation (Yua & Yang, 2000).

2.13.2 Nash Sutcliffe efficiency (NSE)

The NSE is used to evaluate model performance (Nash, 1970). It is defined as 1 minus the sum of the absolute squared differences between the predicted and observed values normalized by the variance of the observed values during the period under investigation (Krause, Boyle, & Bäse, 2005). It is calculated as:

$$\mathrm{NSE} = \frac{1-[\sum(Q_{obsi}-Q_{sim})^2]}{[\sum(Q_{obsi}-\overline{Q_{sim}})]}, \qquad (2.3)$$

In the above equation, Q_{obsi} is the observed streamflow and $\overline{Q}_{sim}$ is the simulated streamflow. The NSE (unitless) measures the relative magnitude of the residual variance (''noise'') to the variance of the flows (''information''). The optimal value is 1.0, and values should be larger than 0.0 to indicate minimally acceptable performance. A value equal to 0.0 indicates that the mean observed flow is a better predictor than the model (Gupta, Sorooshian, & Yapo, 1999). In physical terms, R^2 is the ratio of the residual variance to the initial or 'no-model' variance, and represents the proportion of the initial variance explained by the model (Smit & Seo, 2004).

2.13.3 Coefficient of determination (R^2)

The coefficient of determination (usually denoted R^2) is a concept in the analysis of variance and regression analysis. It is a measure of the proportion of explained variance present in the data. Hence, the higher the value of R^2, the better the model describes the data (Coefficient of determination R2, 2008). It is also defined as the squared value of the coefficient of correlation (Krause, Boyle, & Bäse, 2005). According to Nash and Sutcliffe (1970), it is the proportion of the initial variance accounted for by that model. R^2 is calculated as:

$$R^2 = 1 - \frac{\sum_{i=1}^{n}(y_i-\hat{y}_i)^2}{\sum_{i=1}^{n}(y_i-\bar{y})^2}, \qquad (2.4)$$

Here, $\bar{y}$ denotes the average of the observations and $\hat{y}_i$is the prediction of y_i using the fitted model. In the case that there is no relation between the predictor variable(s) and the response variable, then $\bar{y}$ is the best 'model' to explain the data. Hence, the terms $y_i - \bar{y}$ account for deviations in the case that there is no relation between the predictor variable(s) and the response variable. The range of values of R^2 depends on the type of model to be fitted; in standard cases like linear least-squares regression models they lie between 0 and 1. A value of 0 means no correlation at all, whereas a value of 1 means that the dispersion of the prediction is equal to that of the observation.

2.13.4 Mean ratio of absolute error (MRAE)

Wijesekera and Abeynayake (2003) stated that the mean ratio of absolute error (MRAE) is the difference between the calculated and observed flows with respect to that particular observation. It is calculated as:

$$\text{MRAE} = \frac{1}{n}\left|\sum \frac{Q_{Obs}-Q_{Cal}}{Q_{Obs}}\right|, \qquad (2.5)$$

where: Q_{obs} is the observed streamflow, Q_{cal} is the calculated streamflow, and n is the number of observations used for comparison. Especially, in water resources assessment, it is used by many modellers (Khandu, 2015; Sharifi, 2015; Jayadeera, 2016; Dissanayake, 2017). Mean ratio of absolute error values lie between 0 to 1. A value closer to 0 indicates good a better fit between the observed and simulated values (Sharifi, 2015).

2.13.5 Root mean square error (RMSE)

Another verification measure is the root mean square error (RMSE), which is defined as the square root of the mean of the squared differences between corresponding elements of the forecasts and observations (Barnston, 1992). The RMSE is calculated as:

$$\text{RMSE} = \sqrt{\frac{\sum_{i=1}^{n}(Q_{obs,i}-Q_{model})^2}{n}}, \qquad (2.6)$$

where Q_{obs} is the observed value, Q_{model} is the simulated value, and n is the number of observations. It describes the average model performance error and varies with the

variability of the error magnitudes (or squared errors) as well as with the total-error or average-error magnitude (MAE) (Willmott & Matsuura, 2005).

2.13.6 Ratio of absolute error to mean (RAEM)

The World Meteorological Organization (WMO, 1975) compared conceptual models used for operational hydrological forecasting and recommended several objective functions. The RAEM is calculated as:

$$\text{RAEM} = \frac{1}{n}\left[\frac{\sum|\text{Qobs}-\text{Qcal}|}{\text{Q}_{cal}}\right], \qquad (2.7)$$

where Q_{obs} is the observed streamflow, Q_{cal} is the calculated streamflow, and n is the number of observations used for comparison. This method indicates the ratio between the observed and calculated streamflows with respect to the mean of observed discharges (Khandu, 2015).

2.13.7 Relative error (RE)

The next efficiency criterion used was the relative error of the volumetric fit between the observed runoff series and the simulated series (Xiong & Guo, 1999), which is defined as:

$$\text{RE} = \frac{\sum(\text{Q}_{obs} - \text{Q}_{cal})}{\sum \text{Q}_{obs}} * 100\%, \qquad (2.8)$$

where Q_{obs} is the observed streamflow, and Q_{cal} is the calculated streamflow. The value of RE is expected to be close to zero for a useful simulation of the total volume of the observed runoff series.

2.13.8 Recommended performance ratings

Recommended performance ratings of watershed models based on the above statistical parameters are summarized in Table 2-4, adapted from Moriasi, Arnold, and Van Liew (2007), and Jain and Singh (2003). The PBIAS and NSE ranges were suggested by Moriasi et al. (2007). The MRAE was suggested by Wijesekera and Abeynayake (2003) based on their literature reviews. The ratings range from very good to unsatisfactory.

Table 2-4 General performance ratings for watershed models

Performance rating	**R^2**	**PBIAS/PVE**	**NSE**	**MRAE**
Very good	$0.75< R^2 \leq 1$	PBIAS$\leq \pm 10$	$0.75<$NSE≤ 1	$0<$MRAE<4
Good	$0.65 <R^2 \leq 0.75$	$\pm 10 \leq$PBIAS $<\pm 15$	$0.65<$NSE≤ 0.75	$0<$MRAE<5
Satisfactory	$0.75< R^2 \leq 0.65$	$\pm 15 \leq$PBIAS $<\pm 25$	$0.50<$NSE≤ 0.65	$5<$MRAE<7
Unsatisfactory	$R^2 \leq 0.5$	PBIAS$\geq \pm 25$	NSE≤ 0.5	MRAE>7

3 METHODS AND MATERIALS

The methodology used in this research work is presented in Figure (3-1). Initially, based on the overall objective and specific objectives, the necessity of a hydrological model for the Kelani river basin to simulate low and intermediate flows was determined. Following that, the literature review identified commonly applicable hydrological models and their applications with respect to various objective functions. Considering model availability, flexibility, and reliability, the application of different hydrological models to many river basins were studied. As a result, the HEC-HMS model was selected to simulate runoff for a part of the Kelani Ganga river basin up to Hanwella gauging station.

The model development was carried out in this study by considering three main components: the basin model, the precipitation model, and the control specifications. The sub-model selection under the basin model for rainfall loss, direct runoff, base flow, and channel routing was carried out considering common application, data availability, and works of literature. The maximum drainage area method was used for lumped and distributed models. Three, five, eight, and 12-sub-basin distributed models were developed to compare multiple subdivision effects on the overall efficiency of runoff simulation. Model development, the calculation of initial parameters, and the selection of objective functions are described in Chapter 4. Five years' data from October 2007 to September 2012 was used for model calibration and five years' data from October 2012 to September 2017 was used for model verification.

The model performance was evaluated by different objective functions, using the minimum value of the MRAE as the primary objective function. In addition, percent errors in volume (also referred to as mass balance error), NSE coefficient and the coefficient of determination were also checked. Further, a sensitivity analysis was carried out to figure out the most and the least sensitive parameters in the calibration and parametrization processes. At the end of this chapter, the acquired results are presented and compared. Finally, all the results are discussed, and the conclusion and recommendations for future research are covered in Chapters 5, 6, and 7.

3.1 Methodology flow chart

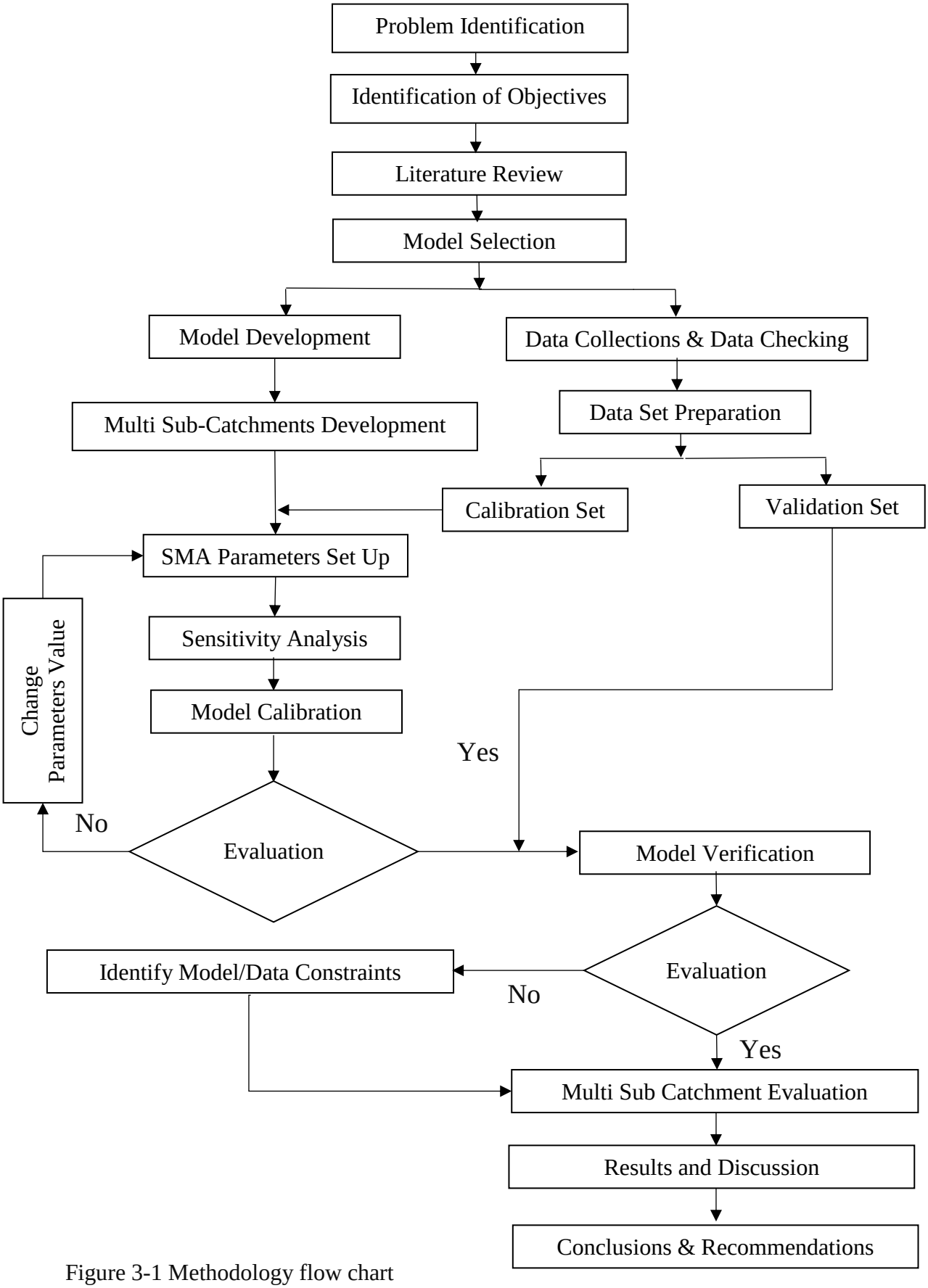

Figure 3-1 Methodology flow chart

3.2 Model selection

After sufficient literature reviews for model selection, it was found that only the HEC-HMS model supports the SMA as one of its loss methods. Therefore, the HEC-HMS model, which was developed by the US Army Corps of Engineers, is used in this study.

3.3 Study area

For the current research, the watershed up to Hanwella in the Kelani river basin was selected with a catchment area of 1,829.2 km^2, as presented in Figure 3-2. Six rainfall gauging stations (Norwood, Kithulgala, Holombuwa, Deraniyagala, Glencourse, and Hanwella) were selected for the current study, which are all within the study area boundary. Besides the six rainfall gauging stations, one streamflow gauging station at the outlet of the catchment in Hanwella was selected. It was determined that the study area is mostly covered by rubber – almost by 40 %. Homesteads and gardens cover the second most area of the study location. The catchment boundary was delineated through contour maps, and streams were generated using a 30-meter resolution Digital Elevation Model DEM.

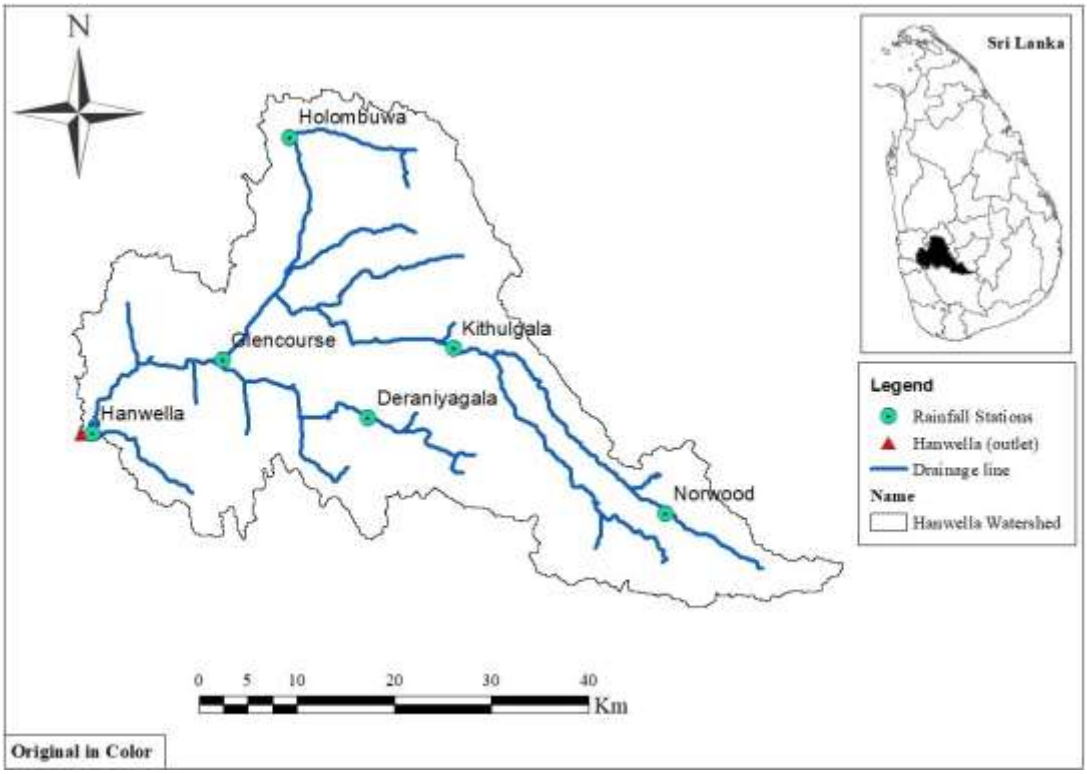

Figure 3-2 Study area map

3.4 Data collection and data checking

Daily data on rainfall, streamflow, and evaporation was collected from the irrigation and meteorological department of Sri Lanka for years 2007 to 2017. The rainfall, streamflow, and evaporation data was checked for inconsistencies. The data checking process included visual and consistency checks. Subsequently, yearly, monthly, and daily water balance checks were carried out for the entire catchment up to the Hanwella streamflow gauging station. Also, single and double mass curves are plotted and used to check the inconsistencies of the rainfall data.

3.5 Land use map

Land use map with scale of 1:50,000 was retrieved from the Survey Department, Sri Lanka, The land use categories consisted of rubber cultivation, homesteads/gardens, tea cultivation, forest, paddy, scrubland, stream, rock, boundary of reservoir, coconut cultivation, marsh, chena, water hole boundaries, grassland, tank, unclassified area, and other cultivations. Rubber cultivation cover 39.8 % of the study area. The land use details are presented in Table 3-1, and graphically shown in Figure 3-3. For the whole study area, a land use map was prepared, which is shown in Figure 3-4.

Table 3-1 Land use distribution of Kelani river basin at Hanwella catchment

Landuse type	Area	Percentage
Rubber	706.45	39.80%
Homesteads/garden	331.77	18.60%
Tea	276.88	15.60%
Forest	238.92	13.40%
Paddy	88.10	4.96%
Scrub land `	49.25	2.77%
Other cultivation	23.44	1.32%
Stream (line/area)	21.78	1.23%
Rock	16.60	0.94%
Boundary of a reservoir	9.60	0.54%
Coconut	6.00	0.34%
Marsh	4.01	0.23%
Chena	1.75	0.10%
Water hole boundaries	0.135	0.01%
Grassland	0.08	0.00%
Tank	0.02	0.00%
Unclassified	0.01	0.00%

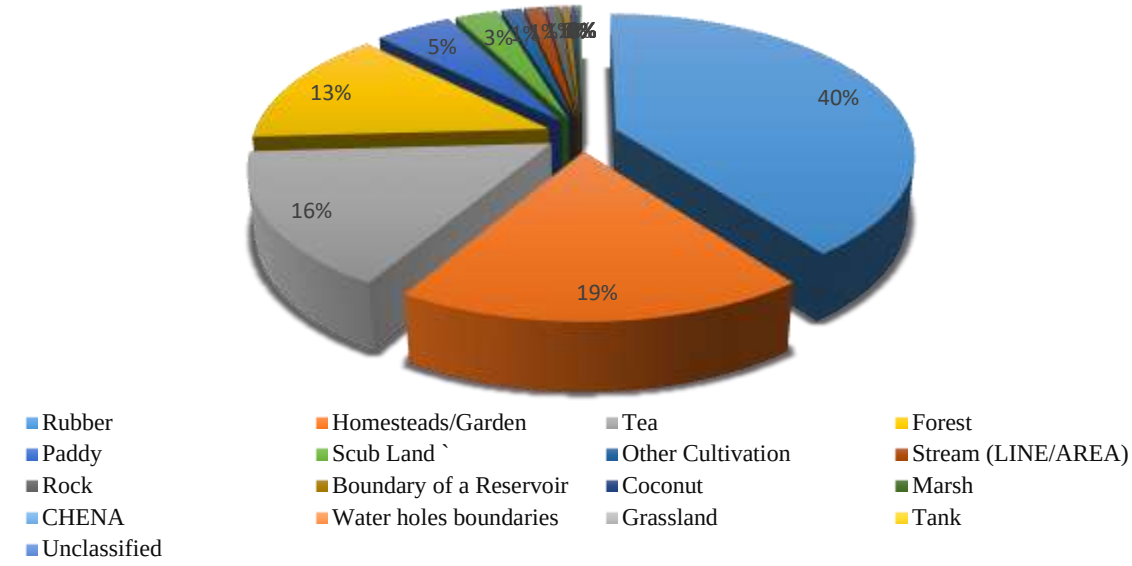

Figure 3-3 Landuse components

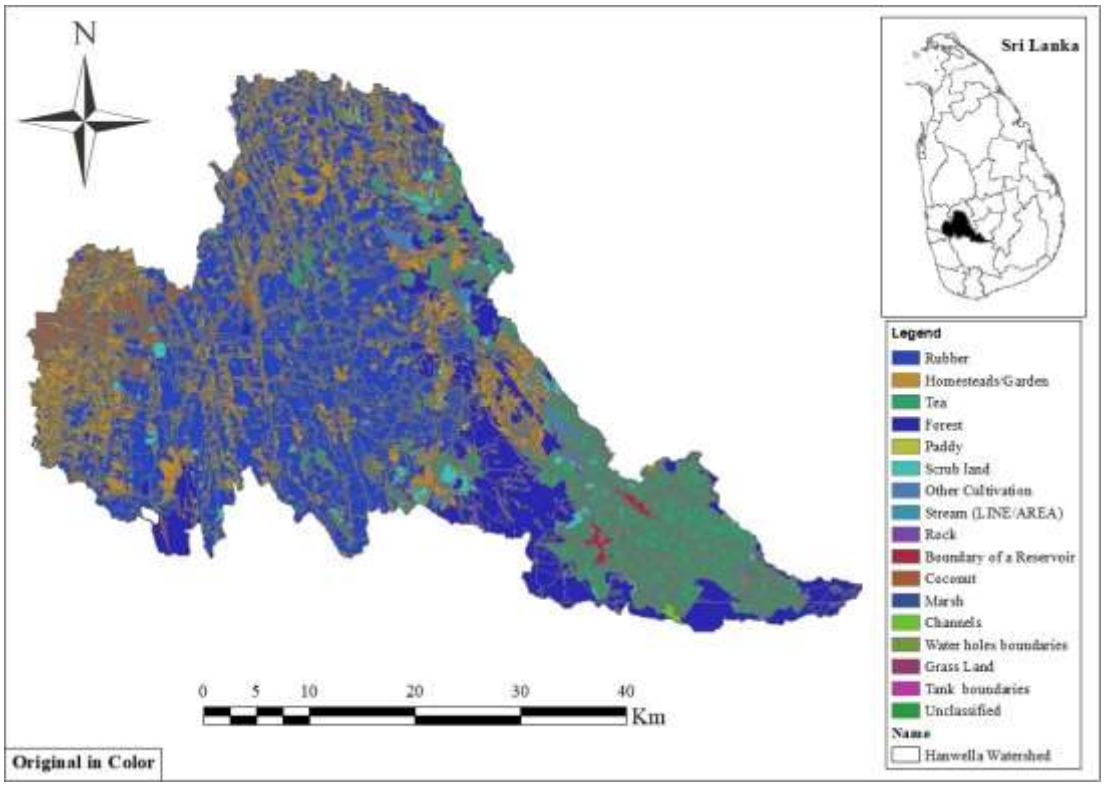

Figure 3-4 Landuse map

Source: Survey Department, Sri Lanka

3.6 Soil data

The soil map of the Kelani river basin up to the Hanwella streamflow gauging station was acquired from the Survey Department of Sri Lanka in the scale of 1: 50,000. The acquired soil map was classified into nine types of soil from the agriculture perspective, as shown in Figure 3-5.

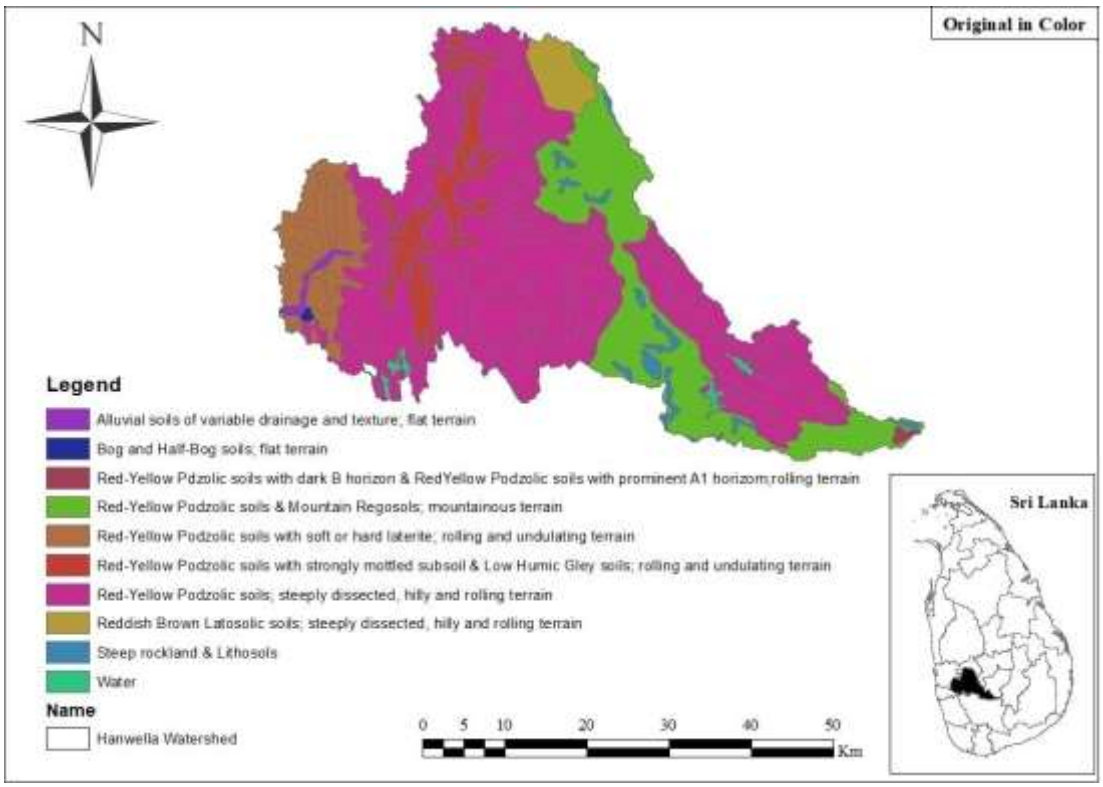

Figure 3-5 Soil map of the Kelani river basin up to Hanwella location

Source: Survey Department, Sri Lanka

3.7 Data and data sources

The main data used in this research was rainfall, streamflow, evaporation, landuse and soil map data. Rainfall and streamflow data for the study area was collected from the Irrigation Department for the period of 2007 to 2017, except for the evaporation data that was collected from the Meteorological Department of Sri Lanka for the same period from the Colombo climate station. For the Kelani river basin at Hanwella watershed, the data sources and resolutions are indicated in Table 3-2 in below.

Table 3-2 Data sources and data availability for the Kelani river basin at Hanwella catchment

Data types	Spatial reference	Resolution	Data period	Source
Rainfall	Norwood	Daily	2007-2017	Dept. of Irrigation
	Kithulgala			
	Holombuwa			
	Deraniyagala			
	Glencourse			
	Hanwella			
Evaporation	Colombo	Daily	2007-2017	Dept. of Meteorology
Streamflow	Norwood	Daily	2007-2017	Dept. of Irrigation
	Kithulgala			
	Holombuwa			
	Deraniyagala			
	Glencourse			
	Hanwella			
Topo-Graphic Map	Negombo, Attangalla, Gampola, Colombo, Avissawellah, Nuwara Eliaya, Badullah, and Balangoda	1:50,000	Updated 2003	Dept. of Survey
Land use	Sri Lanka	1:50,000	Updated 2006	Dept. of Survey
Soil map	Sri Lanka	1:50,000	Updated 2006	Dept. of Survey

3.8 Rainfall and streamflow

Daily rainfall and streamflow data was used in this study as the main input of the model for simulating the Kelani river basin streamflow at Hanwella watershed. The locations of all the stations are indicated in Table 3-3. Similarly, in Figure 3-6 and Figure 3-7, the locations of rainfall and streamflow stations are shown on a location map.

Table 3-3 Gauging station properties for the Kelani river basin at Hanwella catchment

Gauging stations	Location	Period of operation (from)	Data type
Hanwella	Lati - 6.9097 Long - 80.0816	1973	Streamflow & rainfall
Glencourse	Lati - 6.9780 Long - 80.2030	1948	Streamflow & rainfall
Holombuwa	Lati - 6.9597 Long - 79.8767	1962	Streamflow & rainfall
Deraniyagala	Lati - 6.9244 Long - 80.3380	1948	Streamflow & rainfall
Kithulgala	Lati - 6.9891 Long - 80.4177	1948	Streamflow & rainfall
Norwood	Lati - 6.8356 Long - 80.6146	1982	Streamflow & rainfall

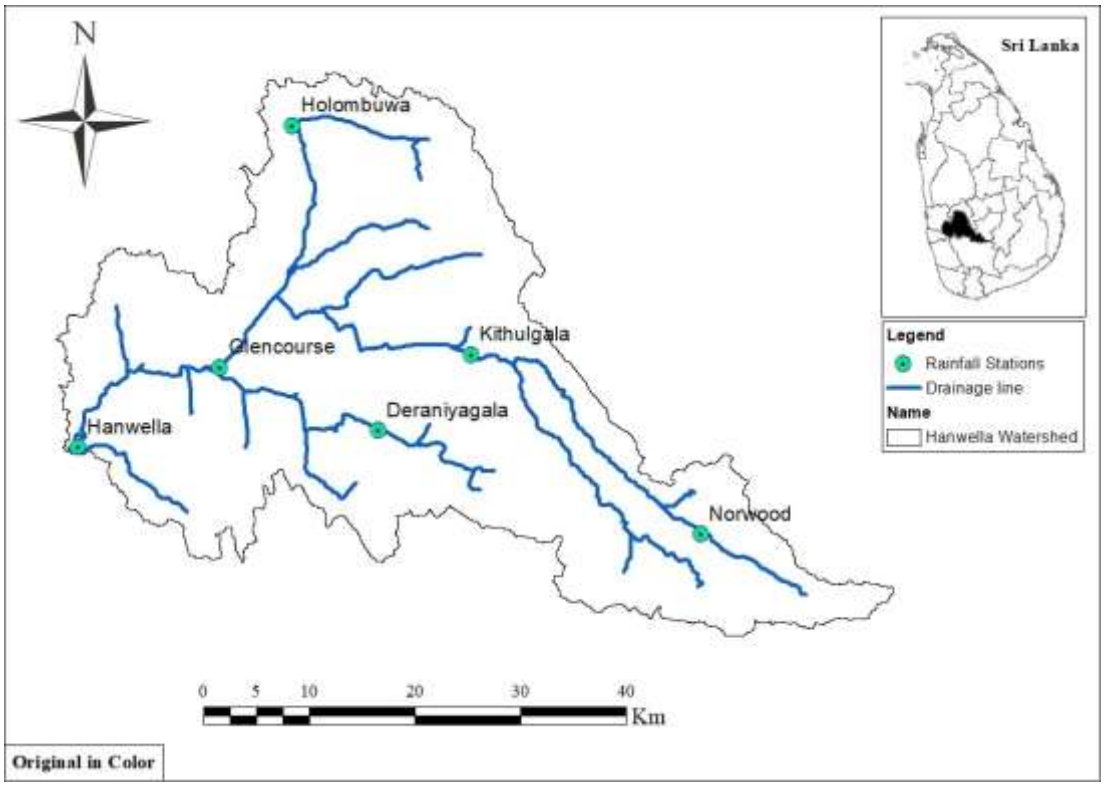

Figure 3-6 Location of the rainfall gauging stations at Hanwella watershed

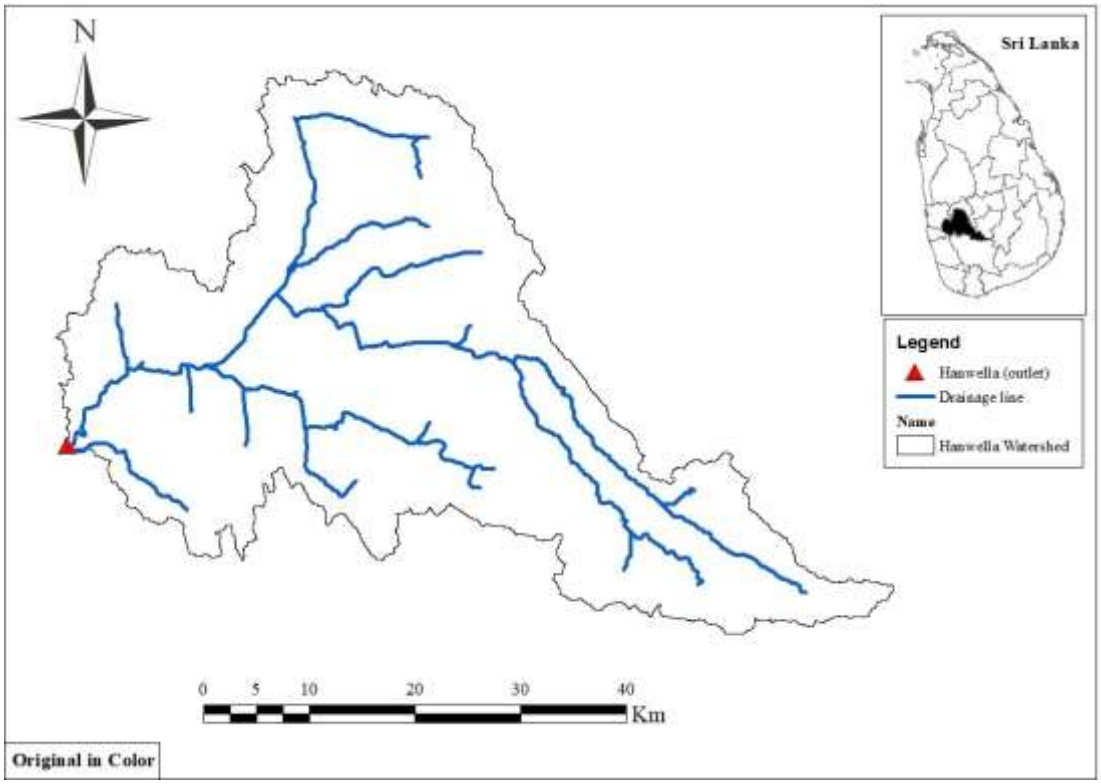

Figure 3-7 Location of the streamflow gauging station at the outlet of Hanwella watershed

3.9 Thiessen average rainfall

A common method used in the literature for deriving the mean areal precipitation is the Thiessen method. This method assigns an area called a Thiessen polygon for each gauging stations. Every point inside this polygon is assumed to have the same rainfall with a constant weight. Thiessen polygons for the Kelani Ganga river basin at the Hanwella outlet were generated by Arc-GIS 10.3 along with Arc Hydro and HEC-GeoHMS extension tools using six rain gauging stations, and are presented in Figure 3-8. In Figure 3-8, the coverage area of every single gauging station is distinguished by colour boundaries. This is the privilege of selecting these station which all of them are lies inside the catchment boundary. Following the generation of the Thiessen polygons, the areas of each Thiessen polygon and its weight were calculated and presented in Table 3-4.

Table 3-4 Thiessen weights for the Kelani river basin at Hanwella catchment

Station name	Thiessen polygon area (km^2)	Thiessen weight
Hanwella	150.55	0.08
Glencourse	372.32	0.20
Holombuwa	280.54	0.15
Deraniyagala	281.78	0.15
Kithulgala	393.74	0.22
Norwood	350.27	0.19
Total	1,829.20	1.00

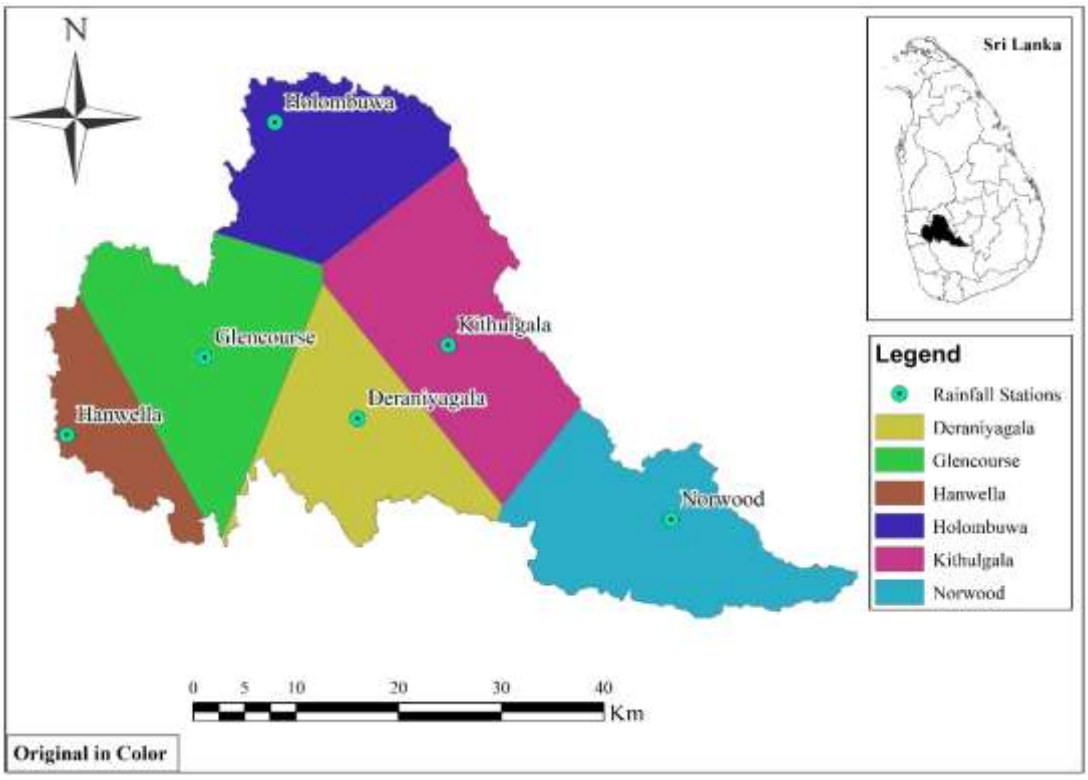

Figure 3-8 Thiessen polygons and rainfall stations at Hanwella watershed

3.10 Data checking

3.10.1 Consistency checking

Prior to use, all rainfall records were checked for continuity and consistency. The double and single mass curves were used for all rainfall stations as common tools. The double mass curve shows the cumulative total of one rainfall station against the total of all rainfall stations. The double mass curve for the current study is illustrated in Figures A-1 and A-2 of Appendix A. For the double mass curve, if the line is straight, it indicates consistency among all rainfall stations, which indicates reliable data. Conversely, if the line does not follow a straight pattern, it indicates a lack of consistency, which indicates unreliable data. The generated double mass curves (Figures A-1 and A-2 of the Appendix-A) show a reasonable consistency of the data by following a straight pattern. The single mass curve generated (shown in Figure A-3 of Appendix-A) also clearly indicates the consistency of individual rainfall stations over the entire period of study. Form the literature, the primary purpose of the single mass curve besides checking the consistency of rainfall is filling missing data. The single mass curve in this study indicates consistency of every station compared to other stations. As a conclusion of these two checks, the available data of rainfall is reliable for modelling purposes without further modification.

3.10.1.1 Visual data checking

In the process of data checking, visual checking is the simplest primary method for identifying errors. The function of visual data checking is to make sure that the graphical representation of rainfall corresponds to streamflow in a graph or a table. The main purpose of this check in this study was identifying the compatibility of rainfall data to the streamflow data in a catchment over a given time period (for a one year). This check is helpful in roughly identifying the mismatching of rainfall and runoff patterns. For better clarification, in this research work, the rainfall versus runoff was plotted in a semi-log, and areas of concern were identified by a blue circles.

In this study, visual checking was conducted for all the periods of study, from the year 2007 to the year 2017 and for each rainfall station. There are six rainfall gauging stations over the Kelani river basin up to Hanwella catchment, and data from these was

acquired from the Irrigation Department of Sri Lanka. At the outlet of the study area in the Hanwella location, a streamflow gauging station was chosen, and the relevant from this was acquired from the Irrigation Department as well.

For the year from October 2007 to September 2008, rainfall-runoff graphs were plotted for every individual rainfall station corresponding to the streamflow gauging station, and these are presented in Figures 3-9 and 3-10. The plotted graphs are in semi-log scale for precisely checking of any incompatibilities. In Figure 3-9, the rainfall in Norwood station for the date of 22nd Dec 2007 is much higher compared than the streamflow. This discrepancy is indicated with a blue circle. Similarly, from the period of 16th Dec 2007 to 06th February 2008, the Deraniyagala rainfall station data does not correspond well to the streamflow (Figure 3-10). In other words, for the mentioned period, no rainfall was happening, but the streamflow graph shows some small peaks. These area also circled in blue line. Likewise, Figure 3-10, where the Hanwella rainfall is plotted alongside the Hanwella streamflow, shows that a high rainfall peak happened on the date 19th of January 2008, but the streamflow did not respond. The rainfall-runoff graphs for the other years from 2008-2017 are similarly plotted and marked in Appendix A, Figures A-5 to A-25.

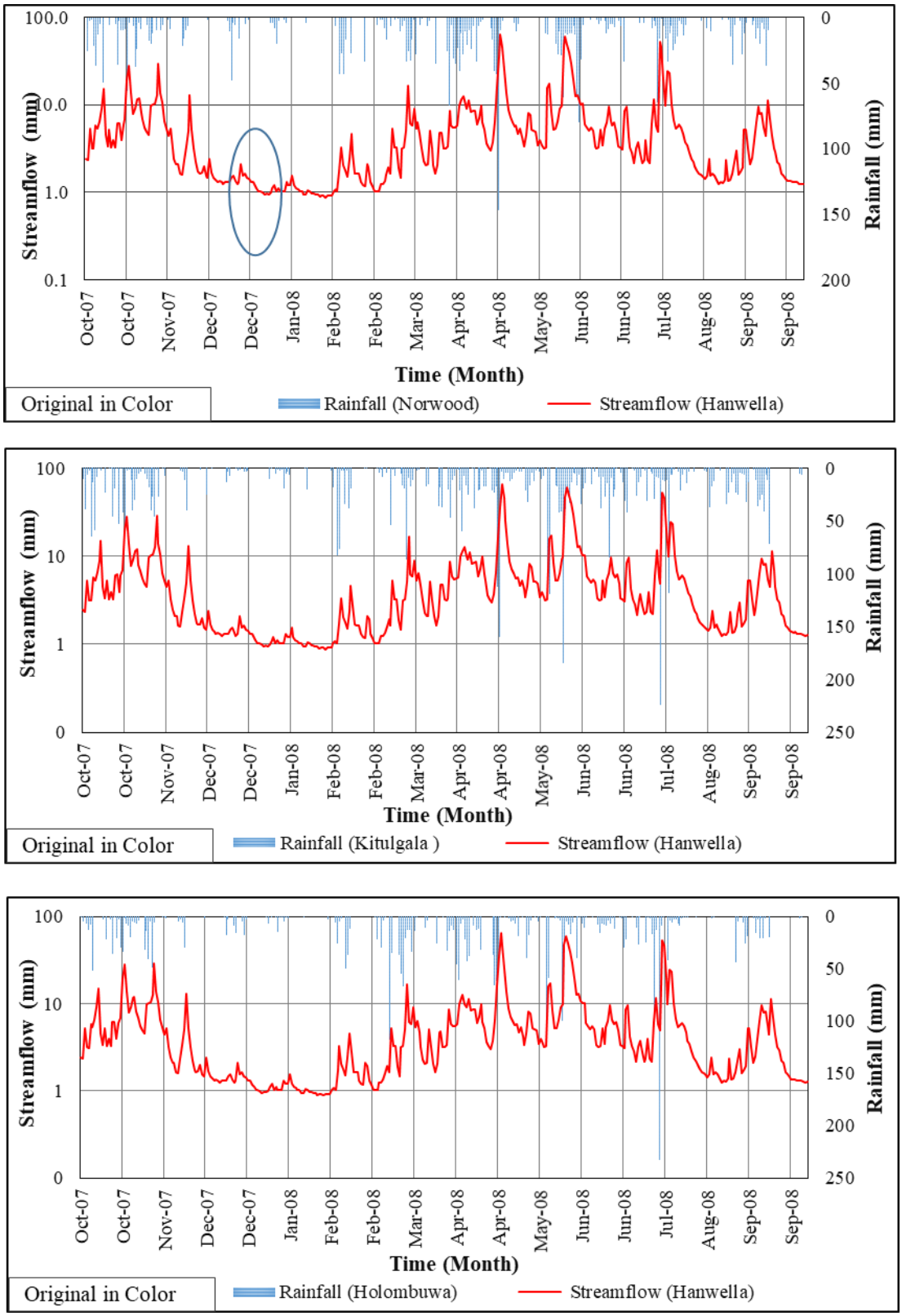

Figure 3-9 Streamflow response of Hanwella watershed with rainfall in 2007/2008

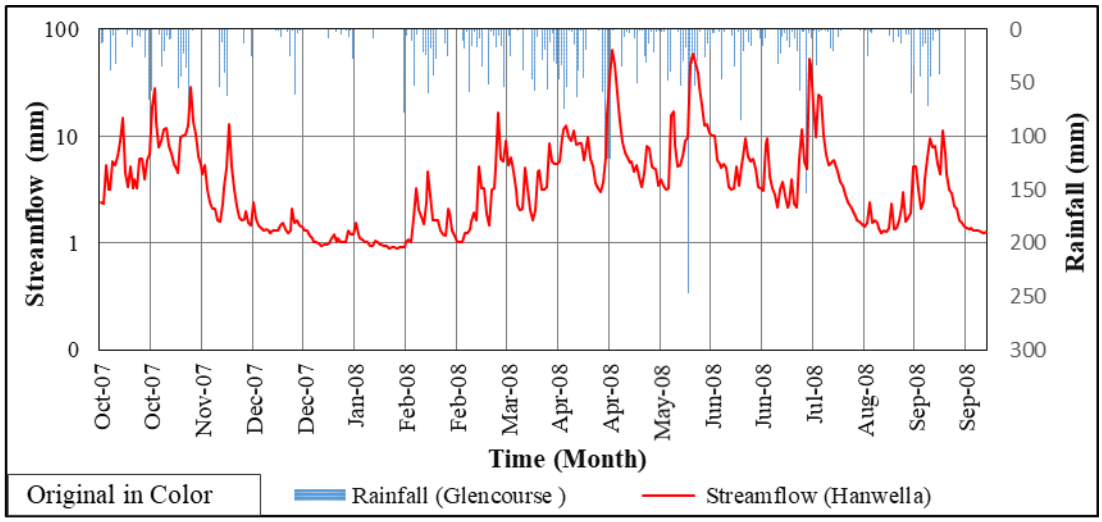

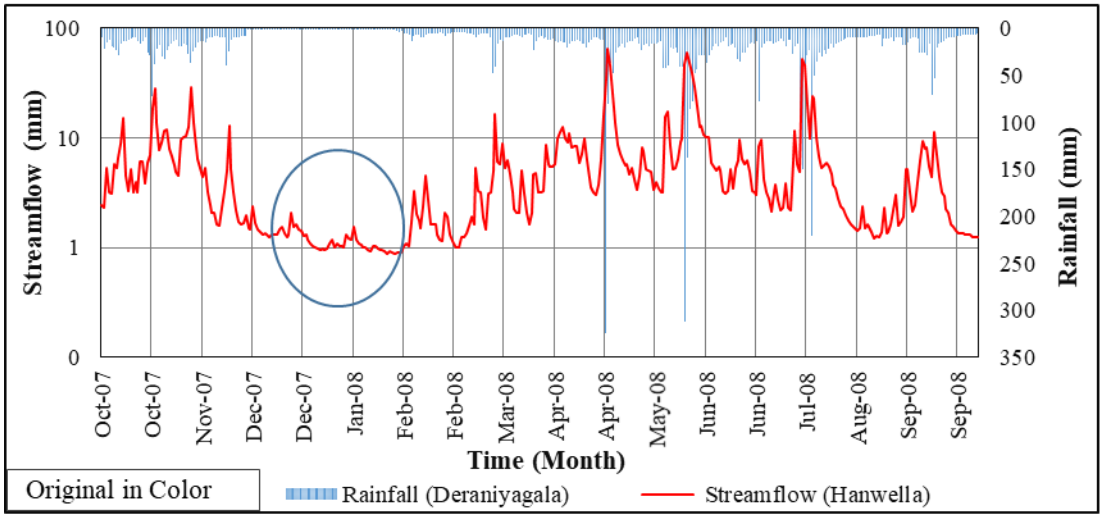

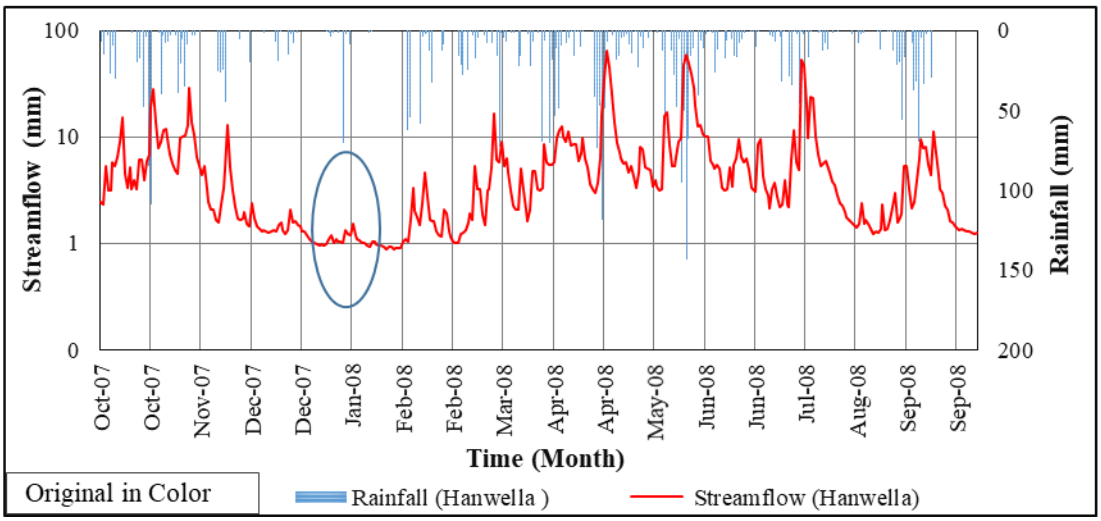

Figure 3-10 Streamflow response of Hanwella watershed with rainfall in 2007/2008

3.10.1.2 Variation of evaporation versus annual runoff coefficient

Calculated annual runoff coefficients varied from 0.26 to 0.57 over the 10 years. It can be seen from Figure 3-11 that in the year 2015/2016, the runoff coefficient was very high compared to other years. In contrast, it was very low in the year 2011/2012. The runoff coefficient values for the Kelani Ganga river basin were verified with the values recommended by literature. In the year 2010/2011, evaporation records showed very low values compared to other years. This is because that the streamflow did not respond well to the rainfall in this year. If this data point is disregarded, there is a slightly increasing trend over the period of study (Figure 3-11). The greatest evaporation can be seen in the year 2015/2016. This is because the highest rainfall was recorded in that year, but the corresponding streamflow was not as high.

Table 3-5 Variation of annual runoff coefficients and evaporation in the Hanwella watershed

Year	Rainfall (mm)	Streamflow (mm)	Runoff Coeff	Pan Evap	Pan Coeff	Actual Evap
2007-2008	4,292	2,094	0.49	1,187	0.80	950
2008-2009	3,505	1,278	0.36	1,272	0.80	1,018
2009-2010	3,872	1,678	0.43	1,206	0.80	965
2010-2011	3,964	1,981	0.50	1,171	0.80	937
2011-2012	2,464	637	0.26	1,264	0.80	1,012
2012-2013	4,251	2,155	0.51	1,207	0.80	966
2013-2014	3,162	1,166	0.37	1,318	0.80	1,054
2014-2015	3,664	1,539	0.42	1,199	0.80	959
2015-2016	3,852	2,188	0.57	1,379	0.80	1,103
2016-2017	3,491	1,504	0.43	1,381	0.80	1,105
Average	3,652	162	0.43	1,258	0.0	1,007

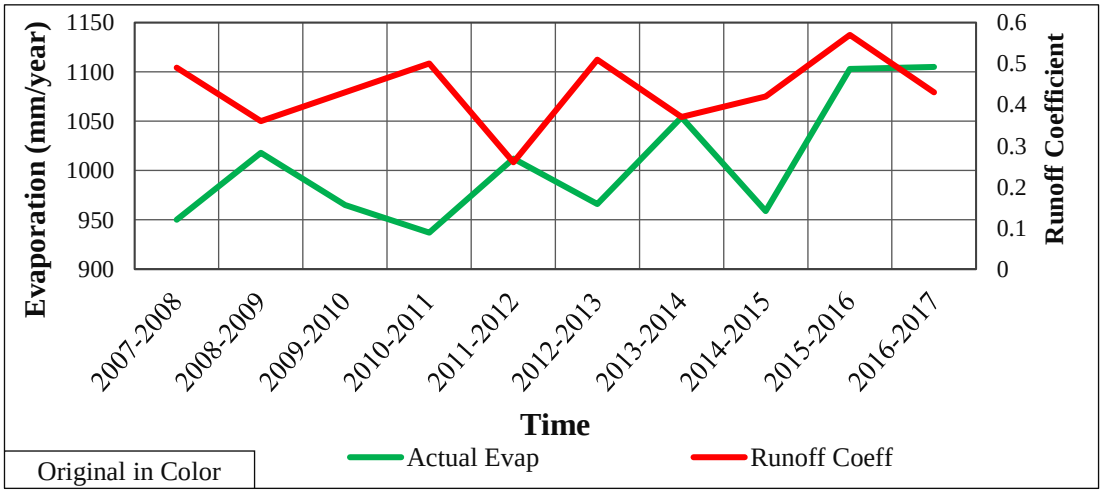

Figure 3-11Variation of annual evaporation and runoff coefficient at Hanwella watershed

3.10.1.3 Variation of annual rainfall and streamflow in the Hanwella watershed

Rainfall patterns increased in the years 2007/2008, 2010/2011, 2012/2013, and 2015/2016. In the years, 2008/2009, 2011/2012, and 2013-2014, rainfall patterns were decreasing. The streamflow followed the same pattern as the rainfall except for the year 2015/2016, which is marked with a circle in Figure 3-12. In this year, the streamflow value was 2,187.56 mm/year, the rainfall was very high. The year 2007/2008, had highest rainfall, but the streamflow was less (2,094.02 mm/year) compared to the year 2015/2016. This reveals that there may be inconsistencies in the streamflow data. However, the rainfall and streamflow data follow nearly the same patterns for the years 2008/2009, 2009/2010, 2013/2014, 2014/2015, and 2016/2017. Figure 3-12, reveals that the year 2011/2012 was observed as the driest year, as both streamflow and rainfall values were very low compared to other years.

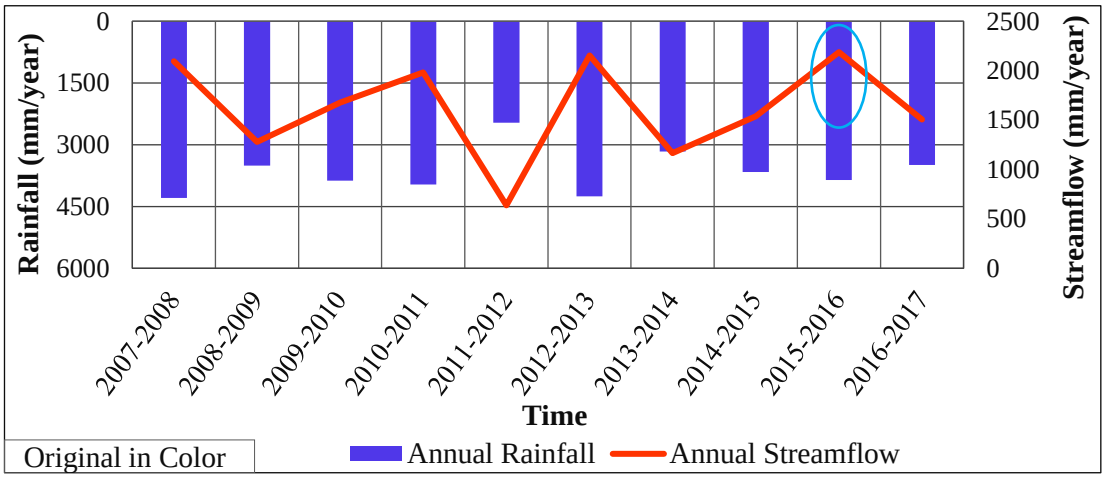

Figure 3-12 Variation of annual rainfall and streamflow

3.10.2 Comparison of annual rainfall

The annual rainfalls from October to September 2017 recorded by each rain gauging station are given in Table 3-6 and plotted graphically in Figure 3-13. The primary purpose of the annual rainfall comparison is checking the variation and consistency of each rainfall station in compare to each other. This comparison shows that there was a considerable increase in the annual rainfall at the Deraniyagala rainfall station for the year 2007/2008. The annual rainfall recorded by the Kithulgala rainfall station shows an irregular pattern in the years 2015/2016 and 2010/2011. It can be observed that there was an increase in rainfall for the year 2012/2013 for all rainfall stations and a

decrease of rainfall in the year 2011/2012, which is marked as the driest year in 10 years of study. Overall, the comparison of the annual rainfall of every station indicates the reliability and accuracy of the data for use in this research and future hydrological and modelling studies.

Table 3-6 Comparison of annual rainfall

Water year	Annual rainfall (mm)					
	Norwood	Kithulgala	Holombuwa	Glencourse	Hanwella	Deraniyagala
2007-2008	2,838	4,654	3,172	4,869	3,532	6,352
2008-2009	2,927	4,226	3,117	3,521	2,826	3,944
2009-2010	3,503	4,689	3,032	4,082	3,690	3,842
2010-2011	2,860	5,236	3,575	3,915	2,982	4,539
2011-2012	1,637	3,016	2,055	2,511	2,339	3,132
2012-2013	3,928	5,050	3,682	3,928	3,476	4,946
2013-2014	2,211	3,756	2,714	3,047	2,663	4,373
2014-2015	2,526	4,350	3,085	3,542	3,211	5,101
2015-2016	2,492	4,908	2,967	3,864	3,363	5,238
2016-2017	2,166	4,064	2,455	3,647	3,637	5,083

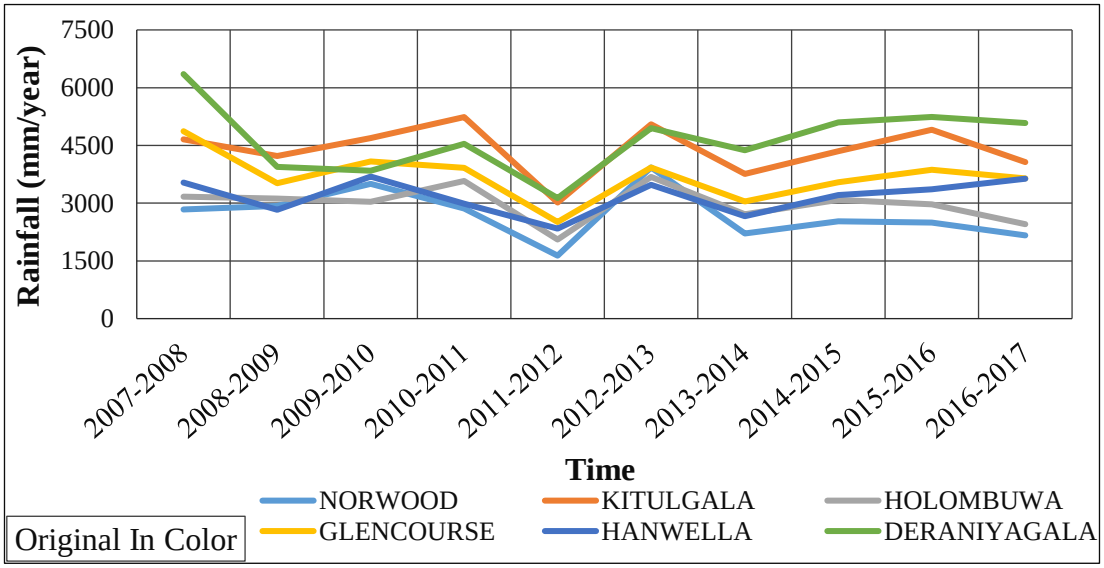

Figure 3-13 Annual rainfall variation at Hanwella watershed

3.10.2.1 Monthly comparison of Thiessen rainfall with observed streamflow for the years 2007-2017

Monthly total rainfall and streamflow data for the years 2007 to 2017 for six rainfall stations and one streamflow gauging station is plotted and shown in Figure 3-14. The Thiessen rainfall means that the average rainfall from these stations is used to illustrate the rainfall over the catchment for each month of the year (Figure 3-14 a). Streamflow graphs were also plotted in respect to check their correspondence with the Thiessen rainfall (Figure 3-14 b). The below figures indicates good matching of the streamflow and Thiessen rainfall data. According to Figure 3-14 (a, b) the month of May in the year 2016-2017 had the highest recorded rainfall and streamflow. Visual checking of this graph shows that the data follows the same pattern, which is further discussed in Chapter 5.

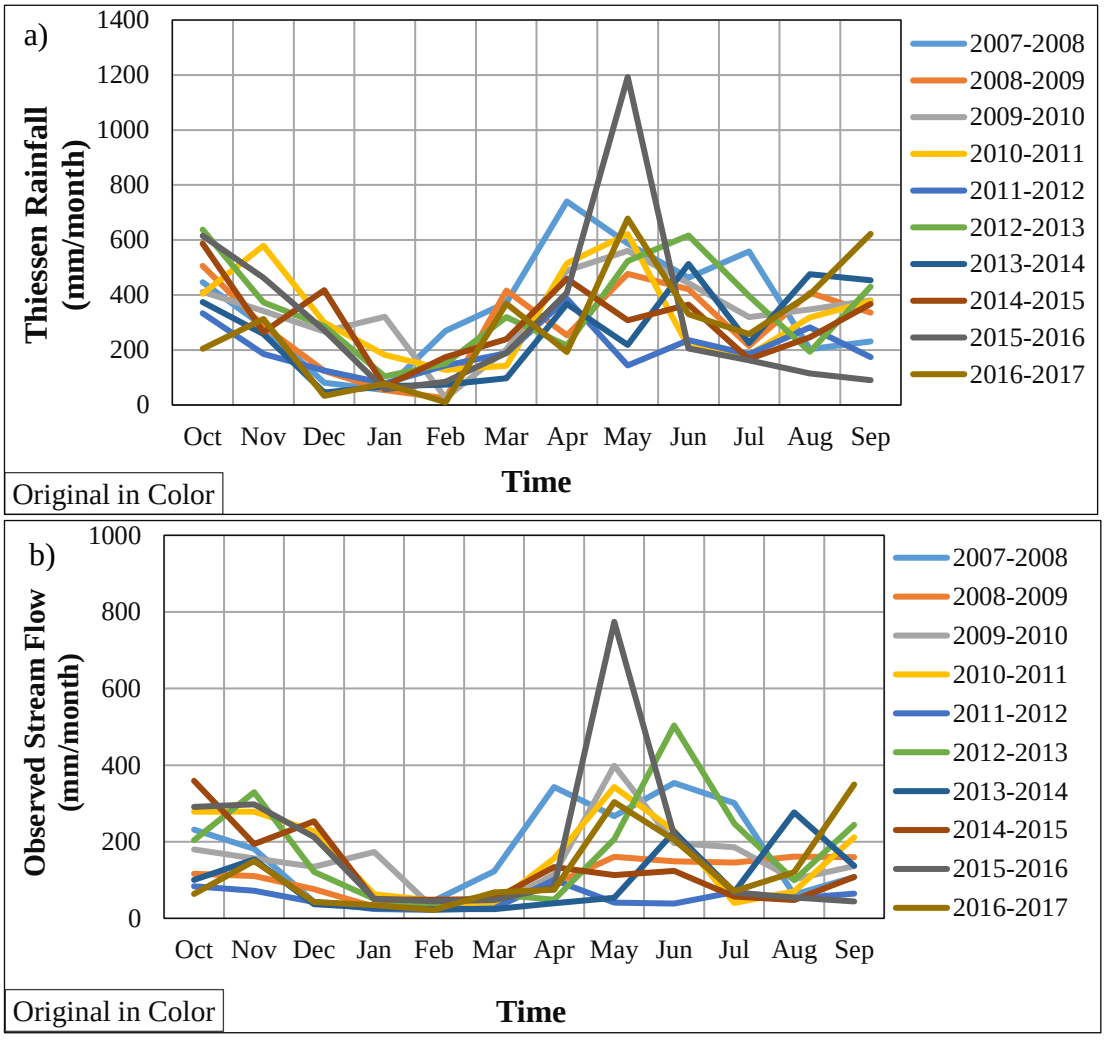

Figure 3-14 Variation of Thiessen rainfall and observed flow in the Kelani river basin (a, b)

3.10.2.2 Monthly comparison of evaporation for the years 2007-2017

A monthly graph of evaporation for the period of study for the years 2007-2017 is plotted and shown in Figure 3-15. The main purpose of these comparisons is determining the consistency of the evaporation pattern for each month of the year. Figure 3-15 indicates good matches of evaporation data for all months of the year, except for in the year of 2015-2016 the month of August shows a comparatively high evaporation rate. This comparison indicates the reliability and accuracy of the evaporation data and that is suitable for modelling and other research purposes.

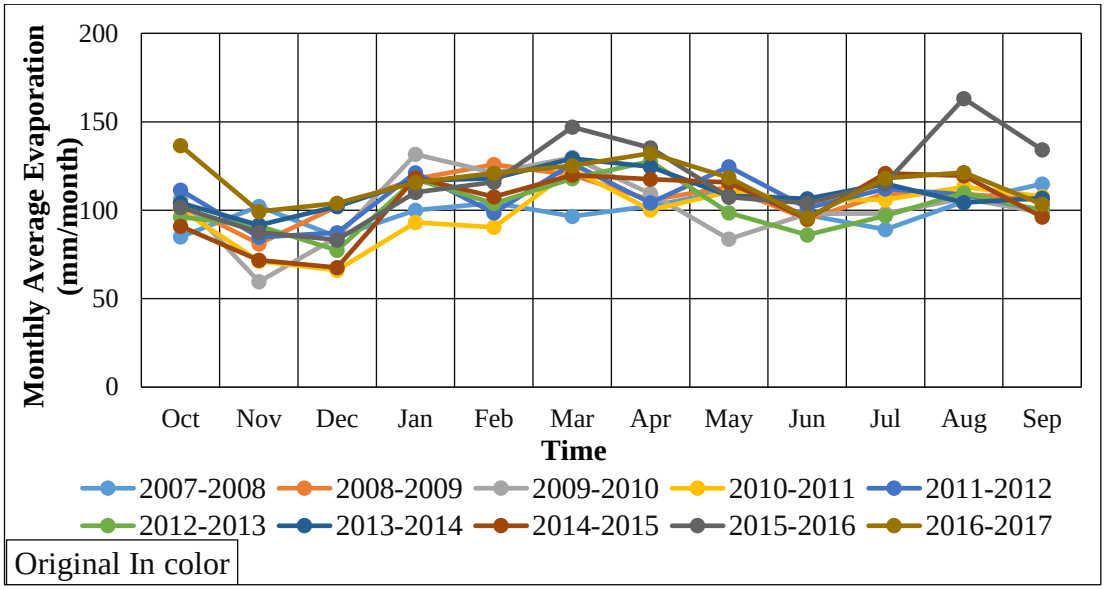

Figure 3-15 Monthly comparison of evaporation

3.10.2.3 Comparison of monthly minimum, maximum and mean (rainfall, streamflow, and evaporation)

The main purpose of this comparison is to ensure that the same patterns of monthly minimum, maximum and mean data are followed for the rainfall, streamflow, and evaporation records over the entire period of study. From Figure 3-16, it can be clearly illustrated that the highest rainfall and runoff happen in May, but the highest amount of evaporation is recorded in August. It can be overall, concluded that the rainfall, streamflow, and evaporation data follow the same pattern throughout the study period.

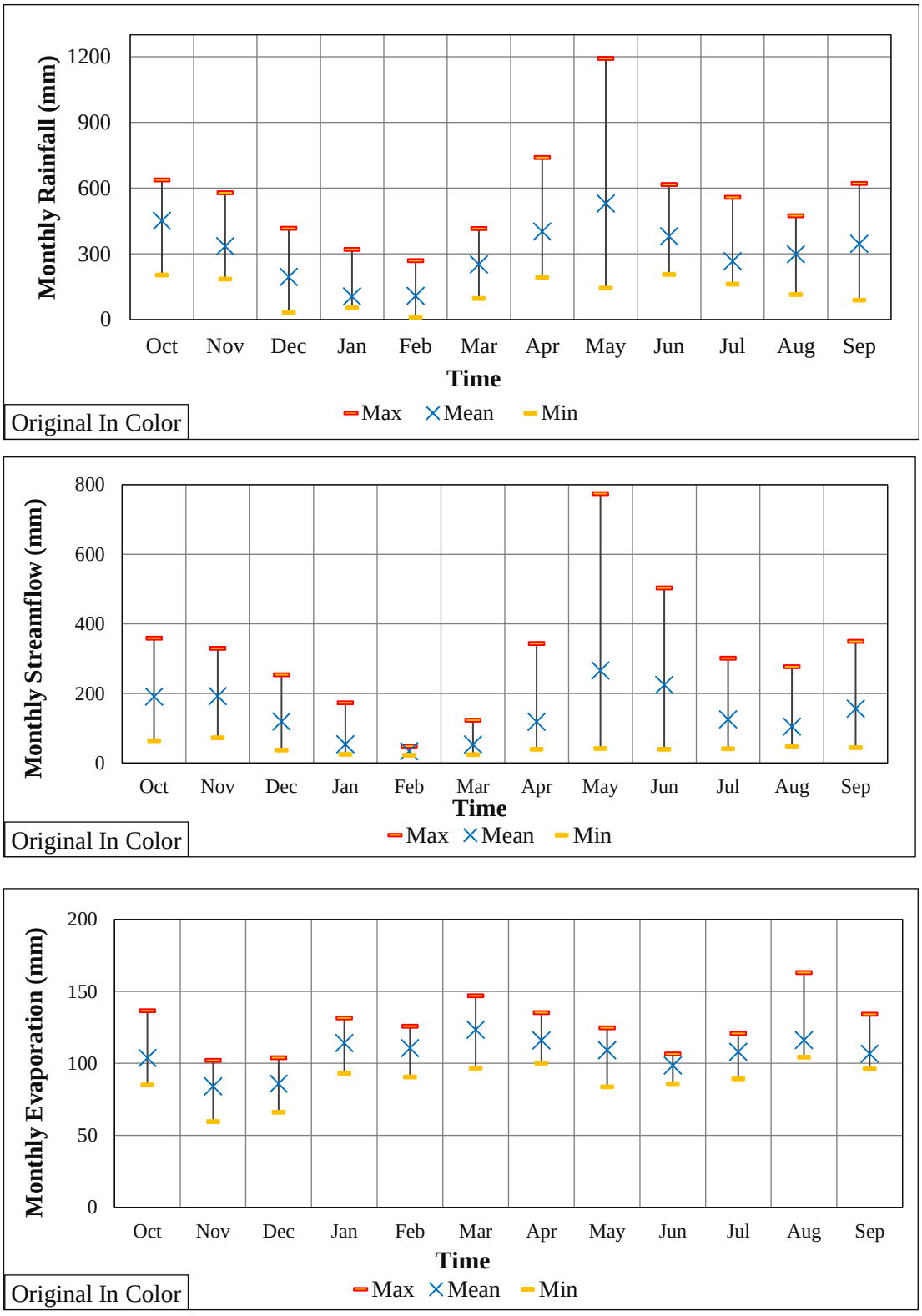

Figure 3-16 Comparison of monthly minimum, maximum and mean data (rainfall, streamflow, and evaporation)

3.10.2.4 Annual water balance for Kelani river basin at Hanwella watershed

Water balance describes the flow of water in and out of a watershed. The main purpose of this check is to identify the data input and computation errors.

Annual water balance is given by;

$$P(t) - E(t) - \text{Seepage}(t) - Q(t) = S_t - S_{t-1}, \qquad (3\text{-}1)$$

where P (t) is the rainfall, E(t) is the evapotranspiration, Q(t) is the outflow, and $S_t - S_{t-1} = \Delta S$ is the change in storage.

The annual water balance was calculated for a part of the Kelani Ganga river basin to compare the annual rainfall, streamflow, and evaporation, as presented in Figure 3-17. This check was conducted for Hanwella watershed from the year 2007 to 2017. The evaporation was checked against the water balance, which indicated a good match, as presented in Figure 3-18.

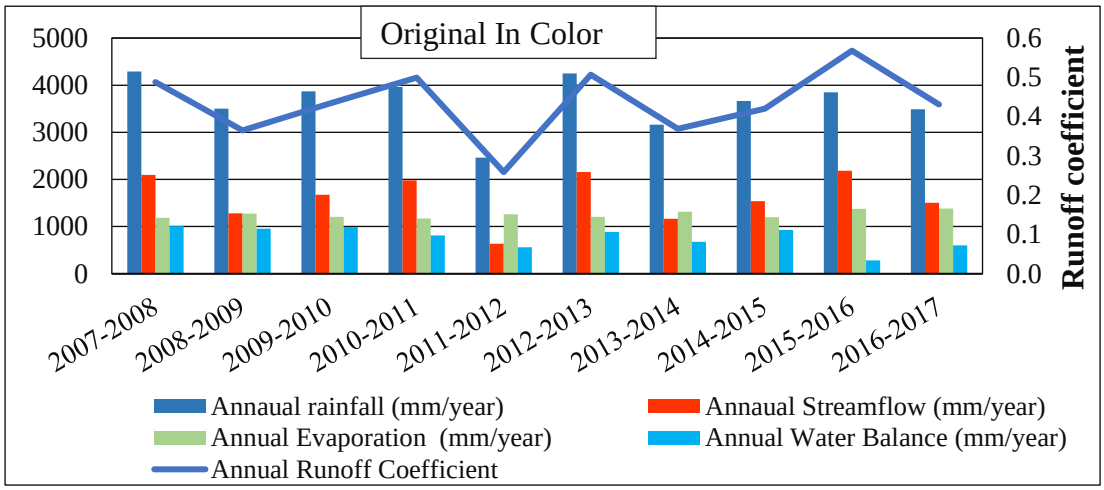

Figure 3-17 Annual water balance for the Kelani river basin at Hanwella catchment

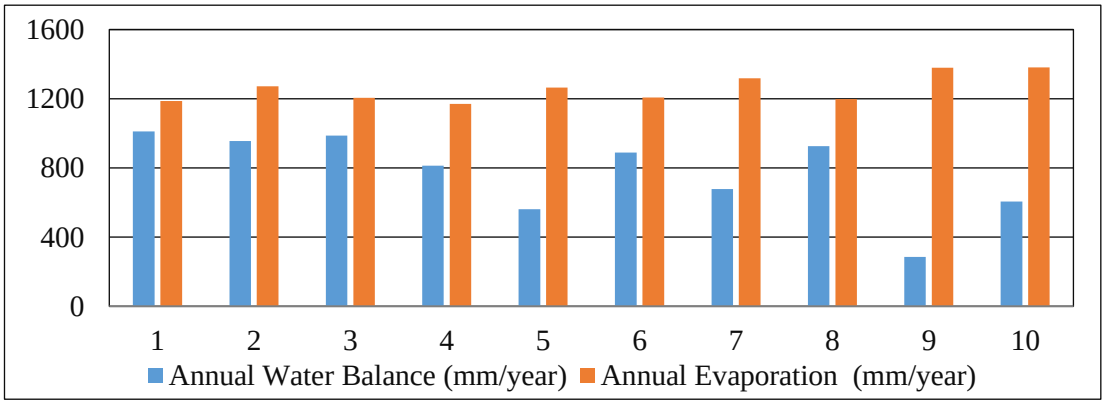

Figure 3-18 Comparison of annual water balance and evaporation

3.11 Multi sub-catchment development

Watershed subdivisions were developed based on the literature review. The critical threshold area method suggested by H. L., Wang, Li, and Wang (2013) was used in this study. The critical threshold area is defined as the minimum upstream drainage area for a river. This study uses ArcGIS, a GIS software developed by ESRI®, to visualize, analyse, compile, and manipulate spatial information. ArcGIS has several toolboxes that help user to perform geospatial analysis. For this study, two external toolbars – Arc Hydro and HEC-GeoHMS – were added to the ArcMap to facilitate the hydrologic modelling process. The Arc Hydro is used to delineate and characterize streams and watersheds and calculate drainage properties such as slope, flow accumulation, stream network, and so on. The HEC-GeeHMS toolbar was used to develop the SMA model parameters automatically and transfer the data to the HEC-HMS model from a geospatial environment.

3.11.1 Lumped model

According to the methodology of this research work, the first model considered the whole catchment as a lumped model. The lumped model schematic for the Hanwella catchment used in the HEC-HMS rainfall-runoff model is presented in Figure 3-19. This consists, of a basin and an outlet.

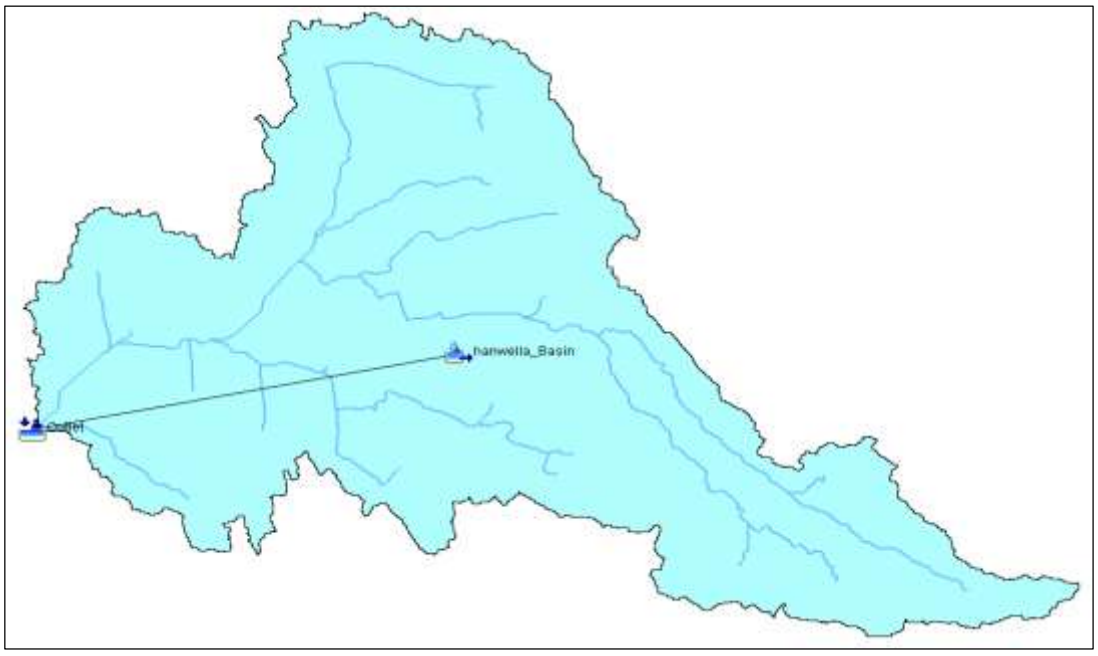

Figure 3-19 Schematic diagram for the lumped model in HEC-HMS

3.11.2 Three-subdivision model

The three-subdivision model generated using ArcGIS with the extensions Arc-Hydro and HEC-GeoHMS is presented in Figure 3-20. The HEC-HMS schematic diagram is shown in Figure 3-21.

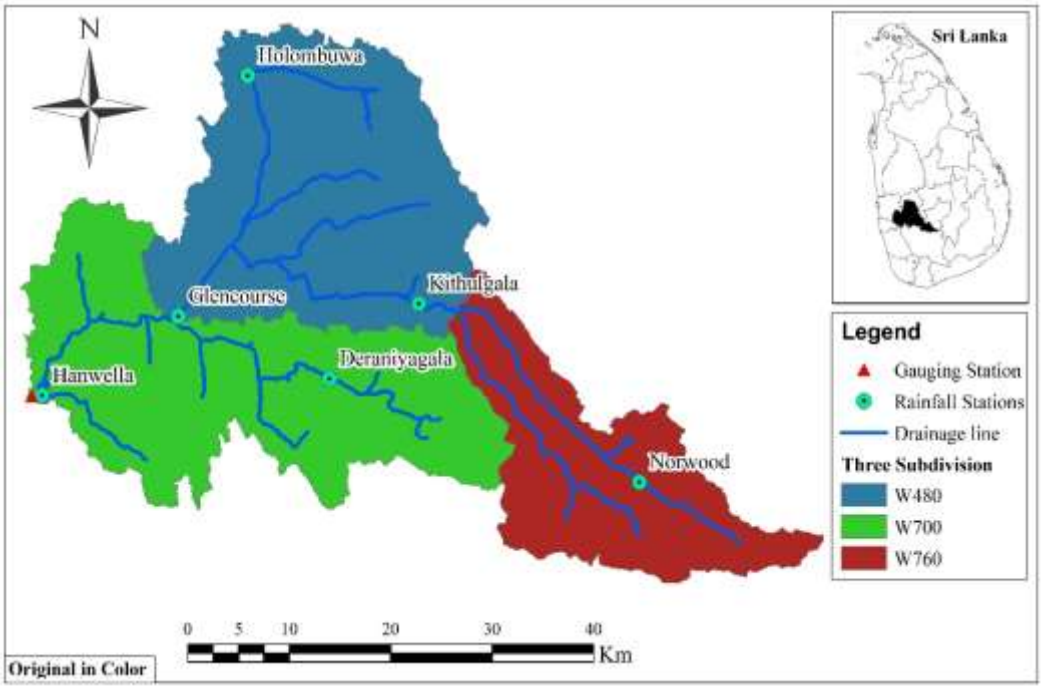

Figure 3-21 Three-subdivision of the Kelani river basin at Hanwella catchment

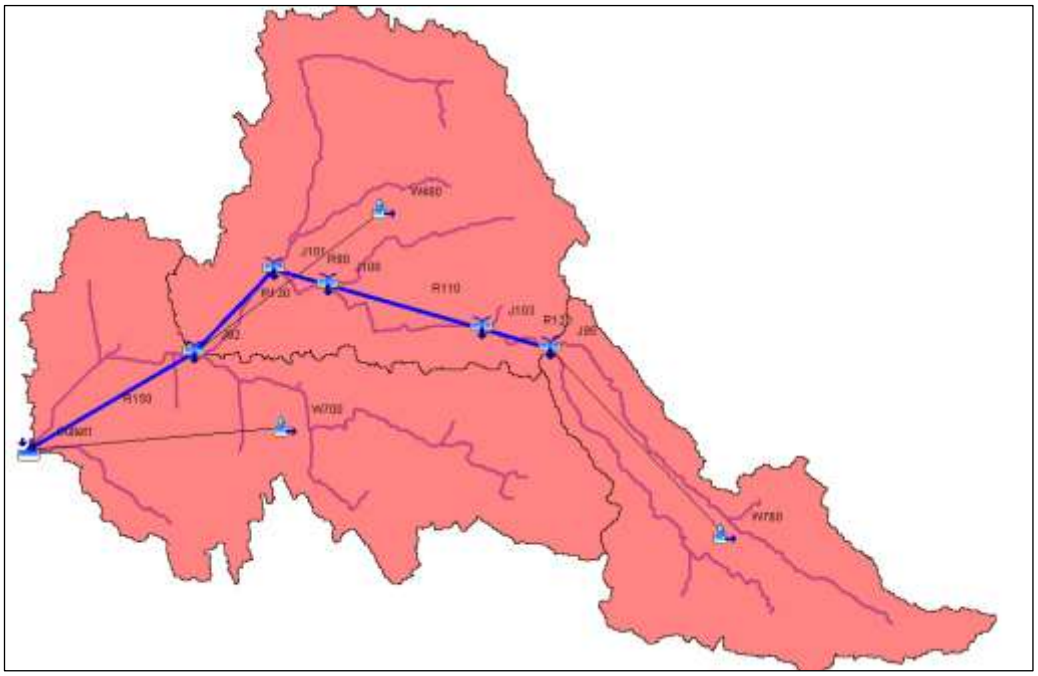

Figure 3-20 Schematic diagram for the three-subdivision model in HEC-HMS

3.11.3 Five-subdivision model

The five-subdivision model generated using ArcGIS with the extensions Arc-Hydro and HEC-GeoHMS is presented in Figure 3-22. The HEC-HMS schematic diagram is shown in Figure 3-23.

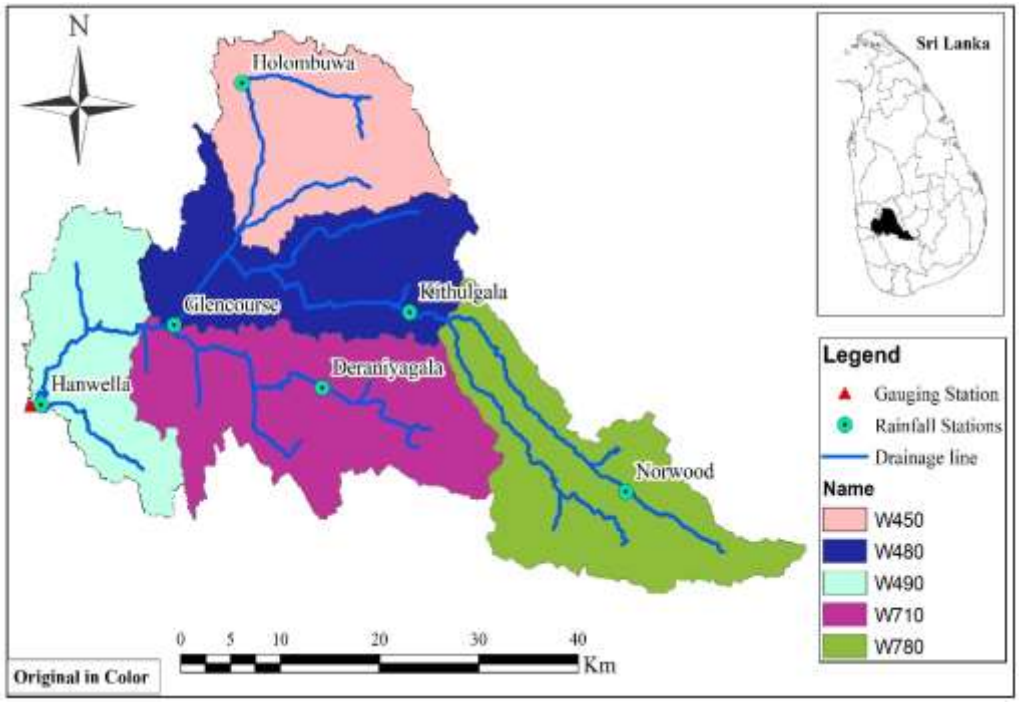

Figure 3-22 Five-subdivision of Kelani river basin at Hanwella catchment

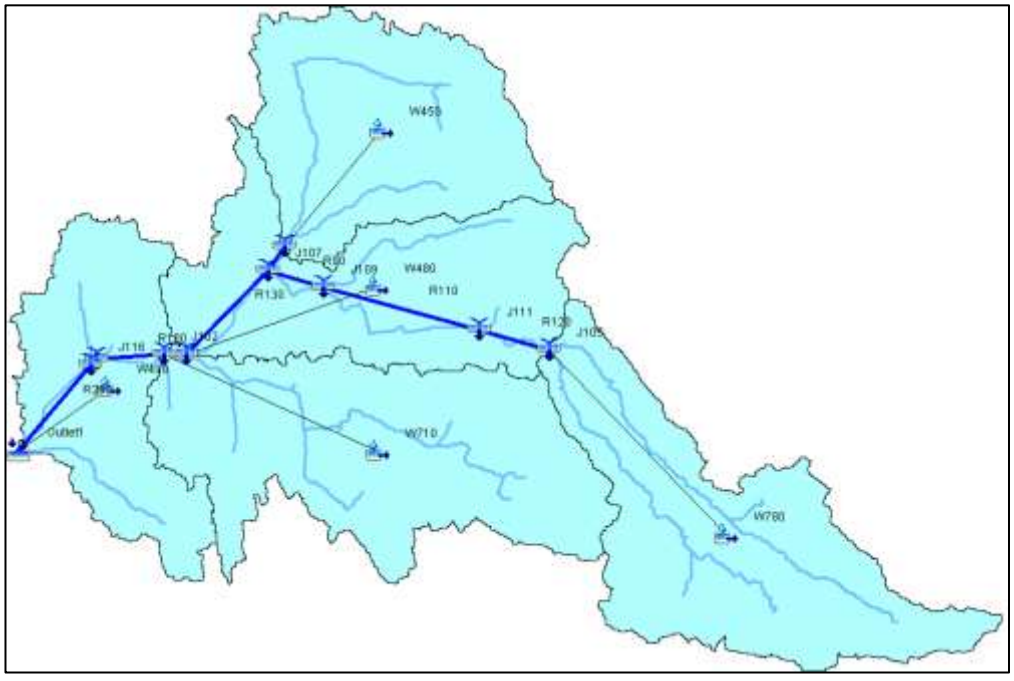

Figure 3-23 Schematic diagram for the five-subdivision model in HEC-HMS

3.11.4 Eight-subdivision model

The eight-subdivision model generated using ArcGIS with the extensions Arc-Hydro and HEC-GeoHMS is presented in Figure 3-24, and the HEC-HMS schematic diagram is shown in Figure 3-25.

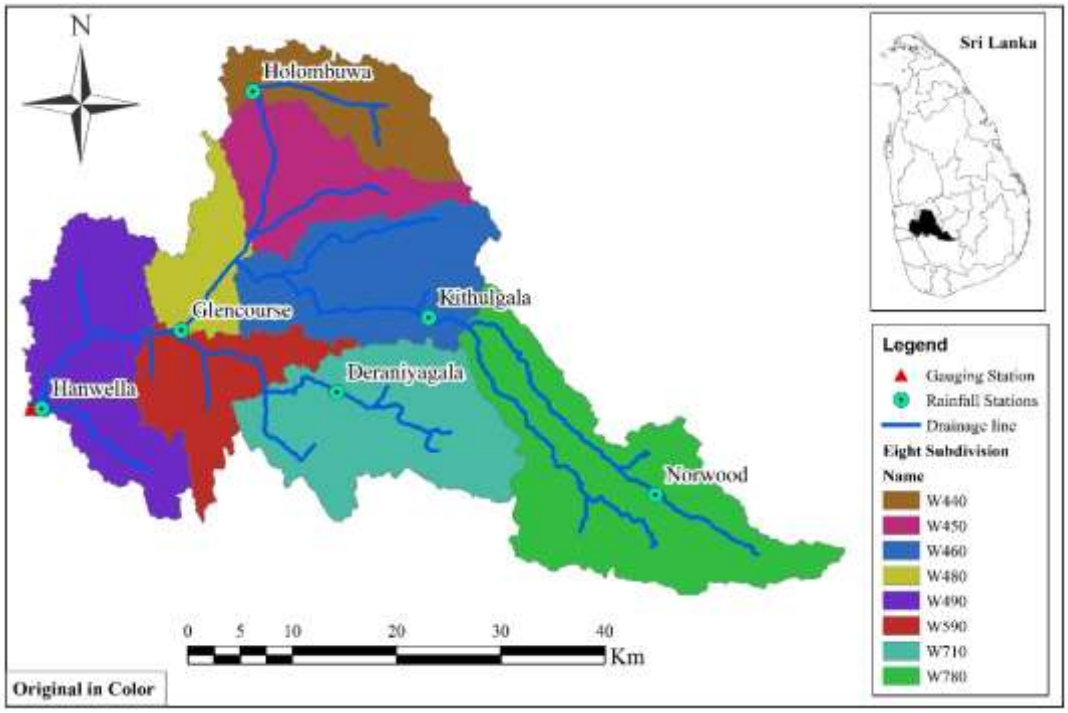

Figure 3-25 Eight-subdivisions of the Kelani river basin at Hanwella catchment

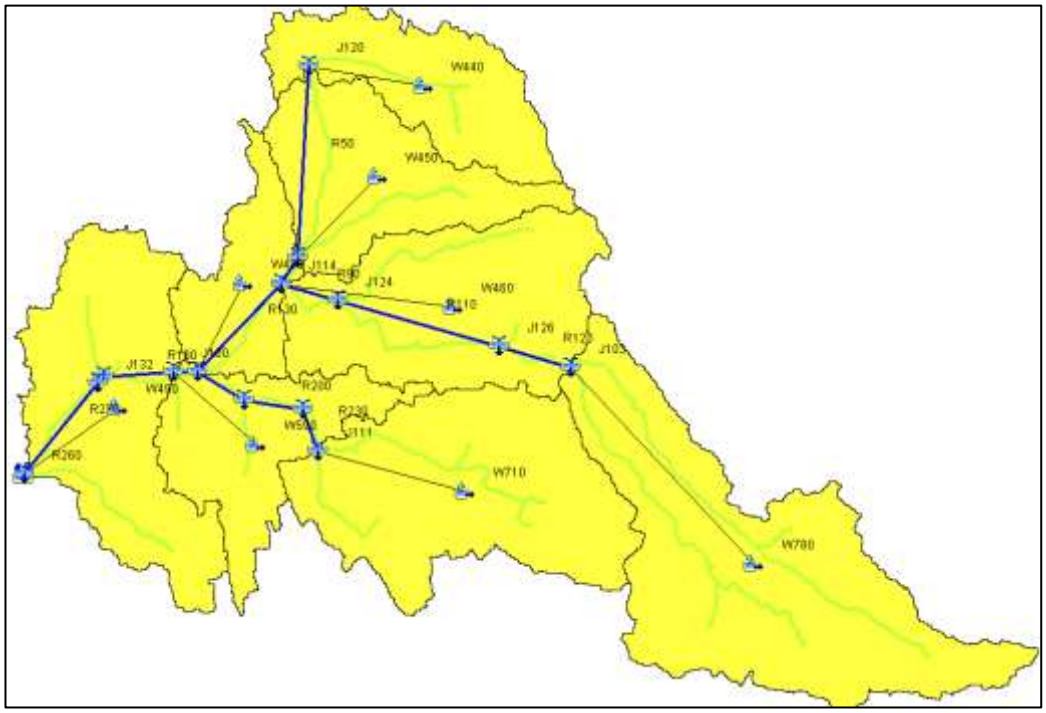

Figure 3-24 Schematic diagram for the eight-subdivision model in HEC-HMS

3.11.5 Twelve-subdivision model

The 12-subdivision model generated using the ArcGIS with the extensions Arc-Hydro and HEC-GeoHMS is presented in Figure 3-26, and the HEC-HMS schematic diagram is shown in Figure 3-27.

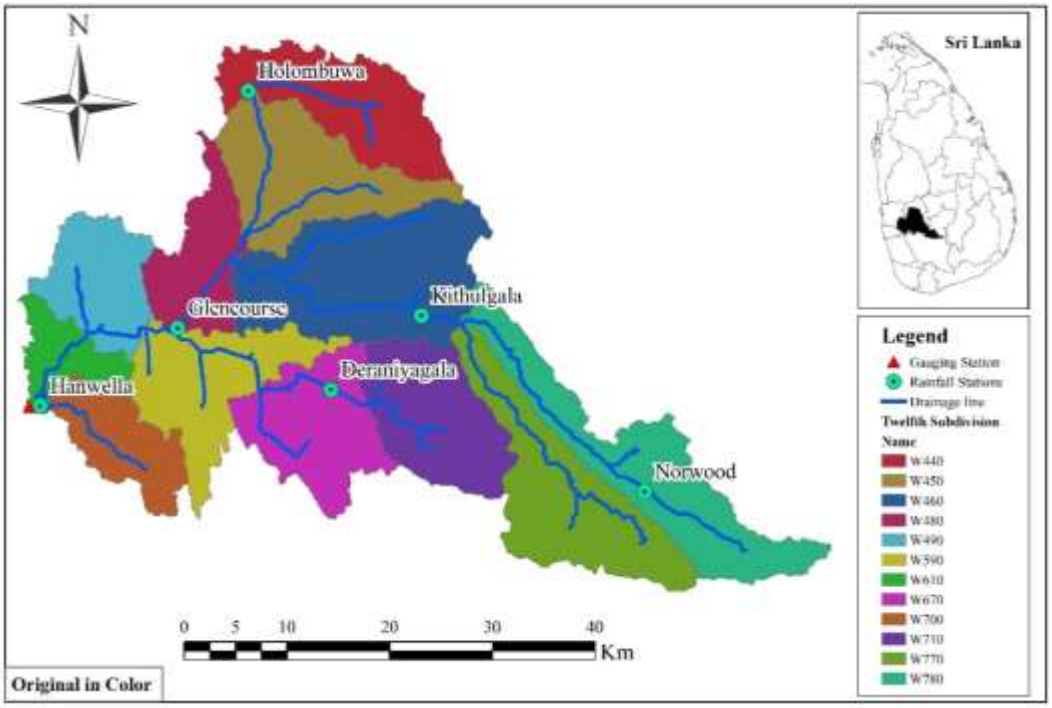

Figure 3-27 Twelve-subdivisions of the Kelani river basin at Hanwella catchment

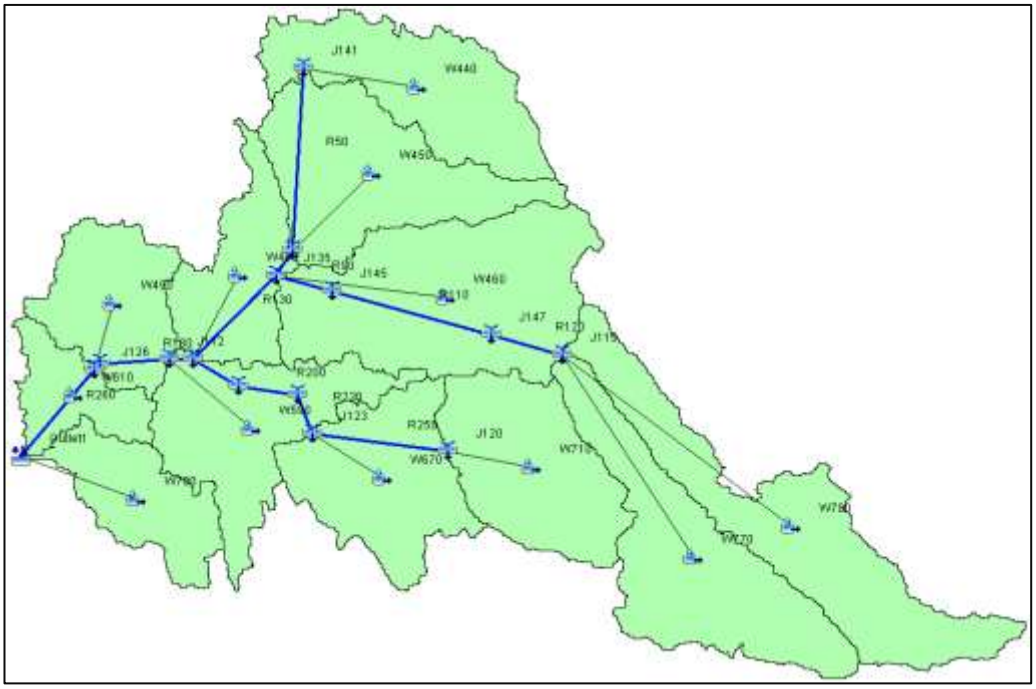

Figure 3-26 Schematic diagram for the 12-subdivision model in the HEC-HMS

4 ANALYSIS AND RESULTS

In this chapter, the methods of analysis, the parameter estimation, and the results are described. The method for the initial parameter estimation using numerous previous studies and techniques is systematically described before explaining any calibration or verification processes. According to several studies in the literature review, it is clear that the soil moisture accounting loss method is among the most difficult methods in hydrological process modelling due to the existence of a huge variety of parameters. The parameter estimation, is further rectified by the calibration process. All the results of this process are compared through the water balance, flow duration curve, hydrograph, and objective functions which will be discussed here in detail.

4.1 SMA algorithm setup and parameter estimation

This study uses ArcGIS, a GIS software developed by ESRI®, to visualize, analyze, compile, and manipulate spatial information. ArcGIS has several toolboxes that help users to perform geospatial analysis. For this study, two external toolbars, – Arc-Hydro and HECGeoHMS– were added to ArcMap to facilitate the hydrologic modelling process. Arc-Hydro is used to delineate and characterize streams and watersheds and calculate drainage properties like slope, flow accumulation, stream network, and so on. The HEC-GeoHMS toolbar is used to develop SMA parameters automatically and transfer the data to HEC-HMS from a geospatial environment.

In addition to building the model schematic in the HEC-HMS model, the SMA model components must be defined for each sub-basin. Regarding the meteorological model, HEC-HMS provides several optional methods for each component. In Table 4-1, a summary of the SMA model components and calculation methods is presented for this study.

Table 4-1 Summary of the SMA model components and calculation methods

Components	Calculation method
Canopy	Simple Canopy
Surface	Simple Surface
Loss	Soil Moisture Accounting (SMA)
Transform	ModClark
Base flow	Recession
Routing	Muskingum

A total of 24 parameters and five initial conditions were required to estimate the canopy, soil, surface, and groundwater storage parameters included in Table 4-1. Out of those 24 parameters, three of them were estimated using the land cover databases in GIS. Four of them were estimated from the streamflow recession analysis, 11 of them were estimated based on the range of values recommended in the literature. In the end, the final parameters with all initial conditions were set, through the calibration procedure. In Table 4-2, the methods for calculation of the mentioned parameters are defined.

Table 4-2 Model parameters and methods of calculation

Parameter	**Method**	**Initial condition**	**Method**
Canopy max storage (mm)	Landuse database	Canopy storage (%)	Calibration
Surface max storage (mm)	Landuse map	Surface storage (%)	Calibration
Max infiltration rate (mm/hr)	Literature and calibration	Soil storage (%)	Calibration
Max soil storage	Literature and calibration	GW1 initial storage (%)	Calibration
Soil tension storage (mm)	Literature and calibration	GW2 initial storage (%)	Calibration
Soil percolation rate (mm/hr)	Literature and calibration	Initial discharge	Streamflow data
GW1 storage	Stream recession		
GW1 max percolation rate (mm/hr)	Literature and calibration		
GW1 storage coefficient (hr)	Stream recession		
GW2 storage (mm)	Stream recession		
GW2 max percolation rate (mm/hr)	Calibration		
GW2 storage coefficient (hr)	Stream recession		
Time of concentration	SCS method		
Storage coefficient	SCS method		
Recession constant	Streamflow recession		
Ratio	Streamflow recession		
Crop coefficient	Default		

4.1.1 Canopy storage parameter estimation

The precipitation intercepted by vegetation is called the canopy interception. When water is falling to the earth's surface, it is falling to the surface of the canopy. After filling the storages capacity of the canopy, surplus water fall to the earth's surface. The SMA loss method considers canopy storage as one of the loss components. The canopy storage capacity varies with the vegetation's surface structure and meteorological factors. Canopy storage can be calculated using the land use and land cover map. The recommended canopy interception values are provided in Table 4-3.

Table 4-3 Canopy storage values

Vegetation type	Canopy interception (mm)
General vegetation	1.27
Grasses and deciduous trees	2.032
Trees and coniferous trees	2.54

Source: Bennett & Peters (2000)

Based on the above-recommended values from the landuse map, the canopy raster was developed. Through developing the canopy raster, its values for the lumped and distributed models could be easily calculated using the Arc GIS tool. For the Kelani river basin at Hanwella catchment, the canopy raster is shown in Figure 4-1. The corresponding values can be found are shown in Table 1-B of Appendix B.

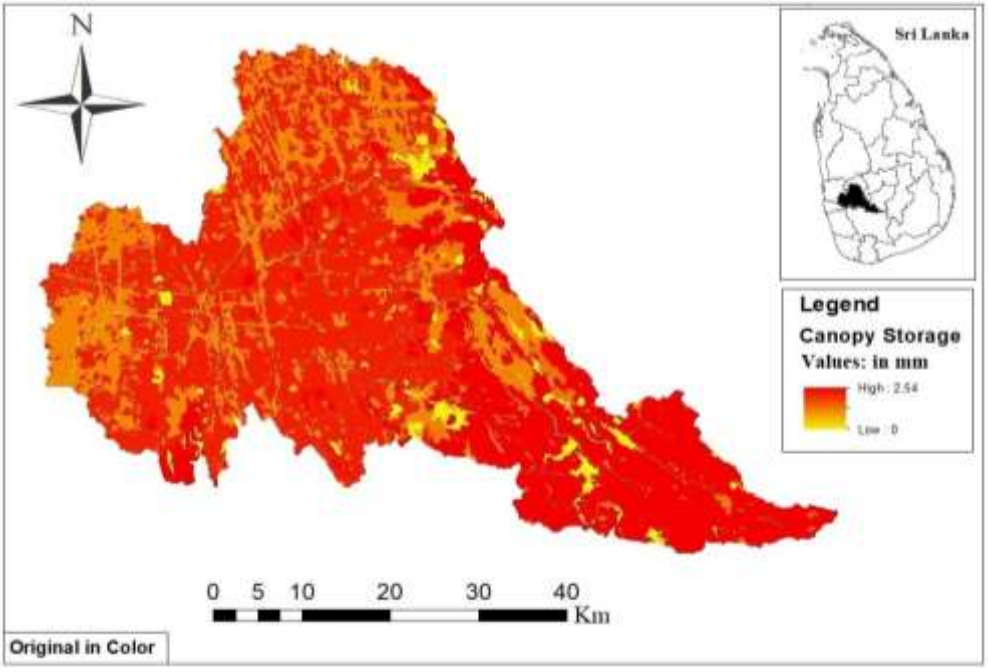

Figure 4-1 Canopy storage raster for the Kelani river basin at Hanwella catchment

4.1.2 Surface storage parameter estimation

Surface storage, or surface depression storage, is defined as the volume of water that is stored in the ground surface. The precipitation that is not captured by the canopy interception or that falls after the canopy's storage capacity is filled moves to the earth surface. Some of this flow infiltrates or evaporates, and some of it is stored in the ground surface. According to Bennett et al. (2000) surface storage capacity is related to the terrain slope. Possible slopes and related storage values are described in Table 4-4 based on Bennett et al.'s (2000) suggestion.

Table 4-4 Surface depression storage values

Description	Slope %	Surface storage (mm)
Paved impervious areas	NA	3.2 - 6.4
Steep and smooth slopes	>30	1.0
Moderate to gentle slope	5-30	12.7 - 6.5
Flat and furrowed land	0-5	50.8

The surface storage raster presented in Figure 4-2 was developed for the Kelani river basin at Hanwella catchment using the recommended values mentioned in Table 4-4. Estimation of the relevant parameters for the lumped and distributed models was carried out using the ArcGIS tool. The surface storage raster is shown in Figure 4-2, and the corresponding values for lumped and distributed models are shown in Appendix B, Table 2-B.

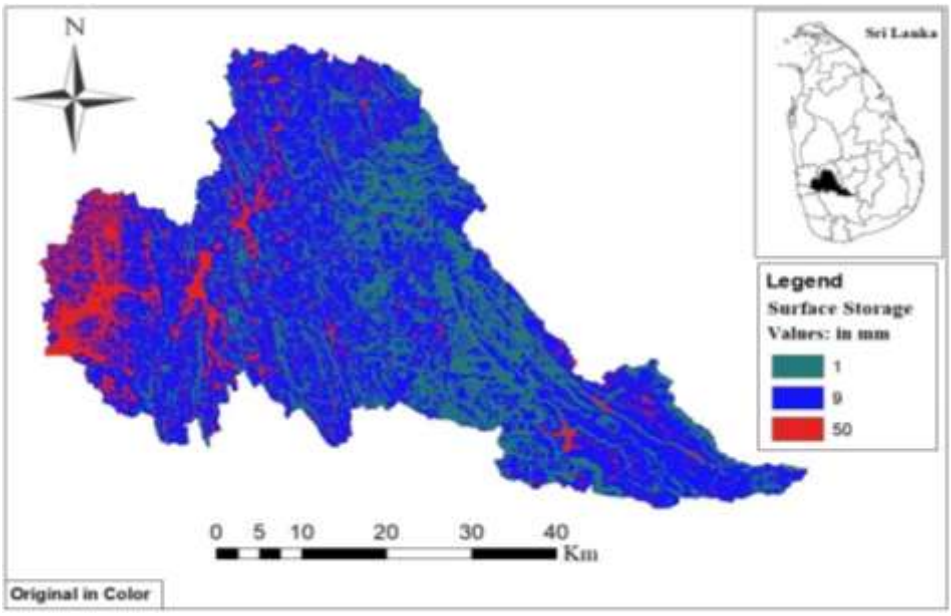

Figure 4-2 Surface storage raster for the kelani river basin at Hanwella catchment

4.1.3 Impervious percentage (%) parameter estimation

The impervious percentage is one of the most important factors in constructing direct runoff in the SMA loss model. This parameter directly affects the peak of the hydrograph. Higher values of this component mean a higher peak in the hydrograph, and vice versa. A high impervious percentage indicates that less water goes through soil layers. In other words, if the values of this factor are lower, then a small amount of water contributes to the surface water. For the Kelani river basin at Hanwella catchment, this parameter was estimated according to the landuse map using the landuse and land cover coefficients. Every component of landuse has a specific coefficient suggested in the literature by Prisloe, Giannotti, and Sleavin (2000). The impervious raster presented in Figure 4-3 was derived using landuse data by entering the specific coefficients. The retrieved mean values for the lumped and distributed models were acquired through ArcGIS software (presented in Table 3-4 B, Appendix B).

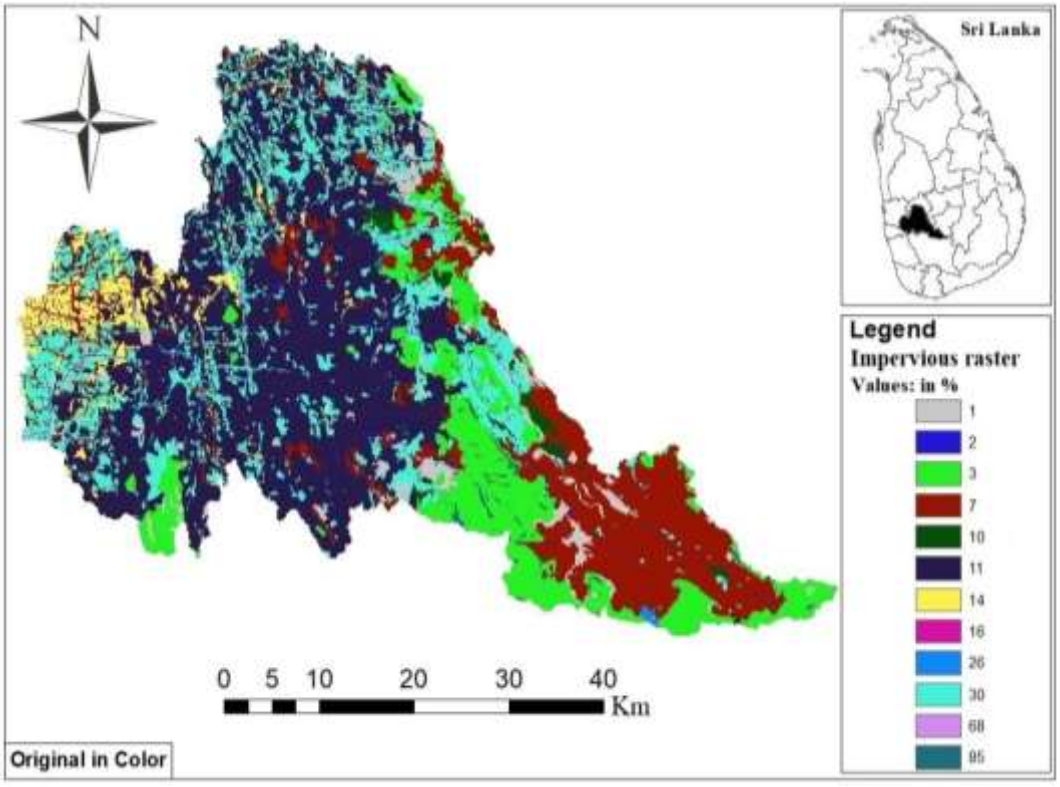

Figure 4-3 Surface storage raster for the Kelani river basin at Hanwella catchment

4.1.4 Transform method parameter estimation

The ModClark unit hydrograph was used as the main tool in the transform method. Through this method, time of concentration and storage coefficients can be estimated. These two parameters were estimated using the grid cell file developed in the ArcGIS software with the extension of the HEC-GeoHMS. The estimation process was conducted using the NRC's formula that considers the curve number (CN) and slopes as a primary data to be input in the model. After acquiring these two parameters, the time of concentration and the storage coefficients can be easily calculated through NRC's formula, as shown in equation 4.1.

$$T_c = \frac{L^{0.8}(\frac{100}{CN} - 9)^{0.7}}{1140S^{0.5}}, \qquad (4.1)$$

In the above formula, the Tc is the time of concentration (Hr), CN is the curve number, L is the longest length in feet, and S is the slope percentage.

The relationship between the time of concentration and storage coefficient is defined in equation 4.2 based on the NRCS method.

$$\frac{T_C}{R} = 1.46 - \frac{0.0867 * L^2}{A}, \qquad (4.2)$$

In the above formula, Tc is the time of concentration, R is the storage coefficient in hour, L is the longest length in miles, and A is the drainage area in square miles. All these factors were generated and calculated using the HEC-GeoHMS extension tool in ArcGIS.

In the above sentences, it is mentioned that to calculate Tc and R, two important parameters (CN and slope) are needed. The CN and slope raster were developed for the Hanwella catchment so that it could be possible to estimate the mean values in lumped and distributed models using ArcGIS software. For generating the slope raster, the 30m DEM resolution published by Survey Department of Sri Lanka was used in this study. Also, the CN grid raster was developed using the landuse and land cover map published by the Survey Department and is shown in Figure 4-4. It is worth mentioning that the CN values for individual landuse were used according to Chow et

al.'s (1988) suggestions. The CN and slope rasters for the Kelani Ganga river basin at Hanwella catchment are shown in Figures 4-4 and 4-5 respectively. All the mean values retrieved from the CN and slope rasters are listed in Table 6-B, Appendix B.

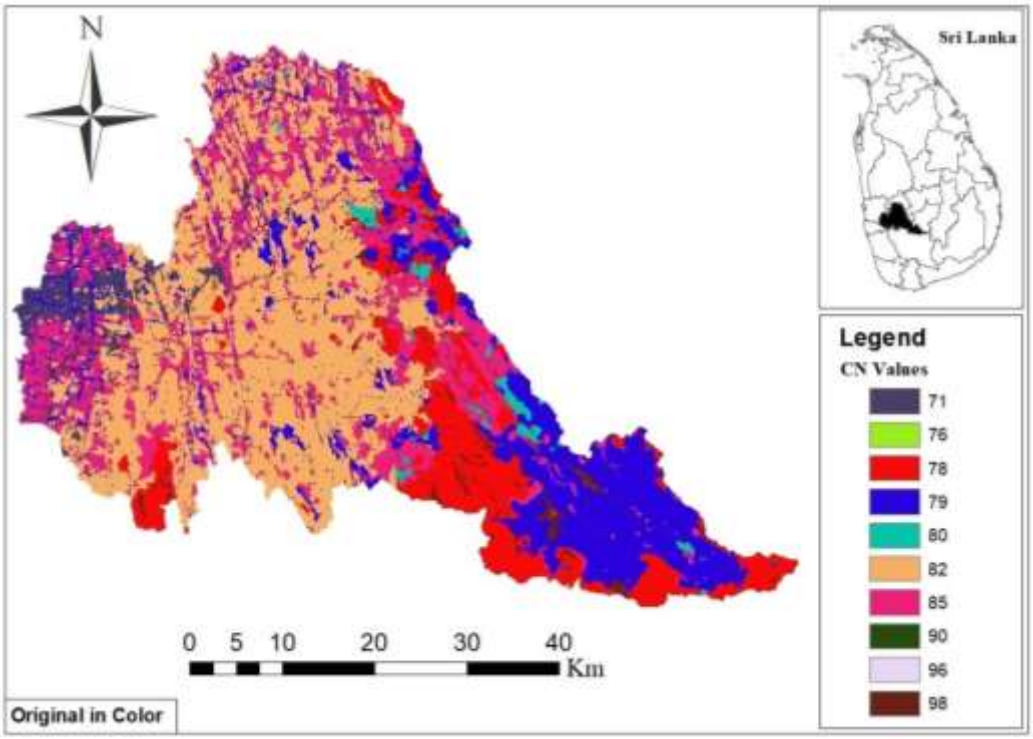

Figure 4-4 CN grid raster for the Kelani river basin at Hanwella catchment

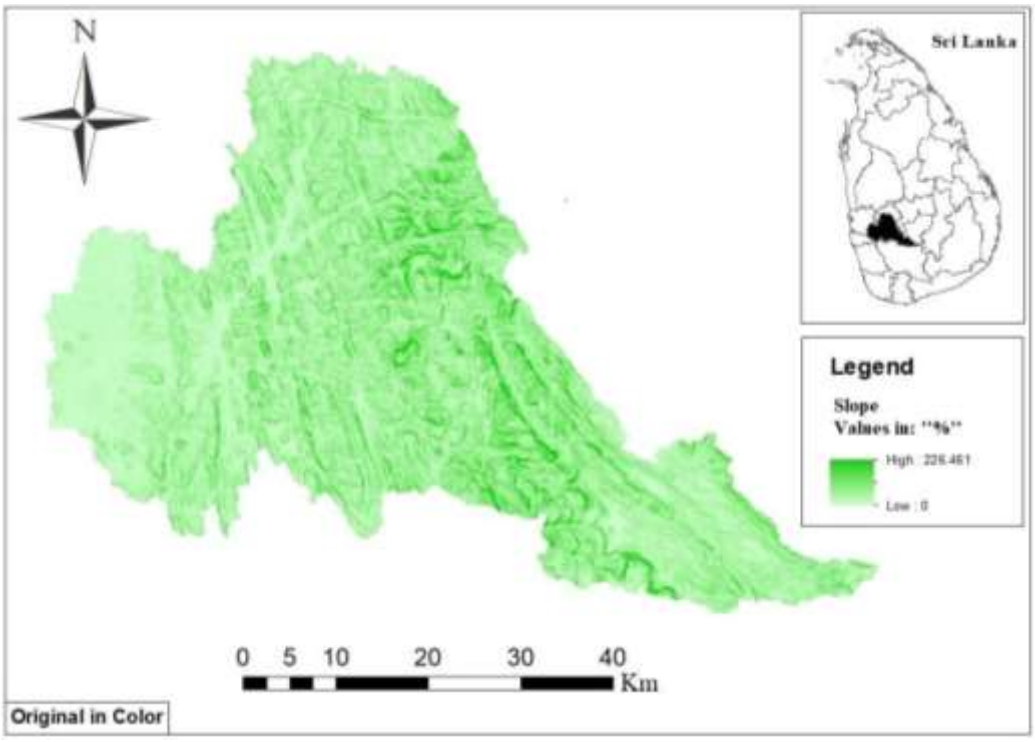

Figure 4-5 Slope raster for the Kelani river basin at Hanwella catchment

4.1.5 Base flow computation

According to the literature review, the base flow computation in many hydrologic modelling around the world is carried out using the exponential recession method (Arnold, Allen, Mutt1ah, & Ber, 1995). The HEC (2000) defines the exponential recession method as a direct relationship between Q_t (the base flow at any time) and Q_0 (the initial base flow). The initial base flow is the flow after whic surface runoff contributes to the streamflow. The relevant formula is shown in equation 4.3 below:

$$Q_t = Q_0 k^t, \qquad (4.3)$$

where Q_0 is the initial baseflow (at time 0) and K is the exponential decay constant, where K is defined as the ratio of the baseflow at time t to the baseflow one day earlier (Arlen & Feldman, 2000).

Before the base flow can be calculated, the HEC-HMS model needs two parameters to be set. These two parameters are K and the ratio of the threshold discharge to the peak discharge. For estimation of these two parameters, a set of rainfall and runoff data from 20th April 2008 to 26th April 2008 was analysed, as presented in Figure 4-6. The optimum values of K and R were set through the calibration procedure.

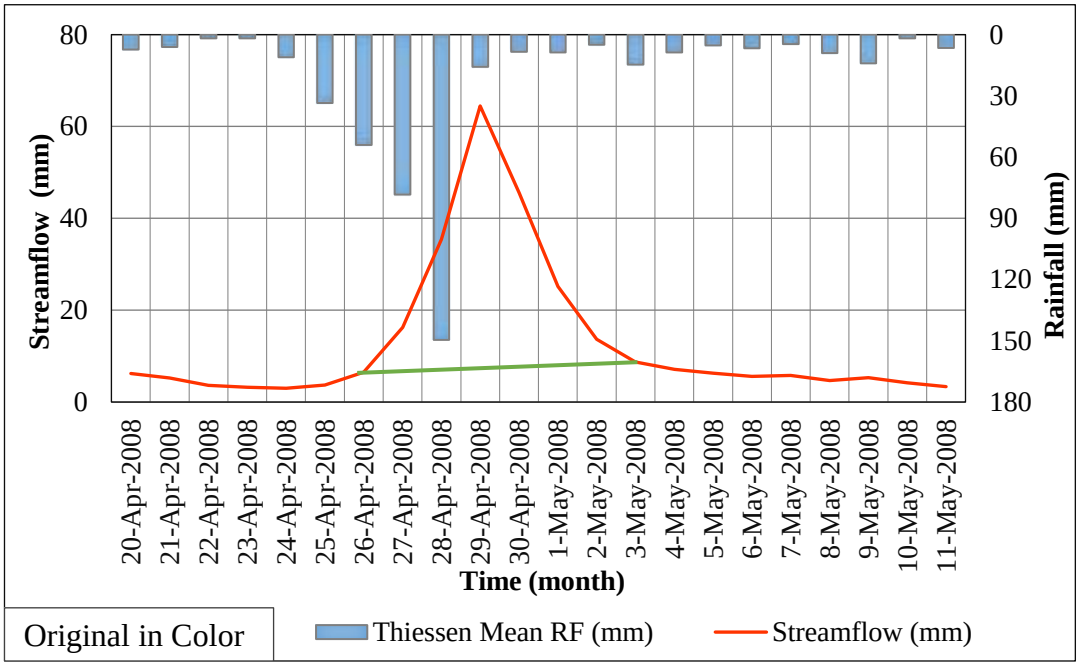

Figure 4-6 Selected hydrograph for baseflow computation at Hanwella catchment

Table 4-5 Rainfall and streamflow values for computation of baseflow parameters

Date	Thiessen mean rainfall (mm/day)	Observed streamflow (mm/day)
20-Apr-08	7.28	6.23
21-Apr-08	6.12	5.24
22-Apr-08	1.85	3.60
23-Apr-08	1.82	3.23
24-Apr-08	11.08	3.00
25-Apr-08	33.51	3.72
26-Apr-08	54.11	6.49
27-Apr-08	78.31	16.23
28-Apr-08	149.58	35.42
29-Apr-08	15.71	64.47
30-Apr-08	8.36	45.55
1-May-08	8.71	25.15
2-May-08	4.93	13.71
3-May-08	14.67	8.71
4-May-08	8.75	7.14
5-May-08	5.21	6.31
6-May-08	6.64	5.61
7-May-08	4.58	5.79
8-May-08	9.02	4.65
9-May-08	14.04	5.34
10-May-08	1.88	4.23
11-May-08	6.56	3.37

The Q_0 and Q_t were found as in Table 3-8. The Q_o was 6.23 (initial flow at any point of time) and Q_t was 6.49 (the time before starting the peak). After Q_t, the hydrograph was the result of the joint contribution of baseflow and direct runoff. According to the mentioned rationalization, the values of the parameters were retrieved for calculation.

According to equation 4.3, the K parameter is calculated:

$$Q_t = Q_0 k^{\,t} \qquad (4.2)$$

$$6.49 = 6.23\mathrm{k}^7$$

After the calculation, the K value was retrieved (k=1.006).

Similarly, the ratio to peak and threshold discharge was calculated using the data in Figure 4-6. The threshold discharge was calculated as $Q_{tr} = 9\ mm/day$, and the peak discharge was calculated as $Q_{peak} = 65\ mm/day$.

Finally, the ratio-to-peak value

$$(R= \frac{Q_{tr}}{Q_{peak}} = \frac{9}{65} = 0.138\ )$$

was calculated.

4.1.6 Parameter estimation using the literature

Some of the parameters related to the hydraulic properties of soil were estimated from the literature. Accurate estimation of those parameters requires an extensive investigation of basin soils, which due to the limits of budget and time in this study, was beyond the scope of this research. In Table 4-6, all of these parameters are mentioned. In this research, the initial values of these parameters were estimated using the ranges of values that were described in previous studies. Optimum values were set through the calibration process.

Table 4-6 Parameters estimated from the literature

Parameters	Source	Range
Max infiltration (mm/h)	Saxton & Rawlas (2006); Gyawali (2013)	5 - 45
Tension storage (mm)	U.S. Army Corps of Engineers (USACE, 2010)	10.2 - 60.6
Soil percolation (mm/h)	WMS (1999); Gyawali (2013)	0.05 - 5
Soil storage (mm)	WMS (1999); Gyawali (2013)	40 - 150

4.1.7 Parameter estimation using streamflow recession analysis

Groundwater layer 1 and 2 storage coefficients and storage depths were estimated using the recession analysis approach suggested by Fleming et al. (2004). Proceeding that, hydrographs of five independent storm events were analysed for the Kelani river basin. The inflection point on the receding limb of a hydrograph marks where the surface flow has stopped contributing to runoff (Linsley, 1975). After this point, the

receding limb represents contributions from both interflow and groundwater flow. Recession analysis of the historical streamflow data provides the constant recession value of the streamflow (Subramanya, 2013).

The following function suggested by Fleming et al. (2004) was used to estimate the recession coefficient and groundwater storage.

$$Q_t = Q_0 k^t, \qquad (4.3)$$

where Q_t is the discharge at time t, Q_o is the initial discharge, and K_r is the recession constant. The recession constant K_r consists of three components to account for three types of storage as follows:

$$K_r = K_{rs}.K_{rt}.\ Krb, \qquad (4.4)$$

where K_{rs} is the recession constant for surface storage, K_{rt} is the recession constant for interflow, and K_{rb} is the recession constant for the base flow. For estimation of two different storage types, equation 4.3 was developed after the mathematical analysis into equation 4.4 as below:

$$\frac{Q_1}{Q_2} = K_r^{(t_1 - t_2)}, \qquad (4.5)$$

Using equation 4.5, the recession constant can be determined from the historical streamflow data. The storage S_t remaining at any time t is obtained as follows:

$$S_t = \int_t^\infty Q_t dt = \int_t^\infty Q_0 e^{-at} dt = \frac{Q_t}{a}, \qquad (4.6)$$

where

$$x = -\ln K_r, \qquad (4.7)$$

To study the streamflow recession analysis, events were selected for the whole calibration period, starting from the year 2007/2008 to the year 2011/2012, for estimation of the mentioned parameters.

Hydrographs were chosen from the different seasons and from those storm events where no rainfall occurred. As a representative example, here one event for the year 2007/2008 is selected from the 16th Nov to the 28th Nov (Figure 4-7). In order to perform streamflow recession analysis for estimation of the groundwater storages parameters, the hydrograph was analysed by subtracting the groundwater, interflow,

surface runoff and interflow from the total hydrograph, as shown in Figure 4-7. The main literature source used for streamflow recession analysis was Linsley (1975). In addition, for every single year of calibration, a similar process wasconducted, which can be seen in Figures 1-B to 4-B in Appendix B.

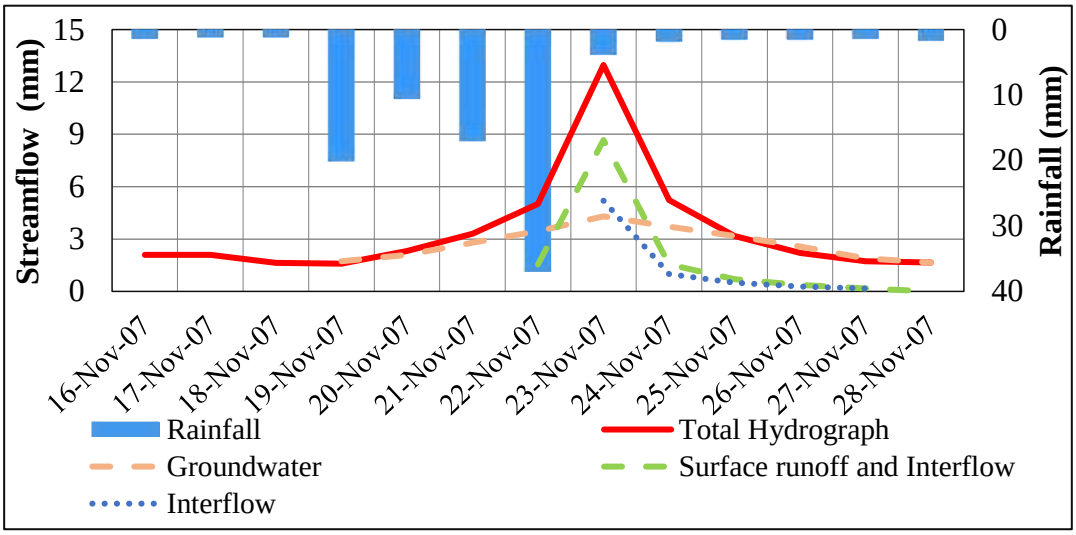

Figure 4-7 Selected event for the year 2007: streamflow recession analysis

The results of the streamflow recession analysis are shown in Table 4-7 for the entire calibration period.

Table 4-7 Streamflow recession analysis results

Parameters	Years					Average
	2007	2009	2010	2012	2013	
Base flow storage (mm)	21.8	15.8	24.1	155.7	102.64	64
Base flow constant (Hr)	240	264	192	144	168	201.6
Interflow storage(mm)	2.2	1.2	1.1	9	13.5	5.4
Interflow recession constant (Hr)	120	120	96	52	72	92

4.2 Objective functions recommendations

The MRAE is used as a primary metric objective function in this research work. This indicator has been used widely in hydrologic modelling of Sri Lankan river basins by major researchers (Wijesekera & Abeynayake, 2003; Perera & Wijesekera, 2011; Khandu, 2015; Sharifi, 2015; Jayadeera, 2016 and Dissanayake, 2017). This objective

function is also suggested by the World Meteorological Organization (WMO, 1975). Besides the MRAE, other objective functions are also used for evaluating the efficiency of current hydrological model performance. These objective functions are the coefficient of determination (R^2); percentage error in volume (PVE), as suggested by Jain and Singh (2003); and the NSE indicator, as suggested by Nash and Sutcliffe (1970) are all used in this study.

Recommended ranges of the mentioned objective functions for evaluating the performance of the hydrological models are summarized in Table 4-8. The MRAE objective function ranges are adopted from Wijesekera et al. (2003); Moriasi, Arnold, and Van Liew (2007); Perera et al.(2011); Khandu (2015); Sharif (2015); Jayadeera (2016) and Dissanayake (2017). The PBIAS and NSE ranges were retrieved based on Moriasi et al.'s (2007) suggestion.

Table 4-8 Objective function recommendations

Performance rating	**R^2**	**PBIAS/PVE**	**NSE**	**MRAE**
Very good	$0.75< R^2 \leq 1$	PBIAS$\leq\pm10$	0.75<NSE≤1	0<MRAE<4
Good	$0.65 <R^2 \leq 0.75$	$\pm10 \leq$PBIAS $<\pm15$	0.65<NSE≤0.75	0<MRAE<5
Satisfactory	$0.75< R^2 \leq 0.65$	$\pm15 \leq$PBIAS $<\pm25$	0.50<NSE≤0.65	5<MRAE<7
Unsatisfactory	$R^2 \leq 0.5$	PBIAS$\geq\pm25$	NSE≤0.5	MRAE>7

4.3 Sensitivity analysis

Sensitivity analysis of the HEC-HMS model with the SMA algorithm was one of the main objectives of this study. For this analysis, all SMA parameters were varied from -50% to +50% in increments of 10%. Each parameter was varied individually while keeping other parameters constant. The percentage changes in simulated volume plotted against the variation of each parameter are presented in Figure 4-8. Figure 4-8 illustrates that soil percolation was the most sensitive parameter and the GW2 coefficient was the least sensitive parameter relating to the changes in simulated volume. Other studies conducted for the Dale Hollow basin, the Cumberland river

basin, the Blue Nile river basin, and the Kulfo and Bilate catchments in the Abaya-Chamo sub-basin frequently found that soil percolation was the most sensitive parameter. After soil percolation, tension zone storage and soil storage parameters were identified as the following most sensitive parameters.

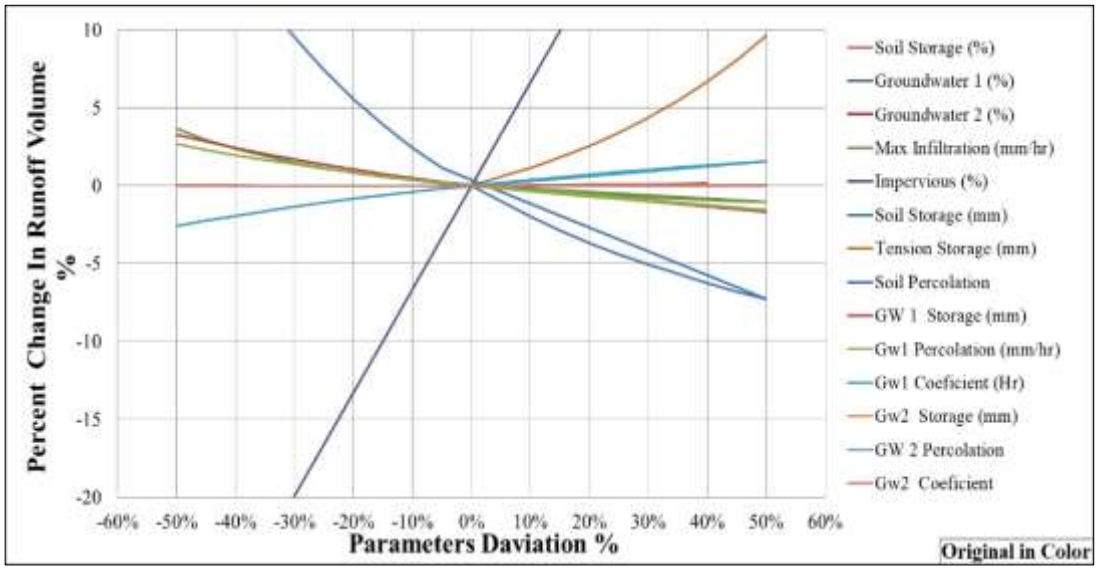

Figure 4-8 Sensitivity analysis for SMA parameters

the same procedure of changing the parameters from -50% to +50% in an increments of 10% was conducted (shown in Figure 4-9). It was found that among all the parameters, the impervious percentage is one of the most sensitive parameters and needs to be accurately estimated for successful modelling purposes.

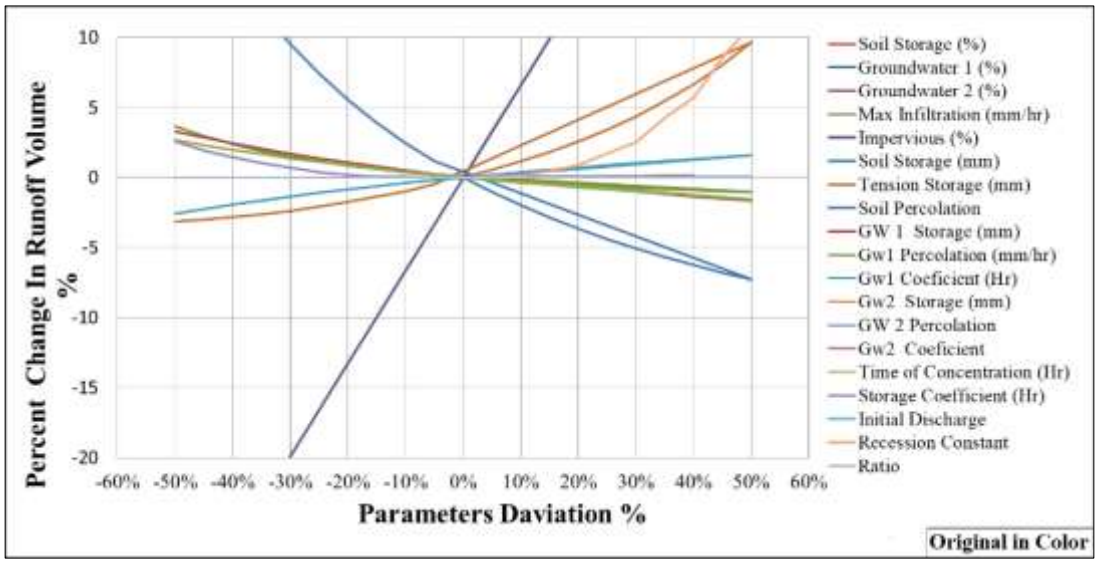

Figure 4-9 Sensitivity analysis for all parameters

4.4 Results for the lumped model

The results of the analysis were embedded in the form of water balance, flow duration curve, hydrographs, and objective functions. All the results are shown below, including the entire calibration and verification periods.

4.4.1 Annual water balance

The results of the model are shown in water balance form to ascertain the accuracy between the observed and simulated streamflows. The annual water balance values for the calibration period are shown in Table 4-9 and Figure 4-10.

Table 4-9 Annual water balance values for the calibration period of the lumped model

Water year	Thiessen averaged rainfall (mm)	Simulated streamflow (mm)	Observed streamflow (mm)	Observed water balance (mm)	Simulated water balance (mm)	Annual water balance difference (mm)
2007-2008	4,294	1,878	2,099	2,195	2,415	221
2008-2009	3,593	1,452	1,367	2,226	2,142	-84
2009-2010	3,872	1,597	1,676	2,196	2,275	79
2010-2011	3,967	1,878	1,986	1,981	2,089	108
2011-2012	2,532	812	639	1,893	1,720	-173

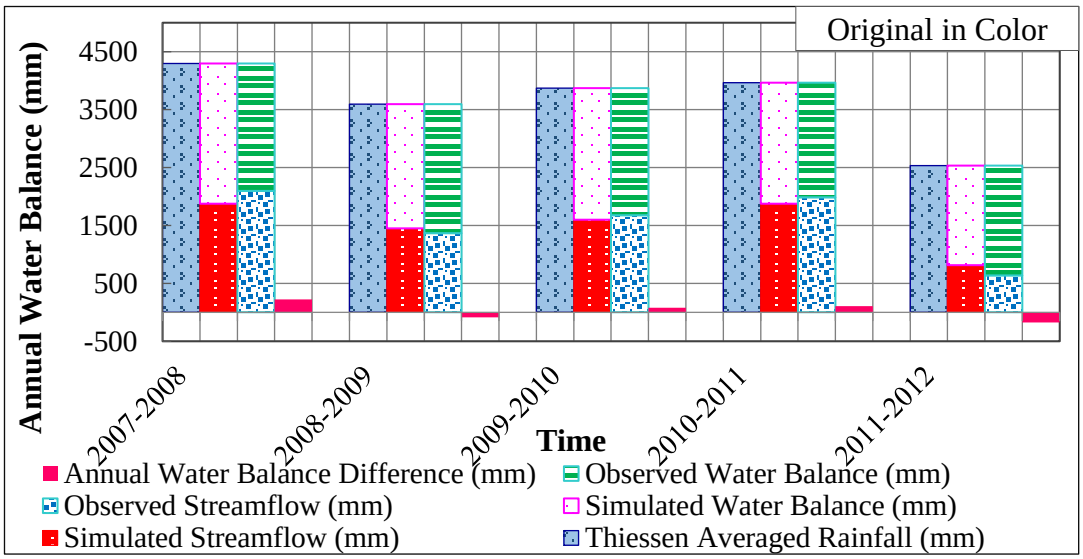

Figure 4-10 Annual water balances for the calibration period of the lumped model

The differences in water balance are illustrated in Figure 4-10 in red and are equal 3.82 % for the entire calibration period. This value indicates the accuracy of the model

due to its existence in an acceptable range as described in the literature review section. Similarly, the annual water balance was carried out for the verification period to verify the accuracy of the amount of water entering and exiting the catchment. The annual water balance for the calibration period is illustrated in Table 4-10 and Figure 4-11. As a result of these checks for the verification period, the maximum difference was near 10 %, and occurred in the year 2015/2016. This value is in the acceptable range according to the literature, which demonstrated a well-defined model during the verification period. Overall, for the verification period, the average error defined in the calculation was 5.87 %, indicating a precise hydrological model.

Table 4-10 Annual water balance values for the verification period of the lumped model

Water year	Thiessen averaged rainfall (mm)	Simulated streamflow (mm)	Observed streamflow (mm)	Observed water balance (mm)	Simulated water balance (mm)	Annual water balance difference (mm)
2012-2013	4,253	1,872	2,161	2,093	2,382	289
2013-2014	3,271	1,145	1,169	2,103	2,126	24
2014-2015	3,666	1,263	1,543	2,123	2,403	280
2015-2016	3,666	1,808	2,196	1,729	2,117	388
2016-2017	3,568	1,378	1,508	2,060	2,191	130

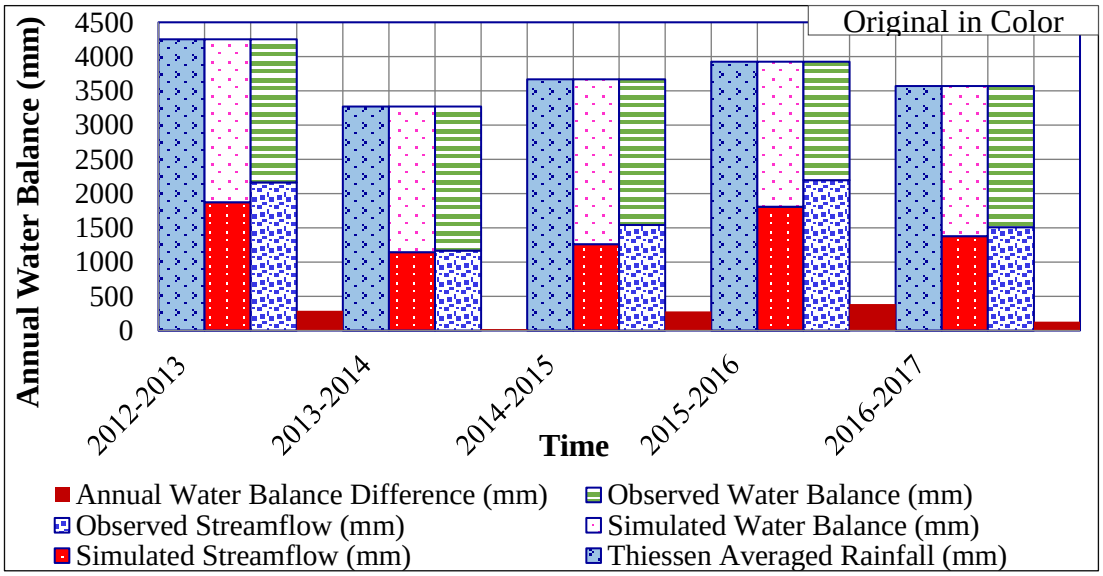

Figure 4-11 Annual water balances for the verification period of the lumped model

4.4.2 Flow duration curve

A flow duration curve for the entire calibration and verification period was generated and contained both observed and simulated streamflows. It is presented in normal and semi-log scale in Figures 4-12 and 4-13. It has been classified into three categories of flows based on studies described in the literature review section high (≤10%), medium (10 % < X ≤ 70%) and low (>70%).

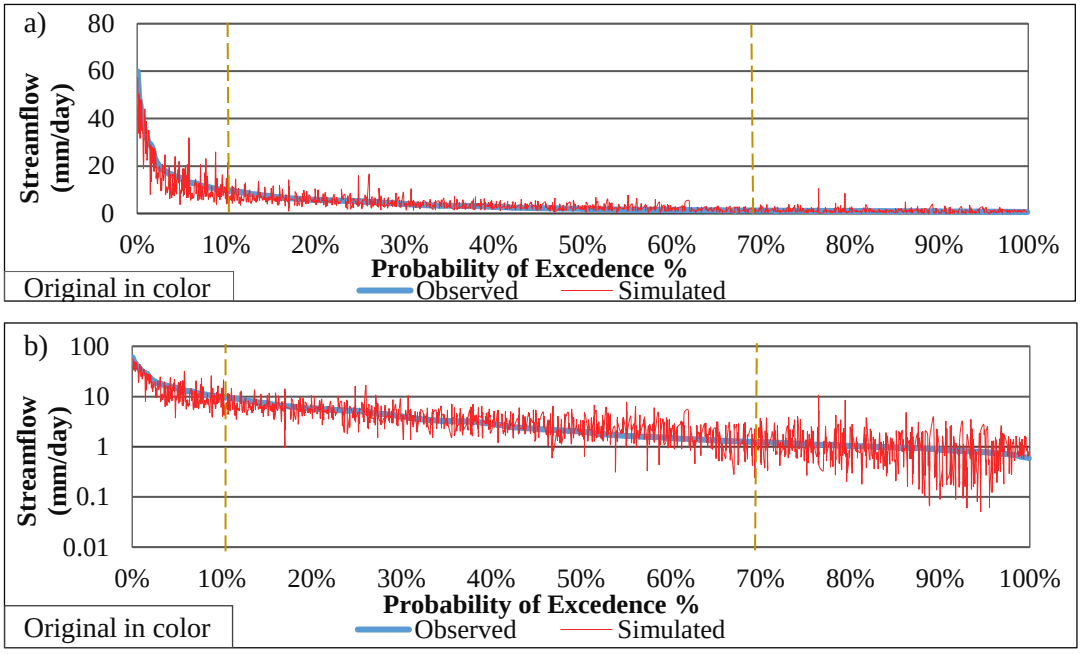

Figure 4-12 Flow duration curve for the calibration period of the lumped model (a, b)

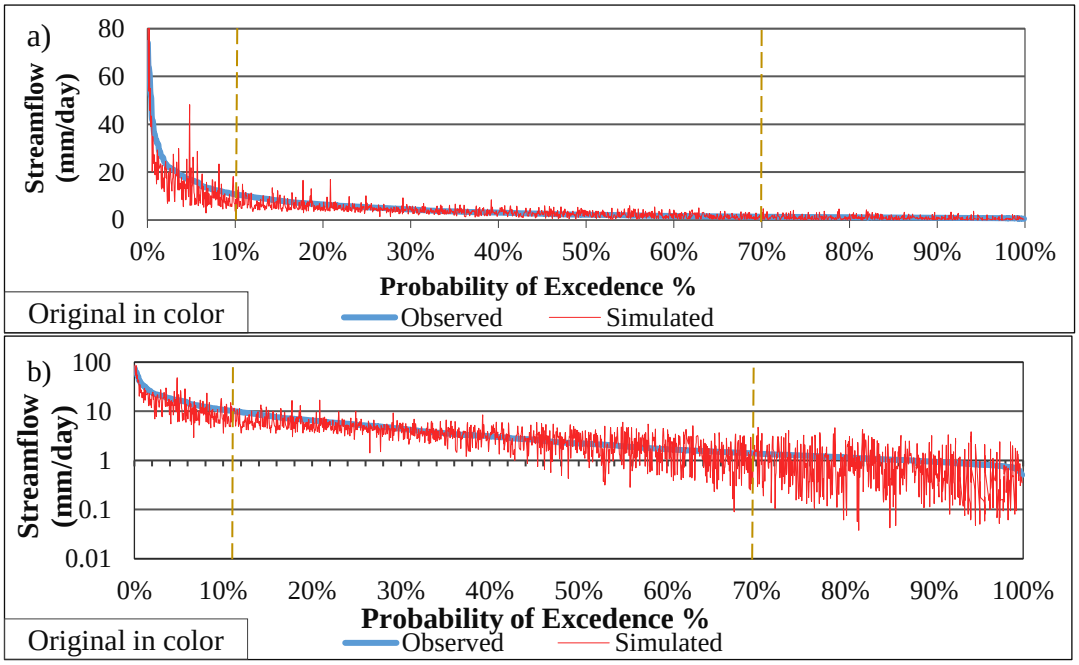

Figure 4-13 Flow duration curve for the verification period of lumped model (a, b)

4.4.3 Outflow hydrograph (calibration period)

The outflow hydrograph results for the entire calibration period are shown in Figure 4-14 and Figure 4-15 in semi-log and normal scales respectively.

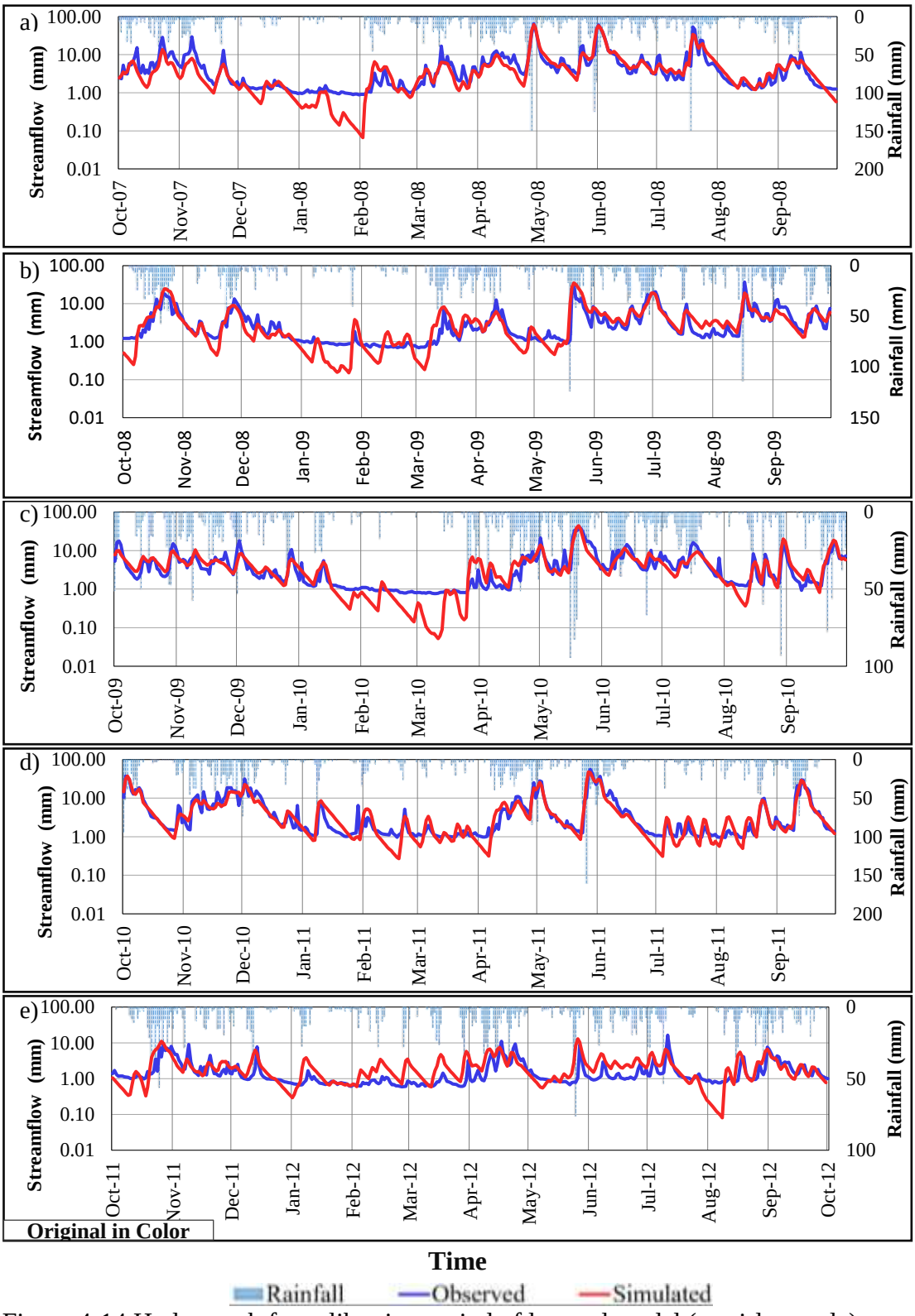

Figure 4-14 Hydrograph for calibration period of lumped model (semi-log scale)

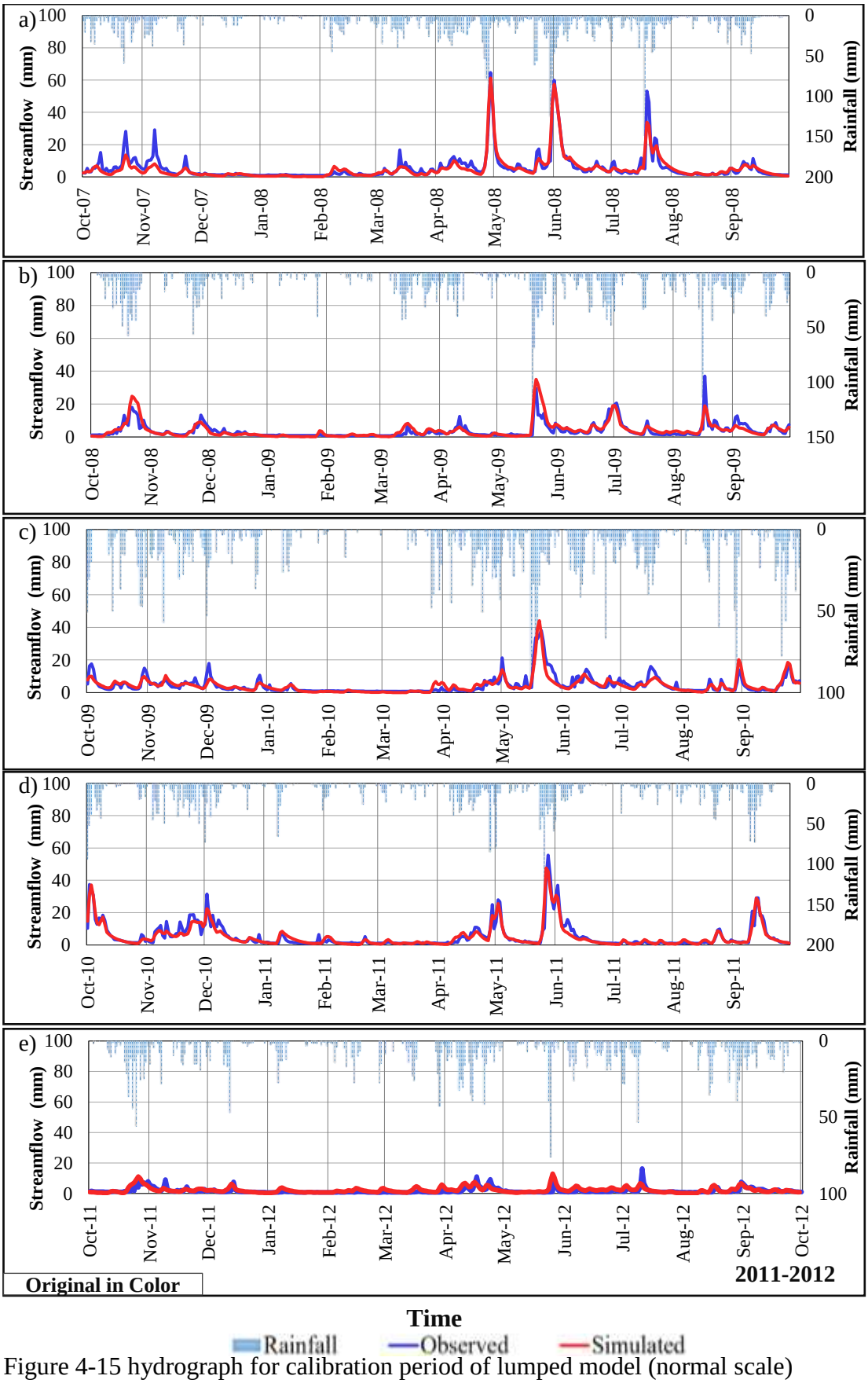

Figure 4-15 hydrograph for calibration period of lumped model (normal scale)

4.4.4 Outflow hydrograph (verification period)

Similarly, the outflow hydrograph results for the entire verification period are shown in Figure 4-16 and Figure 4-17 in semi-log and normal scales respectively.

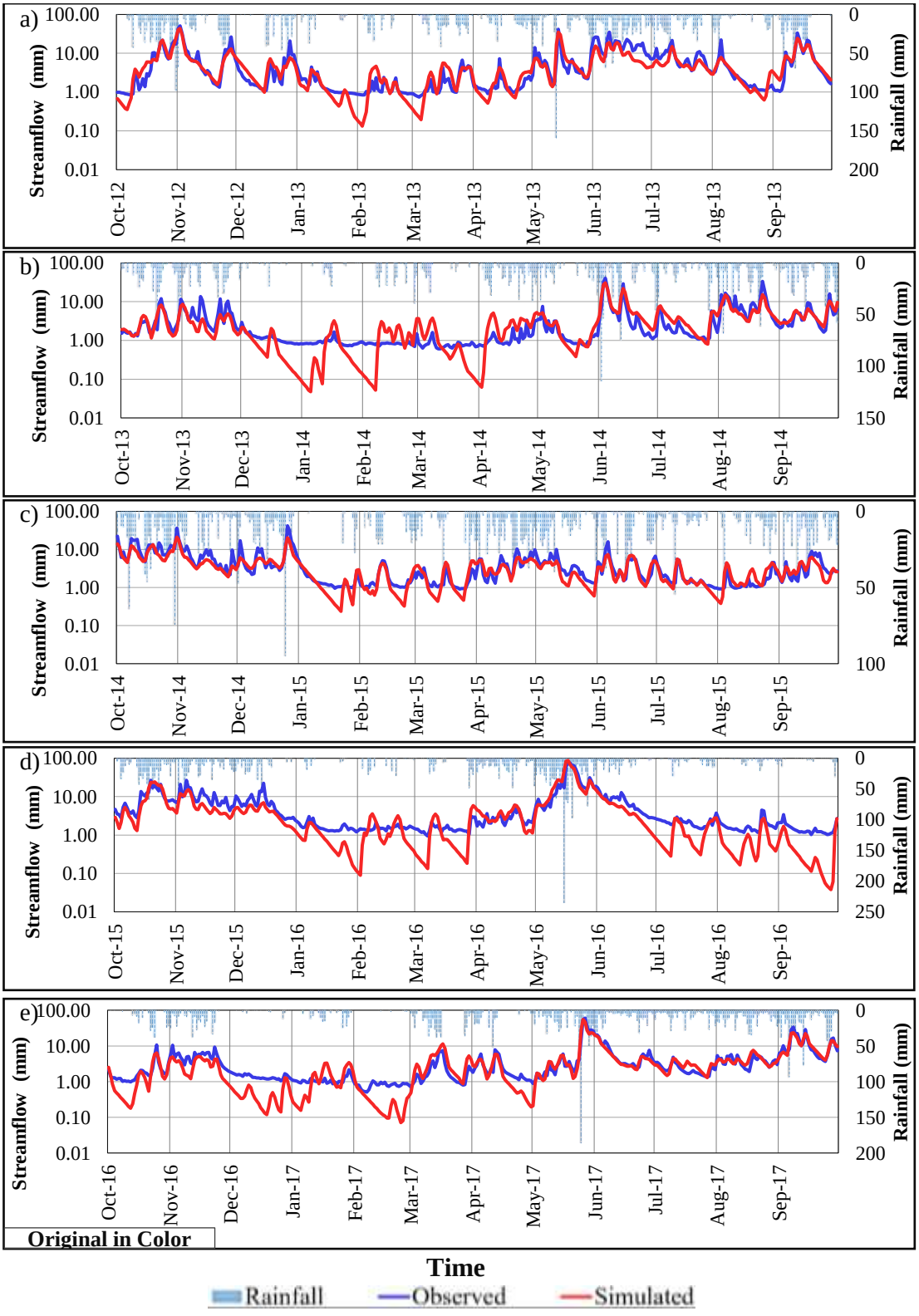

Figure 4-16 Hydrograph for verification period of lumped model (semi-log scale)

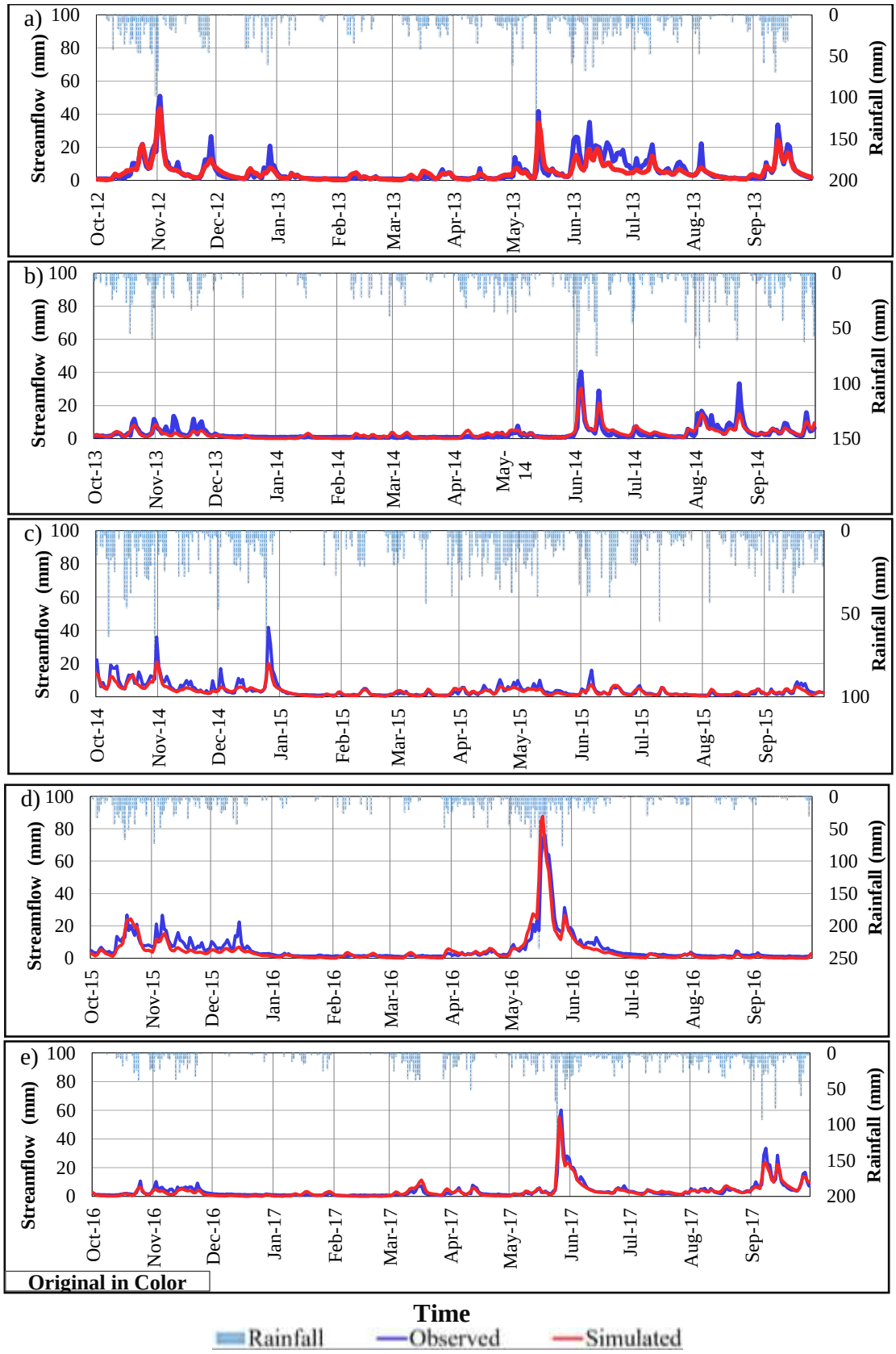

Figure 4-17 Hydrograph for verification period of lumped model (normal scale)

4.4.5 Lumped model performance

The lumped model performance was evaluated with MRAE, Nash, PVE, and R^2 for both the calibration and verification periods in respect to high, medium, and low flows, as presented in Table 4-11.

Table 4-11 Model performance for the lumped model

	Period	Flow classification	MRAE	NASH	PVE	R^2
Summary Flow	Calibration	Overall	0.45	0.85	1.95	0.85
		High	0. 30	0.66	13.25%	0.75
		Medium	0.39	0.41	-5.79%	0.53
		Low	0.64	-33.09	-13.20%	0.04
	Verification	Overall	0.44	0.83	12.95%	0.84
		High	0.32	0.59	19.81%	0.75
		Medium	0.36	0.51	7.60%	0.56
		Low	0.63	-17.53	8.40%	0.06
	Calibration and verification	Average	0.45	0.84	7.45%	0.85

Similarly, the relationship between the observed and simulated streamflows is shown in a scatter plot in Figure 4-18 for the entire period of study. Scatter plots only for calibration and verification periods are shown in Figure 1-C and Figure 2-C in Appendix C, respectively.

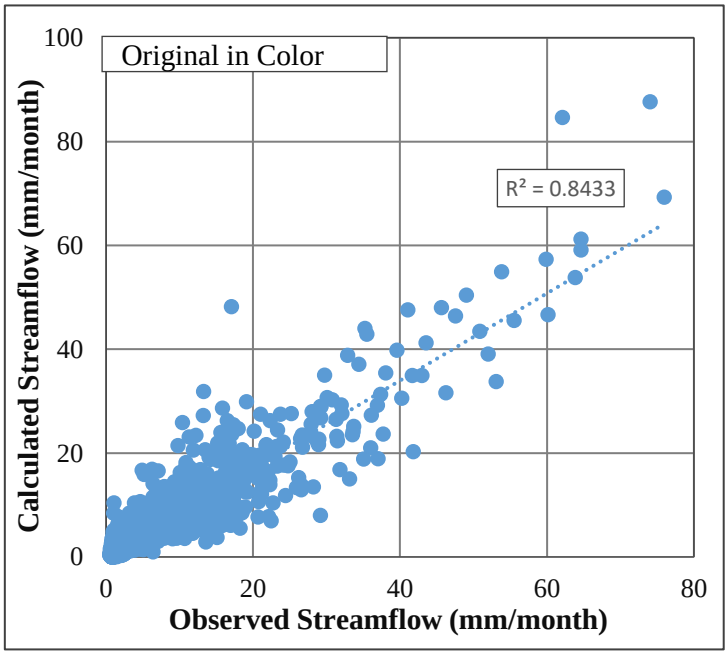

Figure 4-18 Relationship between observed and simulated streamflow in a scatter plot for the lumped model

4.5 Results for three-subdivisions

According to the main scope of this research to compare the efficiency of lumped and distributed models, a three-subdivision model based on the maximum drainage area was generated by the ArcGIS tool. Similar to the lumped model, the results with three-subdivisions are shown in the form of water balance, a flow duration curve, outflow hydrographs, and objective functions for the entire calibration and verification periods.

4.5.1 Annual water balance

Annual water balance is an important method of accuracy evaluation for calculated and simulated water balances. The annual water balance values for the calibration period in the three-subdivision model are shown in Table 4-12 and Figure 4-19, respectively.

Table 4-12 Annual water balance values for the calibration period of the three-subdivision model

Water year	Thiessen averaged rainfall (mm)	Simulated streamflow (mm)	Observed streamflow (mm)	Observed water balance (mm)	Simulated water balance (mm)	Annual water balance difference (mm)
2007-2008	4,294	1,763	2,099	2,195	2,531	336
2008-2009	3,593	1,453	1,367	2,226	2,141	-85
2009-2010	3,872	1,641	1,676	2,196	2,231	35
2010-2011	3,967	1,867	1,986	1,981	2,100	119
2011-2012	2,532	949	639	1,893	1,583	-310

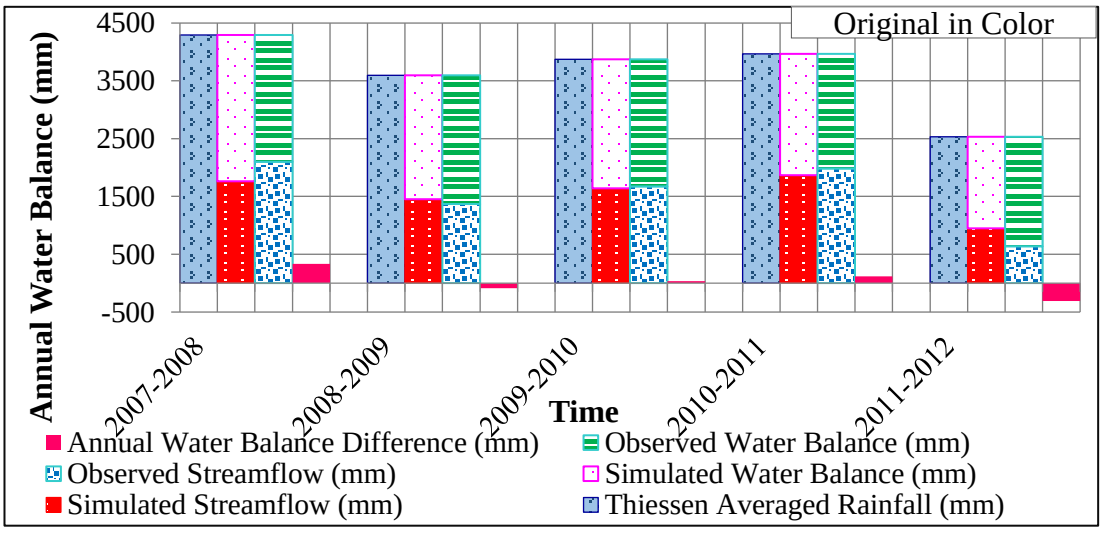

Figure 4-19 Annual water balance for the calibration period for the three-subdivision model

Based on Table 4-12 and Figure 4-19, the maximum errors in water balance occurred for the years 2007/2008 and 2011/2012, at 7.8% and 12.2% respectively. In the same fashion, the overall average error for the entire calibration period was 5.3 %, which according to literature review is in the acceptable range.

Similarly, for the verification period, annual water balance difference for comparisons of observed and calculated streamflow were performed to check the accuracy of the amount of water entering and exiting from the basin. The water balance results are shown in Table 4-13 and Figure 4-20. The comparison illustrated that the maximum error occurred in the year 2012/2013, and was 5.4%. Overall, for the entire period, the average error was equal to 4.98%, which was higher than the calibration period. This value, according to the literature review, is within the acceptable range.

Table 4-13 Annual water balance values for the verification period of the three-subdivision model

Water year	Thiessen averaged rainfall (mm)	Simulated streamflow (mm)	Observed streamflow (mm)	Observed water balance (mm)	Simulated water balance (mm)	Annual water balance difference (mm)
2012-2013	4,253	4,253	2,161	2,093	2,316	223
2013-2014	3,271	1,352	1,169	2,103	1,920	-183
2014-2015	3,666	1,491	1,543	2,123	2,175	52
2015-2016	3,666	1,953	2,196	1,729	1,973	243
2016-2017	3,568	1,722	1,508	2,060	1,846	-214

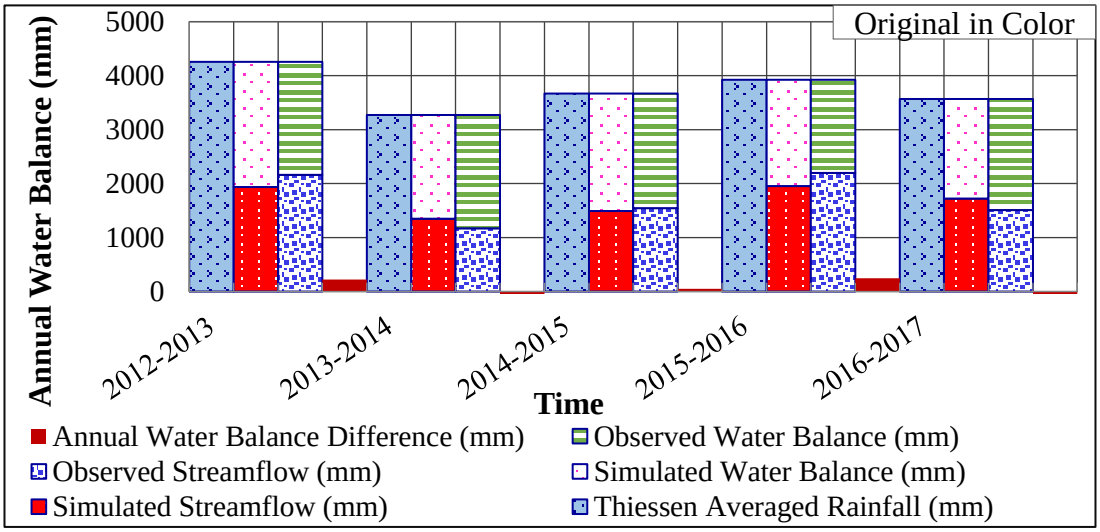

Figure 4-20 Annual water balance for verification period for the three-subdivision model

4.5.2 Flow duration curve

Flow duration curves for the entire calibration and verification periods were generated and contained both observed and simulated streamflow data. These are presented in normal and semi-log scales in Figures 4-21 and 4-22. Flows were classified into three categories of high (≤10%), medium (10 % < X ≤ 70 %) and low (>70%) based on studies described in details in the literature review section.

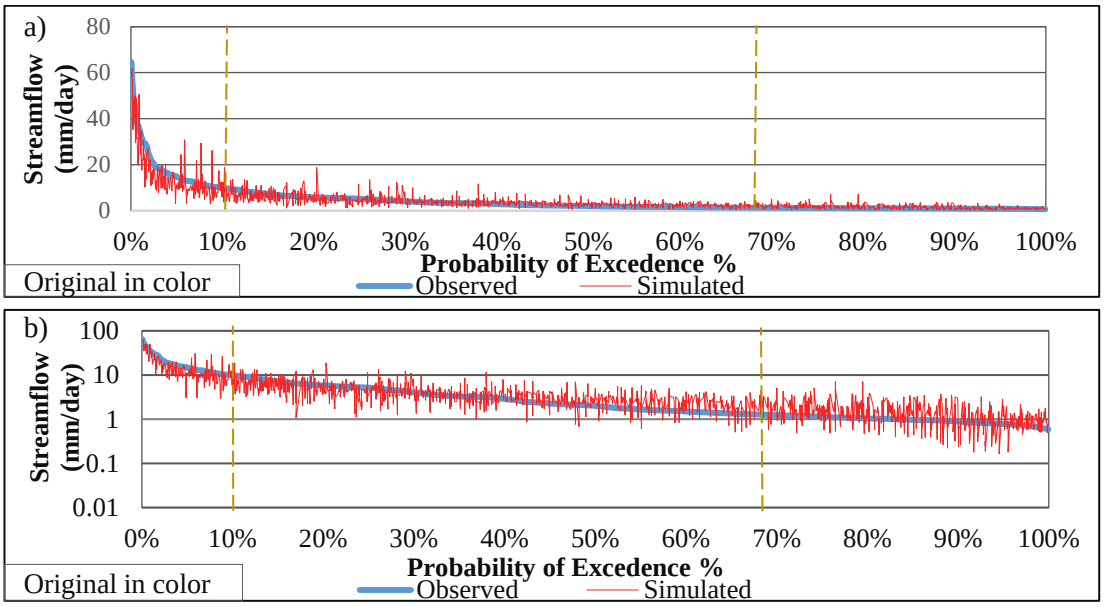

Figure 4-21 Flow duration curve for the calibration period for three-subdivision model (a, b)

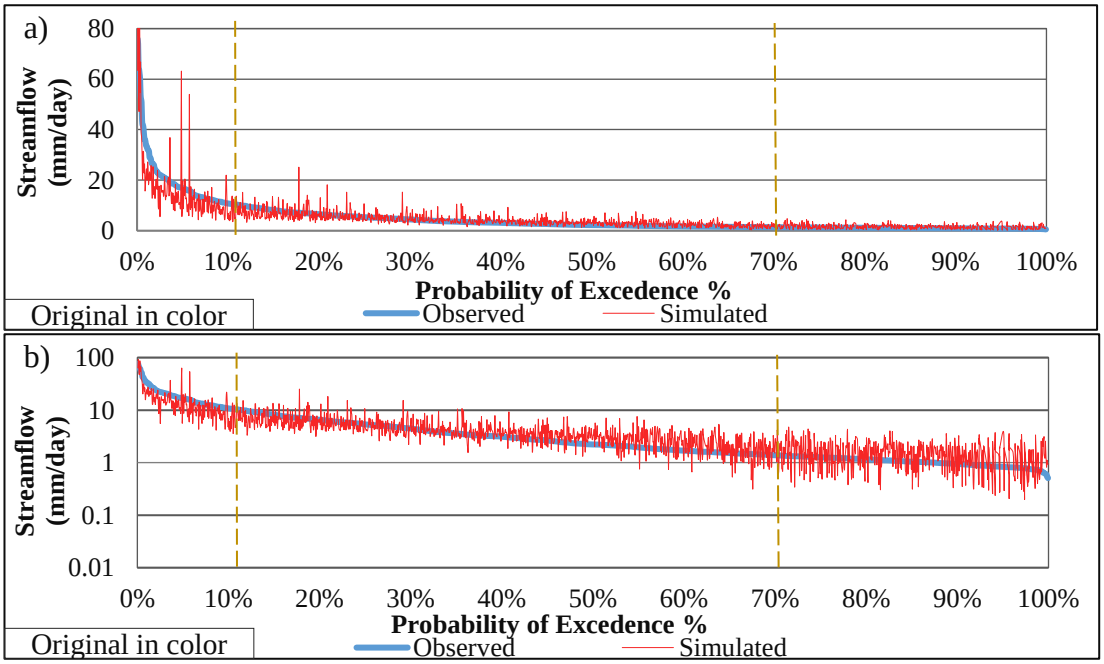

Figure 4-22 Flow duration curve for verification period for the three-sub division model (a, b)

4.5.3 Outflow hydrograph (calibration period)

The outflow hydrograph results for the entire calibration period are demonstrated in Figure 4-23 and Figure 4-24 in normal and semi-log scales respectively.

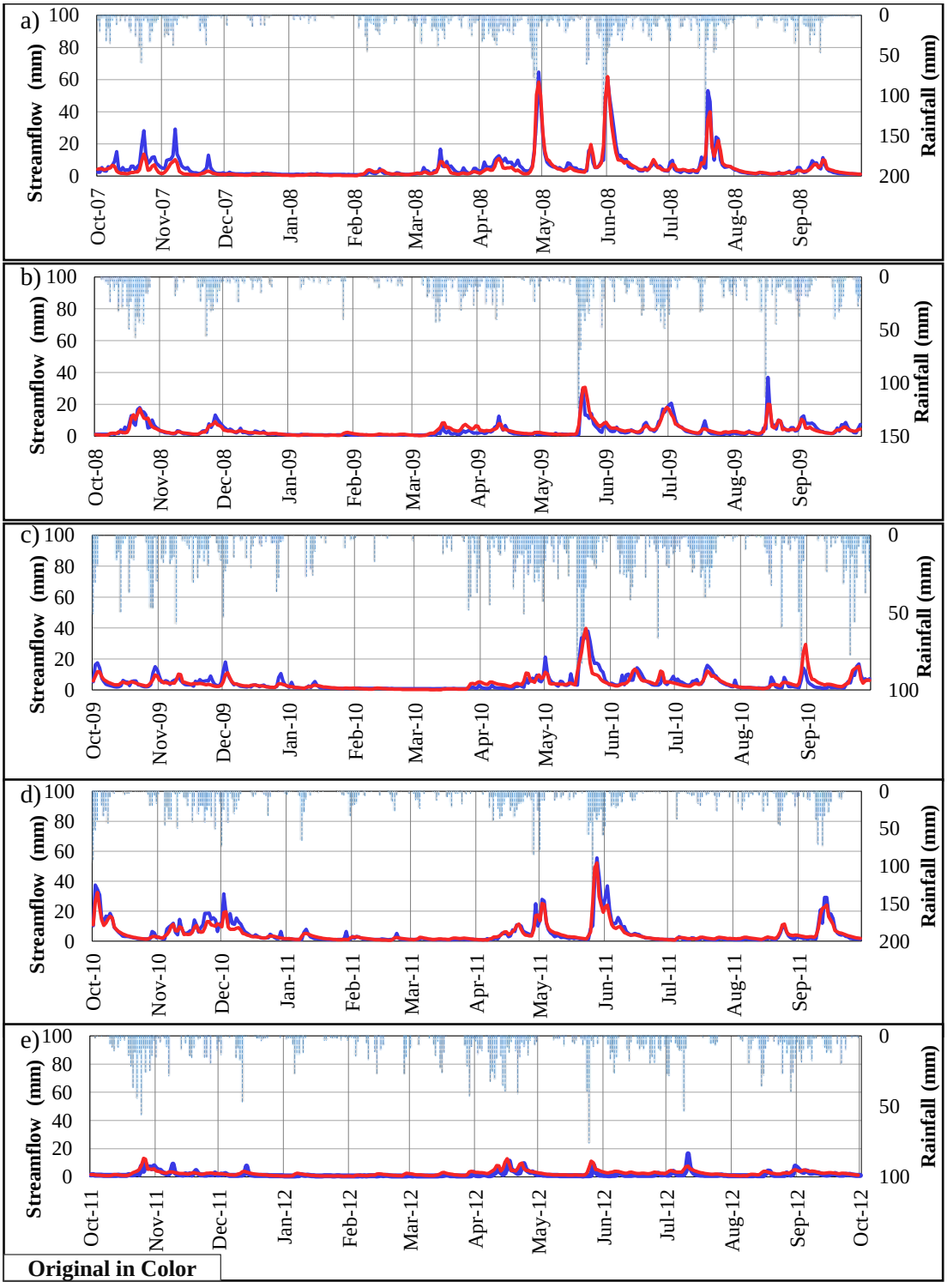

Figure 4-23 Hydrograph for calibration period for the three-subdivision model (normal scale)

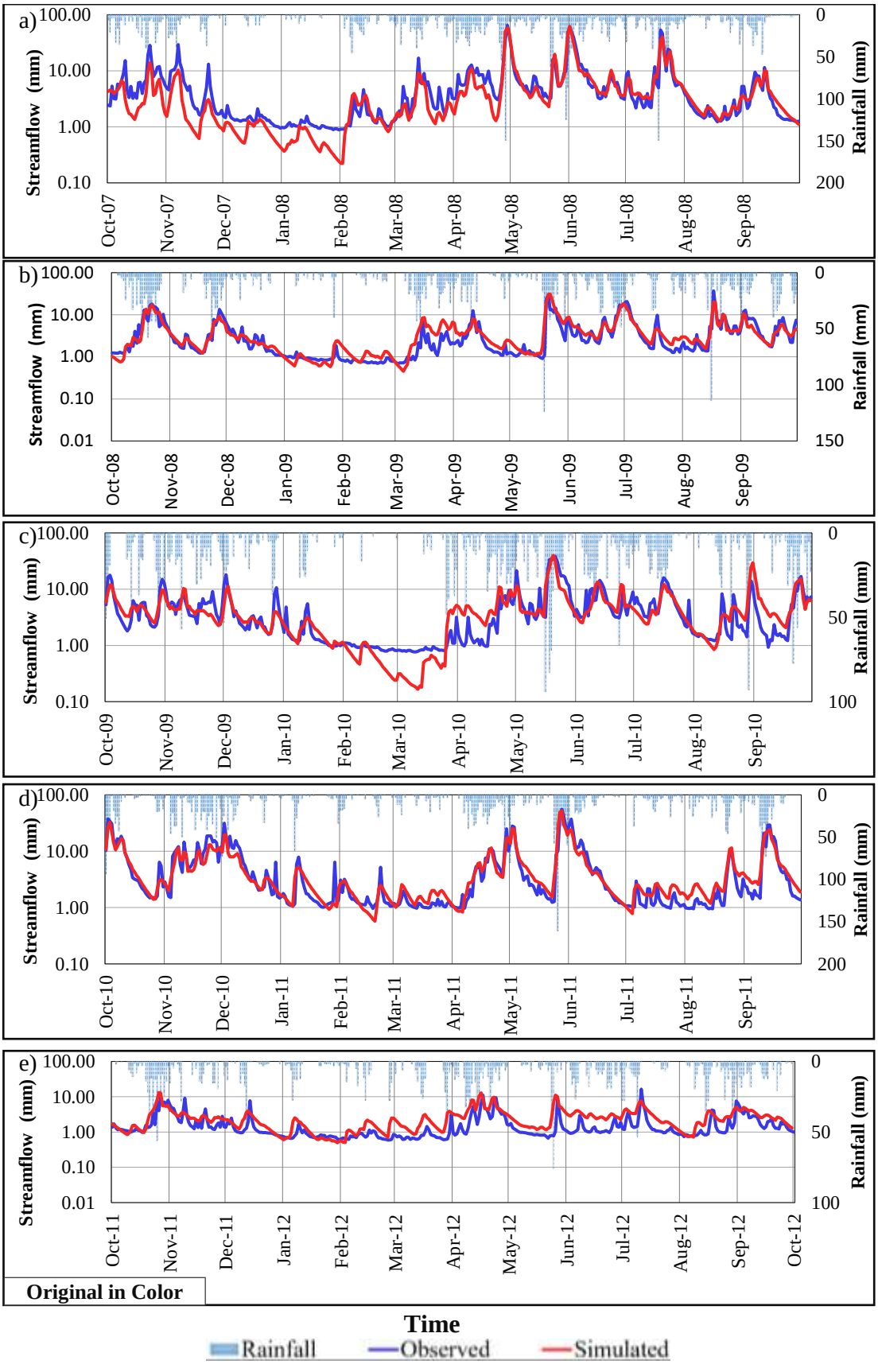

Figure 4-24 Hydrograph for calibration period for the three-subdivision model (semi-log scale)

4.5.4 Outflow hydrograph (verification period)

The outflow hydrograph results for the entire verification period are shown in Figure 4-25 and Figure 4-26 in normal and semi-log scale respectively.

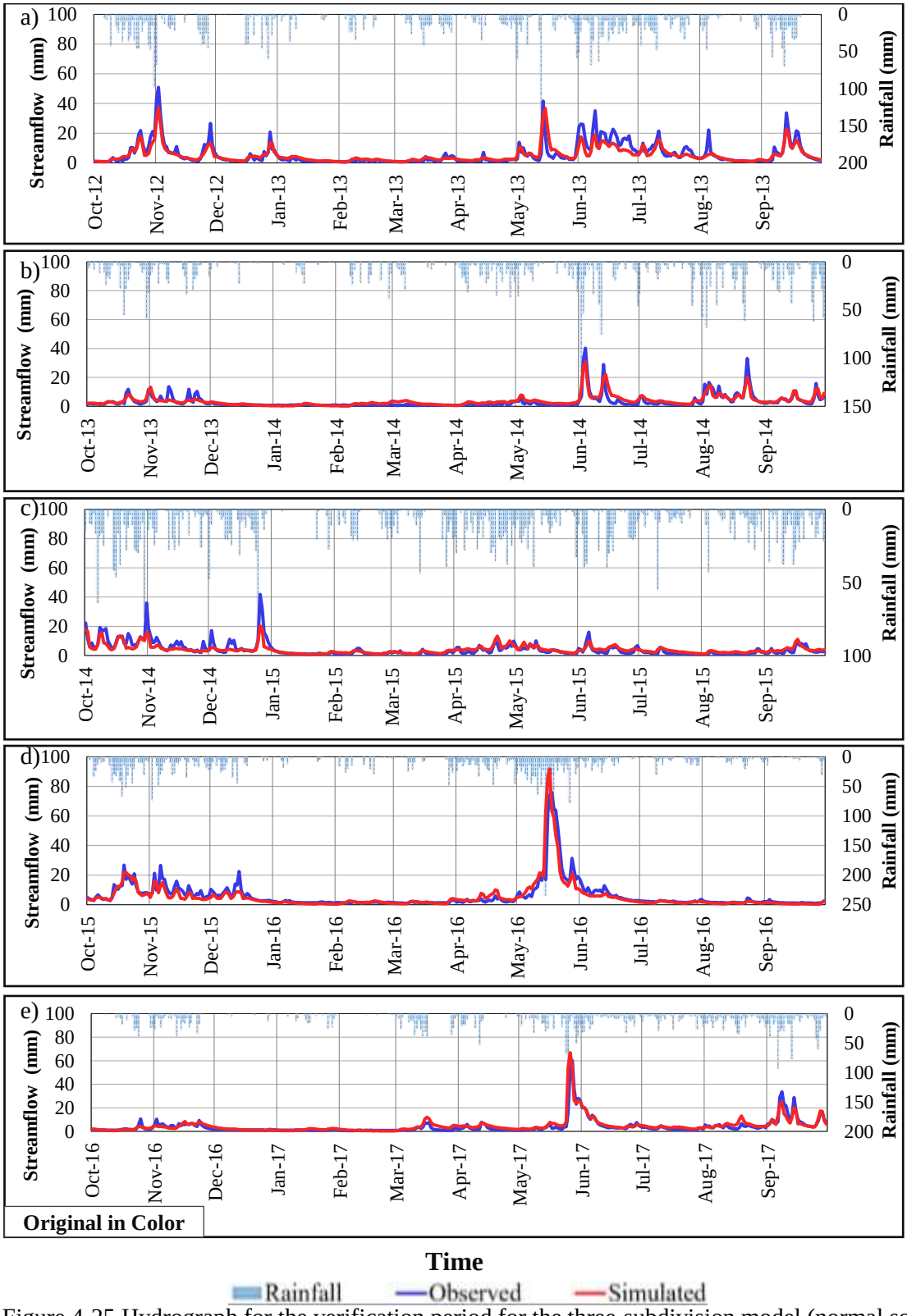

Figure 4-25 Hydrograph for the verification period for the three-subdivision model (normal scale)

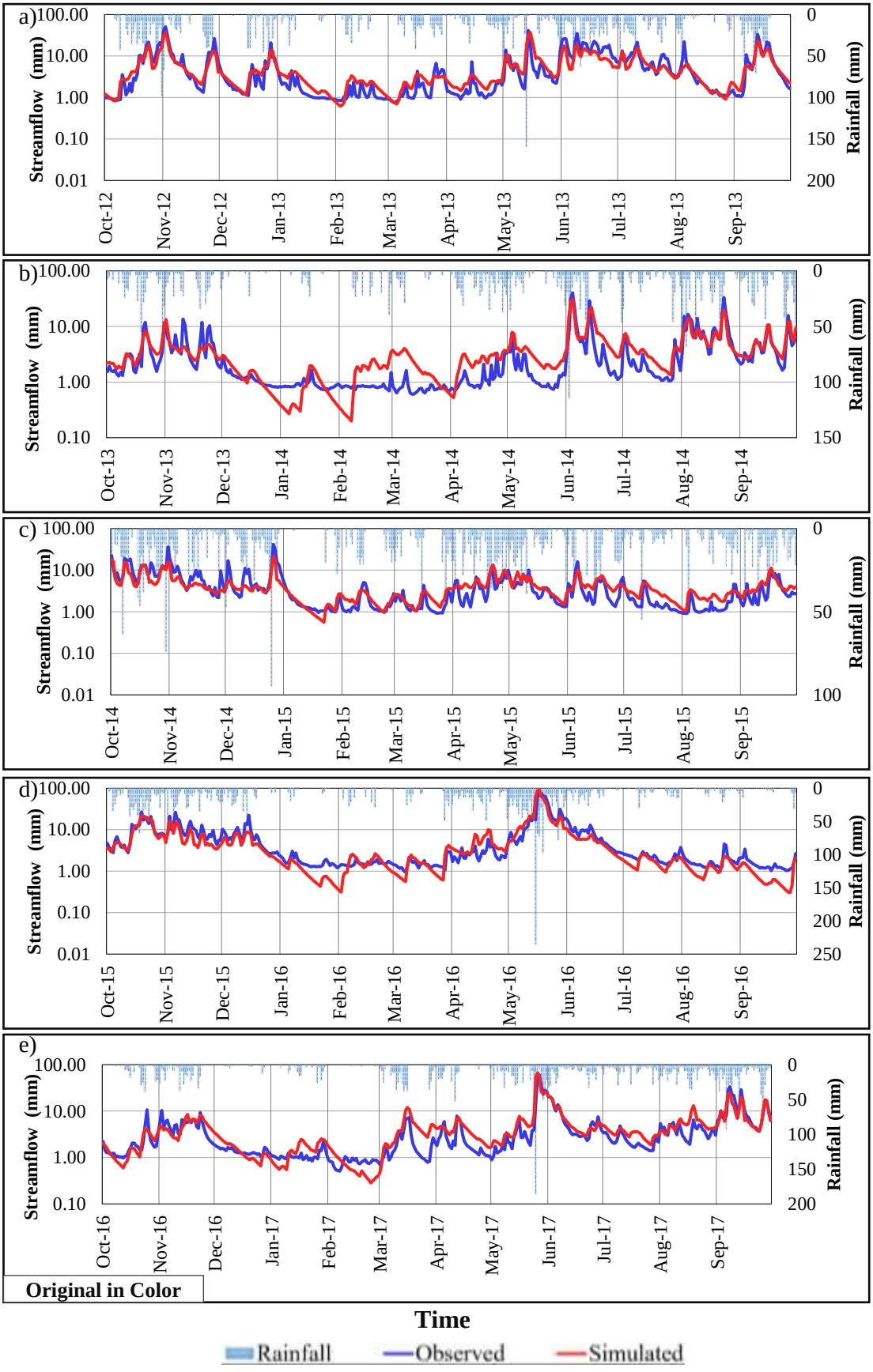

Figure 4-26 Hydrograph for the verification period for the three-subdivision model (semi-log scale)

4.5.5 Model performance

Three subdivision model performance was evaluated with MRAE, NSE, PVE and R^2 for both calibration and verification periods with respect to high, medium, and low flows, as presented in Table 4-14.

Table 4-14 Model performance for the three-subdivision model

	Period	Flow classification	MRAE	NASH	PVE	R^2
Summary Flow	Calibration	Overall	0.47	0.84	1.2%	0.83
		High	0.28	0.65	16.4%	0.76
		Medium	0.41	0.32	-5.9%	0.45
		Low	0.65	-32.25	-43.9%	0.12
	Verification	Overall	0.49	0.79	1.41%	0.79
		High	0.32	0.48	19.63%	0.67
		Medium	0.40	0.34	-8.25%	0.46
		Low	0.72	-23.17	-45.02%	0.05
	Calibration and verification	Average	0.48	0.81	0.01	0.81

Similarly, the relation of observed and simulated streamflow is shown in a scatter plot in Figure 4-27 for the entire period of study. Scatter plots only for calibration and verification period are shown in Figure 3-C and Figure 4-C in Appendix C, respectively.

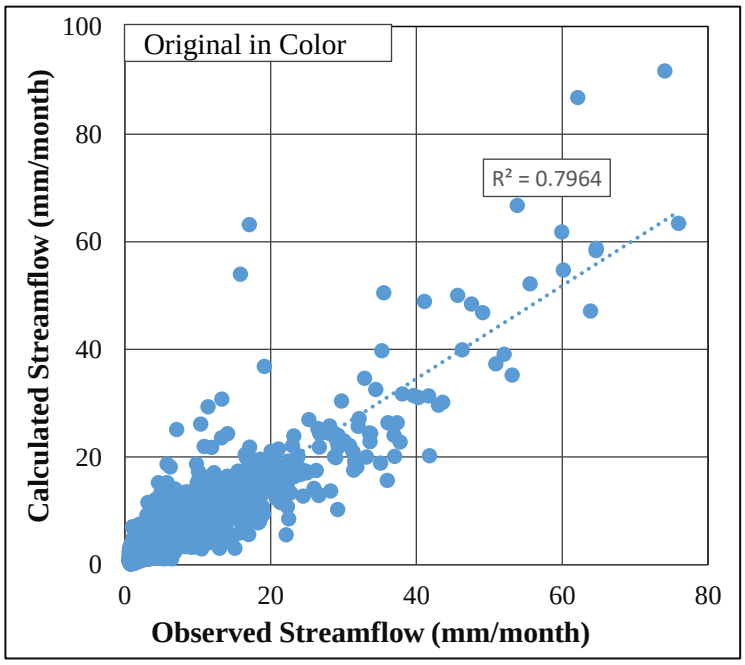

Figure 4-27 Relationship between observed and simulated streamflow in a scatter plot for the three-subdivision model

4.6 Results for five-subdivision model

The five-subdivision model was generated as a part of the distributed models for comparison purposes with lumped and other subdivision models. It was derived through the maximum drainage area method using ArcGIS along with of the HEC-GeoHMS and Arc Hydro extension tools. The results are shown here in the form of water balances, flow duration curves, outflow hydrographs, and objective functions for the entire calibration and verification periods.

4.6.1 Annual water balance

Annual water balance results for the calibration period, considering a five-subdivision model are shown in Table 4-15 and Figure 4-28, respectively. This result is important in specifying the miscalculated flow with respect to the observed flow from an annual water balance perspective.

Table 4-15 Annual water balance values for the calibration period for the five-subdivision model

Water year	Thiessen averaged rainfall (mm)	Simulated streamflow (mm)	Observed streamflow (mm)	Observed water balance (mm)	Simulated water balance (mm)	Annual water balance difference (mm)
2007-2008	4,294	1,882	2,099	2,195	2,412	218
2008-2009	3,593	1,271	1,367	2,226	2,322	96
2009-2010	3,872	1,578	1,676	2,196	2,294	98
2010-2011	3,967	1,860	1,986	1,981	2,107	126
2011-2012	2,532	763	639	1,893	1,769	-124

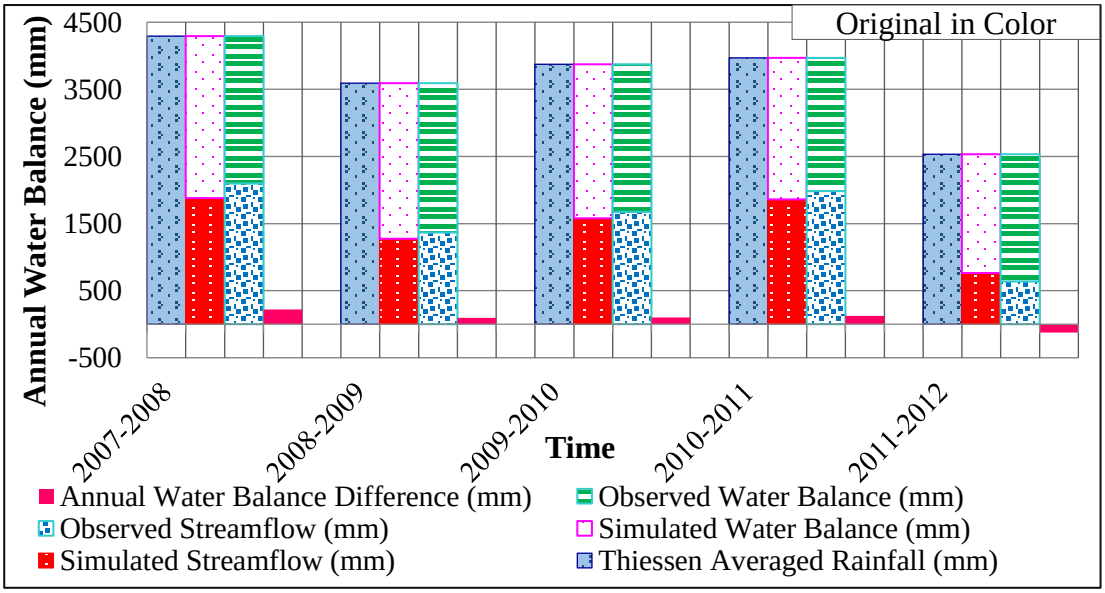

Figure 4-29 Annual water balance for the calibration period of the five-subdivision model

Figure 4-28 illustrates the water balance differences in red. The maximum error in water balance marked in year 2007/2008 corresponds to 5%. Similarly, for the entire calibration period is equal to 3.7%, which, according to the literature indicates an acceptable error.

For the verification period, an annual water balance difference comparison of the observed and calculated streamflow data was performed to check the agreement between the amount of water entering and exiting from the basin. The water balance results are shown in Table 4-16 and Figure 4-29. This comparison illustrated that the maximum error occurred in the year 2012/2013 and corresponds to 10.63%. Overall, for the entire period of study, the error average was equal to 5.8%, which is higher than that in the calibration period. Despite that, it is in an acceptable range as described in the literature.

Table 4-16 Annual water balance values for the verification period of the five-subdivision model

Water year	Thiessen averaged rainfall (mm)	Simulated streamflow (mm)	Observed streamflow (mm)	Observed water balance (mm)	Simulated water balance (mm)	Annual water balance difference (mm)
2012-2013	4,253	1,708	2,161	2,093	2,545	452
2013-2014	3,271	1,141	1,169	2,103	2,131	28
2014-2015	3,666	1,206	1,543	2,123	2,459	336
2015-2016	3,666	1,940	2,196	1,729	1,985	256
2016-2017	3,568	1,459	1,508	2,060	2,109	49

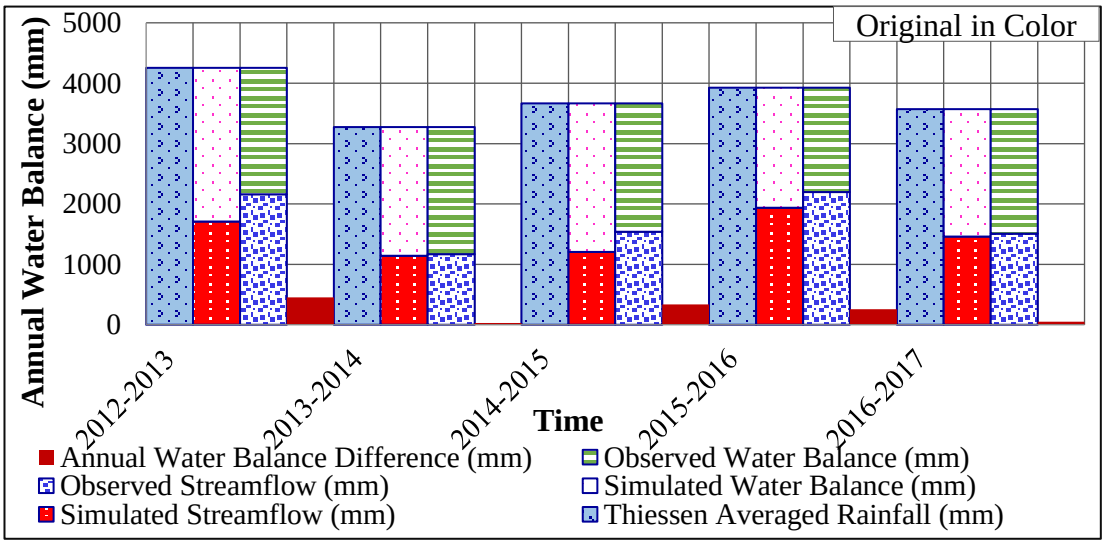

Figure 4-30 Annual water balances for the verification period of the five-subdivision model

4.6.2 Flow duration curve

Flow duration curves for the entire calibration and verification periods were generated and contain both observed and simulated streamflow data. They are presented here in normal and semi-log scales in Figure 4-30 and 4-31 respectively. Further, they are classified into three categories of high (≤10%), medium (10% < X ≤ 70%), and low (>70%) flows based on the studies described in the literature review section.

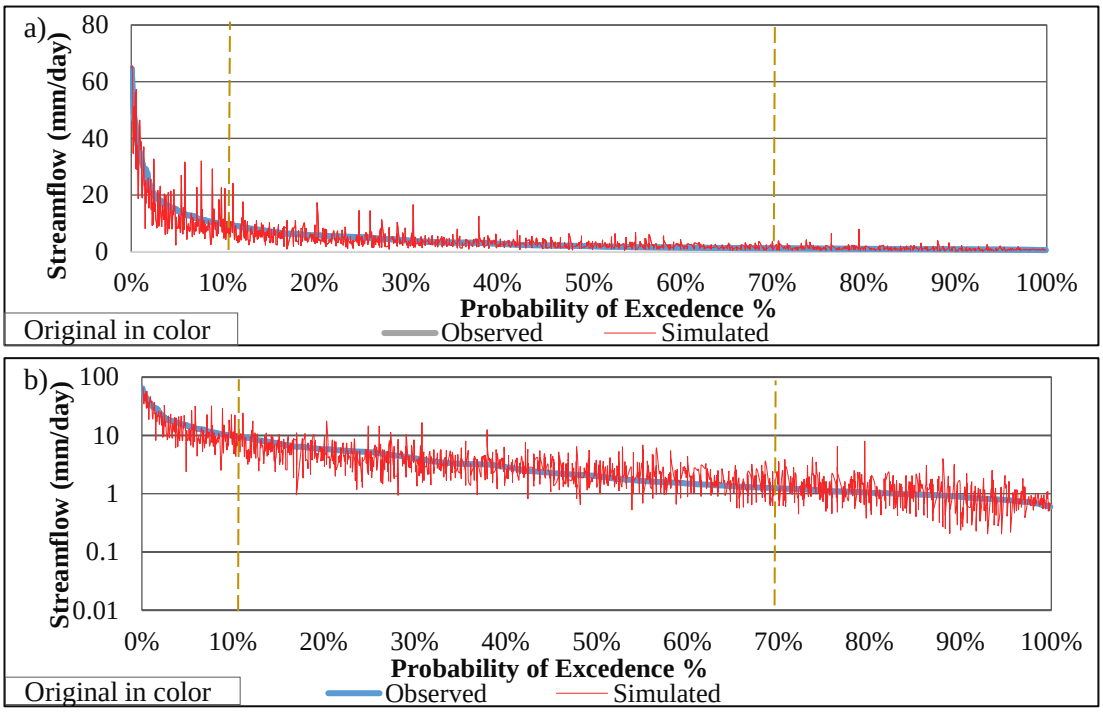

Figure 4-31 Flow duration curve for the calibration period of the five-subdivision model (a, b)

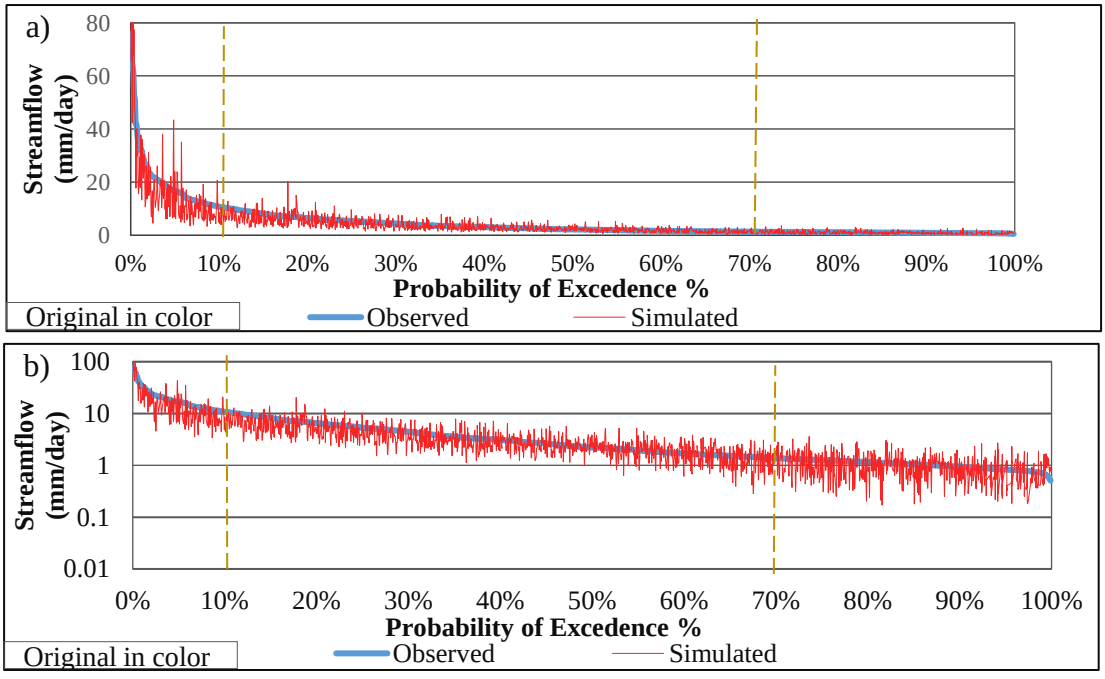

Figure 4-32 Flow duration curve for the verification period of five-subdivision model (a, b)

4.6.3 Outflow hydrograph (calibration period)

The outflow hydrograph results for the entire calibration period of the five-subdivision model are shown in Figure 4-32 and Figure 4-33 in normal and semi-log scales respectively.

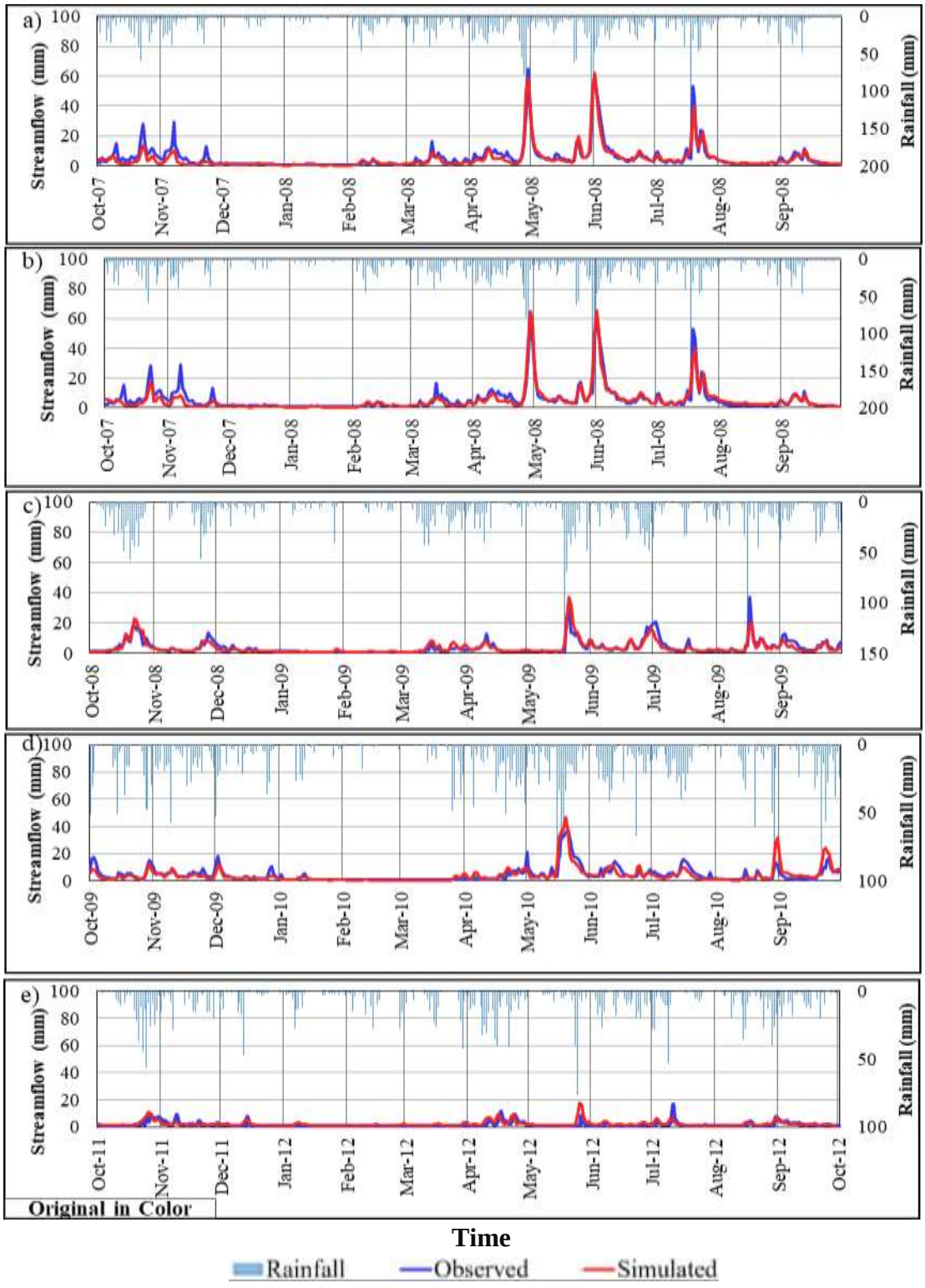

Figure 4-33 Hydrograph for the calibration period of the five sub division model (normal scale)

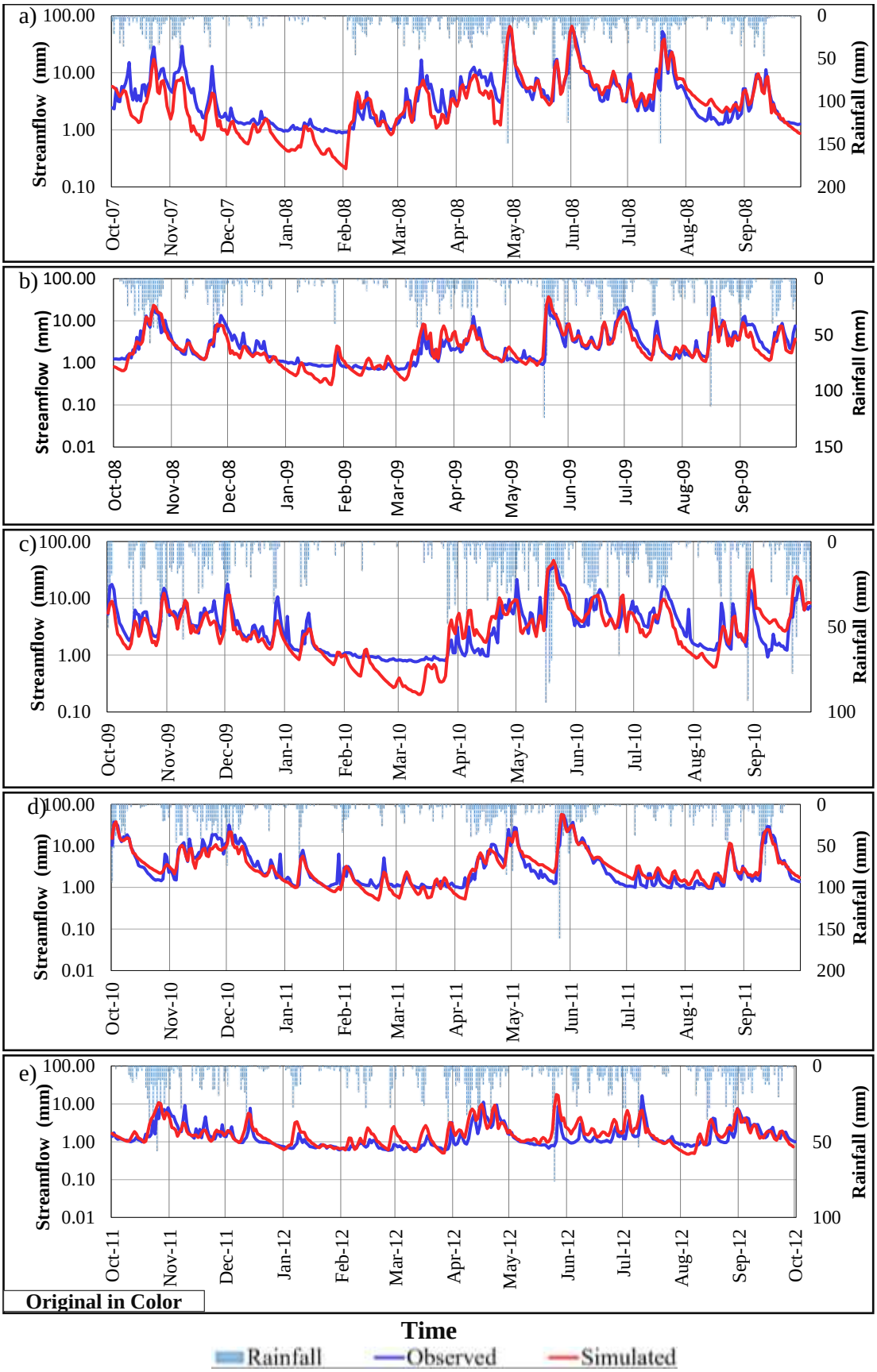

Figure 4-34 Hydrograph for the calibration period of the five-subdivision model (semi-log scale)

4.6.4 Outflow hydrograph (verification period)

The outflow hydrograph results for the entire verification period of the five-subdivision model are shown in Figure 4-34 and Figure 4-35 in normal and semi-log scales, respectively.

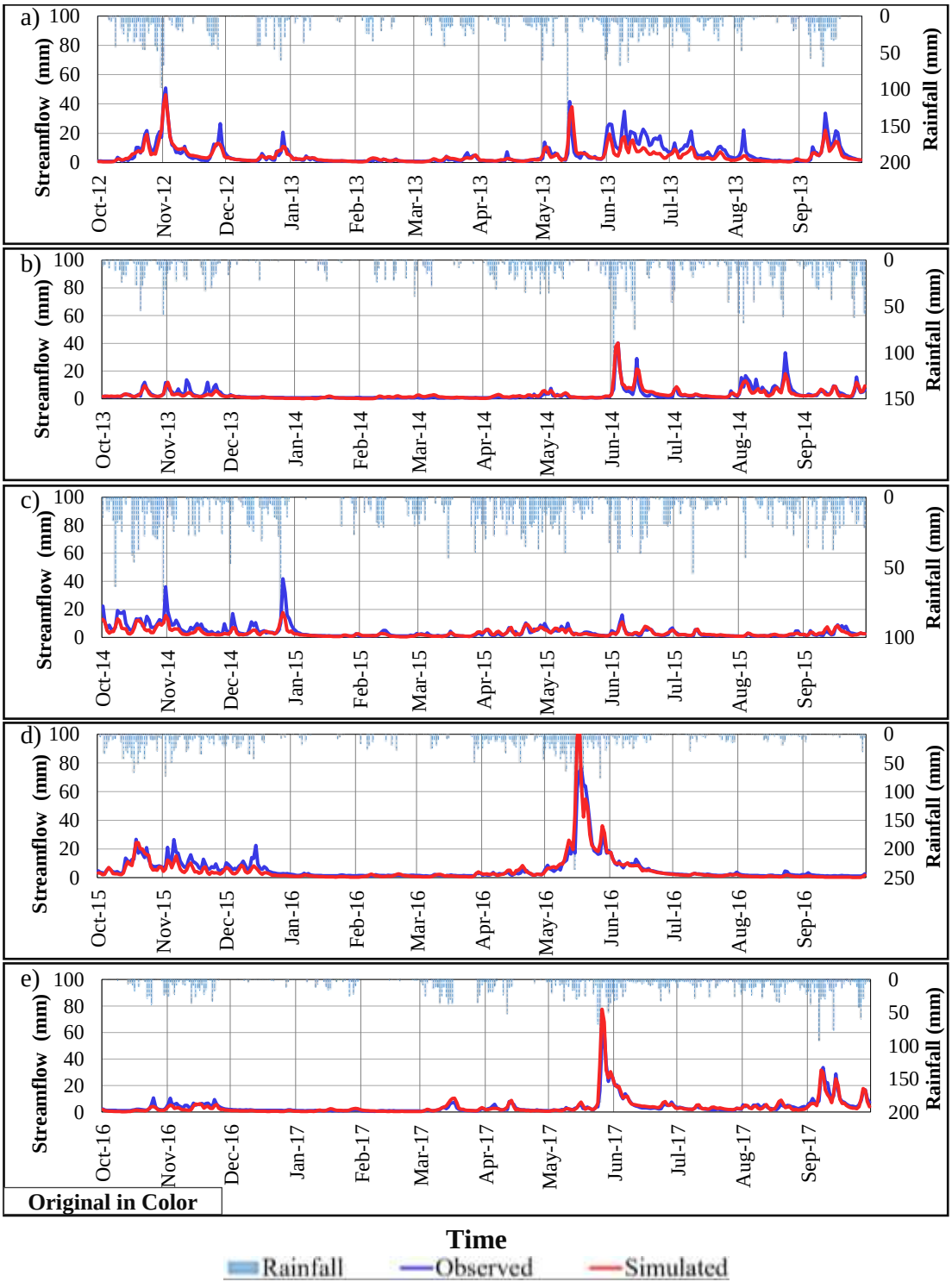

Figure 4-35 Hydrograph for the verification period of the five-subdivision model (normal scale)

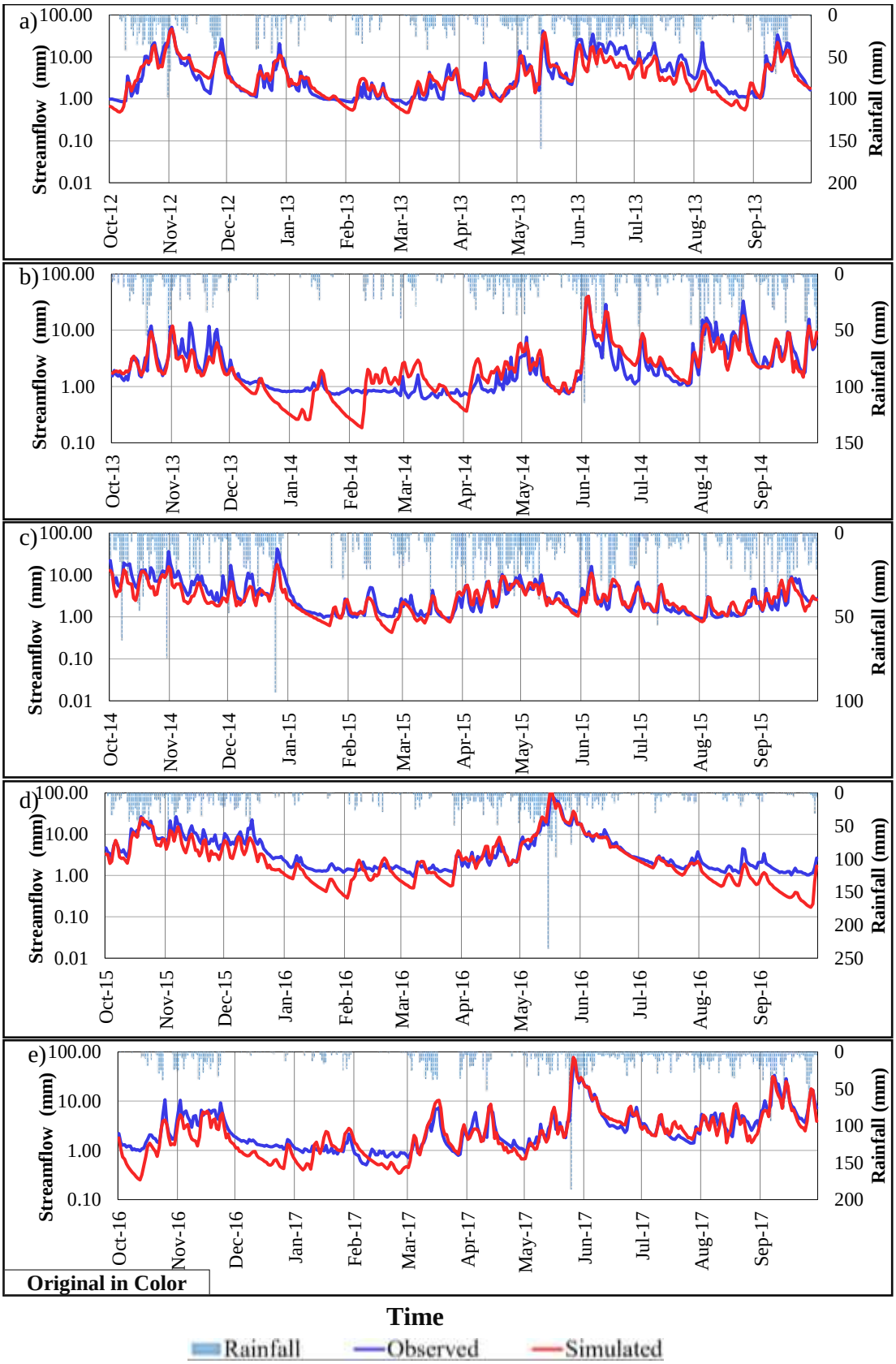

Figure 4-36 Hydrograph for the verification period of the five-subdivision model (semi-log scale)

4.6.5 Model performance

The five-subdivision model performance was evaluated with MRAE, NSE, PVE, and R^2 for the total calibration and verification periods with respect to high, medium, and low flows, as presented in Table 4-17.

Table 4-17 Model performance for the five-subdivision model

	Period	Flow classification	MRAE	NSE	PVE	R^2
Summary Flow	Calibration	Overall	0.38	0.82	5.3%	0.83
		High	0.31	0.60	12.5%	0.73
		Medium	0.37	0.27	1.5%	0.47
		Low	0.44	-16.71	-13.0%	0.12
	Verification	Overall	0.36	0.80	13.07%	0.81
		High	0.30	0.59	14.03%	0.73
		Medium	0.34	0.54	16.24%	0.61
		Low	0.42	-2.84	-13.71%	0.36
	Calibration and verification	Average	0.37	0.81	11.17%	0.82

Similarly, the relationship between the observed and simulated streamflow data is shown in a scatter plot in Figure 4-36 for the entire period of study. Specific plots only for the calibration and verification periods are shown in Figure 5-C and Figure 6-C in Appendix C respectively.

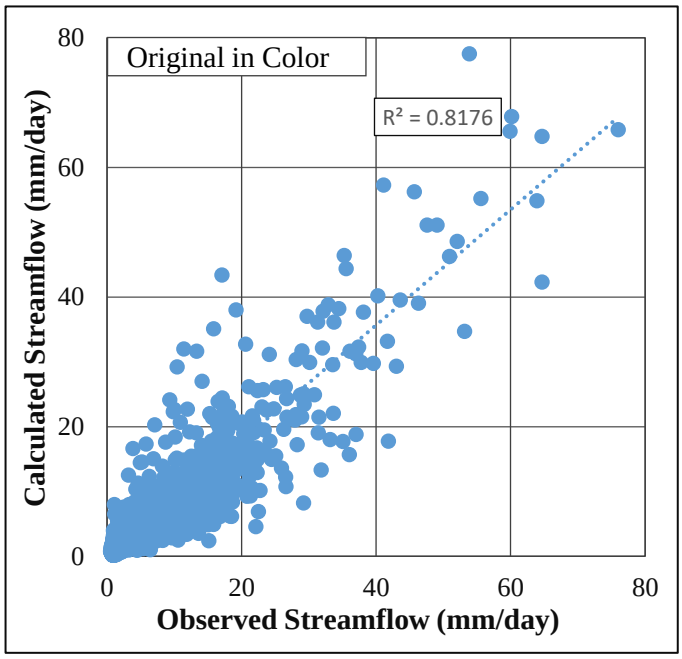

Figure 4-37 Relationship between the observed and simulated streamflow in scatter plot for the five-subdivision model

4.7 Results for the eight-subdivision model

The model with eight subdivisions was one of the distributed models created to be compared with the lumped model and other subdivision models. Eight subdivision models were generated using ArcGIS along with the HEC-GeoHMS and Arc Hydro extension tools through the maximum drainage area method. The results that for the entire calibration and verification periods are shown here with water balances, flow duration curves, outflow hydrographs, and objective functions.

4.7.1 Annual water balance

Annual water balance results for the entire calibration period of the eight-subdivision model are shown in Table 4-18 and Figure 4-37. The importance of this calculation lies in for specifying the accuracy of calculated versus observed flows from the perspective of the annual water balance.

Table 4-18 Annual water balance values for the calibration period of the eight-subdivision model

Water year	Thiessen averaged rainfall (mm)	Simulated streamflow (mm)	Observed streamflow (mm)	Observed water balance (mm)	Simulated water balance (mm)	Annual water balance difference (mm)
2007-2008	4,294	1,975	2,099	2,195	2,319	124
2008-2009	3,593	1,424	1,367	2,226	2,170	-56
2009-2010	3,872	1,723	1,676	2,196	2,149	-47
2010-2011	3,967	1,974	1,986	1,981	1,992	11
2011-2012	2,532	874	639	1,893	1,658	-235

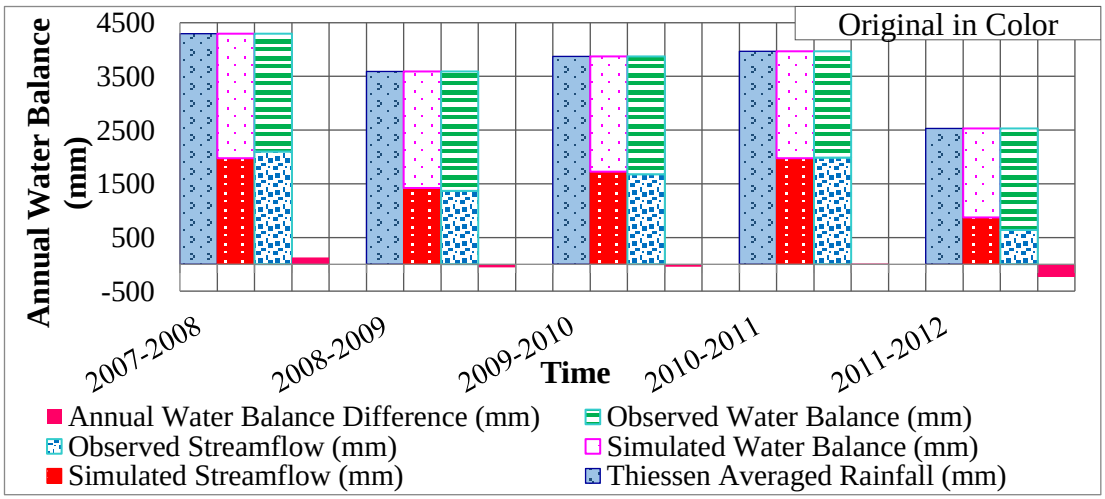

Figure 4-38 Annual water balance for the calibration period of the eight-subdivision model

Based on table 4-18 and Figure 4-37, the maximum error in water balance was recorded in the year 2011/2012 and is 9.3 %. The average difference in the percentage of water balance in the whole calibration period is equal to 3.04 %, which according to the literature, indicates an acceptable error.

Similarly, for the verification period, an annual water balance computation to check the accuracy of the observed and calculated streamflows was performed. This is presented in Table 4-19 and Figure 4-38. The result of this comparison illustrates that the maximum error occurred in the year 2012/2013 and was 6.95%. Overall, for the entire verification period, the average error was equal to 4.65 %, which is higher than that of the calibration period. Despite that, all the errors were within an acceptable range as described in the literature review section.

Table 4-19 Annual water balance values for the verification period of the eight-subdivision model

Water year	Thiessen averaged rainfall (mm)	Simulated streamflow (mm)	Observed streamflow (mm)	Observed water balance (mm)	Simulated water balance (mm)	Annual water balance difference (mm)
2012-2013	4,253	4,253	2,161	2,093	2,388	296
2013-2014	3,271	1,286	1,169	2,103	1,985	-118
2014-2015	3,666	1,463	1,543	2,123	2,203	79
2015-2016	3,666	2,031	2,196	1,729	1,894	165
2016-2017	3,568	1,724	1,508	2,060	1,844	-216

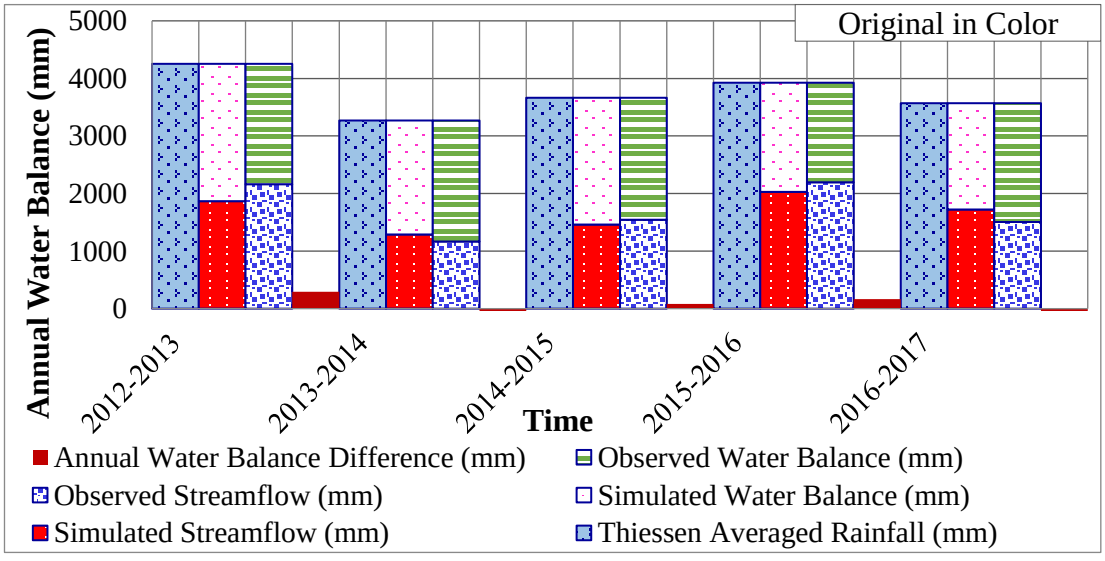

Figure 4-39 Annual water balances for the verification period of the eight-subdivision model

4.7.2 Flow duration curve

Flow duration curves for the calibration and verification periods were generated and contains both observed and simulated streamflows. These are presented in normal and semi-log scales in Figures 4-39 and 4-40 respectively. Flows were classified into three categories of high (≤10%), medium (10% < X ≤ 70%), and low (>70%) based on studies described in the literature review section.

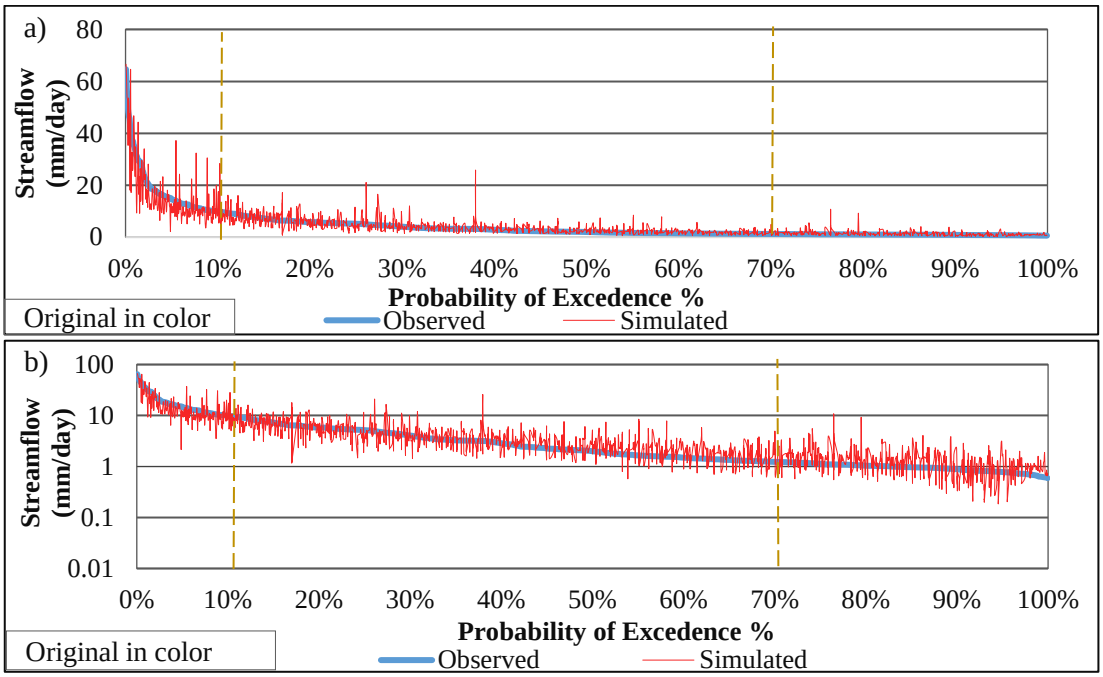

Figure 4-40 Flow duration curve for the calibration period of the eight-subdivision model (a, b)

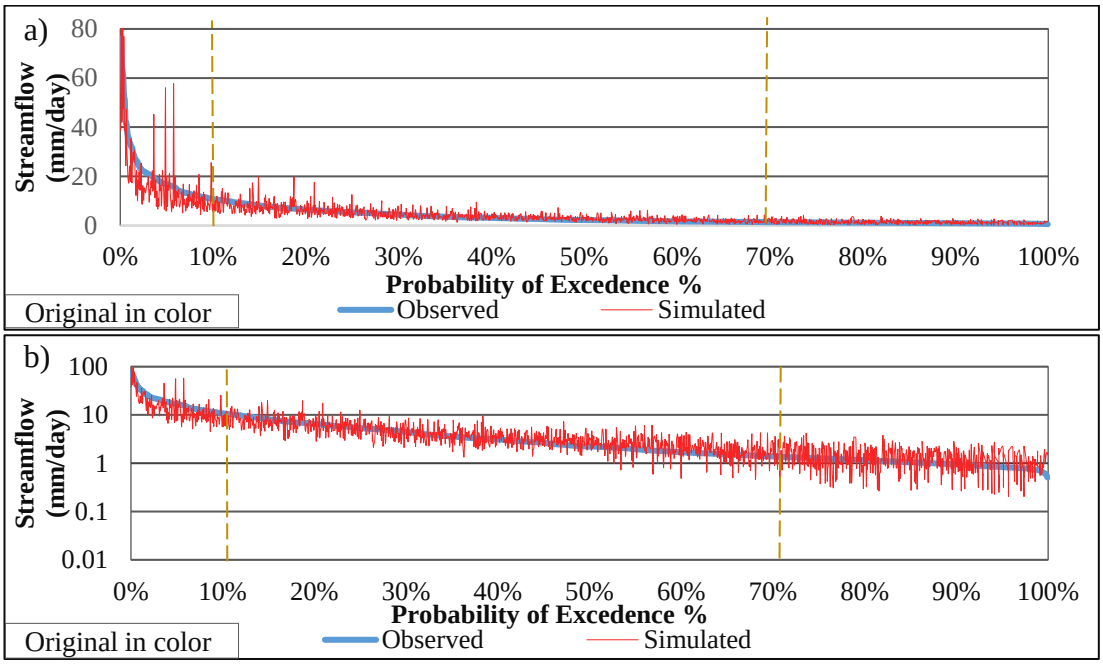

Figure 4-41 Flow duration curve for the verification period of the eight-subdivision model (a, b)

4.7.3 Outflow hydrograph (calibration period)

The outflow hydrograph results for the calibration period of eight subdivision model are shown in Figure 4-41 and Figure 4-42 in normal and semi-log scales respectively.

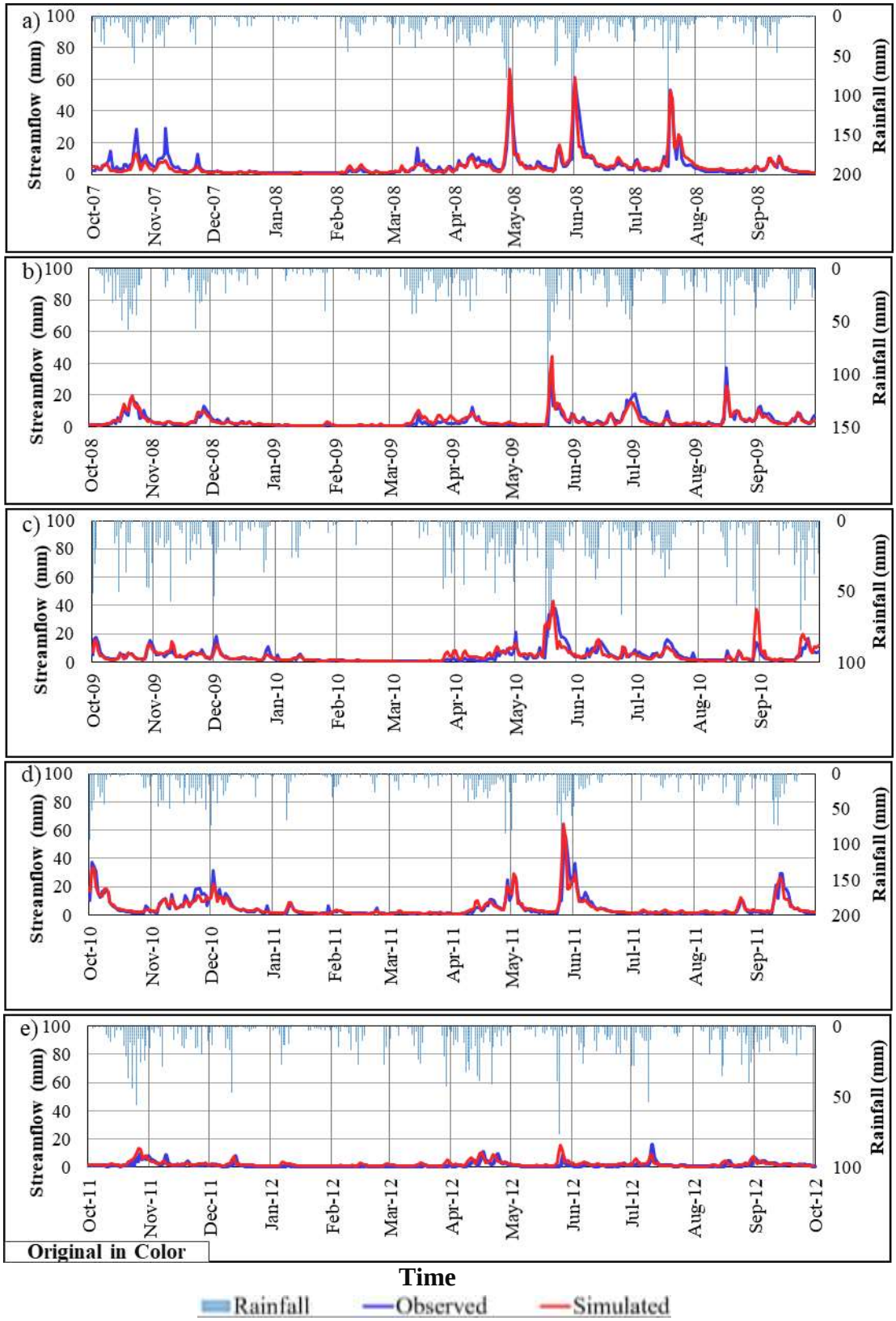

Figure 4-42 Hydrograph for the calibration period of the eight-subdivision model (normal scale)

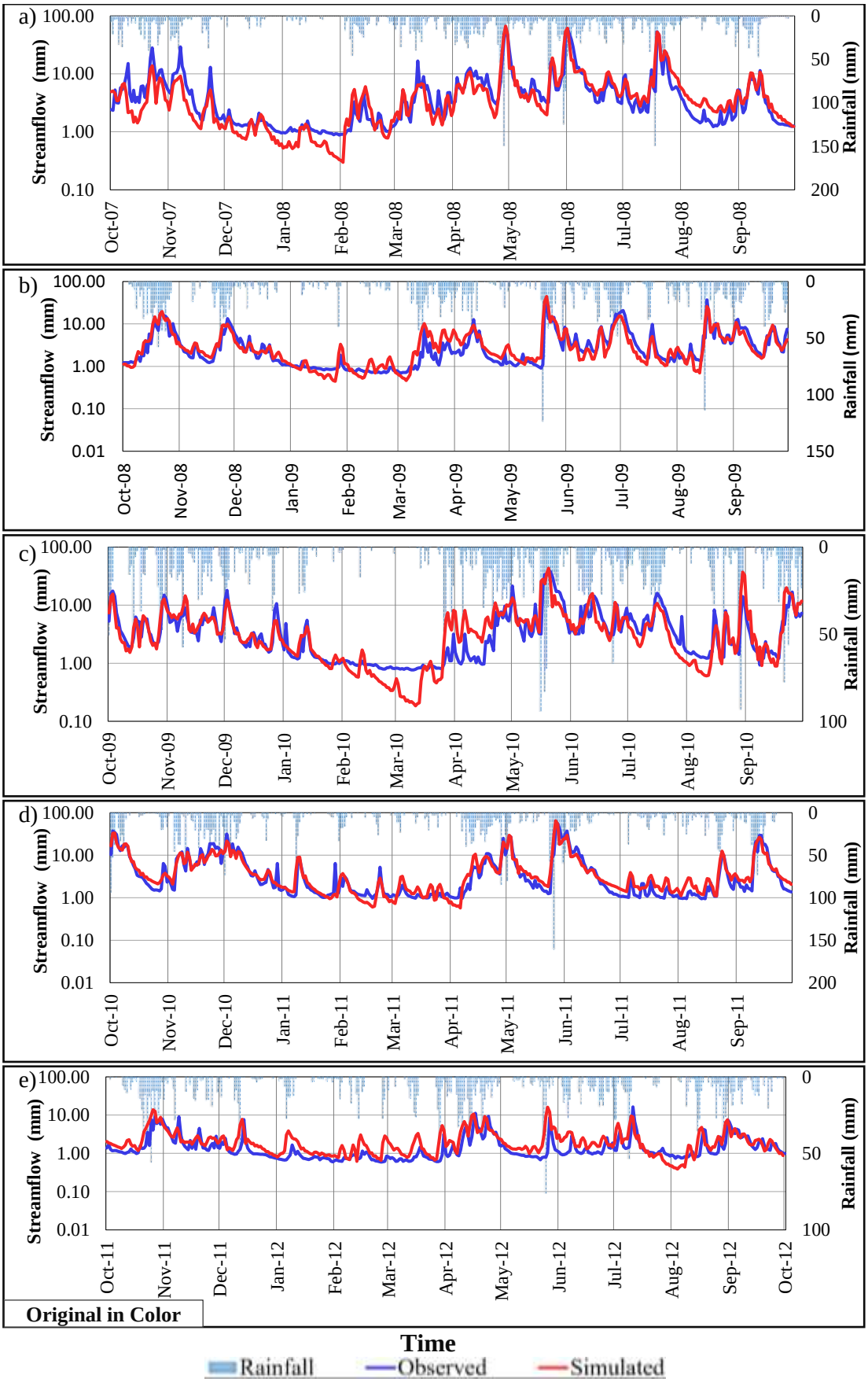

Figure 4-43 Hydrograph for the calibration period of the eight-subdivision model (semi-log scale)

4.7.4 Outflow hydrograph (verification period)

The outflow hydrograph results for the verification period of the eight-subdivision model are shown in Figure 4-43 and Figure 4-44 in normal and semi-log scales respectively.

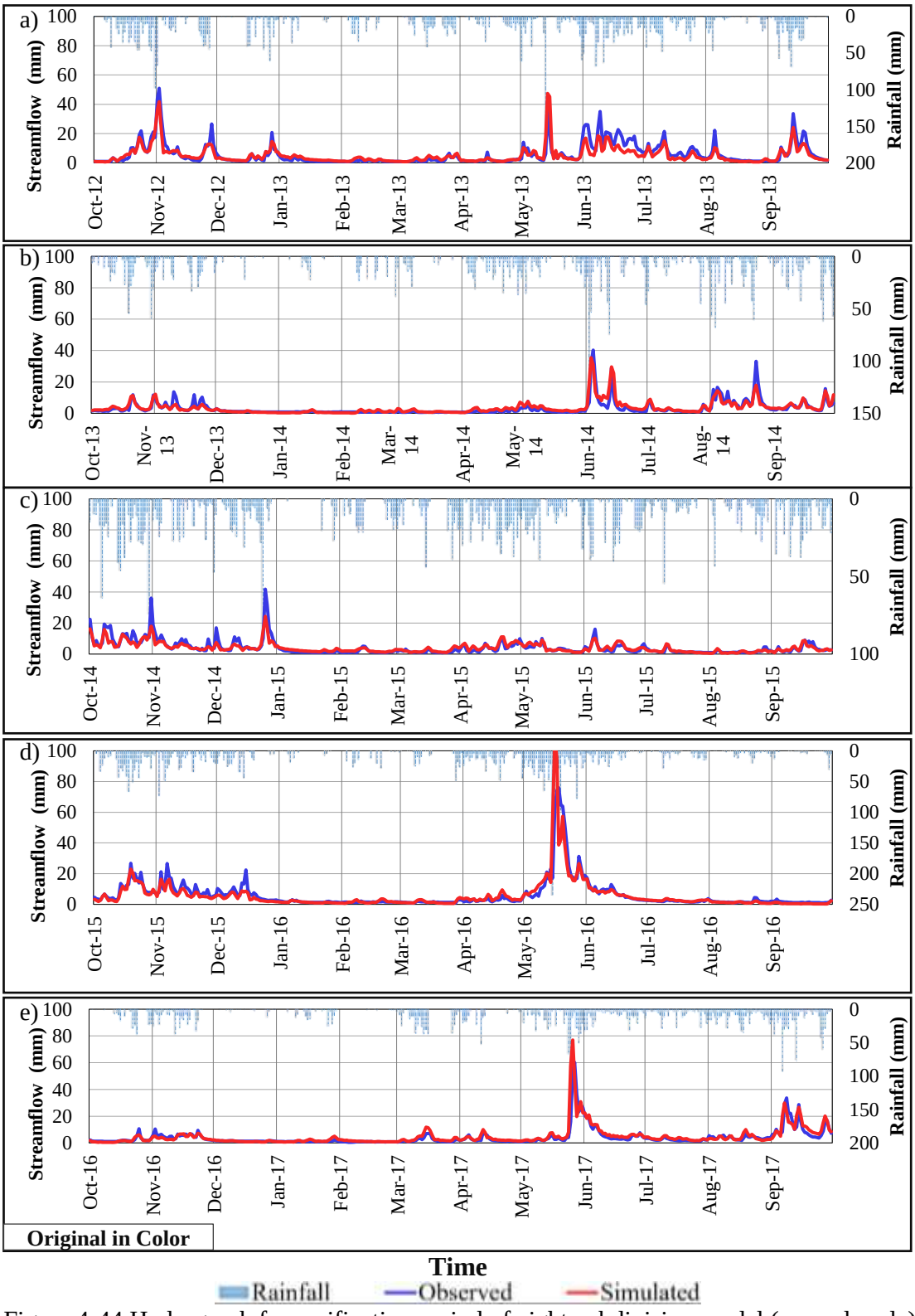

Figure 4-44 Hydrograph for verification period of eight-subdivision model (normal scale)

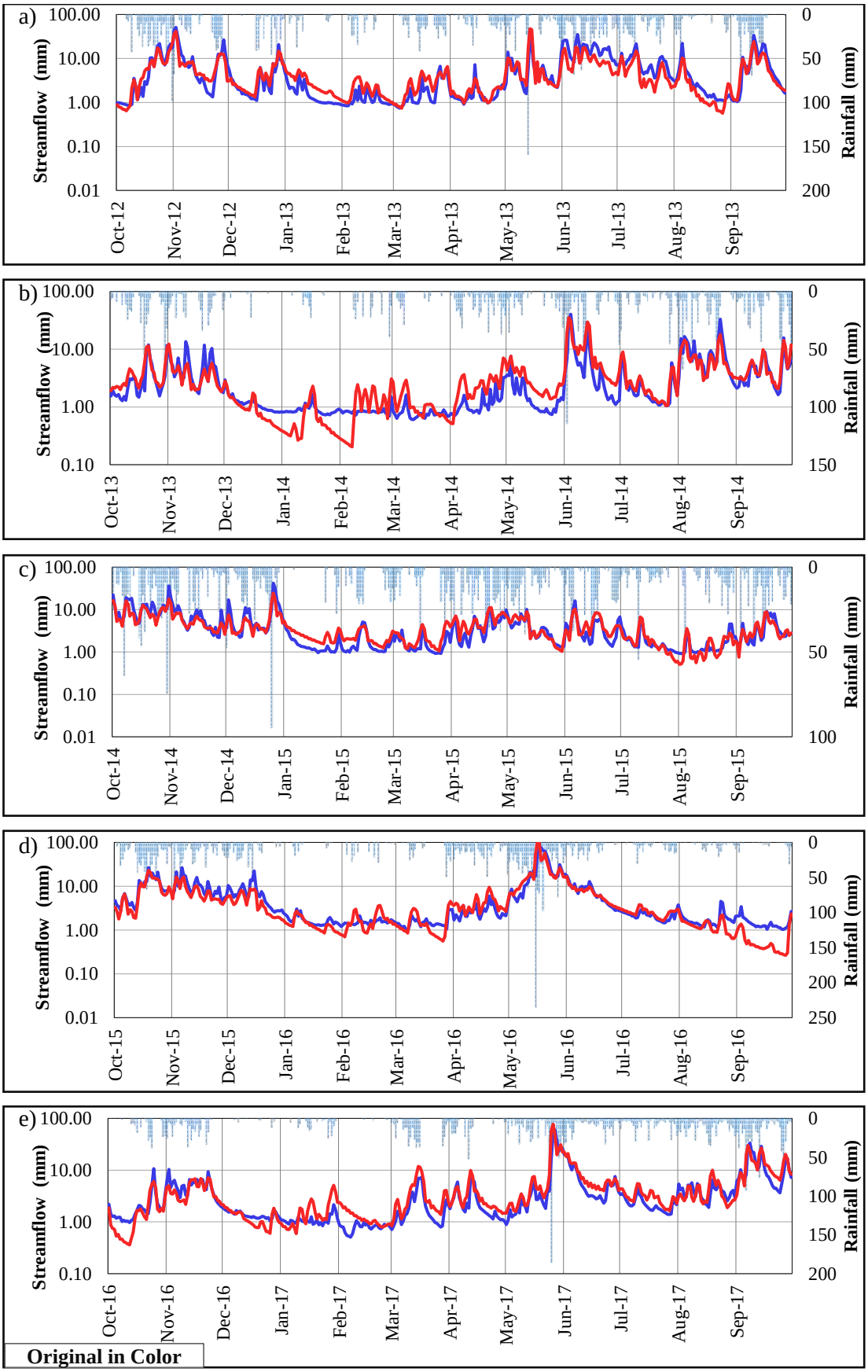

Figure 4-45 Hydrograph for the verification period of the eight-subdivision model (semi-log scale)

4.7.5 Model performance

The eight-subdivision model performance was evaluated with MRAE, NSE, PVE, and R^2 for entire calibration and verification periods with respect to high, medium, and low flows, as presented in Table 4-20.

Table 4-20 Model performance for the eight-subdivision model

	Period	Flow classification	MRAE	NSE	PVE	R^2
Summary Flow	Calibration	Overall	0.44	0.79	-2.7%	0.79
		High	0.29	0.55	12.2%	0.68
		Medium	0.40	0.12	-11.3%	0.48
		Low	0.56	-31.09	-34.7%	0.04
	Verification	Overall	0.40	0.76	2.4%	0.76
		High	0.32	0.35	16.9%	0.60
		Medium	0.34	0.47	-6.4%	0.58
		Low	0.55	-13.24	-26.6%	0.09
	Calibration and verification	Average	0.42	0.78	2.55	0.78

Similarly, the relationship between the observed and simulated streamflows is shown in a scatter plot in Figure 4-45 for the entire period of study. Plots only for the calibration and verification periods are shown in Figure 7-C and Figure 8-C in Appendix C respectively.

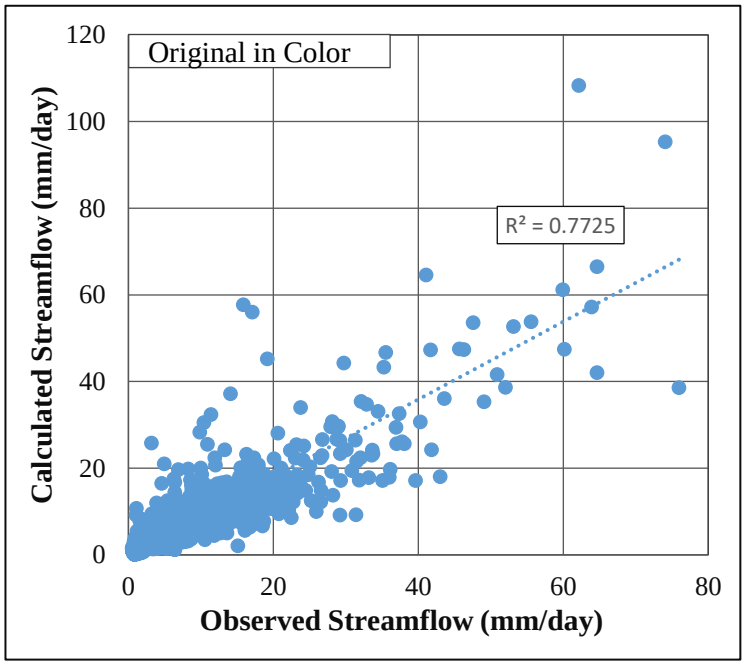

Figure 4-46 Relationship between observed and simulated streamflow in scatter plot for the eight-subdivision model

4.8 Results for the 12-subdivision model

The model with the 12-subdivisions was a distributed models to be compared with the lumped and other subdivision models. The 12-subdivision model was generated using ArcGIS along with HEC-GeoHMS and Arc-Hydro extension tools through the maximum drainage area method. The results for the entire calibration and verification periods are shown here in the forms of water balance, flow duration curves, outflow hydrographs, and objective functions.

4.8.1 Annual water balance

Annual water balance results for the calibration period of the 12-subdivision model are shown in Table 4-21 and Figure 4-46 respectively. This calculation is important to determine the accuracy level of calculated and observed streamflow from the annual water balance perspective.

Table 4-21 Annual water balance values for the calibration period of the 12-subdivision model

Water year	Thiessen averaged rainfall (mm)	Simulated streamflow (mm)	Observed streamflow (mm)	Observed water balance (mm)	Simulated water balance (mm)	Annual water balance difference (mm)
2007-2008	4,294	1,927	2,099	2,195	2,367	172
2008-2009	3,593	1,161	1,367	2,226	2,432	206
2009-2010	3,872	1,451	1,676	2,196	2,421	225
2010-2011	3,967	1,817	1,986	1,981	2,150	169
2011-2012	2,532	610	639	1,893	1,922	29

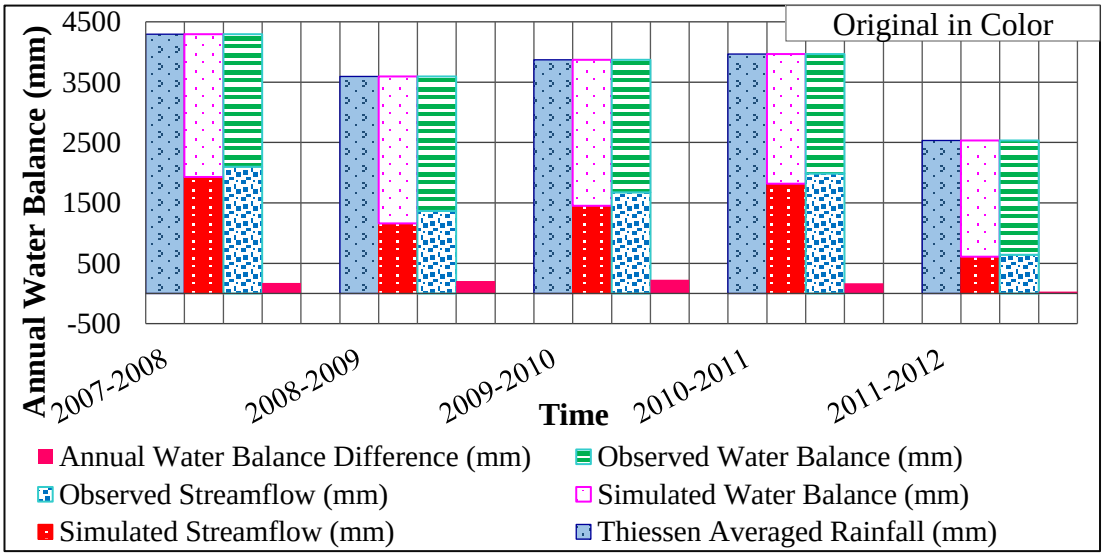

Figure 4-47 Annual water balances for the calibration period of 12-subdivision model

Based on Table 4-21 and Figure 4-46, the maximum error in water balance was from the year 2009/2010 and was 5.8 %. The average difference in the percentage of water balance over the entire calibration period is equal to 4.2%, which is within the range recommended by the literature.

Similarly, for the verification period, the annual water balance difference of observed and calculated streamflow values was studied to identify the accuracy of the model. This computation is presented in Table 4-22 and Figure 4-47. The results of this comparison illustrate that the maximum error occurred in the year 2012/2013 and was14.5%, which is a higher value than to the ranges recommended by the literature. Overall, the average error for the verification period is equal to 7.8 %, which is higher than that of the calibration period but still within the acceptable range recommended by the literature.

Table 4-22 Annual water balance values for the verification period of the 12-subdivision model

Water year	Thiessen averaged rainfall (mm)	Simulated streamflow (mm)	Observed streamflow (mm)	Observed water balance (mm)	Simulated water balance (mm)	Annual water balance difference (mm)
2012-2013	4,253	4,253	2161	2,093	2,710	617
2013-2014	3,271	977	1,169	2,103	2,294	192
2014-2015	3,666	1,066	1,543	2,123	2,600	477
2015-2016	3,666	2,009	2,196	1,729	1,916	187
2016-2017	3,568	1,481	1,508	2,060	2,087	27

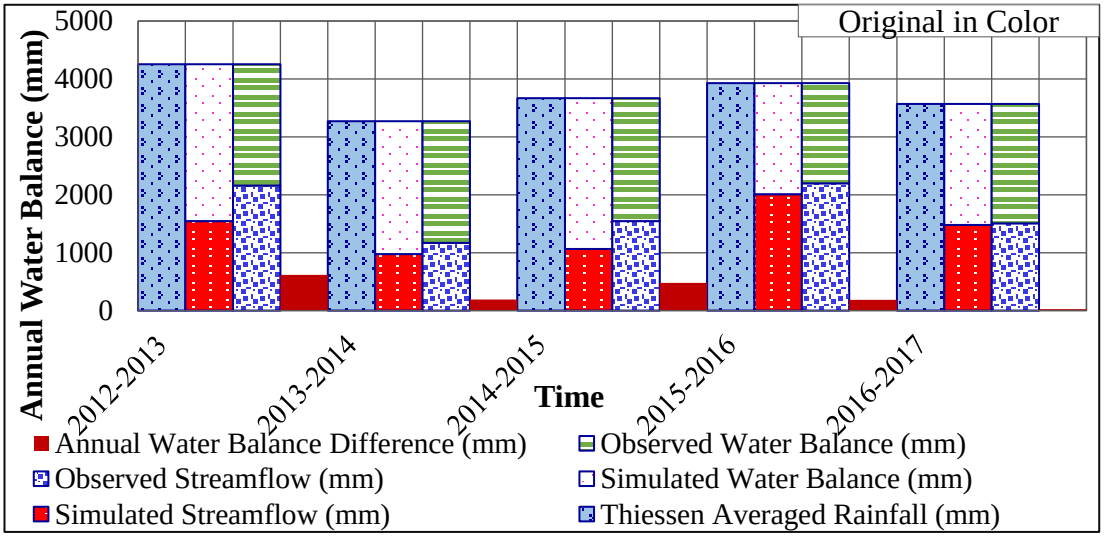

Figure 4-48 Annual water balances for the verification period of the 12-subdivision model

4.8.2 Flow duration curve

Flow duration curves for the entire calibration and verification periods were generated and contain both observed and simulated stream flows. These are presented here in normal and semi-log scales in Figures 4-48 and 4-49, respectively. Further, they are classified into three categories of high (≤10%), medium (10% < X ≤ 70%), and low (>70%) flows based on studies described in the literature review section.

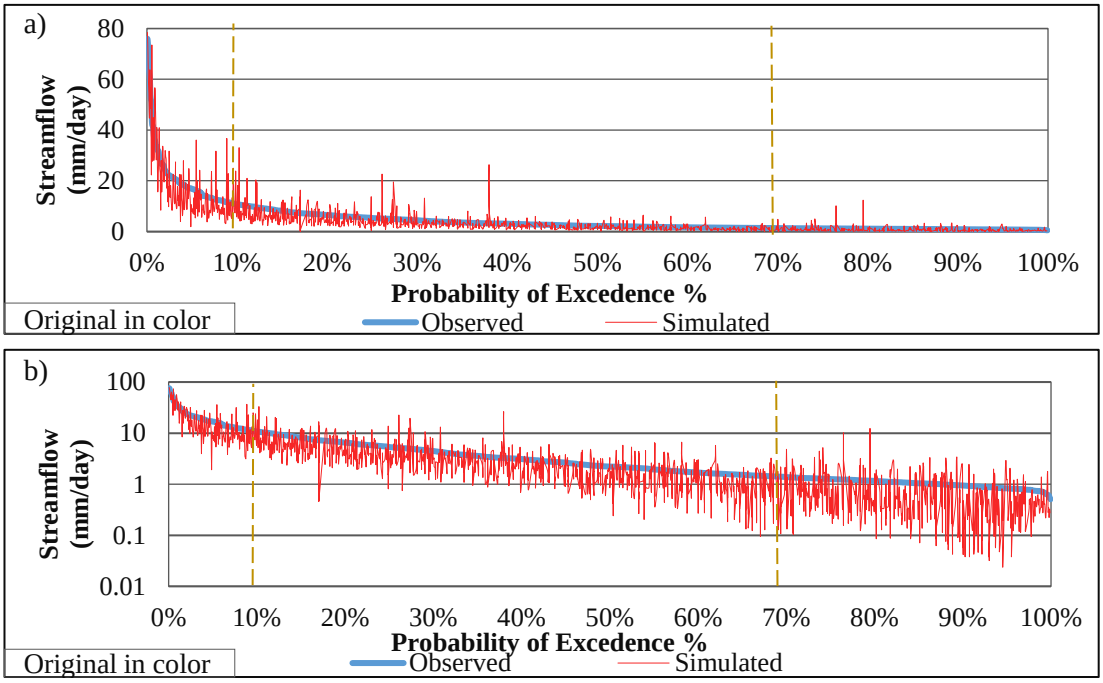

Figure 4-49 Flow duration curve for the calibration period of 12-subdivision model (a, b)

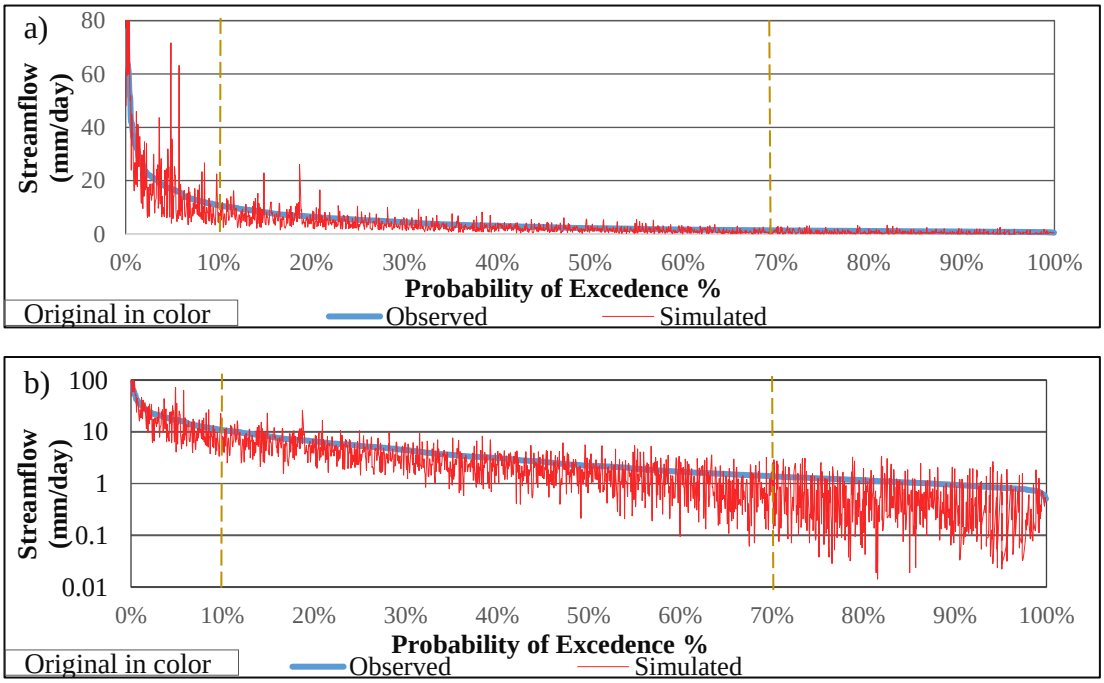

Figure 4-50 Flow duration curves for the validation period of 12-subdivision model (a, b)

4.8.3 Outflow hydrograph (calibration period)

The outflow hydrograph results for the calibration period of the 12-subdivision model are shown in Figure 4-50 and Figure 4-51 in normal and semi-log scales respectively.

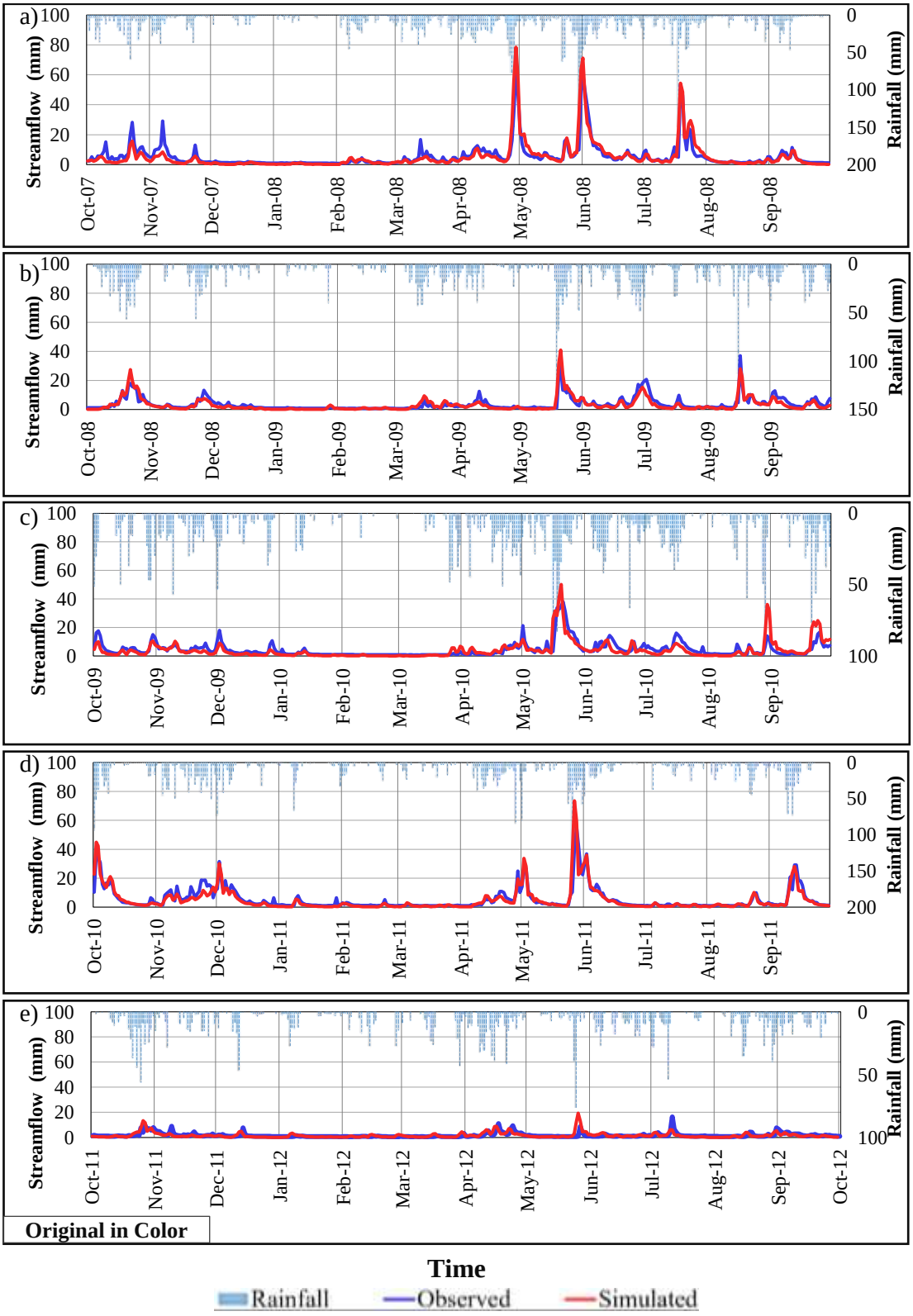

Figure 4-51 Hydrograph for the calibration period of the 12-subdivision model (normal scale)

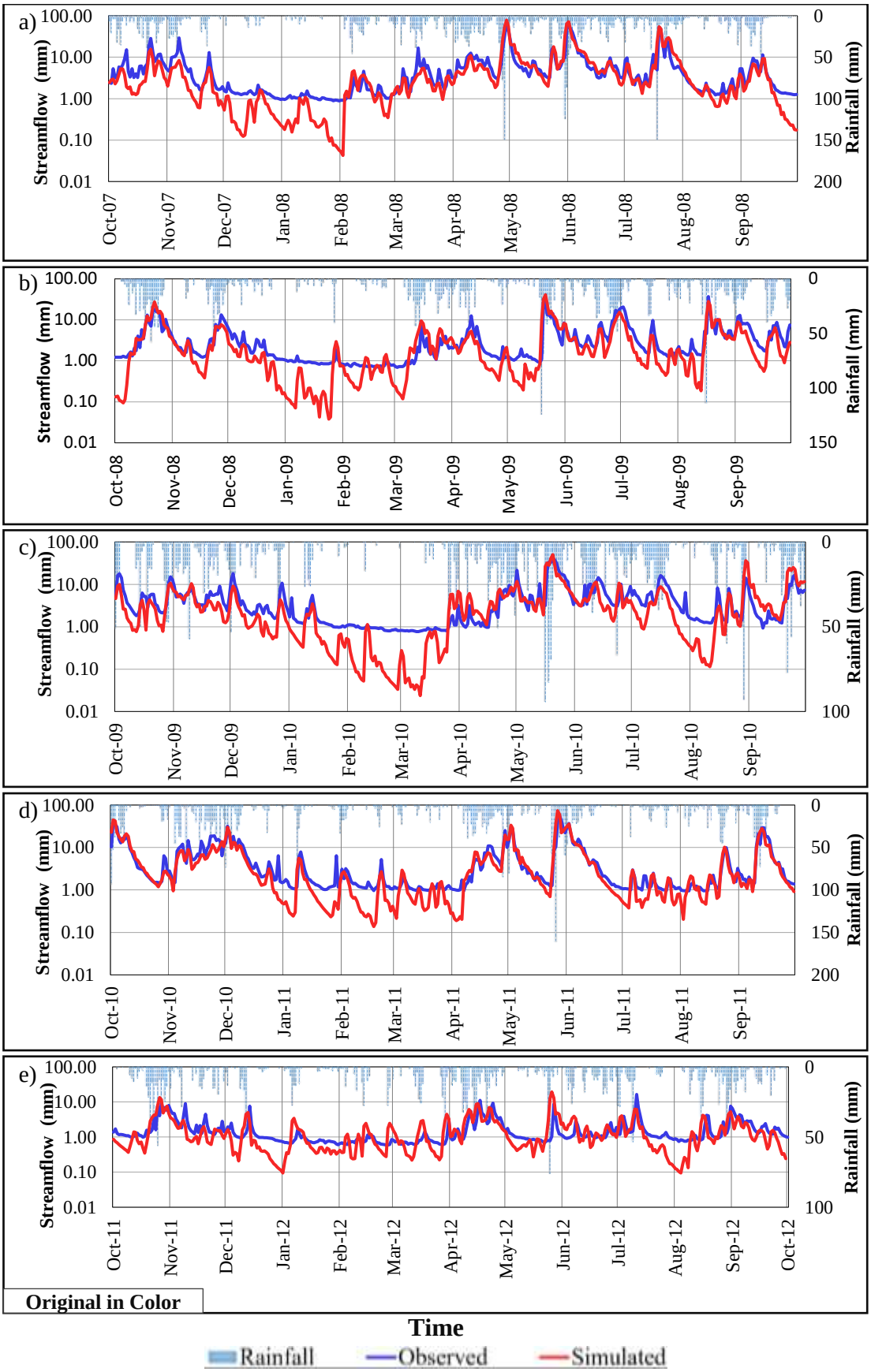

Figure 4-52 Hydrograph for the calibration period of 12-subdivision model (semi-log scale)

4.8.4 Outflow hydrograph (verification period)

The outflow hydrograph results for the verification period of the 12-subdivision model are shown in Figure 4-52 and Figure 4-53 in normal and semi-log scales respectively.

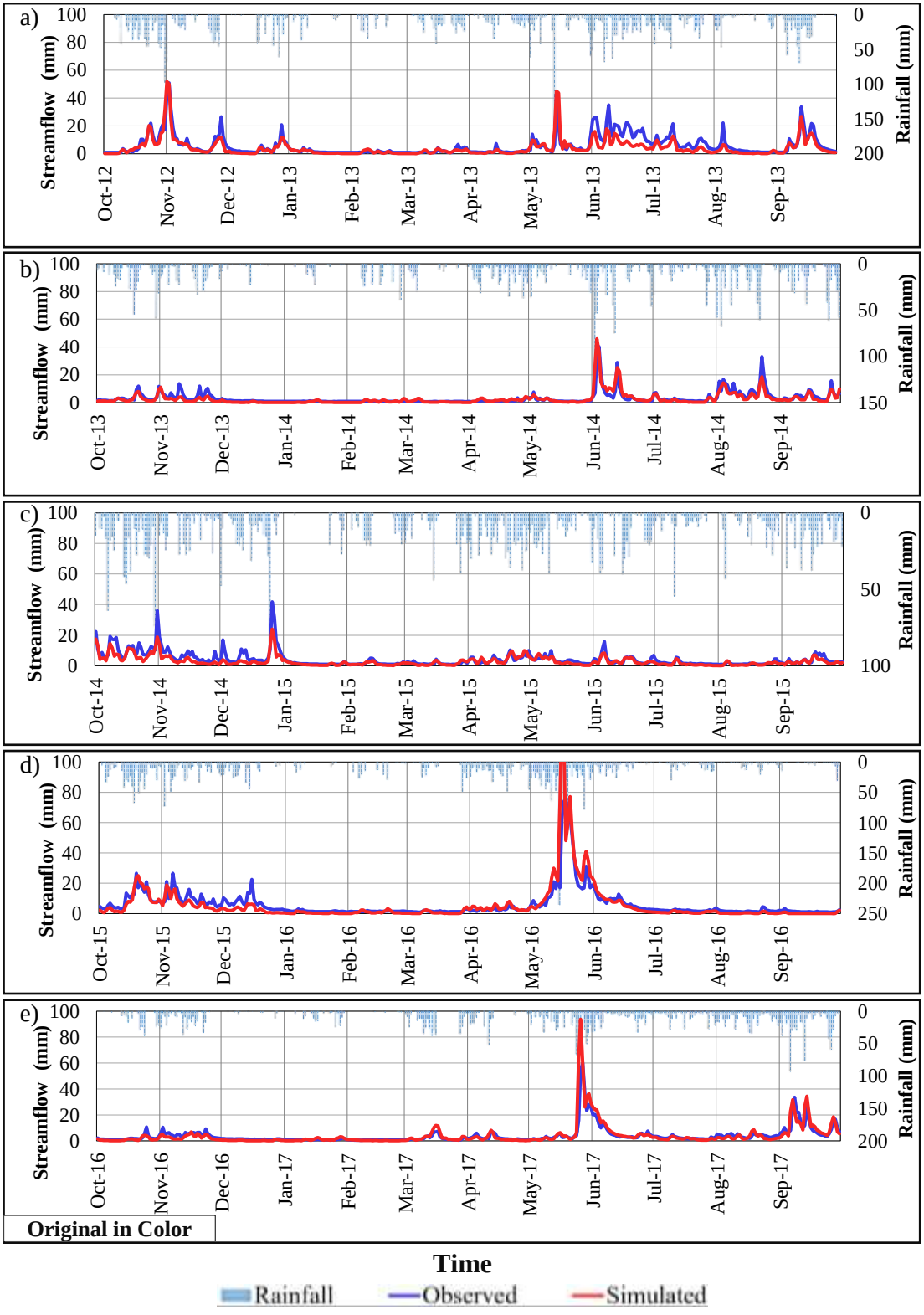

Figure 4-53 Hydrograph for the verification period of the 12-subdivision model (normal scale)

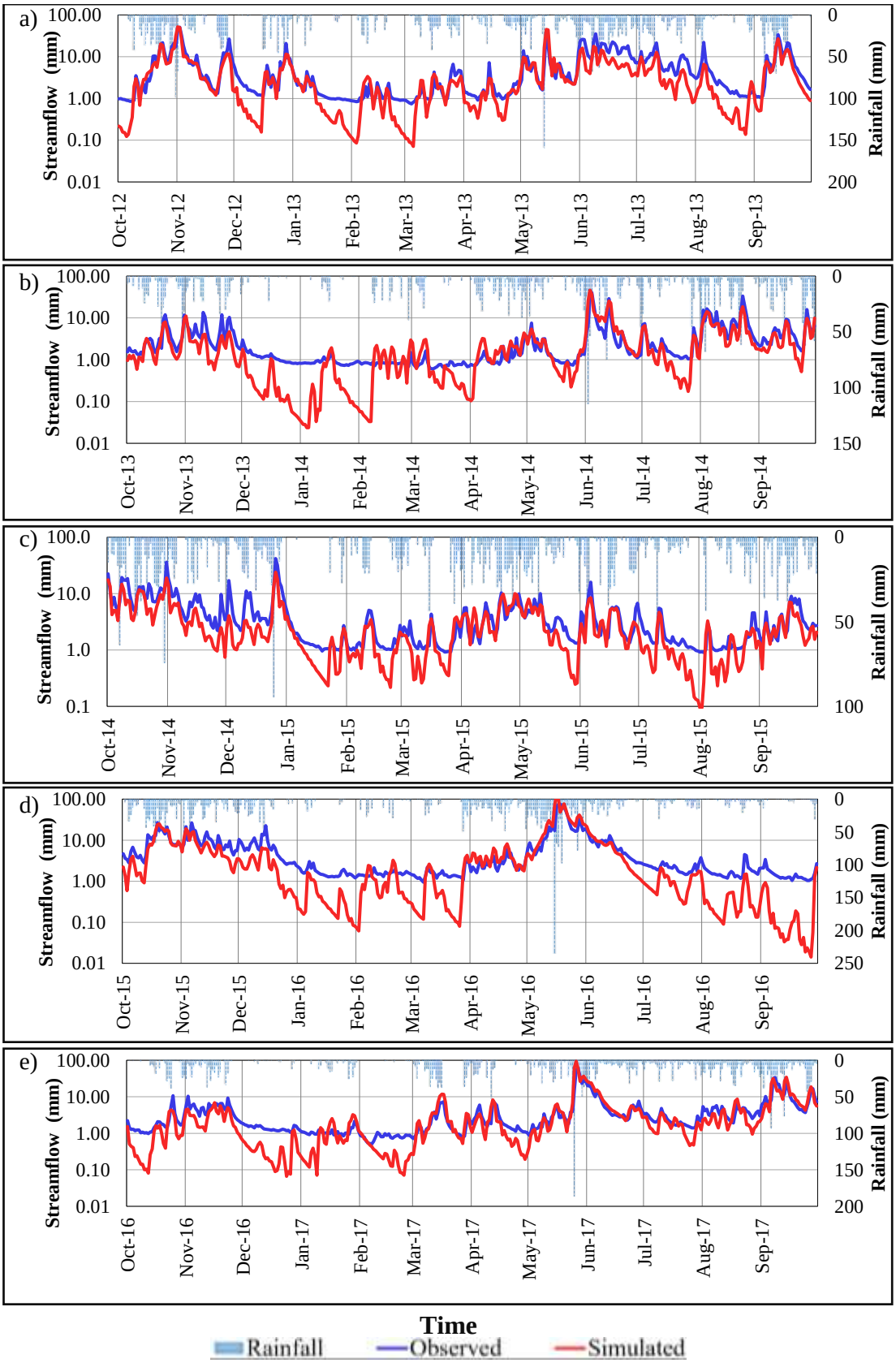

Figure 4-54 Hydrograph for the verification period of the 12-subdivision model (semi-log scale)

4.8.5 Model performance

The 12-subdivision model's performance was evaluated with MRAE, NSE, PVE, and R^2 for the entire calibration and verification periods with respect to high, medium, and low flows, as presented in Table 4-23.

Table 4-23 Model performance of the 12-subdivision model

	Period	Flow classification	MRAE	NSE	PVE	R^2
Summary Flow	Calibration	Overall	0.49	0.75	10.2%	0.80
		High	0.36	0.46	5.7%	0.71
		Medium	0.44	-0.11	12.1%	0.42
		Low	0.65	-33.52	25.9%	0.03
	Verification	Overall	0.49	0.65	17.5%	0.75
		High	0.39	0.43	0.0%	0.68
		Medium	0.47	0.45	27.9%	0.59
		Low	0.56	-1.11	23.1%	0.37
	Calibration and verification	Average	0.49	0.70	2.55	0.77

Similarly, the relationship between observed and simulated streamflow is shown in a scatter plot in Figure 4-54 for the entire period of study. Specific plots only for the calibration and verification periods are shown in Figure 9-C and Figure 10-C in Appendix C, respectively.

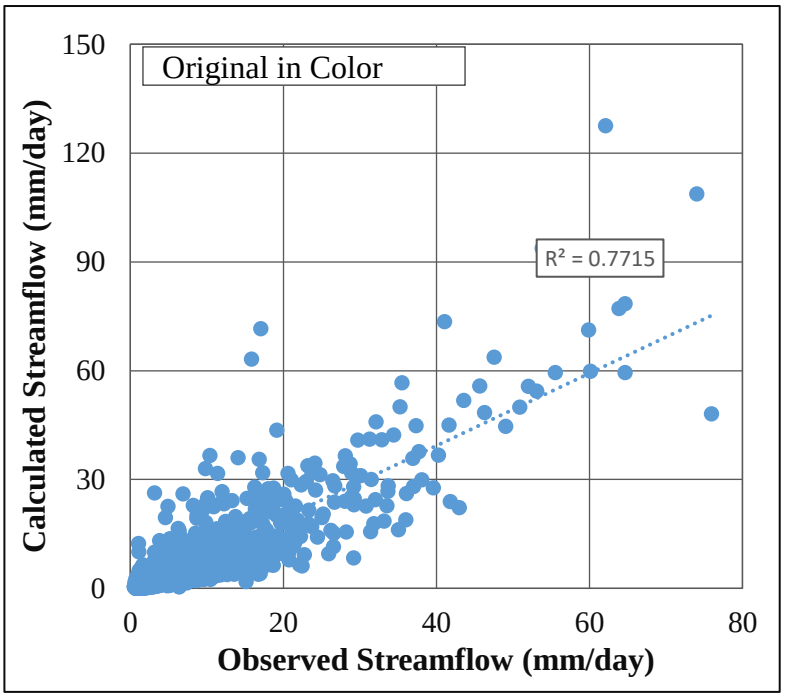

Figure 4-55 Relationship between observed and simulated streamflow for 12-subdivision model

4.9 Results comparison

All the results of this hydrological modelling were compared for better clarification. The comparison is based on the recommended objective functions mentioned in the literature review section, which are MRAE, NSE, PVE, and R^2. The results comparison consists of both the calibration and verification periods, which will be individually compared in here.

4.9.1 Results comparison for the calibration period

The calibration period in this research consisted of 5 years of data on seasonal rainfall in Sri Lanka (Maha and Yala) from the year 2007/2008 to the year 2011/2012. Efforts were made to use the calibration period to increase model efficiency. This effort included looking for the optimum subdivision model suitable for water resource assessment in the Kelani river basin in Sri Lanka. Because of this, the flow duration curves are classified into three categories of high, medium and low flows for ease of comparison.

At first, high flows of all models including the lumped, three, five, eight and 12-subdivisions models were compared (shown in Figure 4-55). Figure 4-55 illustrates that MRAE has a constant low value within the lumped, three, and eight-subdivisions models and a high value in the 12-subdivision model. Likewise, the Nash indicator has high values only in the lumped and five-subdivision models. Present error in volume has a maximum value in the three subdivision model but a minimum value in the 12-subdivision model, in the five and eight-subdivision models it has a constant rate.

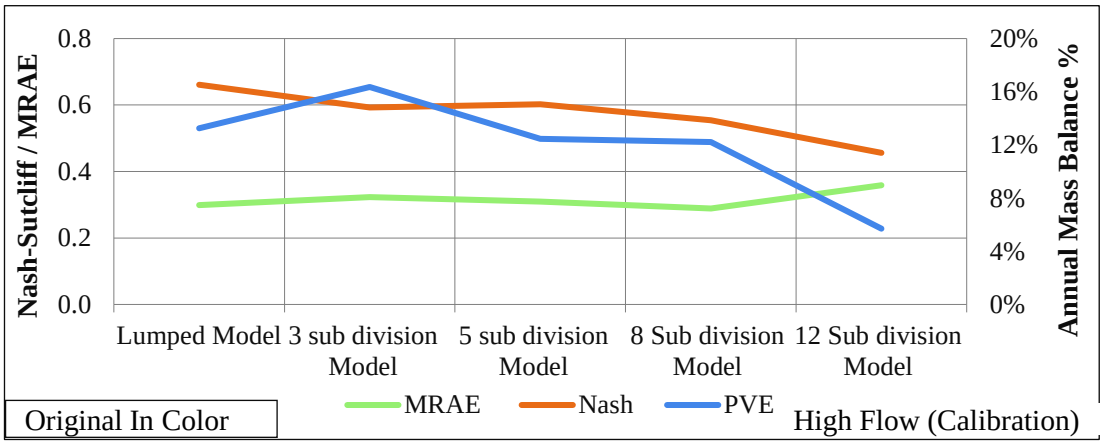

Figure 4-56 High flows comparison for the calibration periods of all models

The medium flows were also compared for all models (shown in Figure 4-56). Figure 4-56 illustrates that the MRAE values displayed a constant rate of 0.3 to 0.4 in all models except for the 12-subdivision model, where they increased. The Nash indicator had a maximum value in the lumped and three-subdivision, but it dramatically decreased with a constant slope of 0.4 to -10 in the models with more subdivisions. The PVE had a constant rate of -5% within the lumped and three-subdivision model. It has its minimum value in the five-subdivision model and maximum values in the eight and12-subdivision models.

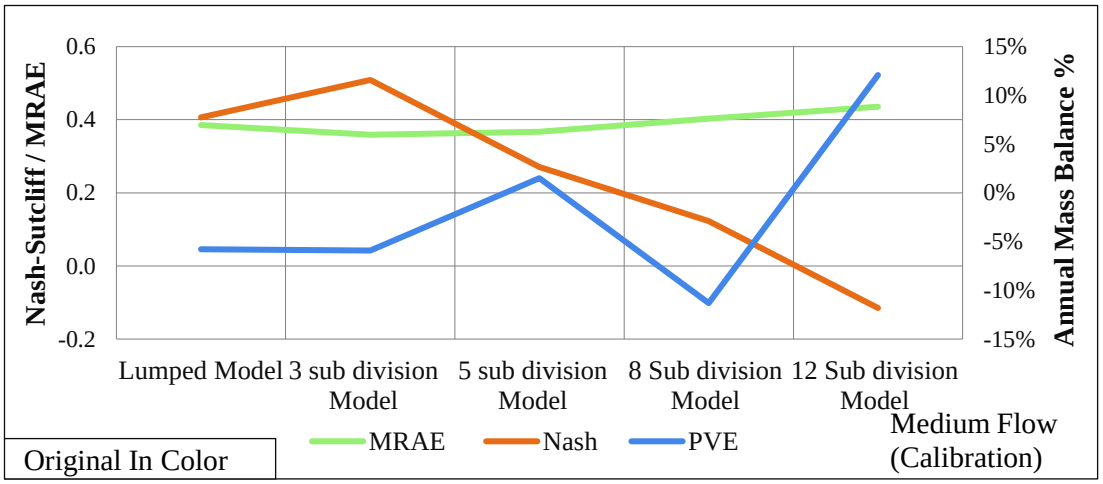

Figure 4-57 Medium flows comparison for the calibration periods of all models

Next, objective functions for the low flows during the calibration period were compared. Figure 4-57 illustrates that MRAE has a nearly constant rate of 0.37 to 0.39 in the lumped model and in the models up to the eight-subdivision one. However, it increased in the 12-subdivision model. The Nash indicator had maximum values in the lumped and three-subdivision models, but it decreased by 0.5 to -10 between the models with three to 12 subdivisions. Subsequently, the PVE had a constant rate near -5% for the lumped and three subdivision models. With respect to five-subdivision model, it had a minimum value (near 0), and respect to the 12-subdivision model, it had a maximum value. It can be concluded that medium and low flows in the five subdivision model showed decent performance with minimum MRAE, a high NSE, and less error in PVE.

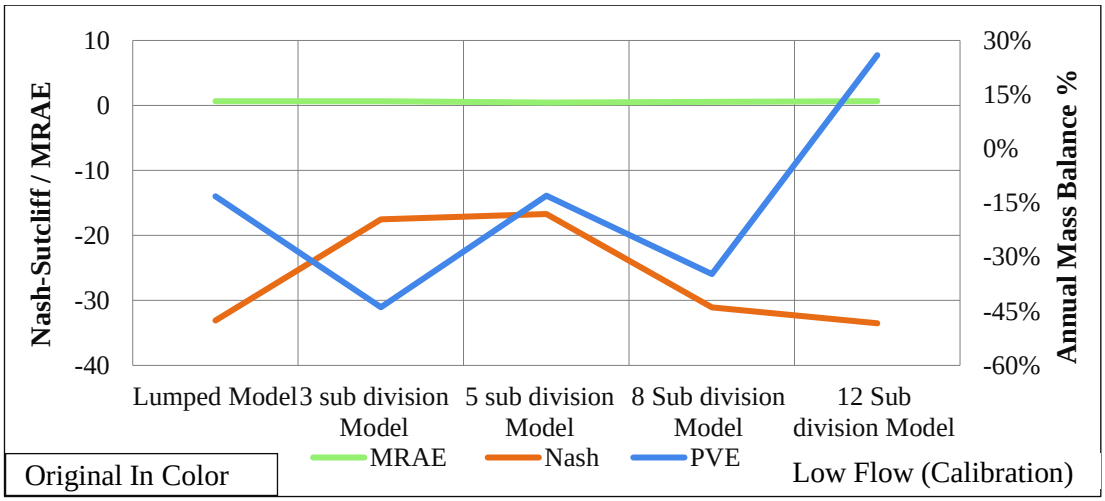

Figure 4-58 Low flows comparison for the calibration periods of all models

In conclusion, the lumped model and all subdivision models (three, five, eight and 12) were compared in an average manner (from high to low), as shown in Figure 4-58. Figure 4-58 demonstrates that the MRAE had a minimum value in the model with five subdivision (less than 0.4) but a greater value (more than 0.4) in the models with other subdivision counts. The NSE objective function had a maximum value in the lumped model and a constant decreasing slope of 0.85 to 0.75 in the models with three to 12 subdivisions. The PVE values had minimum error ranging from 2 to -2% in the lumped, three and eight-subdivisions models. In the five-subdivision model it slightly increased to more than 4 %, but in the 12-subdivision models it increased to 10 %, which shows the maximum error.

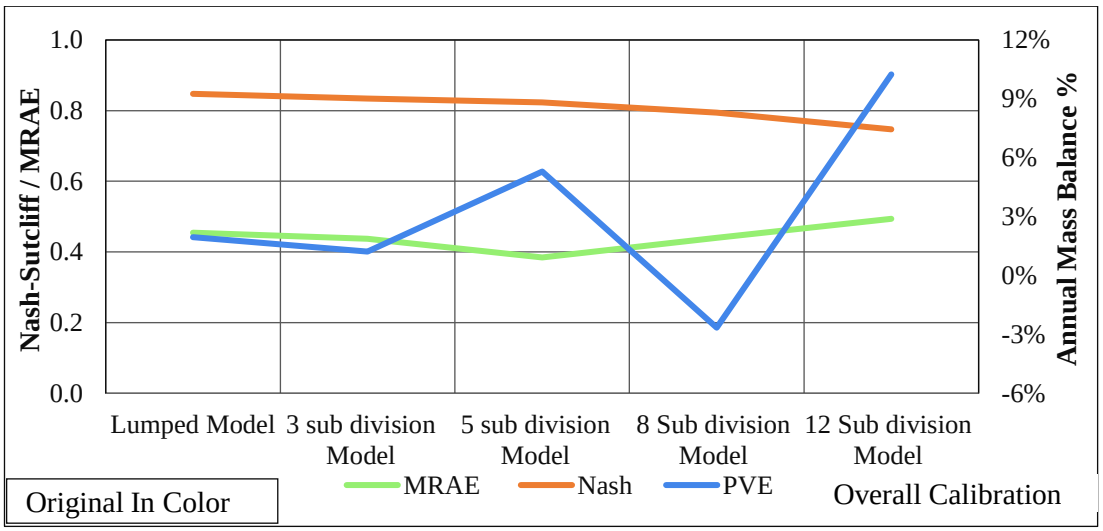

Figure 4-59 Overall flows comparison for the calibration periods of all models

4.9.2 Result comparison for the verification period

A result comparison similar to that for the calibration period was carried out for the verification period to justify the accuracy of the model and parameter estimation methods. The verification period equivalent in length to the calibration period and consisted of five years of data, from 2012/2013 to 2016/2017. The verification assessed the suitability of using the model for various studies over the Kelani river basin in Sri Lanka. In the verification period, similar to the calibration period, flows were compared in high, medium and low categories based on the MRAE, NSE, and PVE.

First of all, all models (Lumped, three subdivision, five subdivision, eight subdivision, and 12 subdivision) were compared with respect to high flows (shown in Figure 4-59). It can be seen in Figure 4-59 that the MRAE had the smallest value in the five-subdivision model (close to 0.3) and the maximum value in the 12-subivision model (close to 0.4). The MRAE had fewer changes within three subdivision model and the lumped model. The Nash indicator had a high value (close to 0.6) only in the lumped and three-subdivision models. Similarly, the PVE had less error in the five-subdivision model (10 to 15 %) compared to the lumped, three-subdivision and eight-subdivision model, although it had a minimum error in the 12-subdivision model that was nearly zero.

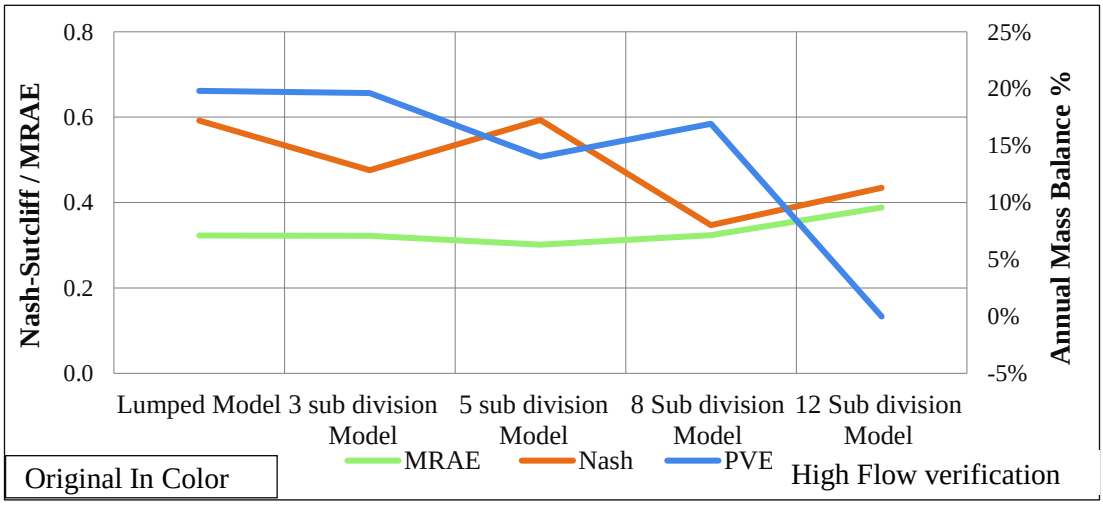

Figure 4-60 High flows comparison for the verification periods of all models

After that, the medium flow comparison was carried out, as shown in Figure 4-60. Figure 4-60 illustrates that the MRAE had low values (closer to 0.35) in the five-subdivision and lumped model. Also, it indicates that MRAE had values near or greater than 0.4 for the rest of the models, with the maximum amount in the 12-subdivision model (near to 0.5). Subsequently, the Nash (NSE) indicator had the maximum value (close to 0.6) in the five-subdivision and lumped models compared to the rest of the models. The PVE indicator had a maximum value (near 30%) in the 12-subdivision model and a minimum value (near 8%) in the lumped model. The PVE had values between -10% and 10% in the models with three to eight subdivisions.

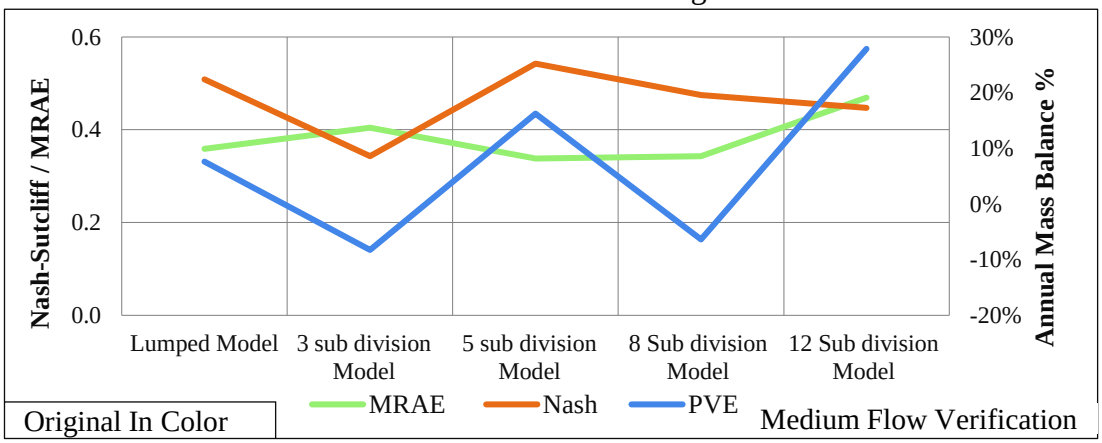

Figure 4-61 Medium flows comparison for the verification periods of all models

Subsequently, low flows were compared in the verification period for all models (shown in Figure 4-61). It can be illustrated from Figure 4-61 that MRAE had a constant rate near 0 in all subdivisions. The Nash indicator had maximum values in the five and 12-subdivision models but minimum values in the other models. The PVE indicator had a minimum error in the five-subdivision model that cannot be compared with other models, which showed higher PVEs.

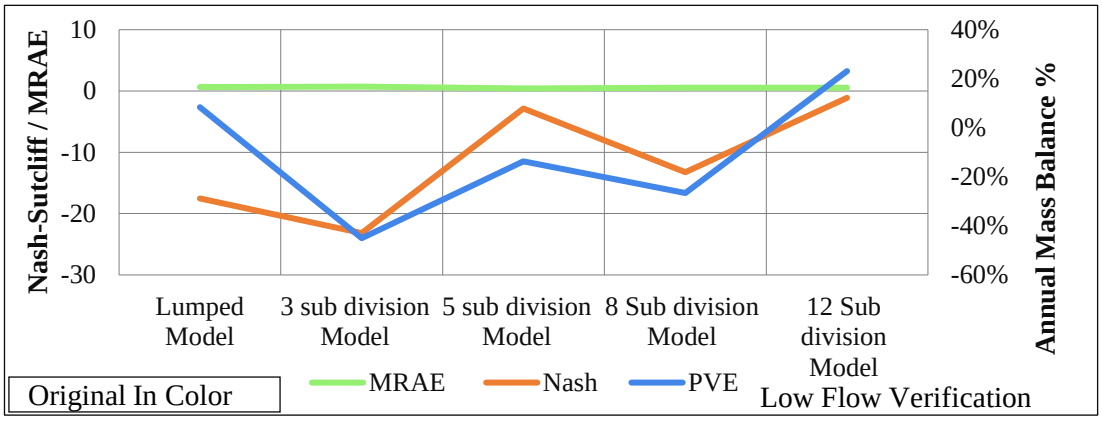

Figure 4-62 Low flows comparison for the verification periods of all models

Finally, all the flows were averaged and compared using the mentioned objective functions, as shown in Figure 4-62. Figure 4-62 illustrates that the MRAE had the lowest value (near 0.35) in the five-subdivision model and the highest values in the three and 12-subdivision models (near 0.5). The Nash indicator had the highest value in the lumped model (near 0.8), but it decreased with increases in subdivisions. In contrast to the MRAE, the PVE indicator had the lowest error (near 0) in the three and eight-subdivision models. It had the maximum error percentage in the 12-subdivision mode. For the lumped and five-subdivision model, the PVE was near 12%.

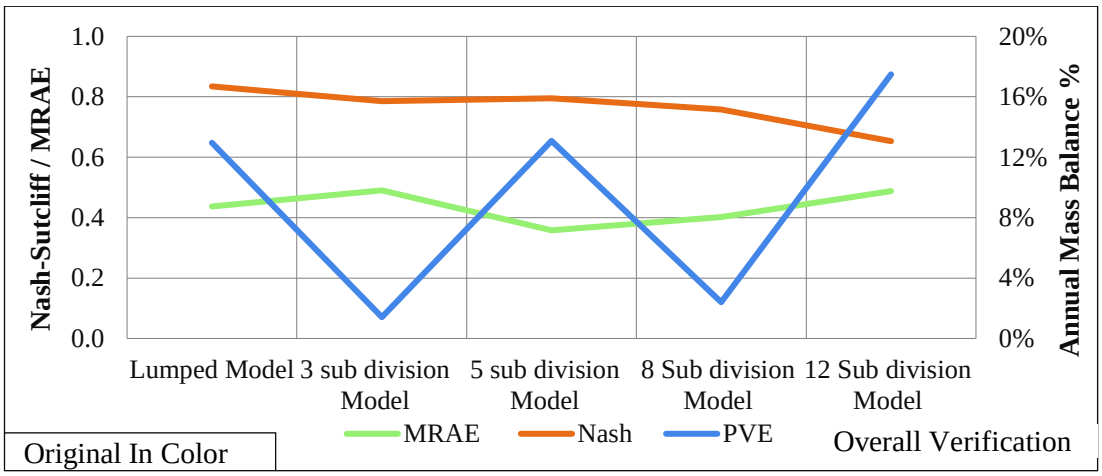

Figure 4-63 Overall flows comparison for the verification periods of all models

5 DISCUSSION

5.1 Model selection

The model selection process was carried out in this research work to select the kind of model that can precisely simulate streamflow, particularly for water resource assessment purposes. Different hydrological models exist for various objectives such as flood and drought assessment, water resource assessment, infrastructure design, and so on. According to the applications of the models, they can be divided into event-based and continuous hydrological models. Event-based models are used when simulating the peak of the hydrograph is the main purpose of the study, and in most cases the evapotranspiration component can be neglected. In continuous models, hydrological modelling more and less focuses on all aspects of a hydrograph. This type of modelling requires an extensive variety of data, including evapotranspiration.

The search for a well-defined model that considers all the natural components in the modelling process for precisely simulating streamflow is a matter of extensive research. Losing water in a natural system through evapotranspiration, seepage, and other anthropogenic phenomena (parks, residential buildings, industries, agriculture, etc.) must considered to help in the improvement of hydrological models. There is a need for a well-defined model of the Kelani river basin that can efficiently simulate runoff with more focus on intermediate and low flows, which is the research objective in this study. After conducting numerous literature surveys, the SMA model was selected as a suitable hydrological model for water resource, environmental, and flood assessment purposes in a river basin. This model considers all the mentioned natural losses and contributions of water from groundwater layers and surface runoff. Due to existence constraints of the SMA model in capturing all natural governing parameters, it is combined with other tools and computer models. Many tools exist, such as Mike, NAM, SWAM, HEC-HMS, and so on. The HEC-HMS hydrological model was used in this research as it supports the SMA model, is free of charge, is accessible, and is frequently used in different contexts around the globe.

In addition to the SMA model, many other models also exist for the estimation of water loss in soil, such as the curve number and the Green and Ampt model. The mentioned

models require fewer parameters and have more conceptual bases rather than a physical bases. Therefore, the SMA model has priority among other methods capturing the water loss in soil layers. Furthermore, the mentioned methods compared with the SMA do not consider the contributions of water from base flow, interflow, and groundwater storage. Those methods rely on some theoretical conceptions rather than physical that are not accurate enough. The possibility of using such methods only exist where the use of SMA models is limited. In Sri Lanka context, due to years of civil war, less attention has been paid to the surveying of soil, landuse, and land cover and maintaining rainfall and hydrological stations. This shortage leads researchers and modellers to ignore the SMA model and choose other models that require data, time, and effort. Because of the mentioned reasons, researchers and hydrological modellers mostly rely on models that cannot simulate the streamflow well. In this research, the SMA model is executed despite the existence of data challenges in hopes of producing more reliable and accurate results compared to past models.

5.2 Data and data checking

5.2.1 Landuse, soil, and DEM

The landuse map used in this study was retrieved from the Survey Department of Sri Lanka and was published in 2006. It needs to be mentioned that the acquired landuse map cannot represent the current status of the basin (2018) due to rapid increases of urbanization and land cover changes. However, the landuse map played a major role in determining the impervious percentage and canopy storage values that were main components of the SMA model. The impervious percentage was determined for individual landuse components as suggested by the literature. During the sensitivity analysis of all parameters, it was found that impervious percentage is among the most sensitive parameters. The sensitivity anlaysis also found that less error in this parameter can lead to a difficult modelling journey. Calibrating this parameter in distributed models is an especially difficult task. In contrast to the impervious percentage, canopy storage has a low impact on the modelling accuracy and directly depends on landuse. Therefore, it can be concluded that the estimated parameters using this landuse map are not very accurate. For compensation of this error, much effort was put into the calibration process.

In the SMA model, as is clears from the model name, soil parameters play a major role in the estimation of relevant parameters. There are certain parameters in the SMA model that can only be calculated through the existence of soil information such as maximum infiltration, soil storage, tension storage, and soil percolation. Another advantage of having the soil information of a basin that it helps in the estimation process of other model parameters, like the time of concentration.

In the Sri Lankan context in general, and particularly in the Kelani river basin, complete and reliable soil information does not exist. The importance of such information in hydrological modelling is for the estimation of the hydraulic properties of soil. The only available soil information (as shown in Figure 3-5) is based on agriculture perspective. Figure 3-4 illustrates that most part of the basin is covered with Podzolic soil, although no further information exists regarding the Podzolic soil in the literature. In this research, the categories of soil according to field visits to the different locations are classified in C groups. Due to lack of soil information, the hydraulic properties of soil were estimated by the range of values suggested in the literature (as shown in Table 4-6). This innovation is used in the soil-data-scarce situations and potentially affects the time length of the calibration process.

A digital elevation model was acquired from the Survey Department of Sri Lanka. The existence of the DEM data played an essential role in determining the catchment boundaries and generating its sub-catchments. The main problem with 30 m resolution DEM was its accuracy for precisely generating catchment boundaries, slopes, and other geomorphologic properties. The catchment area is a main constant input to the hydrological model that affects its overall accuracy. The 30 m DEM resolution is not very high, which directly affected the result of the model. In this research work, due to the only available option of a 30 m DEM, all the relevant characteristics of the catchment were generated using this model.

5.2.2 Data period

The main data used in this study was rainfall and streamflow. Usually, the formation of a river takes a long time, and changing its courses takes hundreds of years. At the same time, natural phenomena such as floods, drought, and erosion also affect the

streamflow course and current. Also, man-made factors such as urbanization, reservoir construction, power stations, retaining walls, and other similar structures are directly and indirectly effected by streamflow course and current. The mentioned phenomena also affect the streamflow simulation process, mainly determining the calibration and verification periods. Some researches indicate that even one –year of data is enough to simulate the streamflow, but this would be only applied in a situation where the influence of the mentioned phenomena is minimum.

Through a survey of the literature, some prominent research proposed using a minimum of three years of data for the calibration period. Some research has indicated that the calibration period needs to be determined based on the runoff coefficient for six years. It declares that the selection of the calibration period depends on years with minimum variation of runoff coefficients. Further, it indicates that the validation period should be selected among years with less variation of runoff coefficients. Most researchers use the split method for the hydrological modelling period: they use half of the data for calibration and half for the validation period.

The main scope of this research work was developing a model for efficient simulation of streamflow uses for water resources assessment. Specifying the simulation period for the Kelani river basin in a situation where rapid progress and development is happening all over its catchment is a challenging task. Considering this reality, most literature suggests six years of data for efficient simulation of the streamflow. Based on the reality of the Kelani river basin, a combination approach of split and runoff coefficient methods was used in determining the length of calibration and verification periods. Ten years of data starting from the year 2007/2008 to the year 2011/2012 was used for calibration and data from the year 2012/2013 to the year 2016/2017 was used for verification. It can be observed that high and low runoff coefficients happened during the calibration period compared to the verification period. It is worth mentioning that using more than 10 years of data was decided against due to time and model constraints. However, in the case of climate change, data needs to be considered for a longer period.

5.3 Using daily versus monthly data for water resources assessment

According to Xu and Singh (1996) monthly data cannot be used for a wide range of purposes such as climate change and long-term streamflow forecasting. Using data on a daily scale provides a better estimation of actual evapotranspiration than does monthly data (Xu & Singh, 1996). Furthermore, the estimation of monthly runoff is easy from daily inputs, but the estimation of daily runoff using monthly inputs is a challenging task. Also, the performance of the daily input model has more usage compared to the monthly input model.

A study on the Bilate river basin located in the Southern Ethiopian Rift valley indicated extreme variability of daily and monthly precipitation. The related research suggests that monthly average precipitation can be used roughly for water availability estimations for cultivation and traditional water harvesting, though it is not very accurate compared to daily average precipitation (Thiemann & Förch, 2004). The variability of daily flow is generally not very important for water resource planning. Monthly variability of flow is used in determining water's average residence time in the ground and in the reservoirs. Water resource assessment using daily variability of flow is necessary for real-life applications (De Geroen, 2012). Further, in models that use monthly time steps, certain fluxes between components of the water resource system like interception, transpiration, recharge, surface, and so on, are governed by daily processes. Most hydrological models that use monthly time steps do not make a distinction between interception and other forms of evaporation, but prefer to combine all evaporation processes in what is generally called evapotranspiration (De Geroen, 2012).

Daily data available for the Kelani river basin up to the Hanwella catchment, and according to the mentioned realities, it is always better to use daily data instead of monthly data if there are no any major constraints. Similarly, results from daily data are more reliable due to consideration of all hydrological processes in detail compared to monthly data. Today, all the water fields are interconnected, and only considering water resources assessment is not sufficient for a useful runoff model. There is an advantage to using multi-purpose (flooding, infrastructures designs, and water resources assessment) models like the SMA model considered in this research work.

5.4 Data errors

In this section, all graphically or numerically existing errors found during the visual and consistency checks are discussed.

5.4.1 Visual checking

This section will discuss all the data checking mentioned in Chapter 3 of this research. This kind of data checking was carried out only for rainfall, streamflow, and evaporation data. This check is not conducted for the landuse and soil maps due to time, resource, and budget constraints.

For the visual checking, it was observed that in Dec 2007 (Figure 3-9) the Norwood rainfall station recorded a high amount of rainfall corresponding with a lower amount of streamflow. Similarly, in this year, the Deraniyagala rainfall station (Figure 3-9) observed no rainfall or streamflow during January or December. Furthermore, for the year 2008 in January for Hanwella rainfall station, it was recognized that a high rainfall amount corresponded to less streamflow (shown in Figure 3-9).

Moving ahead, zero rainfall was recognized in the February 2010 months for the Deraniyagala, Hanwella, Glencourse and Holombuwa rainfall stations, but streamflow was observed, which indicates the existence of an error (shown in Figures A-8 and A-9, Appendix A). Similarly, for October 2010, a high amount of rainfall was recognized compared to the streamflow in the Norwood, Kithulgala, Deraniyagala, and Hanwella rainfall stations (shown in Figure A-9, Appendix A). In February 2011, the Glencourse, Deraniyagala, and Hanwella rainfall stations recognized less rainfall compared to the streamflow (shown in Figure A-10, Appendix A).

In the progress of data checking recognized less streamflow compared to rainfall in November 2011 for all streamflow stations (shown in Figures A-11 and A-12). Similarly, less rainfall compared to streamflow was shown for the year 2012 in the end of November and the middle of April and August for all rainfall stations (shown in Figure A-13 and A-14). Less rainfall compared to streamflow was also recognized in December 2014 for the Hanwella, Deraniyagala, and Glencourse rainfall stations (Figure A-18). Furthermore, in August 2016 and December 2015 for all rainfall stations, less rainfall was observed compare to the streamflow (shown in Figure A-19

and Figure A-20). For the year 2017, the month of April showed less rainfall compared to streamflow (shown in Figure A-21 and Figure A-22, Appendix A).

In summary, during the visual checking of all data, most of the mistakes were found in the years 2007/2008 and 2011/2012, generally in the months of December, January, February, and November. Also, the Deraniyagala rainfall station was found to have the most error compared to all other stations, as rainfall did not match very well with the streamflow.

5.4.2 Consistency checking

During the process of consistency checking, the single mass curve for the year 2011/2012 indicated the existence a little inconsistency almost in all rainfall stations (Figure A-3). Similarly, in the checking process of the annual runoff coefficient with evaporation (Figure 3-10), inconsistencies were found in the pattern for the years 2011/2012 and 2013/2014 compared to other years. In the variation of annual rainfall and streamflow for the year 2015/2016, it was found that streamflow responded much more strongly to rainfall (Figure 3-11) which seem unrealistic. In the same manner, for the years 2007/2008, 2012/2013, and 2014/2015, the rainfall is in high compare to streamflow.

In the continuation of consistency checking process of the annual rainfall of each station (Figure 3-12), in the year 2007/2008 for the Deraniyagala rainfall station the high amount of rainfall was found compared to all other stations, which seems unrealistic. Similarly, for the Hanwella rainfall station, the pattern of rainfall does not match well for years 2009/2010 and 2015/2016 compared to the other stations. Furthermore, in a monthly comparison of Thiessen rainfall with observed streamflow (Figure 3-13), less rainfall was found compared to streamflow in November 2012/2013. Moreover, during the checking of monthly evaporation data over the entire period of study (Figure 3-15), a high amount of evaporation was only found in the months of August, October, and March 2015/2016. Also, during the water balance checks with evaporation, the annual water balance did not matching with evaporation for the years 2011/2012, 2015/2016, and 2016/2017 (shown in Figures 3-17 and 3-18 respectively).

Furthermore, the minimum, maximum and average values of rainfall, streamflow, and evaporation were checked (shown in Figure 3-16). For this check, the mean values need to be in the middle of the minimum and maximum values for the entire period. From the comparison of rainfall values, it was found that the average values were not in the middle for January, July, February, and November. Similarly, the average streamflow values were not in the middle for January, February, April, August, and July. During the comparison of the streamflow and rainfall values (Figure 3-16), it was identified in February and August that the patterns of rainfall and streamflow did not match. Similarly, during monthly comparison of evaporation data (Figure 3-15), it was found for month of August, October and March in the year 2016 the pattern of data did not follow the same respect to other years and the average values were not in the middle (Figure 3-16).

In a summary of consistency checks, it was found during the years 2011/2012, 2013/2014, and 2015/2016 that the streamflow and rainfall were not well matching. Among rainfall stations, the Deraniyagala rainfall station showed a high amount of rainfall for the year 2007/2008 compared to other stations. Similarly, the Hanwella rainfall stations did not well represent the years 2009/2010 and 2012/2013, especially for the month of November. From the comparison of monthly fluctuations of rainfall and streamflow, it was found that January, February, November, and August did not compare well to other months. In the comparison of evaporation data, year 2015/2016 were found with high evaporation in some months compared to other years.

5.5 Subdivisions of the watershed

As a part of this research comparing multiple subdivisions models in the HEC-HMS with the SMA model, the Kelani river basin was divided into several sub-watersheds based on a critical threshold area, which is a more common and precise method compare to other methods mentioned in several previous studies. The selection process was entirely based on the literature reviews that are shown in Table 5-1. The threshold method was the minimum upstream drainage area for a channel to originate and can be specified by a percentage of the total watershed area (Kumar & Merwade, 2009). The schematic diagram of this method is presented in Figure 5-1.

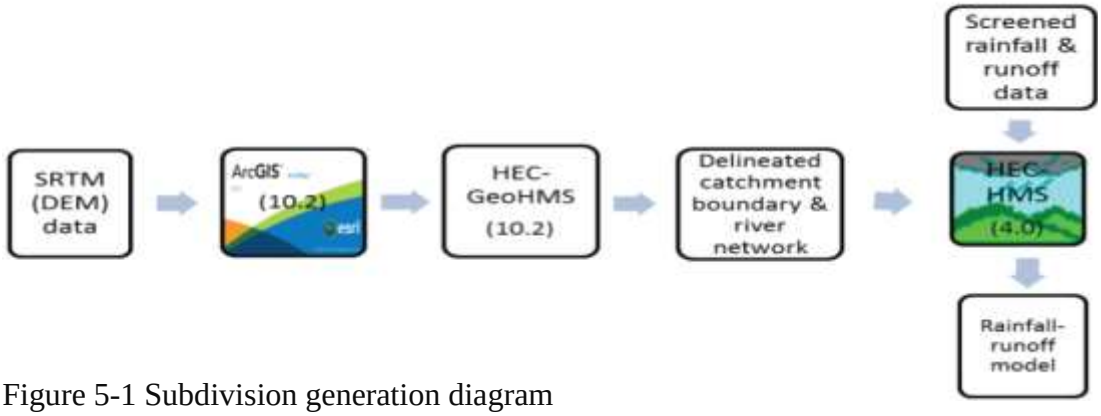

Figure 5-1 Subdivision generation diagram

Source: (Kumar & Merwade, 2009)

According to Figure 5-1, a DEM was used as a primary data source for initiating this process. The ArcGIS software with the extension of Arc-Hydro and HEC-GeoHMS facilitated the delineation of catchment and sub-catchments boundaries. After executing the maximum threshold area method, the remaining number of parameters was developed for the individual sub-watersheds using many tools, primary through HEC-GeoHMS. The HEC-GeoHMS facilitated the importing of boundary and basin parameters to the HEC-HMS model, for developing a rainfall-runoff model, in this case, for the Kelani river basin in Sri Lanka.

Table 5-1 Literature support for delineation of the watershed

Authors	Literature support	Methods
Kanchanamala, D. P. H. M., Herath, H. M. H. K., & Nandalal, K. D. W	Kanchanamala, D. P. H. M., Herath, H. M. H. K., and Nandalal, K. D. W. (2016). Impact of catchment-scale on rainfall-runoff modeling: Kalu Ganga river catchment up to Ratnapura. Engineer: journal of the institution of engineers, Sri Lanka, 49(2).	River network, landuse
Zhang, H. L., Wang, Y. J., Wang, Y. Q., Li, D. X., & Wang, X. K.	Zhang, H. L., Wang, Y. J., Wang, Y. Q., Li, D. X., and Wang, X. K. (2013). The effect of watershed scale on HEC-HMS calibrated parameters: a case study in the Clear Creek watershed in Iowa, US. Hydro. Earth Syst. Sci., 17(7), 2735–2745	Threshold area using stream network
Kim, J.-G., Park, Y., Yoo D., Kim, N.-W., Engel, B. A., Kim, S., … Lim, K. J	Kim, J.-G., Park, Y., Yoo, D., Kim, N.-W., Engel, B.A., Kim, S., Lim, and K. J. (2009). Development of a SWAT patch for better estimation of sediment yield in Steep Sloping watersheds. JAWRA Journal of the American Water Resources Association, 45(4), 963–9	Threshold area using stream network
Narayan Prasad Gautam	Narayan Prasad Gautam (2015).Hydrological modeling with HEC-HMS in different channel sections in case of Gandaki river, basin Global Journals Inc.,(USA) 2249-4596	Stream network
Manoj Jha, Philip W. Gassman, Silvia Secchi, Roy Gu, and Jeff Arnold	Manoj Jha, Philip W. Gassman, Silvia Secchi, Roy Gu, and Jeff Arnold (2004). Effect of the watershed subdivision on SWAT flow, sediment and nutrient predications.	Randomly using stream network
Tripathi, M. P., Raghuwanshi, N. S., and Rao, G. P	Tripathi, M. P., Raghuwanshi, N. S., and Rao, G. P. (2006). Effect of the watershed subdivision on simulation of water balance components. Hydrological Processes, 20, 1137–1156.	Automatic delineation
Thuy Luong	Thuy Luong, 2008.Cleveland subdivision of Texas watersheds for hydrologic modeling, Texas Tech University college of engineering	Equal area method
David B Thompson and Theodore G Cleveland	David B. Thompson, Theodore G. Cleveland. (2009). subdivision of Texas watersheds for hydrologic modeling, Texas Tech University college of engineering	Heuristic approach

5.6 Sensitivity analysis

Sensitivity analysis involves measuring the effect of a parameter on the simulation process. Sensitivity analysis is potentially useful in all phases of the modelling process, including model formulation, model calibration, and model verification (McCuen, 1973). This study found that overall, the impervious percentage was the most sensitive parameter and recession constant was the least sensitive parameters. For the SMA model, the soil percolation and tension storage were the most sensitive parameters and GW2 was the least sensitive parameter. These results were compared with similar studies worldwide, as shown in Table 5-2.

Table 5-2 Comparison of sensitive analysis results based on the literature

Study	River basin	Sensitive parameters
(Rahman Davtalab, et al., 2015)	Karkheh	Recession constant and tension storage
(Sok & Oeurng, 2016)	Tonle Sap Lake	Tension storage, Soil percolation
(Samady, 2017)	Colorado	GW2 percolation, tension storage
(Bhuiyan, McNairn, Powers, & Merzouki, 2017)	Sturgeon Creek	Soil storage, max infiltration, soil percolation
(Begam, Ghosh, Jana, & Roy, 2013)	Eastern India	Soil storage, imperviousness, soil percolation
(Cunderlik & Simonovic, 2004)	Thames	Tension storage, max infiltration
(McEnroe, 2010)	Johnson County	Soil storage, impervious, max infiltration
(Rahul Singh & K.Jain, 2015)	Vamsadhara	Soil storage and soil percolation

It can be illustrated using Table 5-2 that in most research relates to the SMA model, the tension storage, soil percolation, and impervious percentage are found to be the most sensitive parameters. In the current research work, the impervious percentage, soil percolation, and tension storage parameters were found to be the most sensitive parameters (shown in Figure 4-8 and Figure 4-9).

5.7 Results discussion

All the results acquired after the analysis are shown in the form of water balance, flow duration curves, outflow hydrographs and objective functions which will be discussed here in details.

5.7.1 Annual water balance

The summary of annual water balance results for the lumped and distributed models (three, five, eight and 12 subdivisions) are shown in Table 5-3. If the results of that water balance are below 10% compared to the observed water balance, then the model is reliable (Martinez & Gupta, 2010). In this comparison, the eight-subdivision model showed the lowest error during the calibration and verification periods, with percentages of 3.05% and 4.66%, respectively. After that, the lumped mode and the three, five, and eight-subdivision models were marked with the highest error in chronological order. It can be easily observed from Table 5-3 that the lumped model during the entire period of the study indicated the least variation of errors, followed by the eight-subdivision model. The 12-subdivision model shows the most difference over the entire period of study.

Table 5-3 Comparison of annual water balance errors

Period	**Water year**	**Annual water balance absolute error percentage %**				
		Lumped	**3 Sub divisions**	**5 Sub divisions**	**8 Sub divisions**	**12 Sub divisions**
Calibration	2007/2008	5.14	7.82	5.07	2.90	4.01
	2008/2009	2.34	2.37	2.68	1.56	5.74
	2009/2010	2.03	0.89	2.53	1.22	5.80
	2010/2011	2.73	2.99	3.17	0.29	4.27
	2011/2012	6.84	12.26	4.91	9.27	1.13
Verification	2012/2013	6.95	5.25	10.64	6.95	14.51
	2013/2014	3.60	5.59	0.86	3.60	5.86
	2014/2015	2.17	1.42	9.17	2.17	13.01
	2015/2016	4.50	6.63	6.97	4.50	5.10
	2016/2017	6.06	6.01	1.37	6.06	0.75
Average	Calibration	3.82	5.27	3.67	3.05	4.19
	Verification	4.66	4.98	5.80	4.66	7.85
	Overall	4.24	5.12	4.74	3.85	6.02

5.7.2 Flow duration curve

The flow duration curve for the lumped model, as shown in Figure 4-12 indicates many variations of low flows compared to intermediate and high flows in the calibration period. This variation was even higher in the verification periods compared to the calibration periods concerning intermediate and high flows (shown in Figure 4-13).

The three-subdivision model during the calibration period (Figure 4-22) identified the overall lowest variation of calculated flow, with much improvement of low flows compared to the lumped model. The variation of calculated flow did not closely surrounding over the observed flow in half part of high and intermediate flows. For the verification period in the three-subdivision model (Figure 4-23) a similar case was found in respect to the calibration period. Although it showed some improvement for the intermediate flow, in the case of high flows, many fluctuations were identified. For the five-subdivision model's calibration (Figure 4-30) period, the intermediate and low flows indicated much less variation. Also, the calculated flow is surrounding the observed flow around the middle part. For the verification period (Figure 4-31), similar to the calibration period, the flow duration curve showed better variation around the observed flow. In the verification period, less variation occurred during the high flows.

For the eight-subdivision model in the calibration period (Figure 4-39) overall, less fluctuation of simulated flow was identified compared to observed flow. Similarly, for the verification period (Figure 4-40), the variation within the intermediate and low flows was similar to that of the five-subdivision model, for which the calculated flow nearly surrounded the observed streamflow curve. For the final subdivision model (12 subdivisions) in the calibration period (Figure 4-48), high variation was identified within the intermediate and low flows compared to the observed flow. During the verification period (Figure 4-49), the low and intermediate flows indicated high variation, similar to the calibration period. In the verification period, however, the high flows show a huge amount of fluctuation compared to other subdivision models.

In summary of this discussion, the five-subdivision showed the best results out of all the models considering the intermediate and low flows. In the five-subdivision model, the variation of the calculated flow was less around the observed flow, showing fewer

fluctuations compared to other models. Considering the above criteria, the eight-subdivision model and the lumped model can be called the best models. The three-subdivision model is in an average position, but the 12-subdivision model is the worst.

5.7.3 Outflow hydrograph

The outflow hydrograph was discussed mostly through visual observation according to time of peak and matching of high, intermediate, and low flows (Cheng, Cheng, Jet-chau, & Ju-huang, 2013). According to the mentioned criteria, each model is discussed individually in Tables 5-4 to 5-8. Based on the main scope of the model application to water resource assessment purposes, the low and intermediate flows need to be well matched. To improve the low flow accuracy, the lumped model was divided into subdivisions to showing more accuracy. In all subdivided models, calculated flows were well simulate for high flows, but not for the low flows. All models could be used for flooding purposes, but regarding the water resources assessment, the simulation of low and intermediate flows is better in the models with three to eight subdivisions. The lumped and 12-subdivision models showed poorer results.

Table 5-4 Discussion details about the lumped model hydrograph

Lumped model hydrograph results discussion						
Sub divisions	Period	Water year	Time to peak	Peaks (high flow)	Intermediate	Low flow (rainless period)
Lumped	Calibration	2007/2008	Matching	Matching	Matching	Not matching only in Dec 2007, Jan and Feb 2008
		2008/2009	Matching	Matching	Not matching very well	Not matching only in Jan, Feb and March 2009
		2009/2010	Matching	Matching	Matching	Not matching only in Feb and March 2010
		2010/2011	Matching	Matching	Matching	Nearly matching
		2011/2012	Matching	Not matching very well	Not matching very well	Poor matching
	Verification	2012/2013	Matching	Matching	Not matching very well	Not matching only in some days between Jan, Feb, and March
		2013/2014	Matching	Not matching very well	Matching	Not matching only in months between Dec 2013 and Mar 2014
		2014/2015	Matching	Matching	Matching	Not matching very well
		2015/2016	Matching	Matching	Poor matching	Poor matching
		2016/2017	Matching	Matching	Matching	Not matching very well
Conclusion						
Subdivisions		Period	Time to peak	Peaks (high flow)	Intermediate	Low flow (rainless period)
Lumped		Calibration	Matching	Almost matching	Almost matching but not poor	Poor matching
		Verification	Matching	Almost matching	Almost matching but not poor	Poor matching
		Overall	Matching	Almost matching	Almost matching but not poor	Poor matching

Table 5-5 Discussion details about the three-subdivision model hydrograph

Three-subdivision model hydrograph results discussion						
Subdivisions	Period	Water year	Time to peak	Peaks (high flow)	Intermediate	Low flow (rainless period)
3	Calibration	2007/2008	Matching	Not matching only on Oct and Nov 2007	Matching	Not very well matching only in the month of (Nov, Dec 2007) and (Ja, Feb 2008)
		2008/2009	Matching	Matching	Matching	Matching
		2009/2010	Matching	Matching	Matching	Not matching only in Feb March and Sept 2010
		2010/2011	Matching	Matching	Matching	Nearly matching
		2011/2012	Matching	Matching	Not matching very well	Not matching very well
	Verification	2012/2013	Matching	Matching	Not matching very well	Almost matching
		2013/2014	Matching	Matching	Not matching very well	Poor matching
		2014/2015	Matching	Not matching very well	Matching	Not matching very well
		2015/2016	Matching	Matching	Not matching very well	Not matching very well
		2016/2017	Matching	Not matching very well	Matching	Not matching very well
Conclusion						
Subdivisions		Period	Time to peak	Peaks (high flow)	Intermediate	Low flow (rainless period)
3		Calibration	Matching	Almost matching	Almost matching but not poor	Almost matching but not poor
		Verification	Matching	Almost matching	Almost matching but not poor	Almost matching but not poor
		Overall	Matching	Almost matching	Almost matching but not poor	Almost matching but not poor

Table 5-6 Discussion details about the five-subdivision model hydrograph

Five-subdivision model hydrograph results discussion						
Subdivisions	Period	Water year	Time to peak	Peaks (high flow)	Intermediate	Low flow (rainless period)
5	Calibration	2007/2008	Matching	Poor matching only on Oct and Nov 2007	Matching	Almost matching
		2008/2009	Matching	Matching	Matching	Matching
		2009/2010	Matching	Matching	Matching	Almost matching
		2010/2011	Matching	Matching	Matching	Almost matching
		2011/2012	Matching	Matching	Not matching very well	Matching
	Verification	2012/2013	Matching	Matching	Not matching very well	Not matching very well
		2013/2014	Matching	Matching	Matching	Not matching very well
		2014/2015	Matching	Matching	Matching	Matching
		2015/2016	Matching	Matching	Matching	Almost matching
		2016/2017	Matching	Matching	Not matching very well	Almost matching
Conclusion						
Subdivisions		Period	Time to peak	Peaks (high flow)	Intermediate	Low flow (rainless period)
5		Calibration	Matching	Matching	Almost matching	Almost matching
		Verification	Matching	Matching	Almost matching	Almost matching
		Overall	Matching	Matching	Almost matching	Almost matching

Table 5-7 Discussion details about the eight-subdivision model hydrograph

Eight-subdivision model hydrograph results discussion						
Subdivisions	Period	Water year	Time to peak	Peaks (High flow)	Intermediate	Low flow (rainless period)
8	Calibration	2007/2008	Matching	Poor matching only on Oct and Nov 2007	Matching	Matching
		2008/2009	Matching	Matching	Matching	Matching
		2009/2010	Matching	Matching	Matching	Almost matching
		2010/2011	Matching	Matching	Matching	Almost matching
		2011/2012	Matching	Matching	Not matching very well	Not matching very well
	Verification	2012/2013	Matching	Matching	Not matching very well	Not matching very well
		2013/2014	Matching	Matching	Almost matching	Not matching very well
		2014/2015	Matching	Not matching very well	Matching	Almost matching
		2015/2016	Matching	Matching	Matching	Almost matching
		2016/2017	Matching	Matching	Matching	Almost matching
Conclusion						
Subdivisions		Period	Time to peak	Peaks (high flow)	Intermediate	Low flow (rainless period)
8		Calibration	Matching	Matching	Almost matching	Almost matching
		Verification	Matching	Matching	Almost matching	Almost matching
		Overall	Matching	Matching	Almost matching	Almost matching

Table 5-8 Discussion details about the 12-subdivision model hydrograph

12-subdivision model hydrograph results discussion						
Subdivisions	Period	Water year	Time to peak	Peaks (high flow)	Intermediate	Low flow (rainless period)
12	Calibration	2007/2008	Matching	Poor matching only on Oct and Nov 2007	Matching	Not matching only in Dec 2007 and (Jan, Sep) 2008
		2008/2009	Matching	Matching	Not matching very well	Poor matching
		2009/2010	Matching	Matching	Poor matching	Poor matching
		2010/2011	Matching	Matching	Not matching very well	Poor matching
		2011/2012	Matching	Matching	Not matching very well	Poor matching
	Verification	2012/2013	Matching	Matching	Matching	Poor matching
		2013/2014	Matching	Matching	Matching	Poor matching
		2014/2015	Matching	Not matching very well	Matching	Poor matching
		2015/2016	Matching	Matching	Not matching very well	Poor matching
		2016/2017	Matching	Matching	Matching	Poor matching
Conclusion						
Subdivisions		Period	Time to peak	Peaks (high flow)	Intermediate	Low flow (rainless period)
12		Calibration	Matching	Almost matching	Almost matching	Poor matching
		Verification	Matching	Almost matching	Almost matching	Poor matching
		Overall	Matching	Almost matching	Almost matching	Poor matching

5.7.4 Model performance

The main purpose of these models is for water resources assessment studies along the Kelani river basin, Sri Lanka. Therefore, the important primary parts of the flow are medium and low flows. According to this rationalization, the MRAE, PVE, and R^2 play an essential role in determining the accuracy of the model, with more focus on MRAE due to its nature of usage in intermediate flows.

During the comparison of medium flows (Figure 4-81) in the calibration period with the mentioned objective functions, MRAE values were found much lower in the three to eight-subdivision models. Consequently, the PVE had the lowest error in the five-subdivision model (near zero). The PVE indicator has a constant rate between the lumped and three-subdivision models (5 to 10%), but the error percentage increase (greater than 10%) after the eight subdivisions. During the verification period, MRAE had the lowest value in the five-subdivision model (Figure 4-85). Before and after five subdivisions, the MRAE value increased.

For the low flows during the calibration periods in all subdivisions (shown in Figure 4-82), the MRAE values show a constant rate, although it is much lower, for the models with five and eight subdivisions. With respect to PVE, the five-subdivision model had the lowest error, but the three and eight-subdivision models had a constant rate. Furthermore, for the verification period, the comparison of the low flow for all subdivisions as shown in Figure 4-61. It is clearly demonstrated that MRAE had the lowest values from five to eight subdivision models. In the same fashion, the PVE shows the lowest error in the five subdivision model, followed by, the eight and three-subdivision models.

For more clarity, the summary results are shown in Table 5-9. Based on Table 5-9, it can be seen that MRAE has the lowest value in the five-subdivision model. Further, after five subdivisions, eight subdivisions, the lumped model, three subdivisions and 12 subdivisions had the lowest values. With respect to PVE, eight and three subdivisions showed the lowest error, although five subdivisions was in the middle. Regarding the NSE, the maximum value was recorded in the lumped model (Nash=0.84) followed by five and three subdivisions (Nash= 0.81). The Nash value decreased to 0.70 after subdivision five. For R^2, the highest values were recorded in

the lumped model (R^2=0.85). Five subdivisions (R^2 =0.82) was the second highest, and three subdivisions (R^2=0.81) was the third highest. With the 12 subdivisions, R^2 But is reduced to 0.77.

Table 5-9 Summary of the model performance

Model	Nash/NSE	MRAE	PVE	R^2
Lumped	0.84	0.45	7.45%	0.85
3 subdivisions	0.81	0.48	1.31%	0.81
5 subdivisions	0.81	0.37	9.19%	0.82
8 subdivisions	0.78	0.42	-0.13%	0.78
12 subdivisions	0.70	0.49	13.87%	0.77

In summary of this discussion part, it was found from the MRAE perspective that the subdivisions should be between three and eight.

5.7.5 Result comparison with similar studies

For justification of this research work, the acquired results were compared with the similar studies around the world using to HEC-HMS with the SMA algorithm. Most of these studies were used by the study to help set up the initial values. However, the final results in both cases (with data or with data scarcity) directly depend on calibration strategies and data quality.

In Table 5-10, a comparison of this research with other similar studies around the globe is presented. All these comparisons are based on the R^2 (coefficient of determination), PVE (percentage error in volume), and NSE objective functions. From this comparison, both the calibration and verification periods in this study indicate higher R^2 and NSE values compared to most of the studies, except for one by R. Meenu (2012). In that research, the values for the PVE and NASH indicators are greater compared to the current research. It was also found that nearly all studies around the world were conducted for flood and drought issues and used the NSE indicator as a primary objective function. In this research work, the MRAE objective function was used, focusing on medium flow rather than high flow.

Table 5-10 Comparison of the results with similar studies

Study	Methods	Objective functions					
		Calibration period			Verification period		
		R^2	PVE/PBIAS%	NSE	R^2	PVE/PBIAS%	NSE
(Bene & Koch, 2013)	SMA-HMS	0.72	4.66	-	0.60	23.18	-
(Bashar & Zaki, 2005)	SMA-HMS	0.78	-	-	0.69	-	-
(Begam, Ghosh, Jana, & Roy, 2013)	SMA-HMS	0.79	-22.62	0.86	`0.74	-24.14	0.66
(Samady, 2017)	SMA-HMS	0.73	17	0.7	0.86	-12.6	0.73
(Rahul Singh & K.Jain, 2015)	SMA-HMS	0.71	2.64	0.7	0.78	12.33	0.76
(Rahman Davtalab, et al., 2015)	SMA-HMS	0.87		0.7	0.88		0.76
(Ali, Razmkhaha, & Saghafian, 2016)	SMA-HMS	-	0.79	0.76	0.64	-8.09	
(Akay, Koçyiğit, & Yanmaz, 2017)	SMA-HMS	0.63	-28.7	0.76	0.65	-29.9	0.64
(Garcıa, Revilla, & Sainz, 2008)	SMA-HMS	-	-	0.79	-	-	0.72
(Legesse, 2015)	SMA-HMS	0.73	12.3	0.71	0.78	7.49	0.77
(Ahmed, Azmat, Hussain, Qamar, & Umair, 2017)	SMA-HMS	-	22.39	0.77	-	32.51	0.70
(Meenu, Mujumdar, & Rehana, 2012)	SMA-HMS	0.72	0.07	0.48	0.77	1.96	0.59
Current research							
Current research on Kelani river basin, Sri Lank	SMA-HMS	0.83	5.3	0.82	0.81	13.07	0.80

5.8 Model reliability

In this section, the reliability of the model will be discussed in terms of the SMA loss method, meteorological data, SMA algorithm methods, and parameters.

5.8.1.1 Perception loss method

The main purpose of this research was to apply the SMA loss method in a catchment with a lack of soil data. Due to a complete representation of the natural loss of water through the soil layers, the SMA model is recommended by many scholars and modellers, although there is a possibility that other loss methods such as the Green and Ampt, deficit, and constant methods may show better results rather than SMA. It is also worth mentioning that the SMA method was designed in such a way as to be compatible with a catchment having all the necessary soil information. In this study, due to lack of this data, using the SMA in not used with a conventional approach.

5.8.2 Uncertainty in meteorological data

The reliability of this research directly relates to the correctness of the meteorological data along with the accuracy of the interpolation method. The rainfall and evaporation spatial and temporal variability is the main reason for this uncertainty. In the data checking section, it is specified that some meteorological stations have some data issues. The Thiessen method was used for the estimation of average rainfall values, though Thiessen itself is a probable method. There are many interpolation methods that can be used in conjunction with the Thiessen method, like the Inverse Distance Method (IDW) and the Spline. These need to be considered in future research works.

5.8.3 Uncertainty in the SMA algorithm setup

For the SMA algorithm setup, it is required to select a range of methods to calculate the canopy storages, the surface storages, the soil loss, and the transform, baseflow, and routing methods. Due to the existence of a high number of methods, many uncertainties can exist that will be discussed in below.

5.8.3.1 Transform model (direct runoff)

The transform (direct runoff) model was selected for the present study considering the following criterion: (1) physical parameters, (2) number of parameters, (3) compatibility with the SMA, and (4) appropriateness of assumptions.

Considering the above criterion, qualitative method evaluations, and the suggestions of most prominent literature, the modified Clark method (ModClark) was used for the transform model. The Clark Method was used in this study along with gridded meteorological data, defining a linear quasi-distributed unit hydrograph method. Many methods for the transform model exist, such as the Soil conservation service (SCS), the user-specified s-graph, the user-specified unit hydrograph, the Snyder unit hydrograph, the Kinematic wave, and the Clark unit hydrograph. Practically checking the mentioned methods along with the Clark method is a matter for another research works to consider in future studies.

5.8.3.2 Baseflow model

The recession method was selected for the baseflow model out of five available methods in the HEC-HMS model using the following criterion: (1) the number of parameters, (2) the consideration of soil moisture, (3) the usage in the literature, and (4) ease of used in data-poor situations. The limits given in the HEC-HMS model during the optimization process for the recession constant and threshold parameters were between 0 to 1. Primarily for the SMA model, its recommended by HEC (2000) to use the linear reservoir baseflow method rather than the recession constant method. Due to little literature support, the long number of parameters, and the lack of data and time, it was omitted in this research. However, there is a possibility that using the linear reservoir may further improve the baseflow simulation. Practically using the bounded recession, constant monthly, and nonlinear boussinesq base flow methods may influence the results, which needs to be considered in future studies.

5.8.3.3 Routing model

The simple Muskingum routing method was selected out of the six available methods in the HEC-HMS model to route the flow through a channel. The selections process was based on the following criterion: (1) the number of parameters, (2) the

consideration of soil moisture, (3) the usage in the literature, and (4) the ease of use in data-poor situations. The selection of the Muskingum routing model using the mentioned criteria was based on the qualitative approach. In the condition of the existing wide range of data, it is possible that other methods such as the Lag, the Kinematic Wave, the Muskingum-cunge, and the Straddle-stagger method produce would produce better results in practice. Future research works will determine the preciseness of the mentioned methods with the SMA model.

5.8.4 Uncertainty in parameter estimation

All methods used along with the SMA loss model require certain parameters to be estimated. Different studies suggesting different methods, but in a situation where there is not enough data, not all the methods are practical. This difference varies from place to place, with most of the methods having an empirical base rather than a scientific base, which will be discussed in detail in the following sections.

5.8.4.1 Canopy storage

Canopy storage represents the maximum amount of water that can be held on leaves before falling to the earth's surface. The canopy will consume all the potential evapotranspiration until the water in storage has been eliminated. These values were obtained from GIS analysis of landuse and land cover (LULC) maps (Rezaeianzadeh, Stein, & Tabari, 2013). For the current study, the LULC maps do not represent the exact ground situation of vegetation due to being older versions. Another drawback in the current landuse map is that the kinds of vegetation shown generally vary versus reality. In the real scenario, the vegetation cover is widely different that on the generated map (Figure 4-1), because every single vegetation type has a different storage capacity. For this research work using the available landuse map, all vegetation was classified according to Bennett and Peters (2000) into three parts respect to its storage (shown in Table 4-3). Real storage capacity estimations for every single vegetation type requires a huge budget and a huge amount of time.

5.8.4.2 Surface storage

The surface storage retention of earth surface after a rainfall was calculated using the slope map (Figure 4-2) suggested by Bennett et al. (2000) shown (). In reality, the

surface storage capacity can be acquired through land survey and remote sensing techniques after a rainfall. In developing countries such as Sri Lanka, due to a lack of enough equipment, this seems impossible. The slope map (Figure 4-5) in the current study was generated by a 30-meter resolution DEM, which is not very accurate. In the existence of those realities, there is a possibility of miscalculating of surfaces storage. This has a major contribution to streamflow and can affect the model results.

5.8.4.3 Precipitation loss method

The SMA loss method was selected which, requires 14 parameters to be set. Out of that, four parameters are initial that need to be set randomly, and the final values will come through the calibration process (Table 4-2). The impervious percentage was calculated through the landuse map (Figure 4-3), which was not very accurate it was published in 2006. Another four parameters – groundwater 1 storage, groundwater 2 storage, the groundwater 1 coefficient, and the groundwater 2 coefficient – were calculated through the streamflow recession analysis (Equation 4-3 to 4-7) . The groundwater 1 percolation and groundwater 2 percolations were set through the calibration procedure. In fact, these parameters can be calculated by observed inspection wells, which was not considered in this case.

The remaining four parameters, which are the maximum infiltration, soil storage, tension storage, and soil percolation rate, were calculated from similar studies due to the lack of hydraulic property data of the soil. In this method, a range of values has to be put to every parameter that needs to be further calibrated. Indeed, the real value of these parameters requires having complete hydraulic properties of the soil, which in the Sri Lankan context is very rare.

Finally, it is easy to judge that because of the data limitations, the final parameter values cannot represent the real situation as it expected. There is an always possibility of the incorrectness which can affect the final results. It can be concluded that all efforts in this research rely on calibration, which takes much of time and effort.

5.8.4.4 Transform model

The ModClark method was selected for the transform model, which mainly requires two parameters: time of concertation (Tc) and storage coefficient (S). For the

calculation of these two parameters, many methods exists, such as the Bransbey Willium, Dooge Micking, Ven te Chow, Pickering, and SCN methods. Most of the mentioned methods are empirical, and some of them require one or two basic parameters. But the Soil Conservation service (SCN) method is widely used by most researcher due to it considering the physical properties of a channel (length, slope, and soil). Other methods are more conceptual. For this research, based on the literature review, the SCN method was selected (Equation 4-1), but the parameters like slope, length and curve number were estimated form sources that were not very precise or updated.

5.8.4.5 Baseflow method

The recession constant method was used for the base flow computation. This requires three parameters: initial discharge, recession constant, and ratio to peak. The initial discharge was set to the initial discharge from the observed streamflow. The recession constant and the ratio to the peak were calculated using the selected events. The main issue with the estimation of those parameters was existence of various events. The outcome of the final values was based on the calibration procedure. Increasing the number of subbasins with the SMA model is a challenging task, especially during the calibration process. As a result of that, all the burden is put on the automatic calibration procedure. This takes a longer time, and parameters do not well-presenting the real situation.

5.8.4.6 Routing method

The Muskingum routing method is based on a simple conservation of mass approach the defines the route through the stream. This approach was widely used in flow routing processes (Andreassian, Berthet, Javelle, & Perrin, 2009). The Muskingum method requires two parameters, which are K and X. The K defines the travel time through the reach and can be estimated through the knowledge of the cross section and flow properties. The X parameter is the weighing between inflow and outflow influence, which ranges between 0 and 0.5. For this study, all values were based on assumptions using different previous studies and ranges of values. The final values were optimized using the calibration procedure. These values affect the time of peak, but in this study due much effort put into the calibration process, the peaks were well matching in the lumped and all subdivision models.

6 CONCLUSIONS

1. The HEC-HMS model with SMA algorithm was successfully calibrated and verified for the Kelani river basin in Sri Lanka on a continuous daily time scale and can be used for a variety of purpose including water resources assessment, engineering and management.
2. The result of flow duration curve, outflow hydrograph, water balance, and statistical performance indicates an increasing efficiency in the determination of intermediate and low flows with the distributed models between three to eight subdivisions. The optimum result was with five-subdivision model.
3. The MRAE error was decreased by increasing the number of subdivisions to three and eight, with an optimum of five subdivisions giving an MRAE of 0.38 during calibration and 0.36 during the verification period.
4. This study reveals that the soil moisture parameters could have a significant impact on the streamflow, especially on peak flows. This is because the soil percolation rate was found to be the most sensitive parameter.
5. This study shows that moisture parameters for the SMA model can be derived from similar studies and streamflow records in case of a soil-data-scarce situation.
6. The results of statistical analyses indicate that the simulated values are well correlated with the measured flow in the five subdivisions model with overall MRAE 0.37, a Nash 0.81 and a PVE 9.2%.
7. The low flows was underestimated during the long rainless period in the lumped model, but improved with the distributed models, and especially for the five subdivisions.
8. Increasing the number of subdivisions with the HEC-HMS model and SMA algorithm add to the complexity of the calibration and optimization process which requires a lot of computing time and high processing power.

7 RECOMMENDATIONS

1. This verified model (HEC-HMS with SMA algorithm) can be used for water resources assessment, flood forecasting and infrastructure design over the Kelani river basin, Sri Lanka.
2. The number of sub-catchment should be minimized when using the HEC-HMS model with SMA algorithm, but more attention should be paid to the correct estimation of the initial parameters.
3. The results can be further improved by using multiple gauging stations, and it is recommended that multiple gauging stations be used instead of a single station for better calibration.
4. Incorporating hourly and monthly data should be compared with daily data for further studies for further improvement of the results.
5. Other loss methods besides the SMA such as the Green Ampt and the SCN curve method needs to be checked for overall result comparison.
6. Spatial variability should be checked beside the Thiessen interpolation methods for increasing the mode result efficiency.
7. For continuation of this research work, this model should be compared with mathematical models, such as two, three and four parameter models.

REFRENCES

Ahmed, S., Azmat, M., Hussain, E., Qamar, M., & Umair, M. (2017). Application of HEC-HMS for the event and continuous simulation in high altitude scarcely-gauged catchment under changing climate. *European water, 57*, 77-84. doi:10.1007/s12665-015-5059-2

Akay, H., Koçyiğit, M., & Yanmaz, A. (2017). Estimation of hydrologic parameters of Kocanaz watershed by a hydrologic model. *International journal of engineering & applied sciences (IJEAS), 9*(4). doi:http://dx.doi.org/10.24107/ijeas.342039

Ali, A., Razmkhaha, H., & Saghafian, B. (2016). *Water resources, 43*(4), 699-710. doi:0.1134/S0097807816040072

Ali, M. M., Narzis, A., & Haque, S. (2016). Impacts of climate changes on peak flow of upper Meghna river basin. *Journal of PU, Part: B, 3*(2), 54-63. Retrieved from https://doi.org/10.1002/joc.1076

Andreassian, V., Berthet, L., Javelle, P., & Perrin, C. (2009). How crucial is it to account for the antecedent moisture conditions in flood forecasting? comparison of event-based and continuous approaches on 178 catchments. *Hydrology and earth system sciences, 13*, 819-831. Retrieved from https://doi.org/10.5194/hess-13-819-2009

Arekhi, S. (2012). Runoff modeling by HEC-HMS model (case study: Kan watershed, Iran). *International journal of agriculture and crop sciences, 4*(23), 1807-1811. Retrieved from http://pakacademicsearch.com/pdf-files/agr/70/1807-1811.pdf

Arlen, D., & Feldman. (2000). *Hydroligal modeling system technical reference manual.* Davis: US amy corps of engineer. Retrieved from http://www.hec.usace.army.mil/software/hec-hms/documentation/HEC-HMS_Technical%20Reference%20Manual_(CPD-74B).pdf

Arnold, J. G., Srinivasan, R., Muttiah, R. S., & J. (1998, February). Large area hydrologic modeling and assesment. *American water resources association, 34*(1), 73-89. Retrieved from http://ssl.tamu.edu/media/11951/large%20area%20dyrologic%20modeling%20and%20assessment%20part%201.pdf

Arnold, J., Allen, P., Mutt1ah, R., & Ber, G. (1995). Automated base flow separation and recession analysis techniques. *Association of ground water scientists and engineers, 33*, 1010-1018. doi:https://doi.org/10.1111/j.1745-6584.1995.tb00046.x

Barnston, A. (1992). *Correspondence among the correlation, RMSE, and Heidke forecast verification measures; refinement of the Heidke Score.* Washington,

D.C.: Climate analysis center, NMC/NWS/NOAA,. doi:https://doi.org/10.1175/1520-0434(1992)007<0699:CATCRA>2.0.CO;2

Bashar, K., & Zaki, A. (2005). SMA based continuous hydrologic simulation Of The Blue Nile. *International conference of UNESCO Flanders Fust Friend/Nile project towards a better cooperation and the 5th project management meeting and 9th steering committee* (pp. 1-10). Cairo: UNESCO chair in water resources. Retrieved from http://www.unesco.org/new/fileadmin/MULTIMEDIA/FIELD/Cairo/pdf/SMA_Based_Continuous_Hydrologic_Simulation_Of_The_Blue_Nile.pdf

Begam, S., Ghosh, S., Jana, S., & Roy, D. (2013, January). Calibration and validation of HEC-HMS model for a river basin in eastern India. *Journal of engineering and applied sciences, 8*(1), 40-56. Retrieved from www.arpnjournals.com/jeas/research_papers/rp_2013/jeas_0113_847.pdf

Bene, K., & Koch, R. (2013, June). Continuous hydrologic modeling with HMS in the Aggtelek Karst region. *Science publishing group, 1*, 1-7. doi:10.11648/j.hyd.20130101.11

Bennett, T. (1998). *Development and application of a continuous soil moisture accounting algorithm for the Hydrologic Engineering Center Hydrologic Modeling System (HEC-HMS).* University of California, Davis. doi:https://doi.org/10.1061/(ASCE)1084-0699(2004)9:3(175)

Bennett, T., & Peters , J. (2000). Continuous soil moisture accounting in the hydrologic engineering center hydrologic modeling system (HEC-HMS). *Water resouces*, 1-10. Retrieved from https://doi.org/10.1061/40517(2000)149

Beven, K. (2001). How far can we go in distributed hydrological modelling? *Hydrology and earth system sciences, 5*(1), 1-12. doi:https://doi.org/10.5194/hess-5-1-2001

Bhuiyan, H., McNairn, H., Powers, J., & Merzouki, A. (2017). Application of HEC-HMS in a cold region watershed and use of RADARSAT-2 soil moisture in initializing the model. *Hydrology*, 1-19. doi:10.3390/hydrology4010009

Bouvier, C., Tramblay, Y., & Martin, C. (2010, April). Assessment of initial soil moisture conditions for event-based rainfall–runoff modelling. *Journal of hydrology, 387*, 176-187. doi:https://doi.org/10.1016/j.jhydrol.2010.04.006

Cai, Y., Wang, B., Xu, L., & Yue, W. (2016). An inexact two-stage stochastic programming model for sustainable utilization of water resource in Dalian city. *International journal of smart home, 10*, 27-38. Retrieved from http://www.sersc.org/journals/IJSH/vol10_no5_2016/4.pdf

Canfield, H., & Goodrich, D. (1995). Studies of scale and processes in hydrologic modeling on the Lucky Hills watershed. *Agricultural research service (USDA-ARS)*, 444-450. Retrieved from https://www.tucson.ars.ag.gov/unit/Publications/PDFfiles/1488.pdf

Cheng, C.-d., Cheng, S.-j., Jet-chau, W., & Ju-huang, L. (2013, June). Time and flow characteristics of component hydrographs related to rainfall–streamflow observations. *Journal of hydrologic engineering*. doi:https://doi.org/10.1061/(ASCE)HE.1943-5584.0000675

Chow, V., Maidment, D., & Mays, L. (1988). *Applied hydrology.* Singapore: McGraw-Hill. Retrieved from https://ponce.sdsu.edu/Applied_Hydrology_Chow_1988.pdf

Chu, X., & Steinman, A. (2009). Event and continuous hydrologic modeling with HEC-HMS. *Journal of irrigation and drainage engineering, 135*, 119-124. doi:https://doi.org/10.1061/(ASCE)0733-9437(2009)135:1(119)

Coefficient of determination R2. (2008). In F. Ruggeri, R. Kenett, & F. W. Faltin, *Major reference works.* Retrieved from http://sci-hub.hk/https://doi.org/10.1002/9780470061572.eqr173

Cunderlik, J. (2003). *Hydrologic model selection for the CFCAS project: assessment of water resources risk and vulnerability to changing climatic conditions.* Ontario: Department of civil and environmental engineering, the university of Western Ontario. Retrieved from https://www.eng.uwo.ca/research/iclr/fids/publications/cfcas-climate/reports/Report%20I.pdf

Cunderlik, J., & Simonovic, S. P. (2004). *Calibration, verification and sensitivity analysis of the HEC-HMS hydrologic model CFCAS project: assessment of water resources risk and vulnerability to changing climatic condition.* University of Western Ontario, civil and environmental engineering. Ontario: University of Western Ontario. Retrieved from https://www.scribd.com/document/268689590/Calibration-Verification-and-Sensitivity-Analysis-of-the-HEC-HMS

Davis. (1998). *Algrithm for the hydrologic engineering center hydrologic modeling system (HEC-HMS).* University of California. doi:https://doi.org/10.1061/40976(316)632

De Geroen, M. M. (2012). *Modelling interception and transpiration at monthly time steps introducing daily variability through Markov Chains.* Netherlands. Retrieved from http://108.kinetia.com.ar/modelling-interception-and-transpiration-at-monthly-time-steps-introducing-daily-variability-through-markov-chains.pdf

Devi, G. K., Ganasri, B. P., & Dwarakish, G. S. (2015). A review on hydrological models. *Aquatic Procedia, 4*, 1001-1007. doi:https://doi.org/10.1016/j.aqpro.2015.02.126

Dharmasena, G. T. (1997). Application of mathematical models for flood forecasting in Sri Lanka. *Destructive water: water-caused natural disasters, their abatement and control. 239*, pp. 225-235. Anaheim, California: Department of irrigation, Butlers road, Colombo 7, Sri Lanka. Retrieved from https://pdfs.semanticscholar.org/36a3/47a11cf9e5cebaccd1f94ad948a319d7a72b.pdf

Dissanayake, P. M. (2017). *Applicability of a two paramter water balance model to simulate daily rainfall-runoff a case study of Kalu and Gin river basins In Sri Lanka.* Department of civil engineering. Moratuwa: University of Moratuwa Sri Lanka. Retrieved from http://dl.lib.mrt.ac.lk/handle/123/13027

Fleming, M., & Neary, V. (2004). Continuous hydrologic modeling study with the hydrologic modeling system. *Jouranl of hydrologic engineering*, 183. doi:https://doi.org/10.1061/(ASCE)1084-0699(2004)9:3(175)

Ford, D., Pingel, N., & DeVries, J. (2008). *Hydrologic modeling system HEC-HMS.* Washington, DC: US army corps of engineers institute for water resources hydrologic engineering center. Retrieved from http://www.hec.usace.army.mil/software/hec-hms/documentation/HEC-HMS_Applications_Guide_March2008.pdf

Garcıa, A., Revilla, J., & Sainz, A. (2008, April). Surface water resources assessment in scarcely gauged basins in the north of Spain. *Journal of hydrology*, 312-326. doi:https://doi.org/10.1016/j.jhydrol.2008.04.019

Gautam, N. (2015). Hydrological modeling with HEC-HMS in different channel sections in case of Gandaki river basin. *Global journal of researches in engineering, 7*(2), 2249-4596. Retrieved from https://globaljournals.org/GJRE_Volume15/1-Hydrological-Modeling-with-HEC-HMS.pdf

Geethalakshmi, V., Umetsu, C., Palanisamy, K., & Yatagai, A. (2009, January). Impact of ENSO and the Indian ocean Dipole on the north-east monsoon rainfall of Tamil Nadu state in India. *Hydrological processes, 23*, 633-647. doi:https://doi.org/10.1002/hyp.7191

Ghaffari, G. (2011). The impact of DEM resolution on runoff and sediment modelling results. *Research journal of environmental sciences, 5(8)*, 691-702. Retrieved from http://digitalcommons.mtu.edu/etds/454/

Guo, S., & Wang, J. (2002, March). A macro-scale and semi-distributed monthly water balance model to predict climate change impacts in China. *Journal of hydrology, 268*, 1-15. doi:https://doi.org/10.1016/S0022-1694(02)00075-6

Gupta, H. V., Sorooshian, S., & `Yapo, P. O. (1995, April). Status of automatic calibration for hydrologic models: comparison with multi level expert calibration. *Journal of hydroloigc engineering, 4*, 135-143. doi:https://doi.org/10.1061/(ASCE)1084-0699(1999)4:2(135)

Gupta, H. V., Sorooshian, S., & Yapo, P. O. (1999, April). Status of automatic calibration for hydrologic models: comparison with multilevel expert calibration. *Journal of hydrologic engineering, 4*, 135-143. doi:https://doi.org/10.1061/(ASCE)1084-0699(1999)4:2(135)

Gupta, H., Sorooshian, S., & Yapo, P. (1999, April). Status of automatic calibration For hydrologic models: comparison with multilevel expert calibration. *Journal of hydrologic engineering, 135*, 135-143. doi:10.1061/(ASCE)1084-0699(1999)4:2(135)

Gyawali, R. (2013). *A hydro-climatic modeling framework for adaptive water resources management In the Great Lakes basin.* Environmental engineering. Michigan technological university. Retrieved from http://digitalcommons.mtu.edu/etds/454/

H. L, Z., Wang, Y. J., Li, D. X., & Wang, X. K. (2013). The effect of watershed scale on HEC-HMS calibrated parameters: a case study in the Clear Creek watershed in Iowa, US. *Hydrology and earth systme science, 17*(7), 2735-2745. doi:https://doi.org/10.5194/hess-17-2735-2013

Haque, S., Hossain, M., Hashimoto, M., & Salehin, M. (2017). Sensitivity analysis of SMA based continuous hydrologic simulation for Sari-Gowain river basin. *International conference on engineering research, innovation and education* (pp. 752-756). Sylhet, Bagaladesh: ICERIE. Retrieved from https://www.researchgate.net/publication/31233231

HEC. (2000). *Hydrologic modeling syste HEC-HMS: Technical reference manual.* Davis,Calif: U.S army corps of rngineers, hydrologic engineering center. Retrieved from http://www.hec.usace.army.mil/software/hec-hms/documentation/HEC-HMS_Technical%20Reference%20Manual_(CPD-74B).pdf

Holberg, J. (2015, May). *Downward model development of the soil moisture accounting loss method in HEC-HMS: revelations concerning the soil profile.* Purdue university, civil engineering. West Lafayette, Indiana: Purdue university. doi:https://docs.lib.purdue.edu/open_access_theses/501

Jain, S., & Singh, V. (2003). *Water resources systems planning and management.* USA: Elsevier science. doi:https://trove.nla.gov.au/work/27941617

Jajarmizadeh, M., Harun, S., & Salarpour, M. (2012). A review on theoretical consideration and types of models in hydrology. *Journal of environmental*

science and technology, 249-261. Retrieved from http://docsdrive.com/pdfs/ansinet/jest/2012/249-261.pdf

Jayadeera, P. M. (2016). *Development of A rainfall-runoff model For Kalu Ganga Basin of Sri Lanka Using HEC-HMS model.* Department of civil engineering. Moratuwa: University of moratuwa Sri Lanka. Retrieved from dl.lib.mrt.ac.lk/bitstream/handle/123/12800/pre-text.pdf?sequence=1

Jha, M., Gassman, P., Secchi, S., Gu, R., & Arnold, J. (2004, June). Effect of watershed subdivision on SWAT flow, sediment, and nutrient predictions. *Journal of the american water resources association*, 811-825. doi:https://doi.org/10.1111/j.1752-1688.2004.tb04460.x

Kanchanamala, D., Herath, H., & Nandalal, K. (2016). Impact of catchment scale on rainfall-runoff modeling: Kalu Ganga river catchment upto Ratnapura. *The institution of engineers, Sri Lanka, 49*, 1-17. doi:http://doi.org/10.4038/engineer.v49i2.7003

Khandu, D. (2015). *A monthly water balance model for evalution of climate change impacts on the streamflow of Gingaga and Kelani Ganga basins, Sri Lanka.* University of Moratuwa Sri Lanka, department of civil engineering. Moratuwa, Sri Lanka: University of Moratuwa Sri Lanka. Retrieved from http://dl.lib.mrt.ac.lk/handle/123/12893

Kim, J.-G., Park, Y., Yoo, D., Kim, N.-W., Engel, B., Kim, S.-j., . . . Lim2, K. (2009, August). Development of A SWAT patch for better estimation of sediment yield in steep sloping watersheds. *American water resources association, 45*(4), 963-972. doi:https://doi.org/10.1111/j.1752-1688.2009.00339.x

Krause, P., Boyle, D., & Bäse, F. (2005, Dec). Comparison of different efficiency criteria for hydrological model assessment. *Advances in geosciences, 5*, 89-97. Retrieved from https://hal.archives-ouvertes.fr/hal-00296842

Kumar , S., & Merwade, V. (2009, October). Impact of watershed subdivision and soil data resolution on SWAT model calibration and parameter uncertainty. *American water resources association, 45*(5), 1179-1156. doi:https://doi.org/10.1111/j.1752-1688.2009.00353.x

Legesse, S. (2015, May). Application of the HEC-HMS model for runoff simulation of upper Blue Nile river basin. *Sintayehu Legesse Gebre, 6*(2), 3-8. doi:http://dx.doi.org/10.4172/2157-7587.1000199

Li, D., Zhang, H., & Wang, Y. (2013). The effect of watershed scale on HEC-HMS calibrated parameters: a case study in the Clear Creek watershed in Iowa, US. *Hydrology and earth system sciences*, 2735-2745. Retrieved from https://www.hydrol-earth-syst-sci.net/17/2735/2013/hess-17-2735-2013.pdf

Linseley, Koiuer, R., M.A, & Paulus, J. (1958). *Applied hydrology.* New York: Mc Graw Hill.

Linsley, R. K. (1975). *Hydrology For engineers.* New York: New York: McGraw-Hill, [1975]. Retrieved from https://books.google.com.af/books/about/Hydrology_for_engineers.html?id=4fBOAAAAMAAJ&redir_esc=y

Luong, T. (2008). *Subdivision of watersheds for modeling.* University of Houston, civil and environmental engineering. Retrieved from http://www.rtfmps.com/resumes/MyWebPapers/thesis/thuy_thesis/0-5822_ThuyThesis.pdf

Madsen, H. (2000, May). Automatic calibration of a conceptual rainfall–runoff model using multiple objectives. *Journal of hydrology, 235*, 276-288. Retrieved from https://pdfs.semanticscholar.org/8d3b/ea25f6981cc1ad3c4bad630f298f0e218a37.pdf

Martinez, G., & Gupta, H. (2010). Toward improved identification of hydrological models: A diagnostic evaluation of the "abcd" monthly water balance model for the conterminous United States. *Water resources research, 46*, 1-21. doi:10.1029/2009WR008294

McColl, C., & Aggett, G. (2007). Land-use forecasting and hydrologic model integration for improved land-use decision support. *Journal of environmental management, 84*, 494-512. doi:https://doi.org/10.1016/j.jenvman.2006.06.023

McCuen, R. H. (1973). The role of sensitivity analysis in hydrologic. *Journal of hydrology, 18*, 37-53. doi:https://doi.org/10.1016/0022-1694(73)90024-3

McEnroe, B. (2010). *Guidelines for continuous simulation of streamflow in Johnson County, Kansas, with HEC-HMS.* University of Kansas, department of civil, environmental and architectural engineering. Kansas: Johnson county public works and infrastructure stormwater management program. Retrieved from https://www.jocogov.org/sites/default/.../continuous-simulation-with-HEC-HMS.pdf

Meenu, R., Mujumdar, P., & Rehana, S. (2012, December). Assessment of hydrologic impacts of climate change in Tunga–Bhadra river basin, India with HEC-HMS and SDSM. *Hydrological processes*, 1-18. doi:10.1002/hyp.9220

Moriasi, D., Arnold, J., & Van Liew, M. (2007). Model evalution guidlines for systematic quantificaiton of accuracy in watershed simulations. *American society of agricultural and biological engineers, 50*(3), 885-900. Retrieved from https://swat.tamu.edu/media/1312/moriasimodeleval.pdf

Nash, J. E. (1970). River flow forecasting through conceptual models part I-A discussion of principles. *Journal of hydrology, 10*, 282-290. doi:https://doi.org/10.1016/0022-1694(70)90255-6

Oleyiblo, J., & LI, Z.-j. (2010). Application of HEC-HMS for flood forecasting in Misai and Wan'an catchments in China. *Water science and engineering, 3*(1), 14-22. doi:https://doi.org/10.3882/j.issn.1674-2370.2010.01.002

Perera, K., & Wijesekera, N. (2011, July). Identification of the spatial variability of runoff coefficients of three wet zone watersheds of Sri Lanka. *The institution of engineers, Sri Lanka, 3*, 1-10. Retrieved from http://geoinfo.mrt.ac.lk/waterresources/publications/B059.pdf

Ponce, V. (1989). *Engineering hydrology principles and practices.* Prentice Hall College Div.

Prisloe, M. (., Giannotti, L., & Sleavin, W. (2000). *Determining impervious surfaces for watershed modeling applications.* Hartford, Connecticut: National nonpoint source monitoring conference. Retrieved from http://nemo.uconn.edu/tools/impervious_surfaces/pdfs/Prisloe_etal_2000.pdf

R. Meenu, 1. S. (2012). Assessment of hydrologic impacts of climate change in Tunga–Bhadra river basin, India with HEC-HMS and SDSM. *Hydrological processes*. doi:https://doi.org/10.1002/hyp.9220

Rahman Davtalab, A., Ali Mirchi, Khatami, S., Gyawali, R., Massah, A., Farajzadeh, M., & and Kaveh Madani. (2015). Improving continuous hydrologic modeling of data-poor river bsins using hydrologic engineering center's hydrologic modeling system: case study of Karkheh River Basin. *Hydrology*. doi:10.1061/(ASCE)HE.1943-5584.0001525

Rahul Singh, W., & K.Jain, M. (2015, October). Continous hydroligcal modeling using soil moisure accounting algorithm in Vamsadhara river basin, India. *Water resource and hydralulic engineering, 4*, 398-408. doi:10.5963/JWRHE0404011

Refsgaard, J., & Knudsen, J. (1996, July). Operational validation and intercomparison of different types of hydrological models. *Water resources research, 32*(7), 2189-2202. doi:https://doi.org/10.1029/96WR00896

Rezaeianzadeh, M., Stein, A., & Tabari, H. (2013). *Assessment of a conceptual hydrological model and artificial neural networks for daily outflows forecasting.* Islamic Azad University. Tehran, Iran: Springer . doi:10.1007/s13762-013-0209-0

Samady, K. (2017). *Continuous hydrologic modeling for analyzing the effects of drought on the lower colorado river in texas.* Michigan: Michigan

technological university. Retrieved from http://digitalcommons.mtu.edu/etdr/460/

Saxton, K., & Rawls, W. (2006, October). Soil water characteristic estimates by texture and organic matter for hydrologic solutions. *Soil & water management & conservation, soil physics, 70*, 1569-1578. doi:10.2136/sssaj2005.0117

Sharifi, M. (2015). *Calibration and verificaion of a-two paramter montly water balance model and Its application potential for evalution of water resources-a case study of Kalu and Mahaweli rivers of Sri Lanka.* Department of civil engineering. Moratuwa: University of Moratuwa Sri Lanka. Retrieved from http://dl.lib.mrt.ac.lk/handle/123/12954

Smakhtin, V. (2000, September). Low flow hydrology: a review. *Journal of hydrology, 240*, 147-186. doi:https://doi.org/10.1016/S0022-1694(00)00340-1

Smit, M., & Seo, D.-J. (2004, Marh). The distributed model intercomparison project (DMIP): motivation and experiment design. *Journal of hydrology, 298*, 4-26. doi:https://doi.org/10.1016/j.jhydrol.2004.03.040

Sok, K., & Oeurng, C. (2016). *Application of HEC-HMS model to assess streamflow and water resoruces availbility in Stung Sangker catchment of Mekong Tonle Sap lake basin in Cambodia.* Csmbodia: department of rural engineering institute of technology Cambodia. doi:10.20944/preprints201612.0136.v1

Subramanya, K. (2013). *Engineering hydrology.* New Delhi, India: McGraw-Hill Education (India) private limited.

Thiemann, S., & Förch, G. (2004). Water resources assessment in the bilate river catchment - precipitation variability. In S. Thiemann, & G. Förch (Ed.), *Lake Abaya research symposium. 4*, pp. 73-78. Research institute for water and environment. Retrieved from https://www.researchgate.net/publication/238681859

Thompson, D., & Cleveland, T. (2009). *Subdivision of texas watersheds for hydrologic modeling.* Texas Tech University, department of civil and environmental engineering. Lubbock, Texas: Center for multidisciplinary research in transportation. Retrieved from https://ttu-ir.tdl.org/ttu-ir/bitstream/handle/2346/22812/0-5822.pdf?sequence=1

Todd H, B., & John C , P. (2004). *Continuous soil moisture accounting in the hydrologic engineering center hydrologic modeling system (HEC-HMS).* New York: ASCE. Retrieved from https://ascelibrary.org/doi/10.1061/40517%282000%29149

Tripathi , M., Raghuwanshi, N., & Rao, G. (2005, December). Effect of watershed on simulation of water balance components. *Wiley interScience*. doi:https://doi.org/10.1002/hyp.5927

Tripathi, M., Raghuwanshi, N., & Rao, G. (2006). Effect of watershed subdivision on simulation of water balance components. *Hydrological process, 20*, 1137-1156. doi:10.1002/hyp.5927

USACE. (2016). *HEC-HMS hydrologic modeling system-technical reference manual.* US army corps of engineers institute for water resouces hydrologic engineering center. Retrieved from http://www.hec.usace.army.mil/software/hec-hms/documentation/HEC-HMS_ReleaseNotes421.pdf

Wijesekera, N., & Abeynayake, J. (2003, April). Watershed similarity conditions for peakflow transposition – a study of river basins in the wet zone of Sri Lanka. *Journal of the institution of engineers, Sri Lanka, 36*(`2), 26-31. Retrieved from http://geoinfo.mrt.ac.lk/waterresources/publications/B026.pdf

Wijesekera, S. N. (2018). *Classification of streamflow observations for water management.* Moratuwa: University of Moratuwa. Retrieved from https://www.academia.edu/35829487/Classification_of_Streamflow_Observations_for_Water_Management

Willmott, C., & Matsuura, K. (2005, December). Advantages of the mean absolute error (MAE) over the root mean square error (RMSE) in assessing average model performance. *Climate research, 30*, 79-82. doi:192.148.225.18

Wood, E., & Sivapalan, M. (1988). Effects of spatial variability and scale with implications of hydroloigic modeling. *Journal of hydrology, 102*, 29-47. doi:https://doi.org/10.1016/0022-1694(88)90090-X

Xiong, L., & Guo, S. (1999). A two-parameter monthly water balance model and its application. *Journal of hydrology, 216*, 11-123. doi:https://doi.org/10.1016/S0022-1694(98)00297-2

Xu, C., & Singh, V. (1996). A review on monthly water balance models for water resources investigations. *Water resources management, 12*, 31-50. Retrieved from http://folk.uio.no/chongyux/papers_SCI/WARM_3.pdf

Xu, C.-y. (2002). *Hydrologic models.* Uppsala: Textbooks of Uppsala University. Department of earth sciences hydrology. Retrieved from http://www.soil.tu-bs.de/lehre/Master.Unsicherheiten/2012/Lit/Hydrology_textbook.pdf

Yildiz, O., & Barros, A. (2009). Evaluating spatial variability and scale effects on hydrologic processes in a midsize river basin. *Scientific research and essay, 4*, 217-225. Retrieved from https://www.researchgate.net/publication/228630711

Yilmaz, K. K., Gupta, H. V., & Wagener, T. (2008, September). A process-based diagnostic approach to model evaluation: application to the NWS distributed hydrologic model. *Water resources research, 44*, 1-18. doi:10.1029/2007WR006716

Yua, P.-S., & Yang, T.-C. (2000, August). Fuzzy multi-objective function for rainfall-runoff model calibration. *Journal of hydrology, 238*, 1-14. doi:https://doi.org/10.1016/S0022-1694(00)00317-6

Yusop, Z., Chan, C., & Katimon, A. (2007). Runoff characteristics and application of HEC-HMS for modelling stormflow hydrograph in an oil palm catchment. *Water science & technology, 56*(8), 41-48. Retrieved from citeseerx.ist.psu.edu/viewdoc/download?doi=10.1.1.502.8682&rep=rep1&type=pdf

Zhang, H., Wang, Y., Wang, Y., Li, D., & Wang, X. (2013, July). The effect of watershed scale on HEC-HMS calibrated parameters: a case study in the Clear Creek watershed in Iowa, US. *Hydrology and earth system sciences, 17*, 2735-2745. doi:https://doi.org/10.5194/hess-17-2735-2013

Appendix A: Data checking

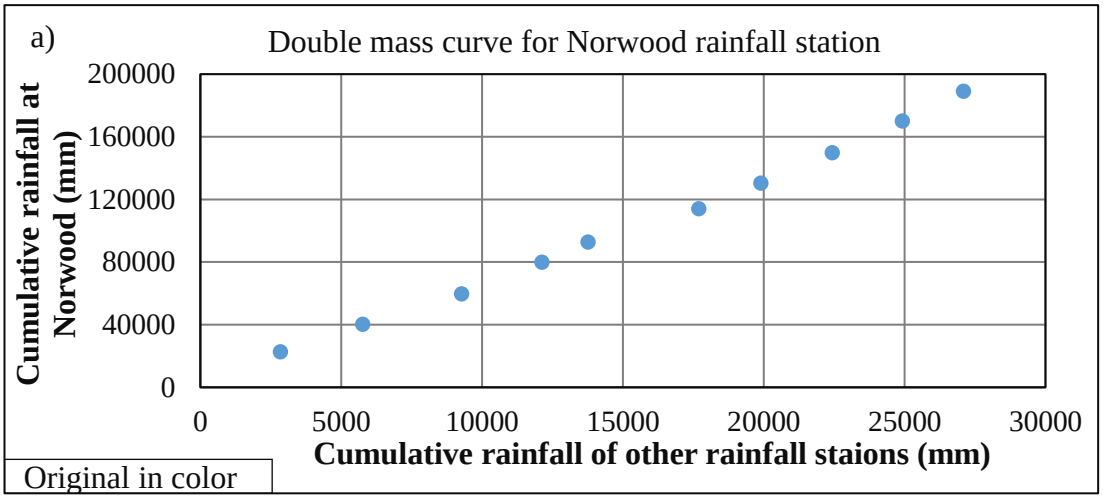

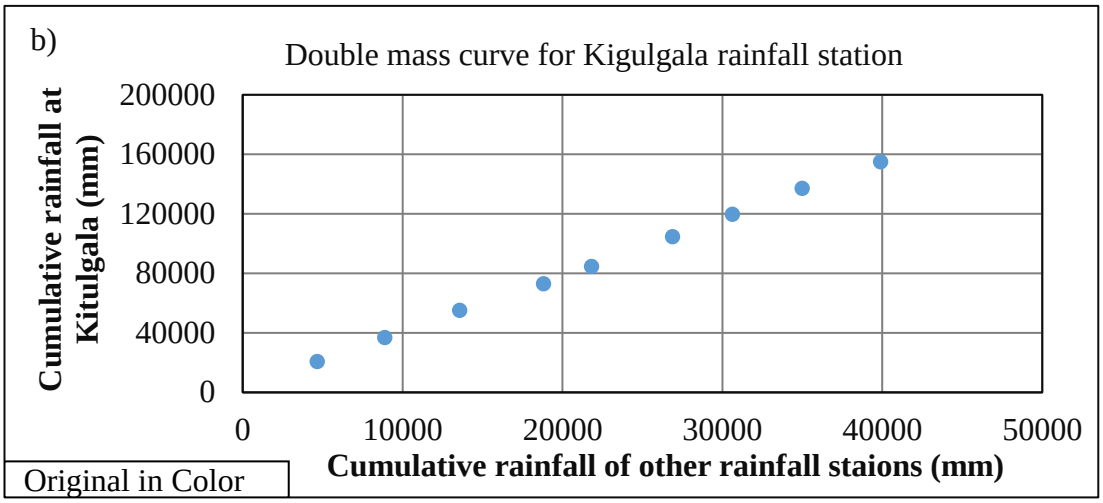

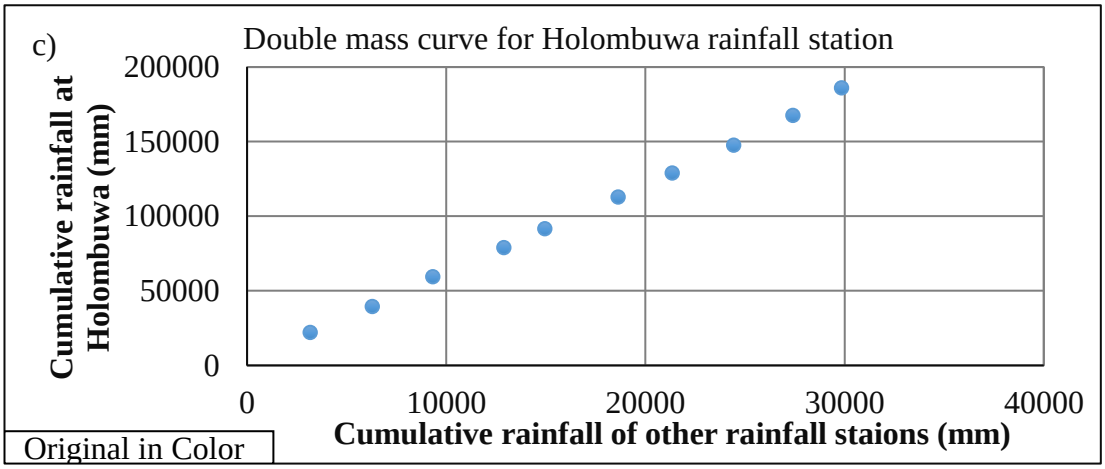

Figure A 1: Double mass curve for all rainfall stations for the Kelani river basin (a-c)

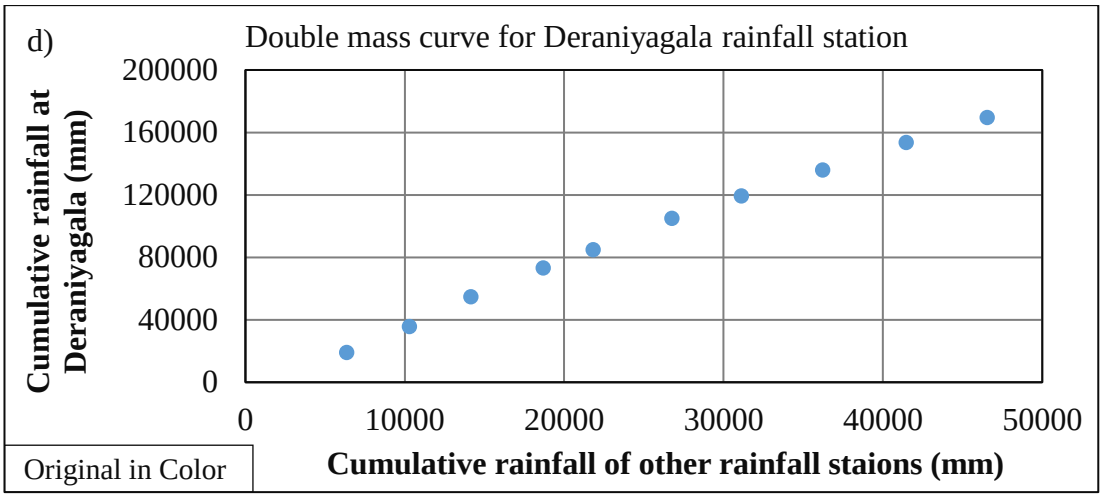

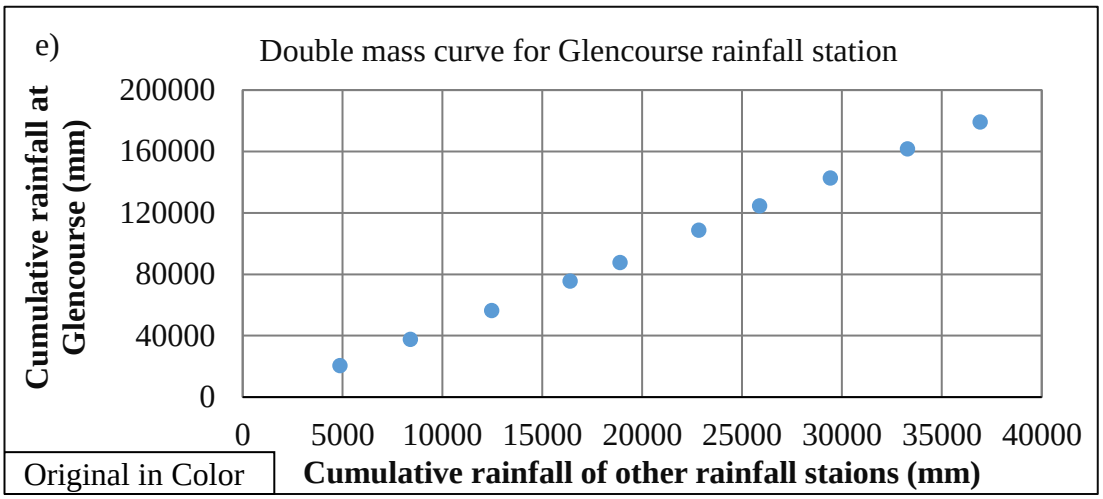

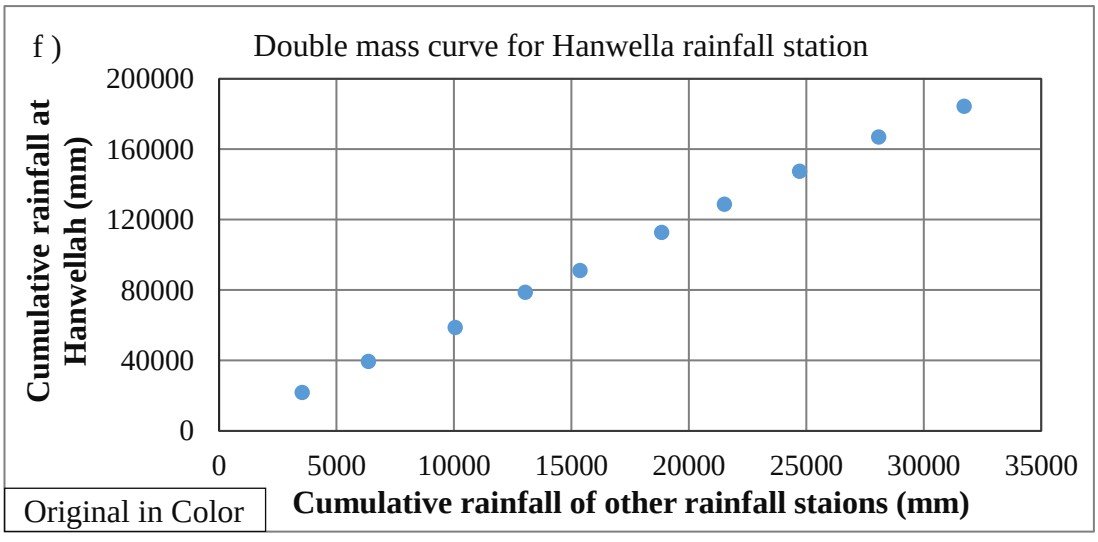

Figure A 2: Double mass curve for all rainfall stations for the Kelani river basin (d-f)

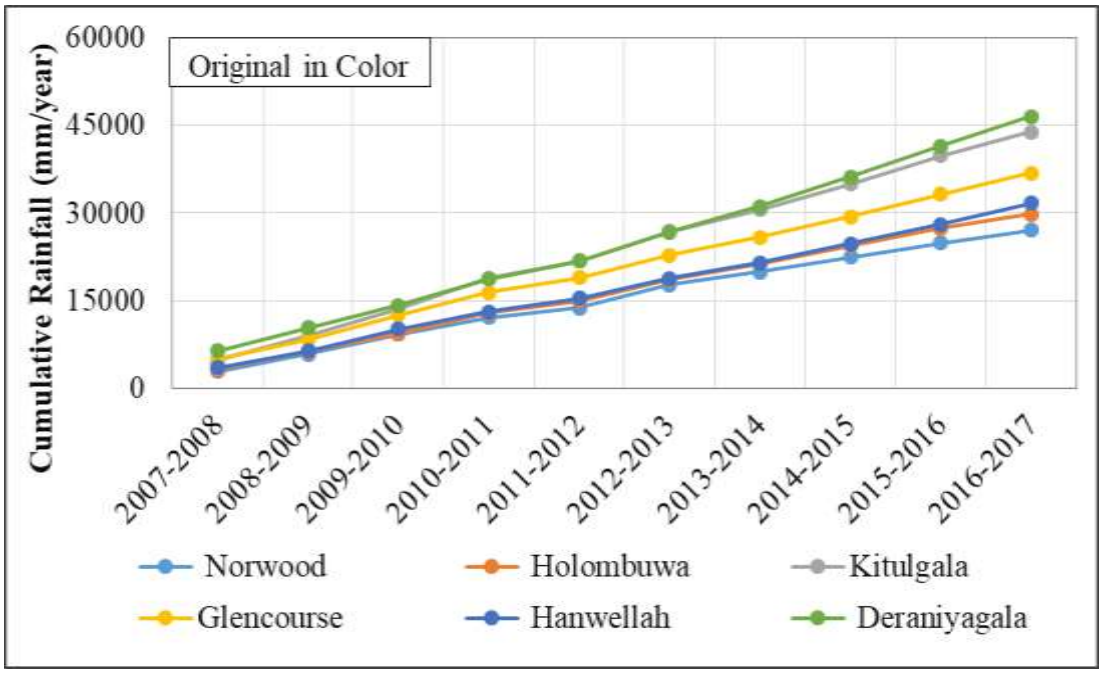

Figure A 3: Single mass curve for each rainfall station

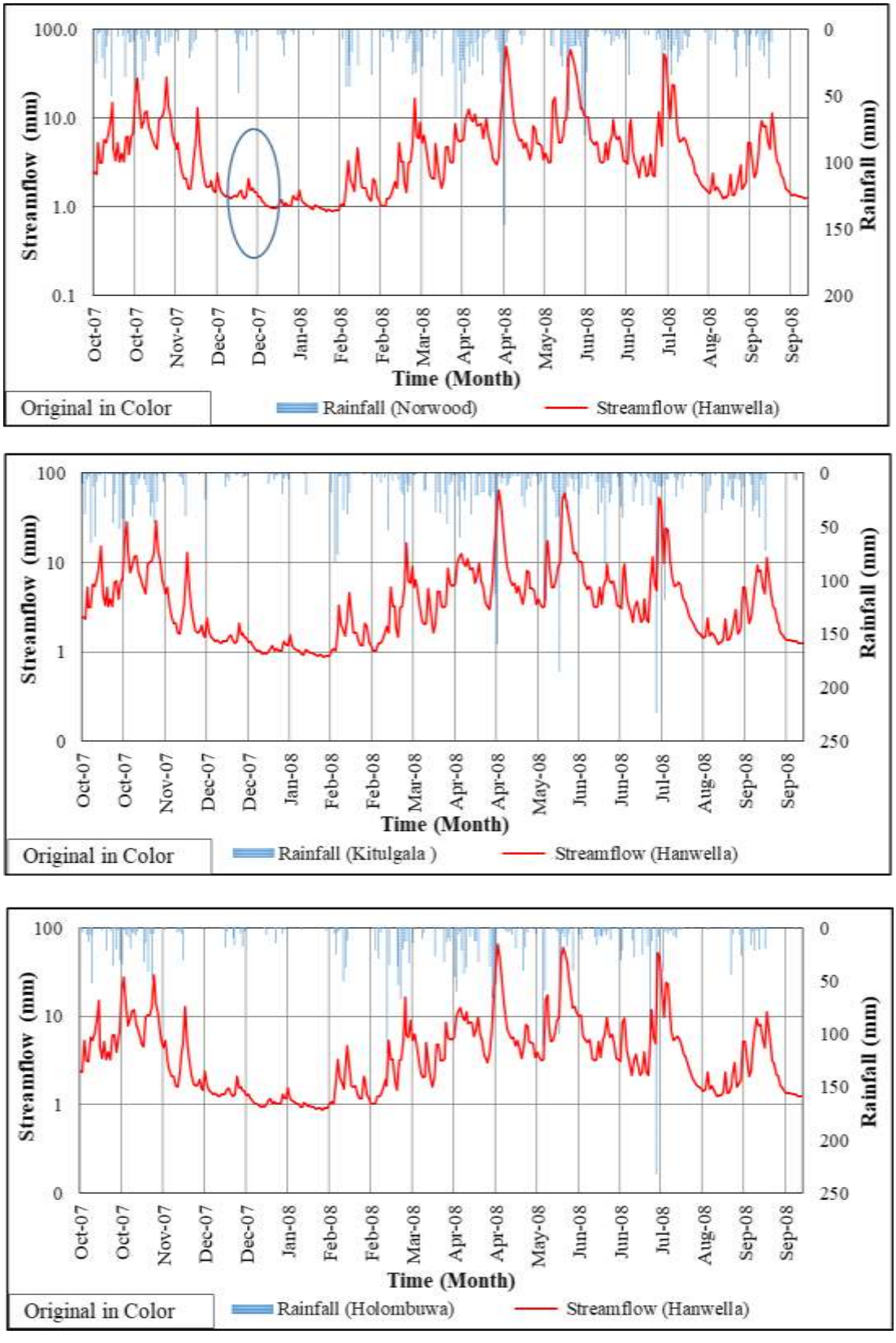

Figure A- 4: Streamflow response of Hanwella with rainfall in year 2007/2008

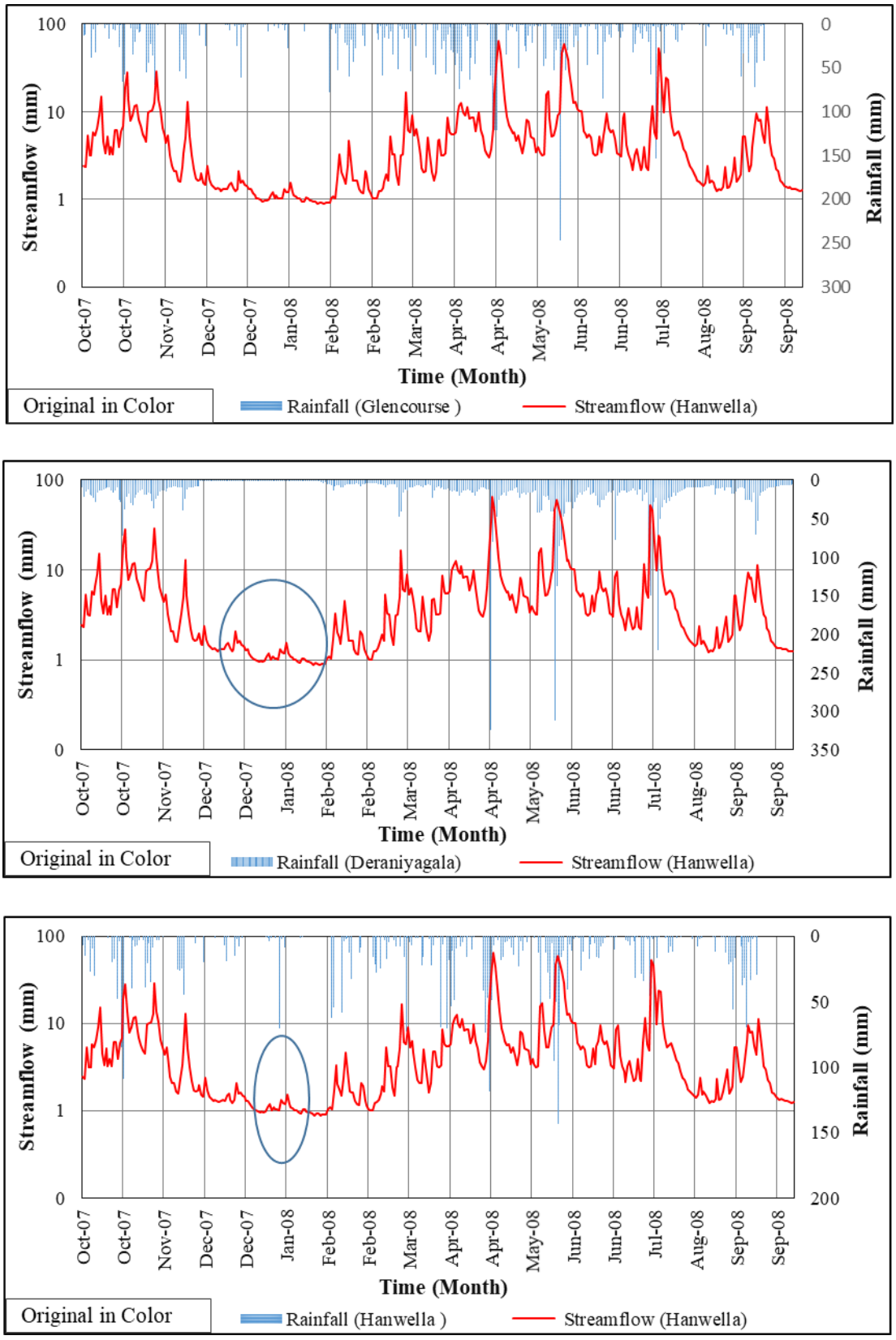

Figure A-5: Streamflow response of Hanwella with rainfall in year 2007/2008

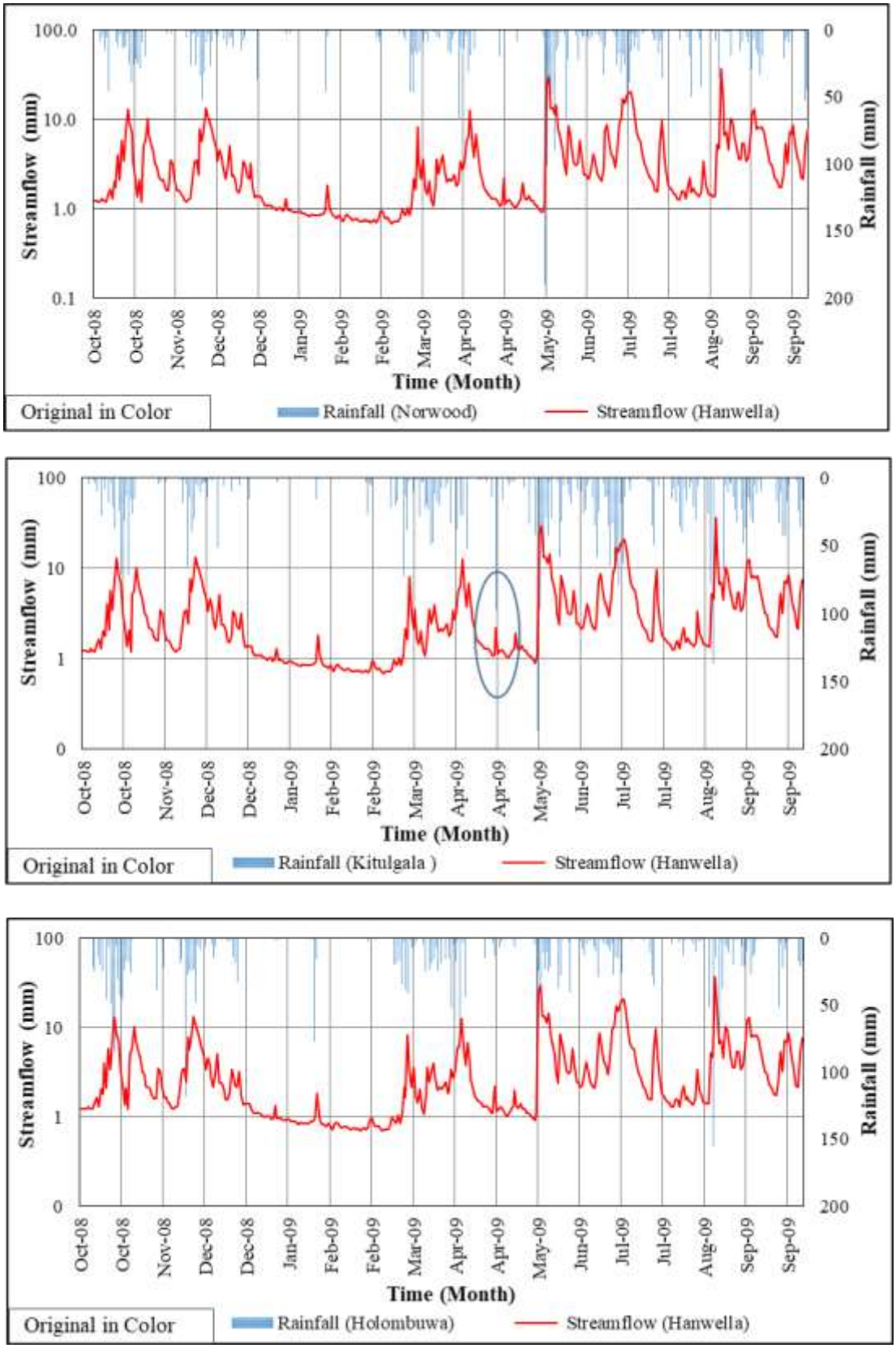

Figure A-6: Streamflow response of Hanwella with rainfall in year 2008/2009

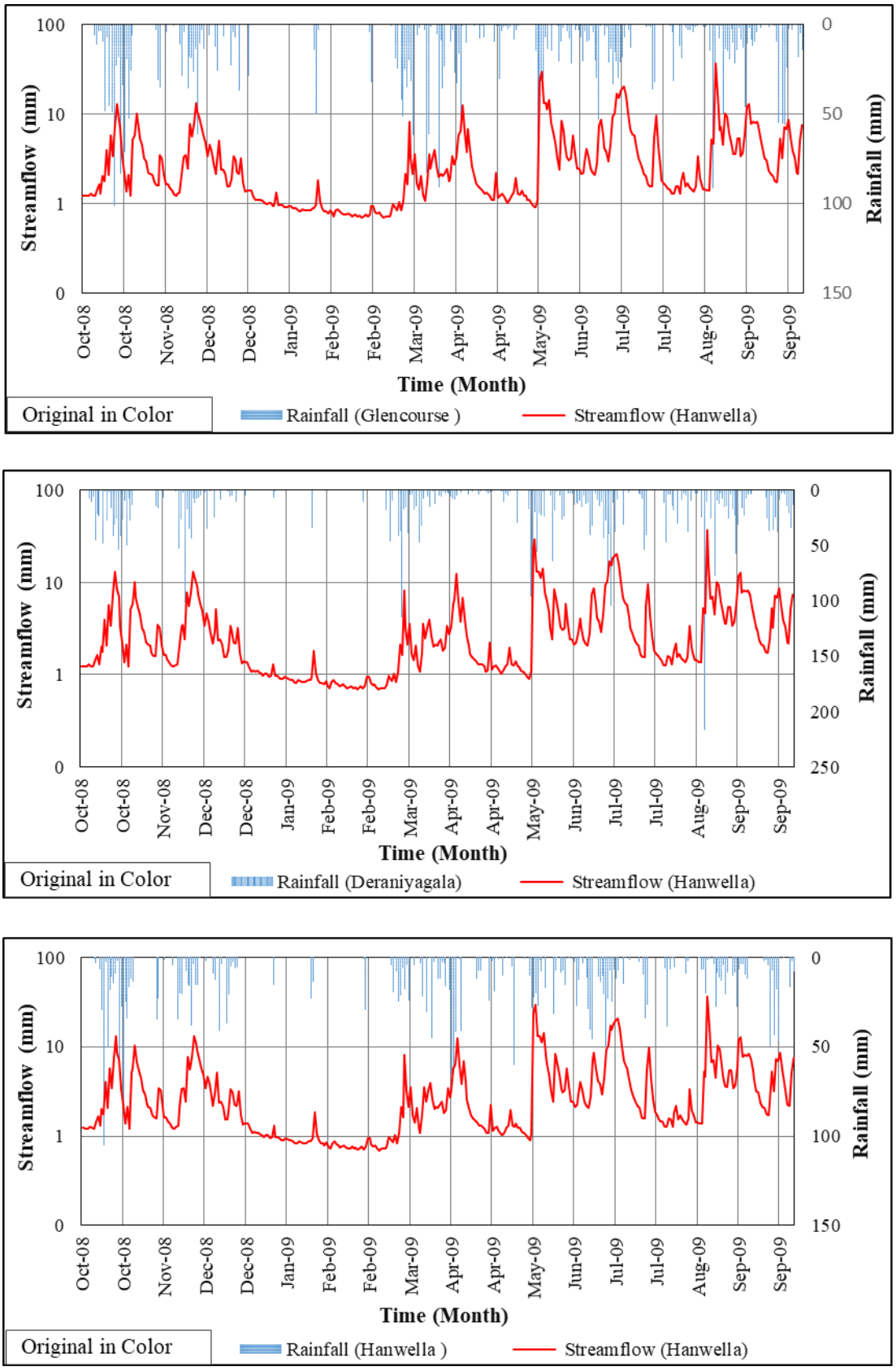

Figure A-7: Streamflow response of Hanwella with rainfall in year 2008/2009

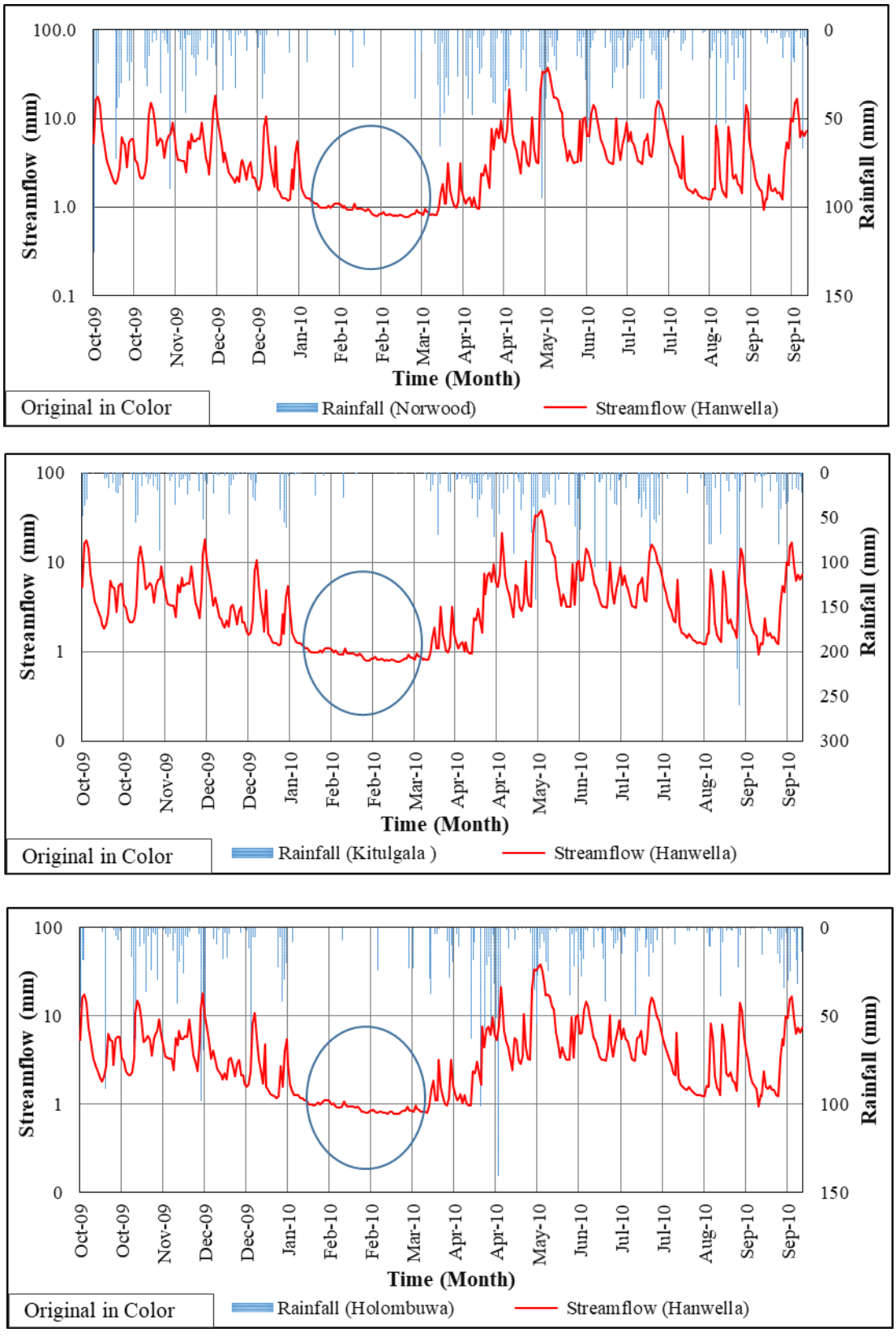

Figure A-8: Streamflow response of Hanwella with rainfall in year 2009/2010

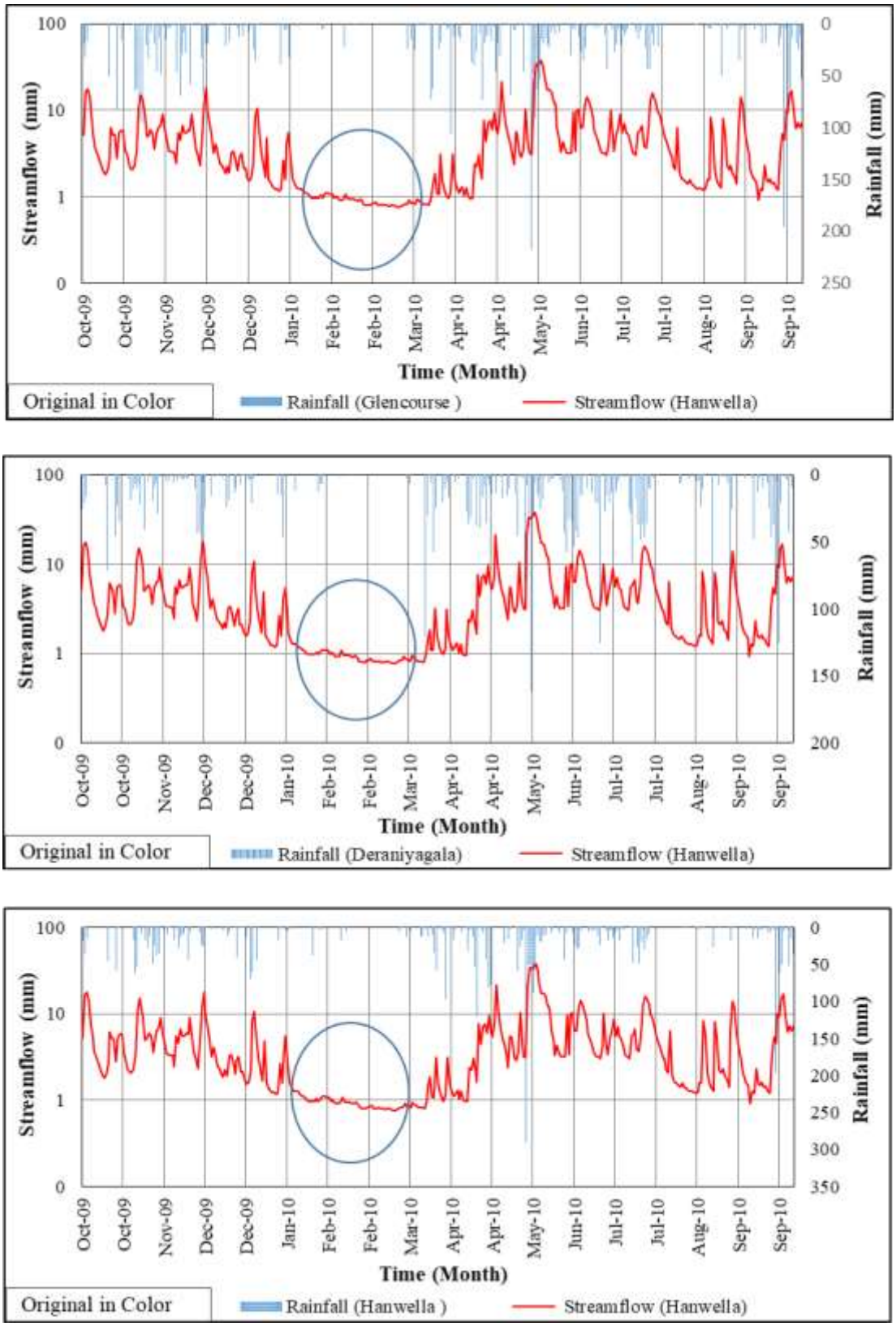

Figure A-9: Streamflow response of Hanwella with rainfall in year 2009/2010

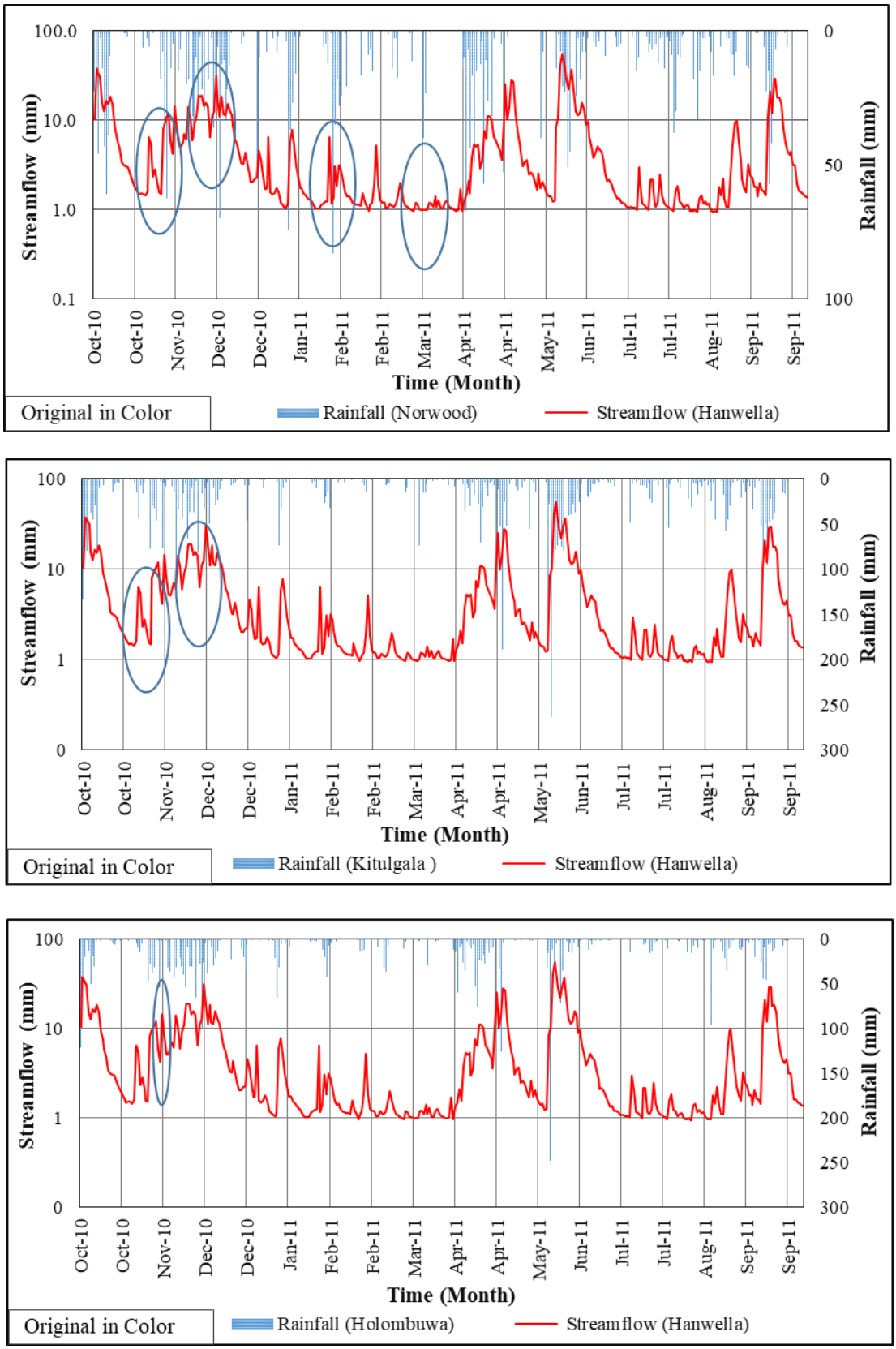

Figure A-10: Streamflow response of Hanwella with rainfall in year 2010/2011

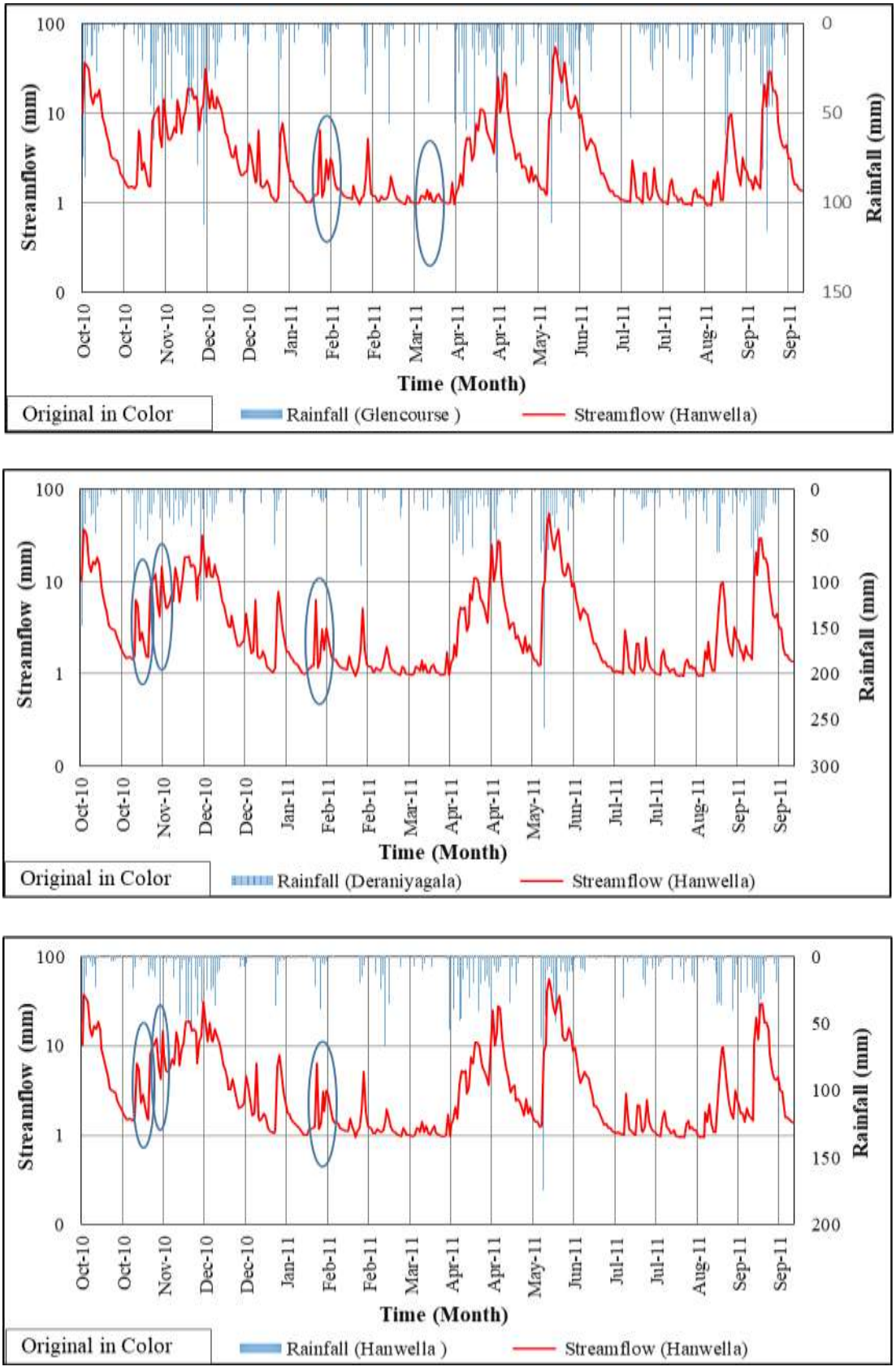

Figure A-11: Streamflow response of Hanwella with rainfall in year 2010/2011

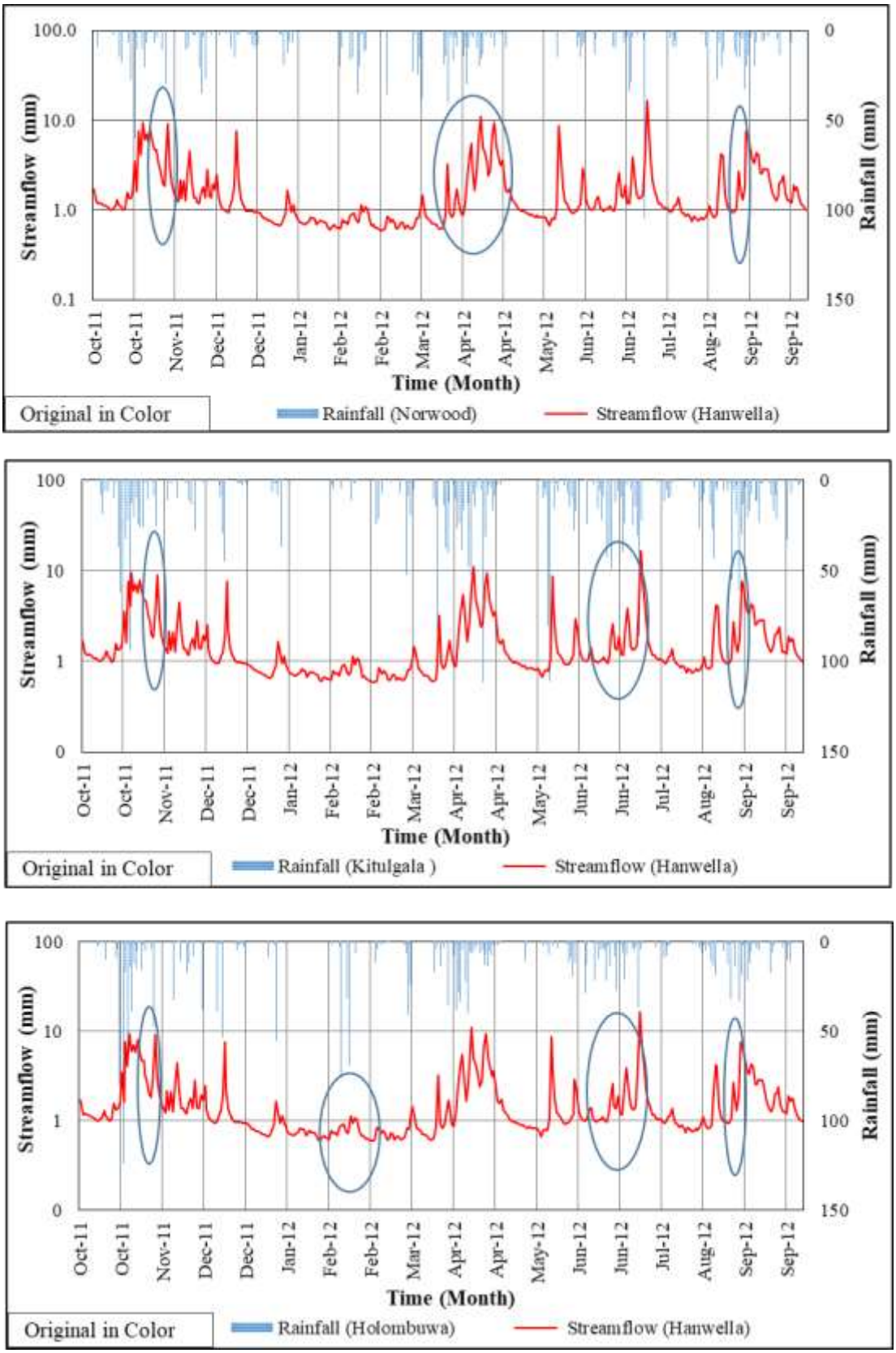

Figure A-12: Streamflow response of Hanwella with rainfall in year 2011/2012

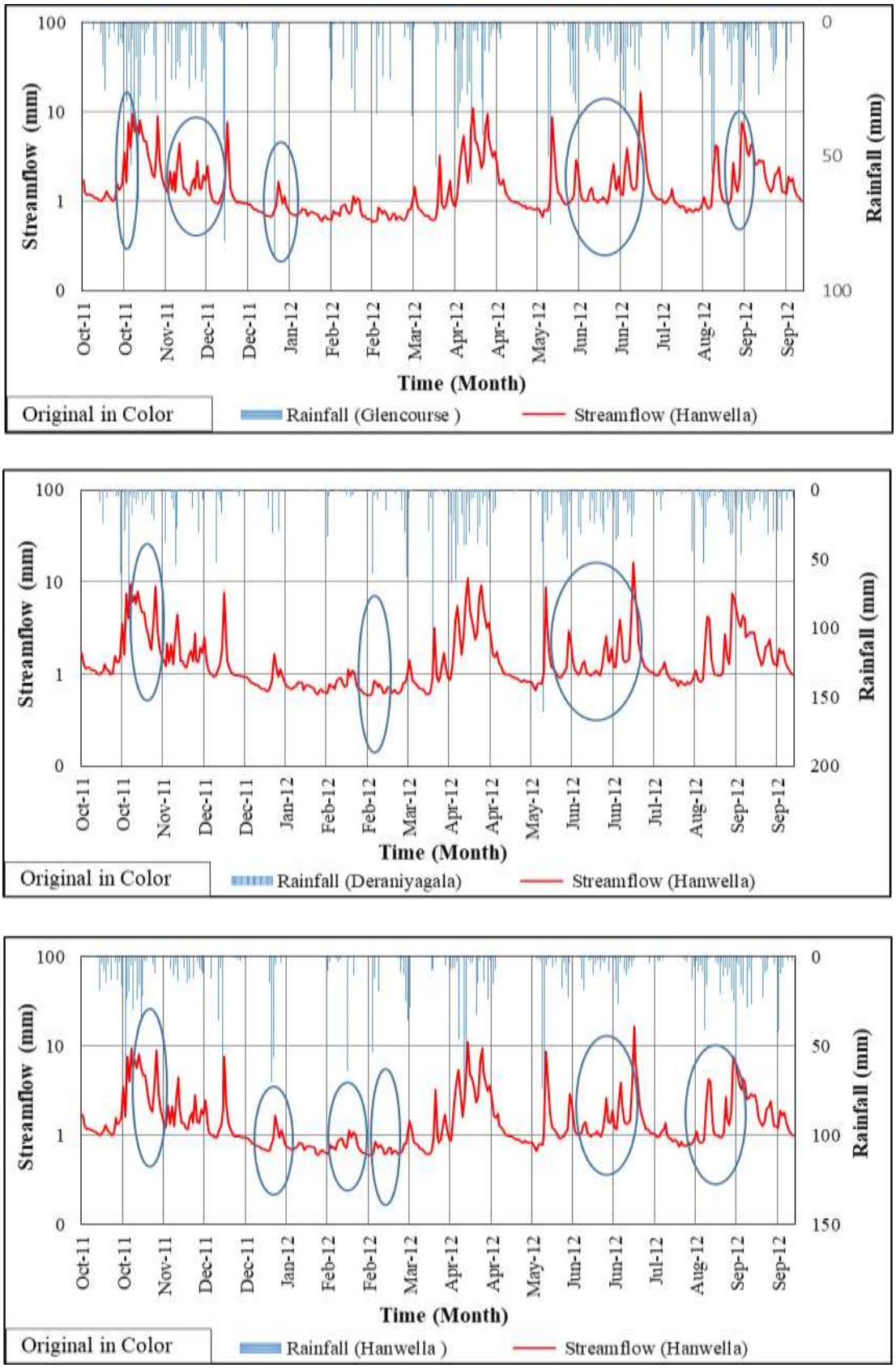

Figure A-13: Streamflow response of Hanwella with rainfall in year 2011/2012

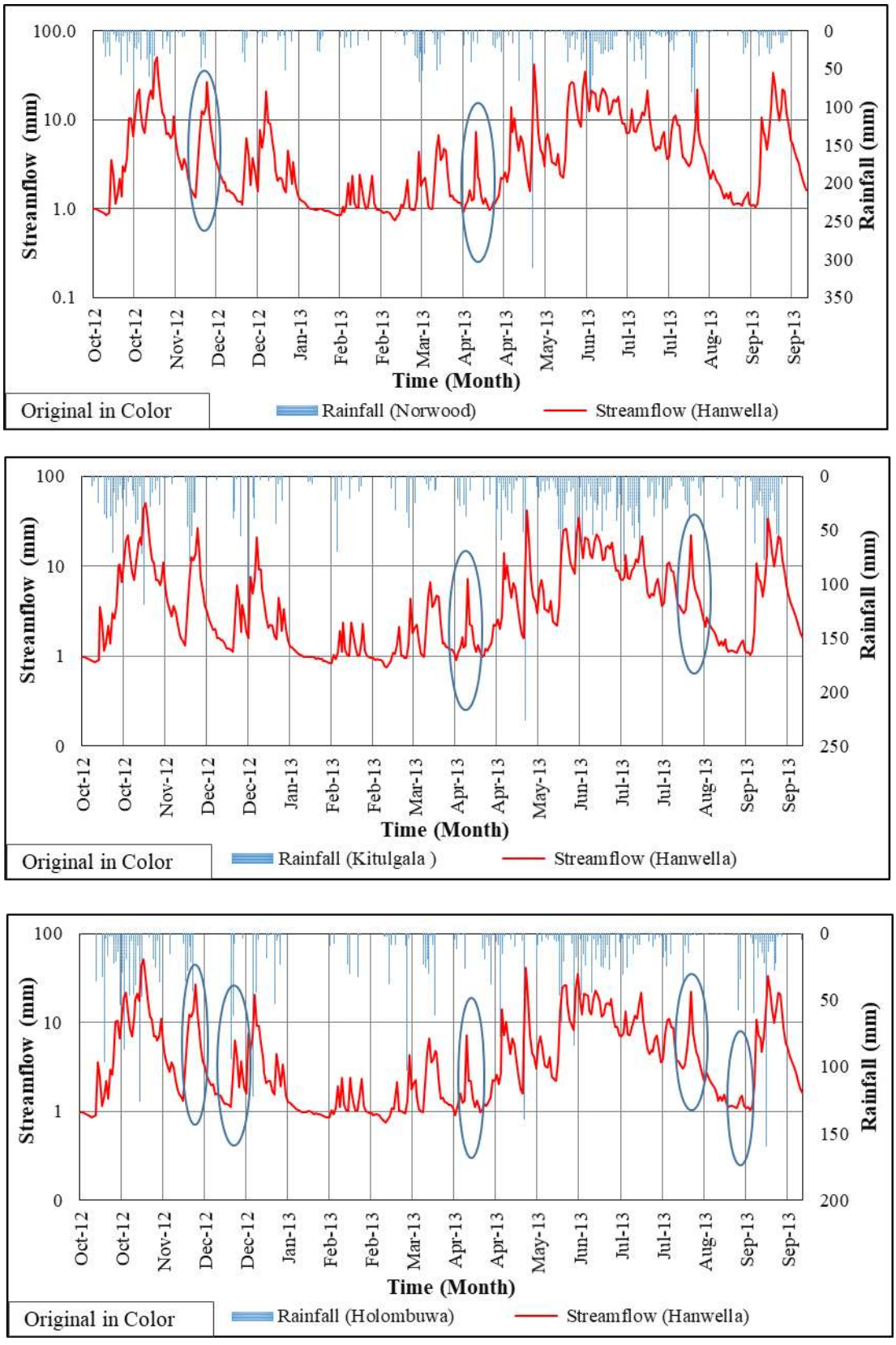

Figure A-14: Streamflow response of Hanwella with rainfall in year 2012/2013

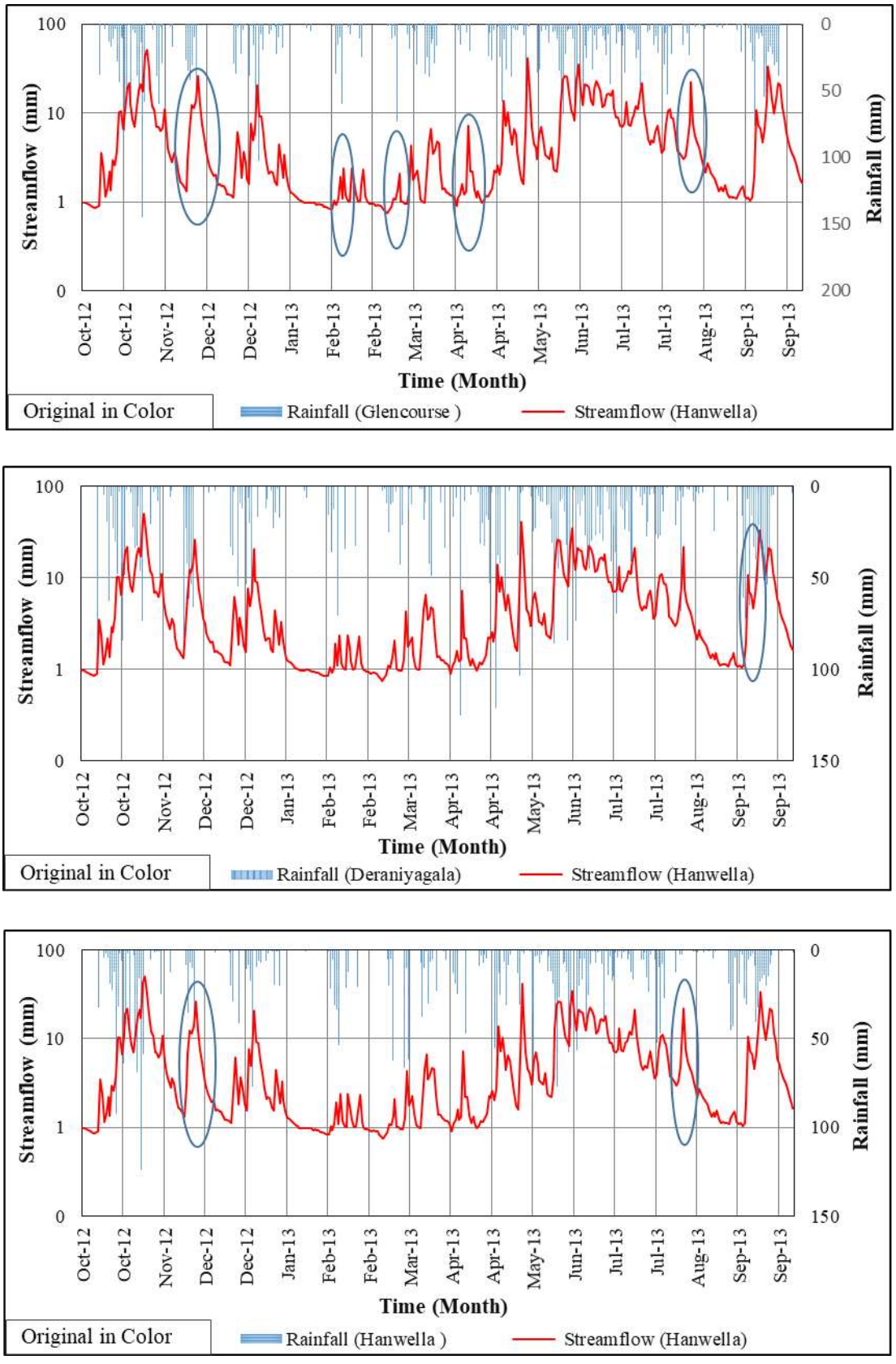

Figure A-15: Streamflow response of Hanwella with rainfall in year 2012/2013

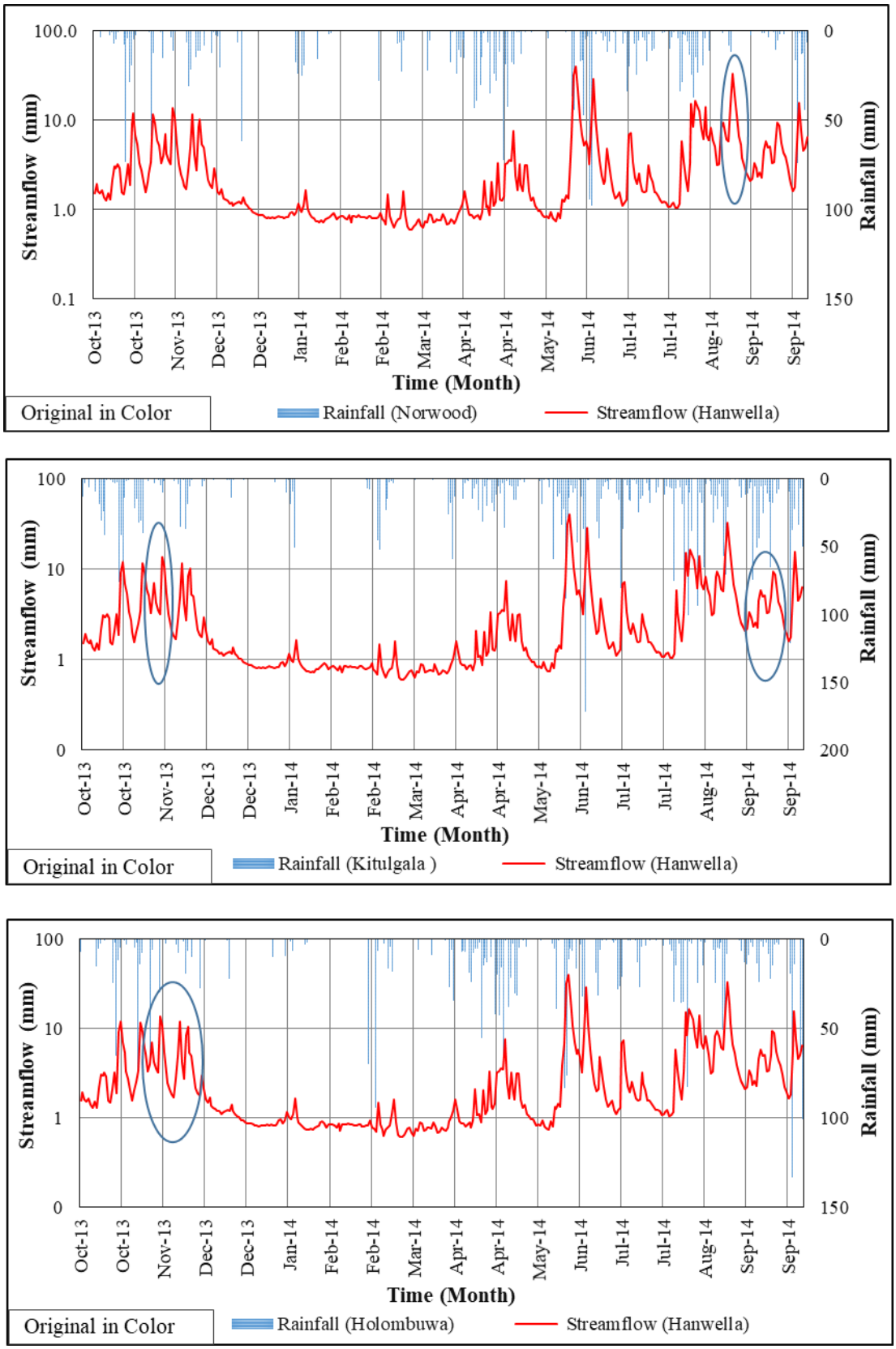

Figure A-16: Streamflow response of Hanwella with rainfall in year 2013/2014

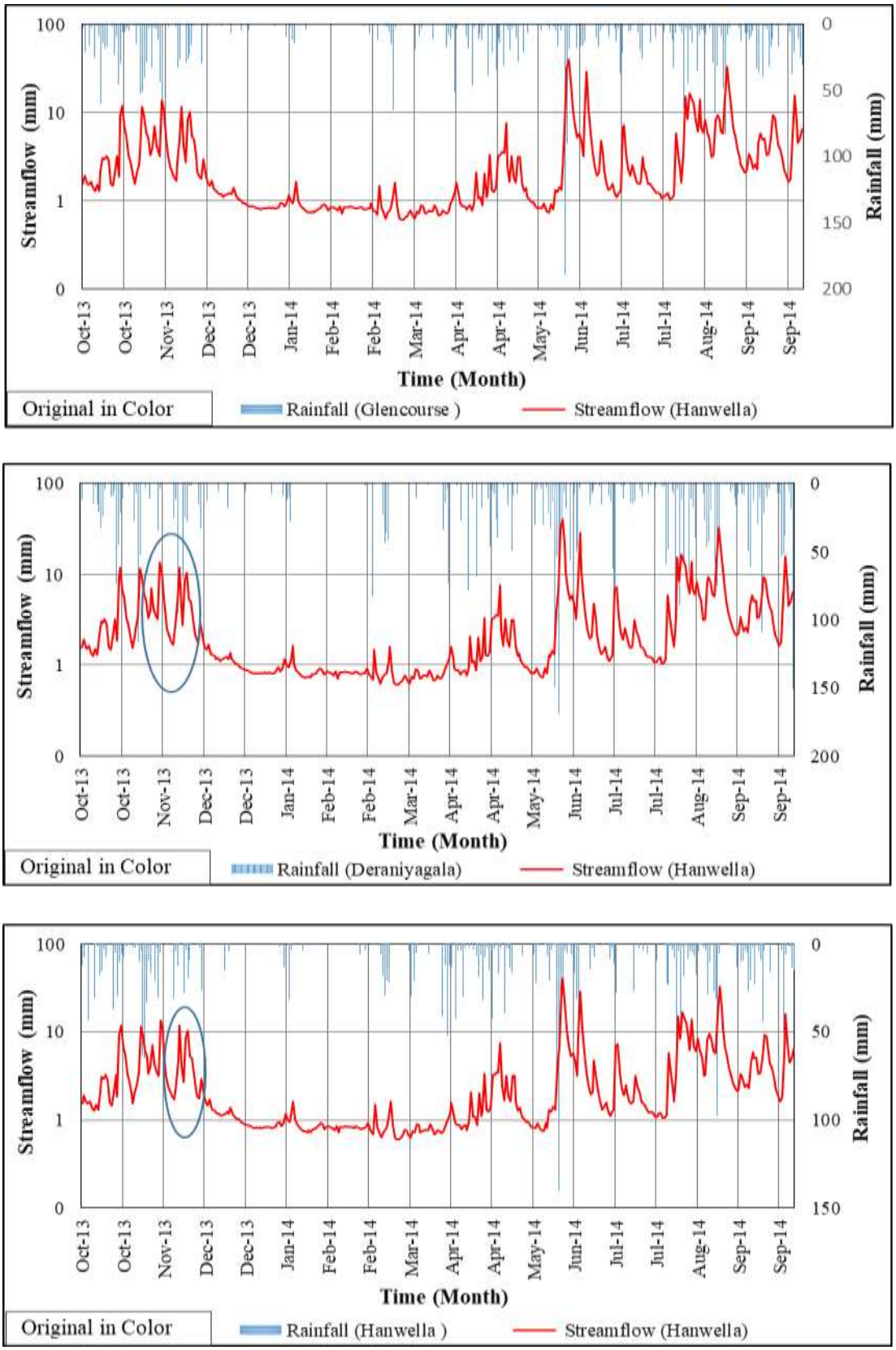

Figure A-17: Streamflow response of Hanwella with rainfall in year 2013/2014

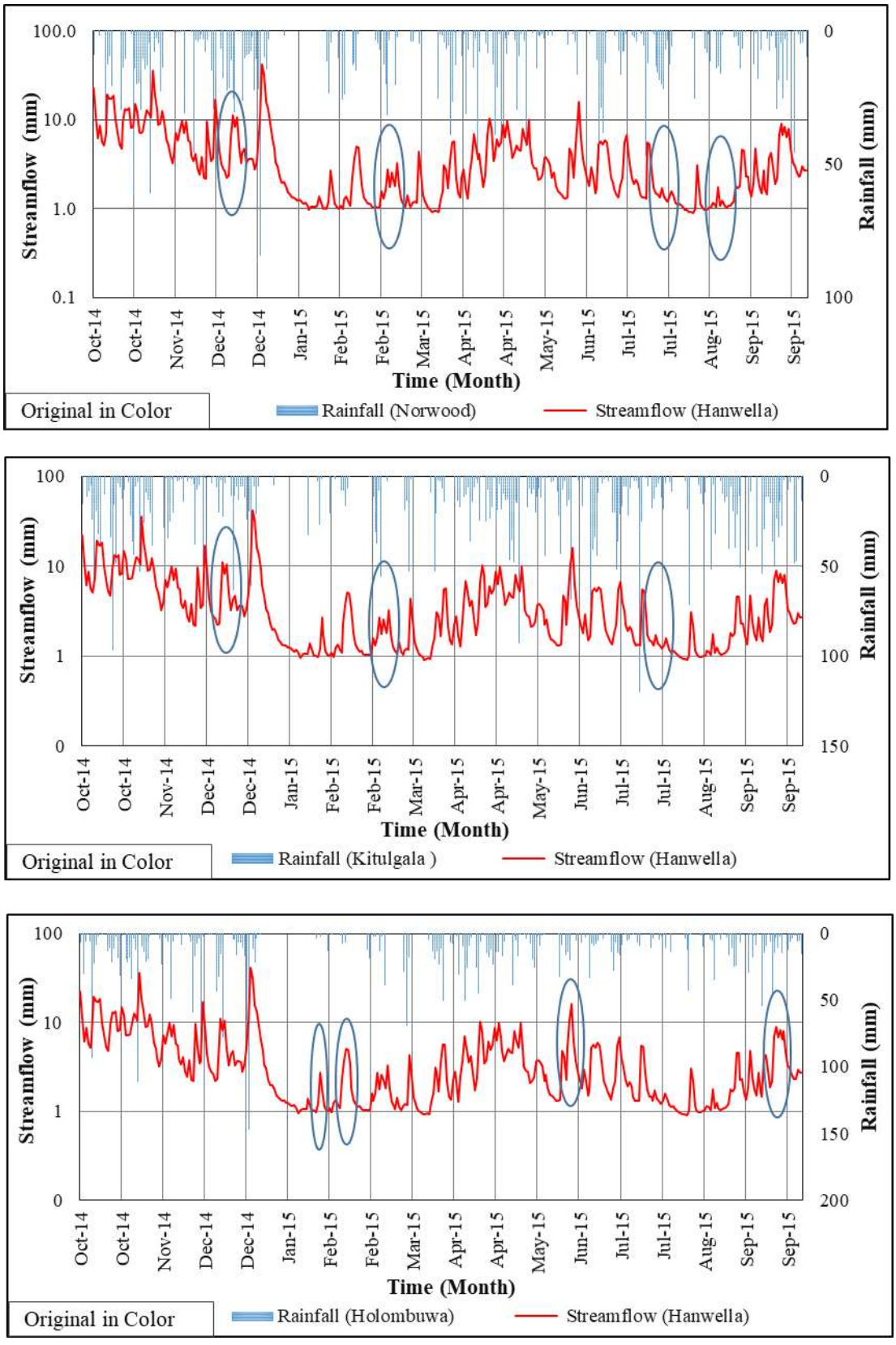

Figure A-18: Streamflow response of Hanwella with rainfall in year 2014/2015

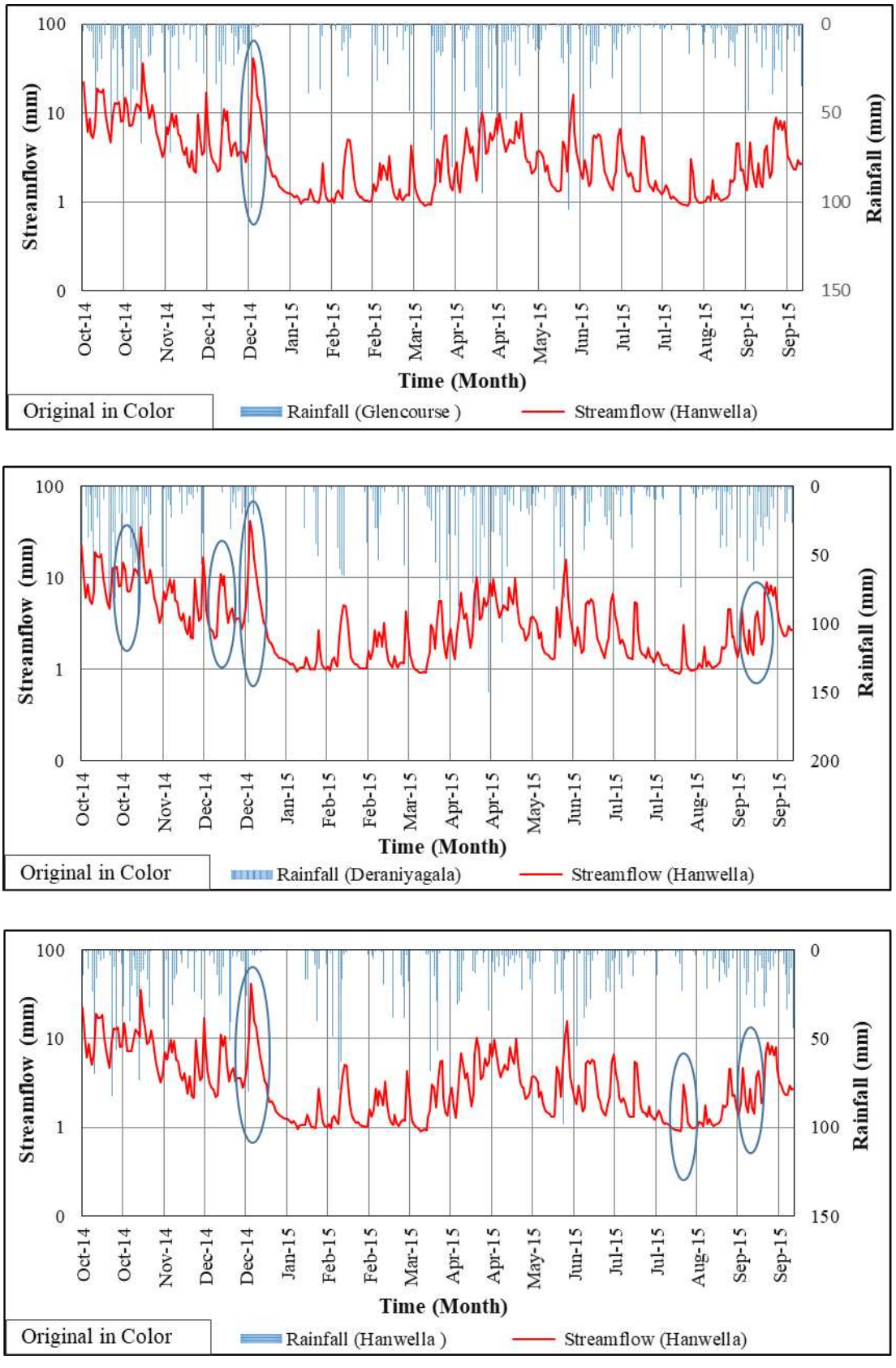

Figure A-19: Streamflow response of Hanwella with rainfall in year 2014/2015

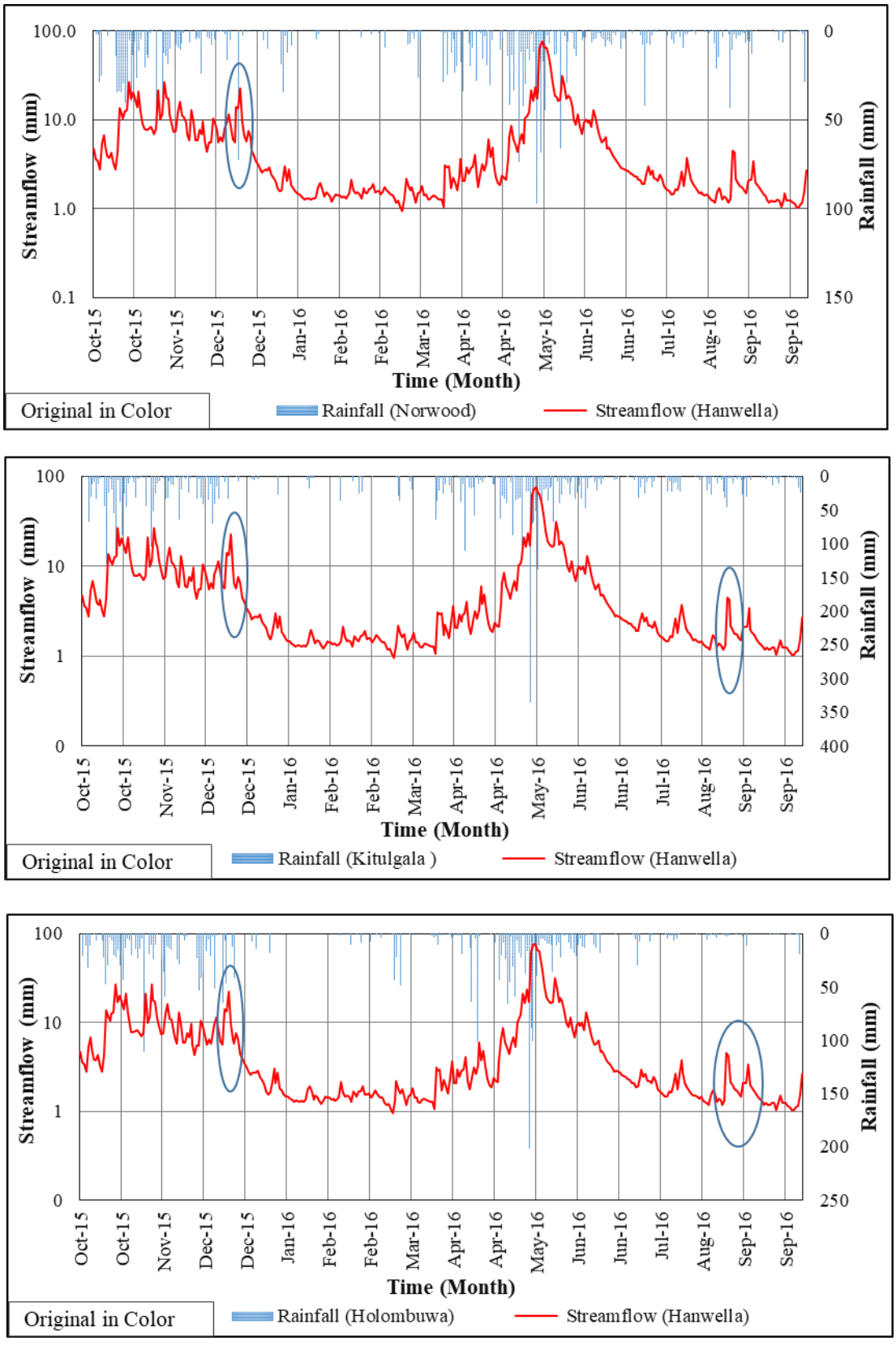

Figure A-20: Streamflow response of Hanwella with rainfall in year 2015/2016

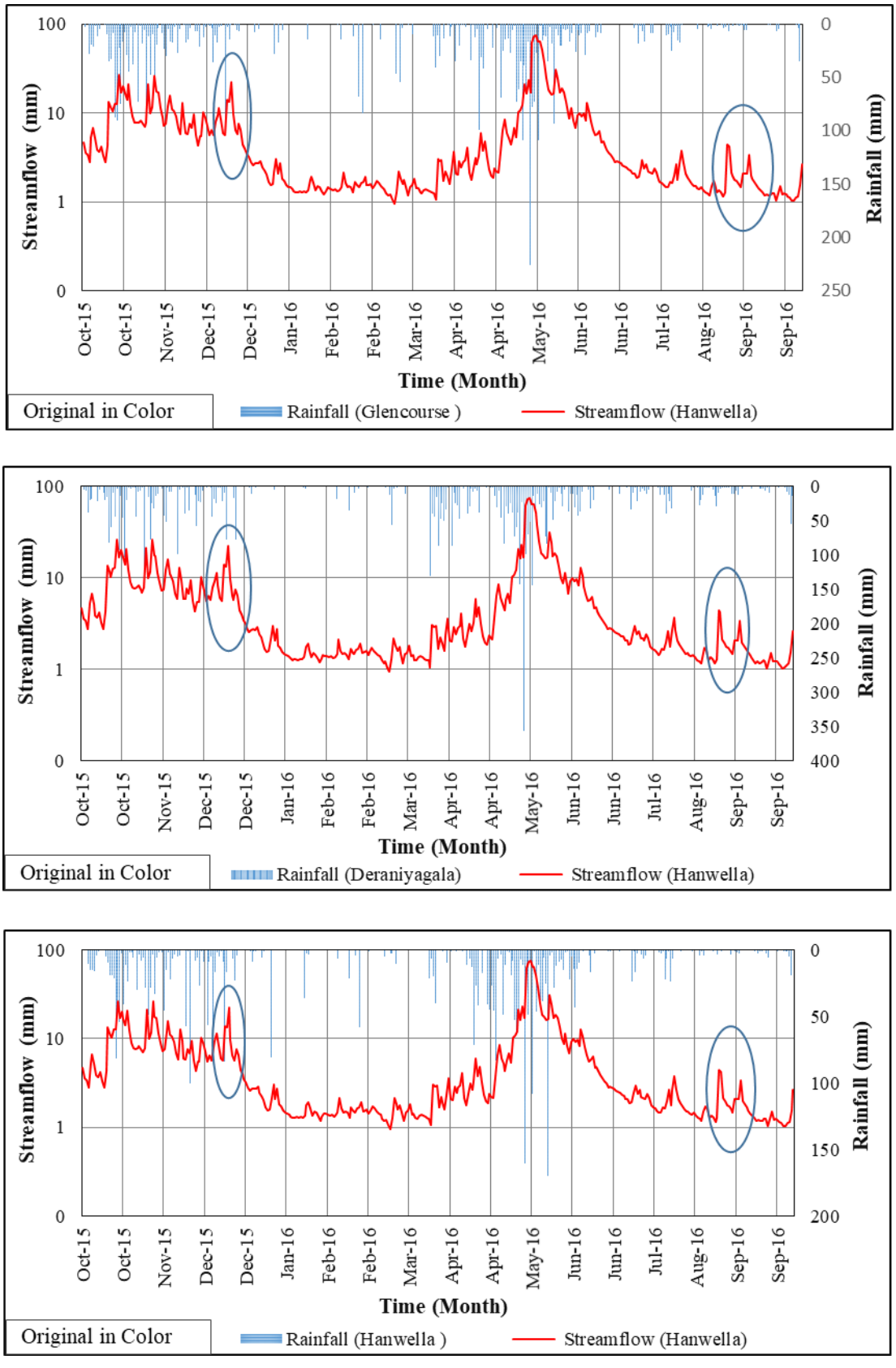

Figure A-21: Streamflow response of Hanwella with rainfall in year 2015/2016

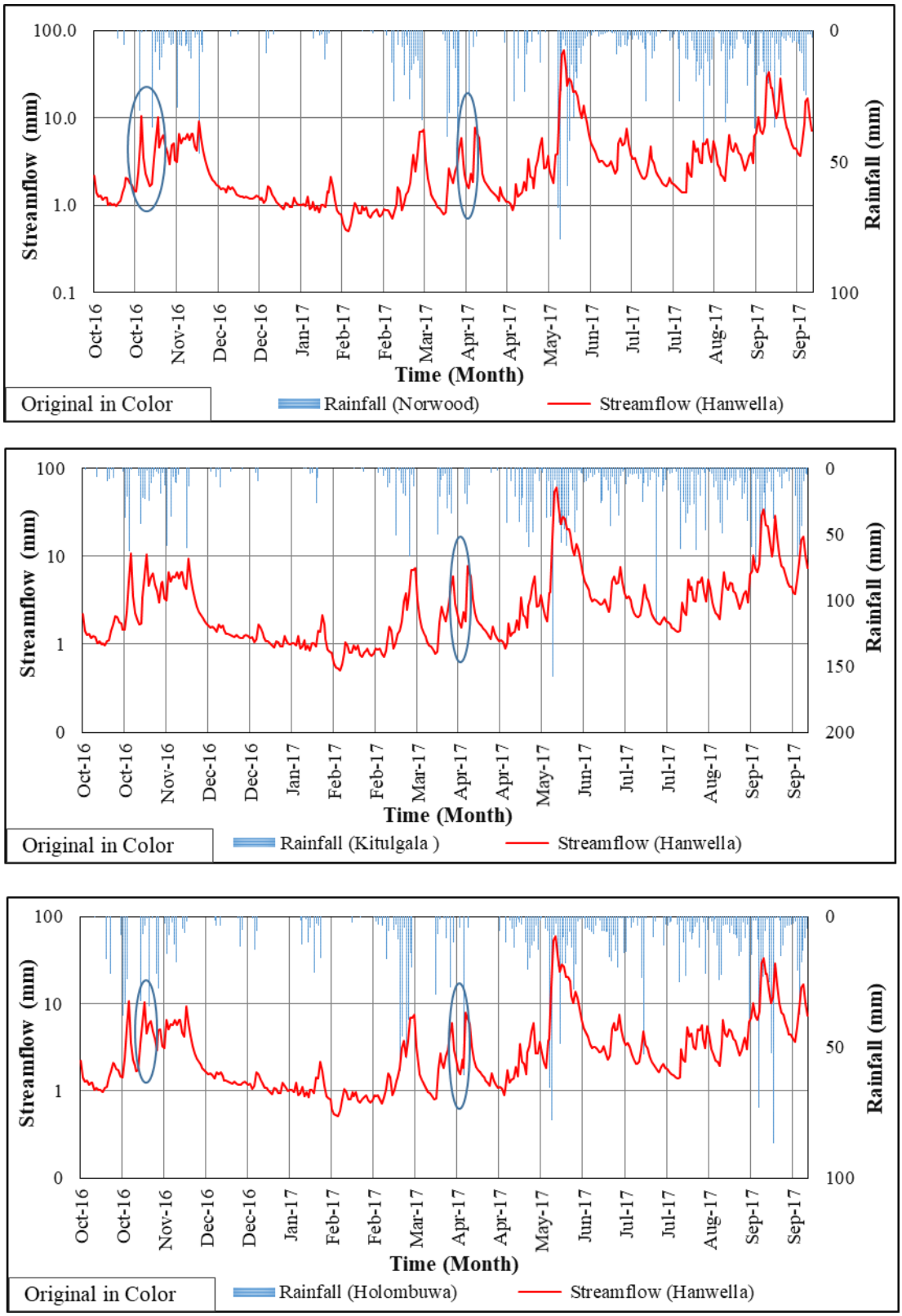

Figure A-22: Streamflow response of Hanwella with rainfall in year 2016/2017

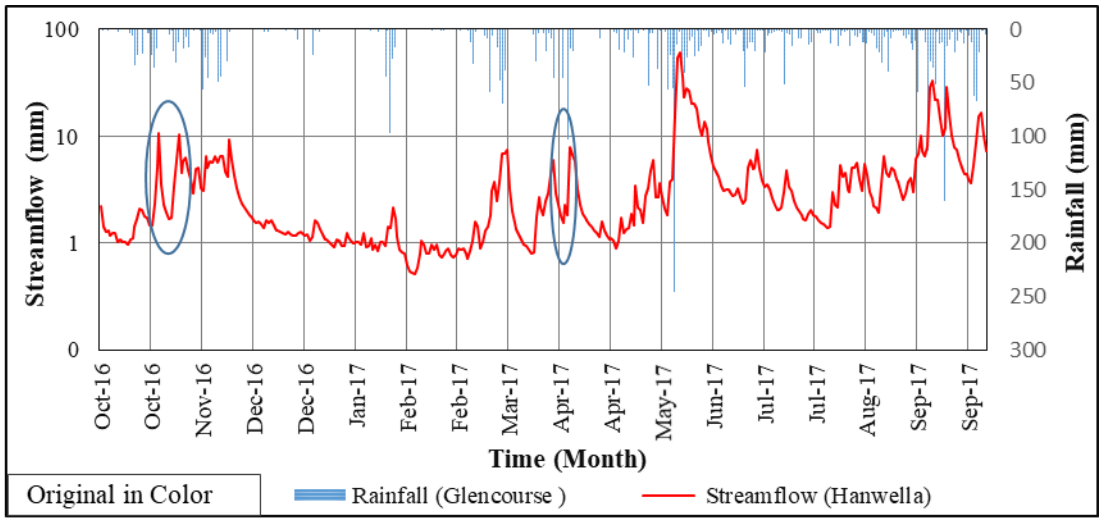

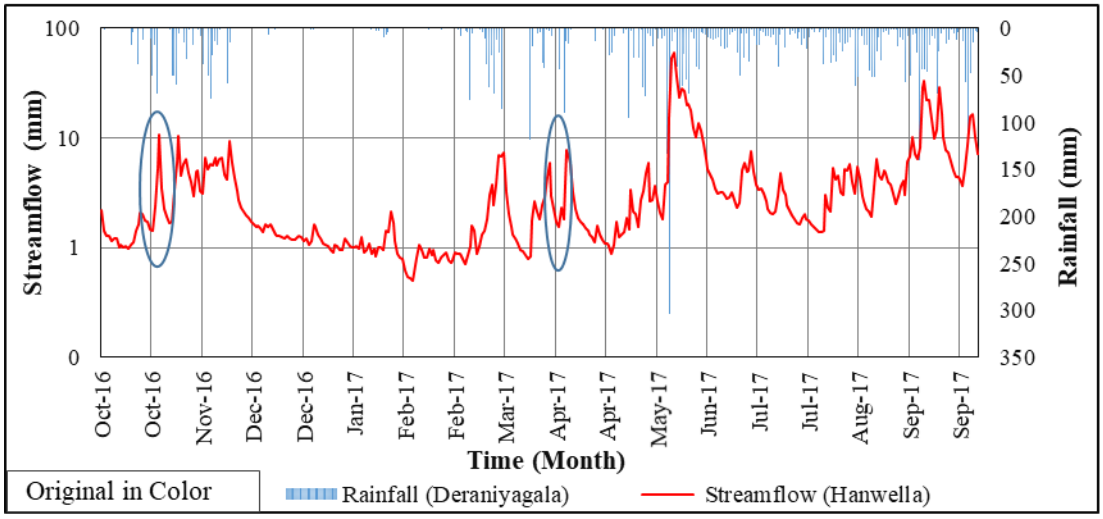

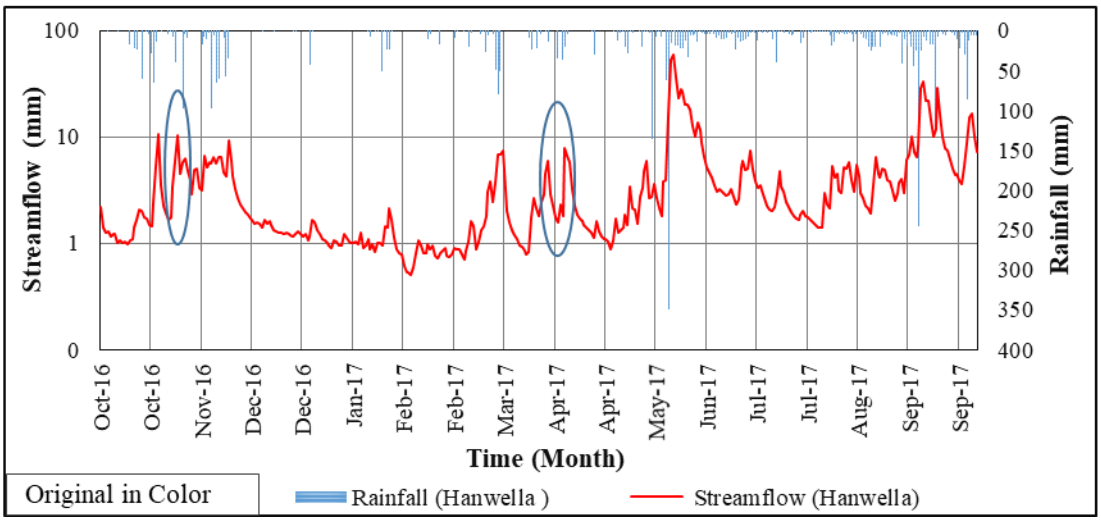

Figure A-23: Streamflow response of Hanwella with rainfall in year 2016/2017

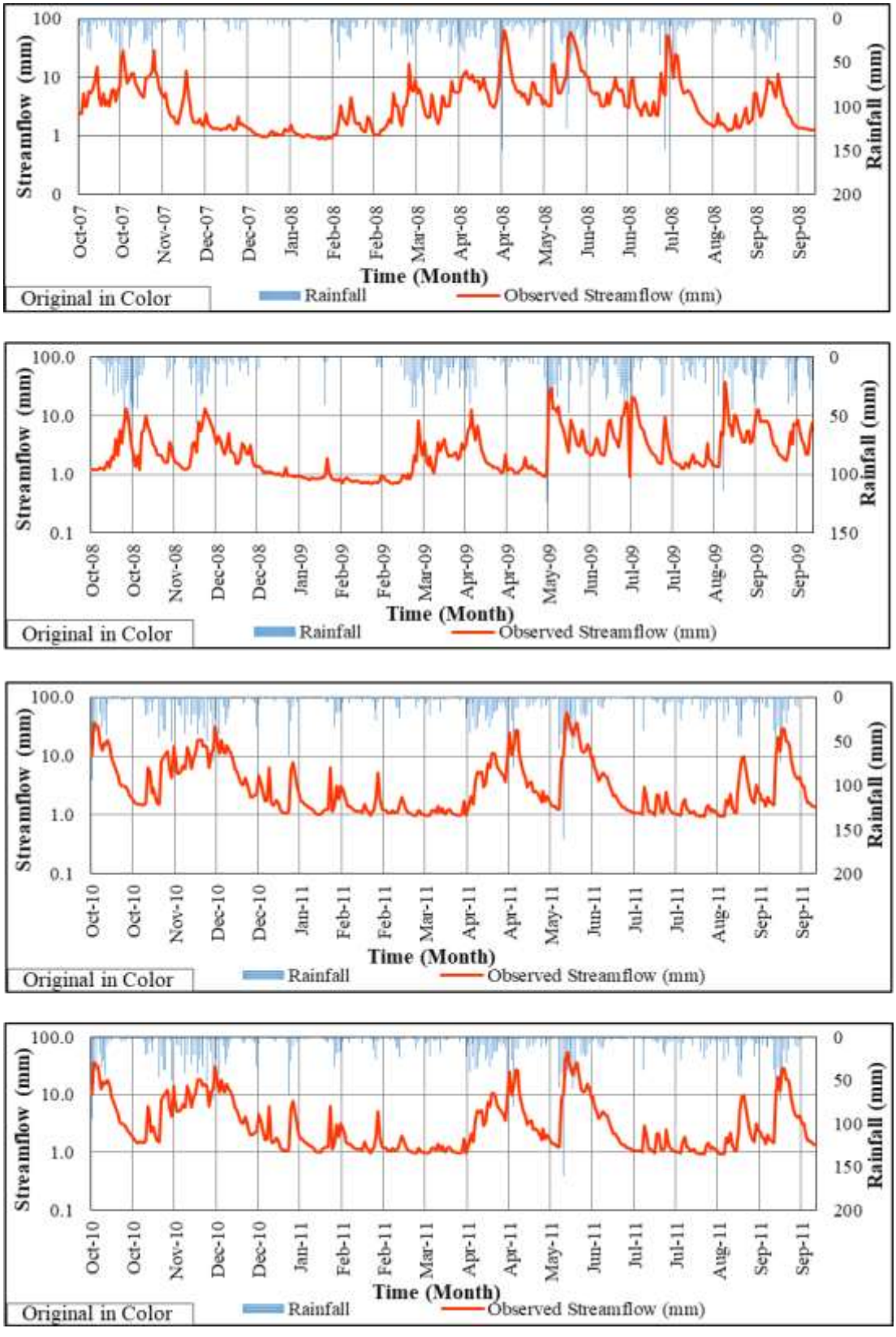

Figure A-24: Streamflow response of Hanwella with Thiessen rainfall for year 2007-2011

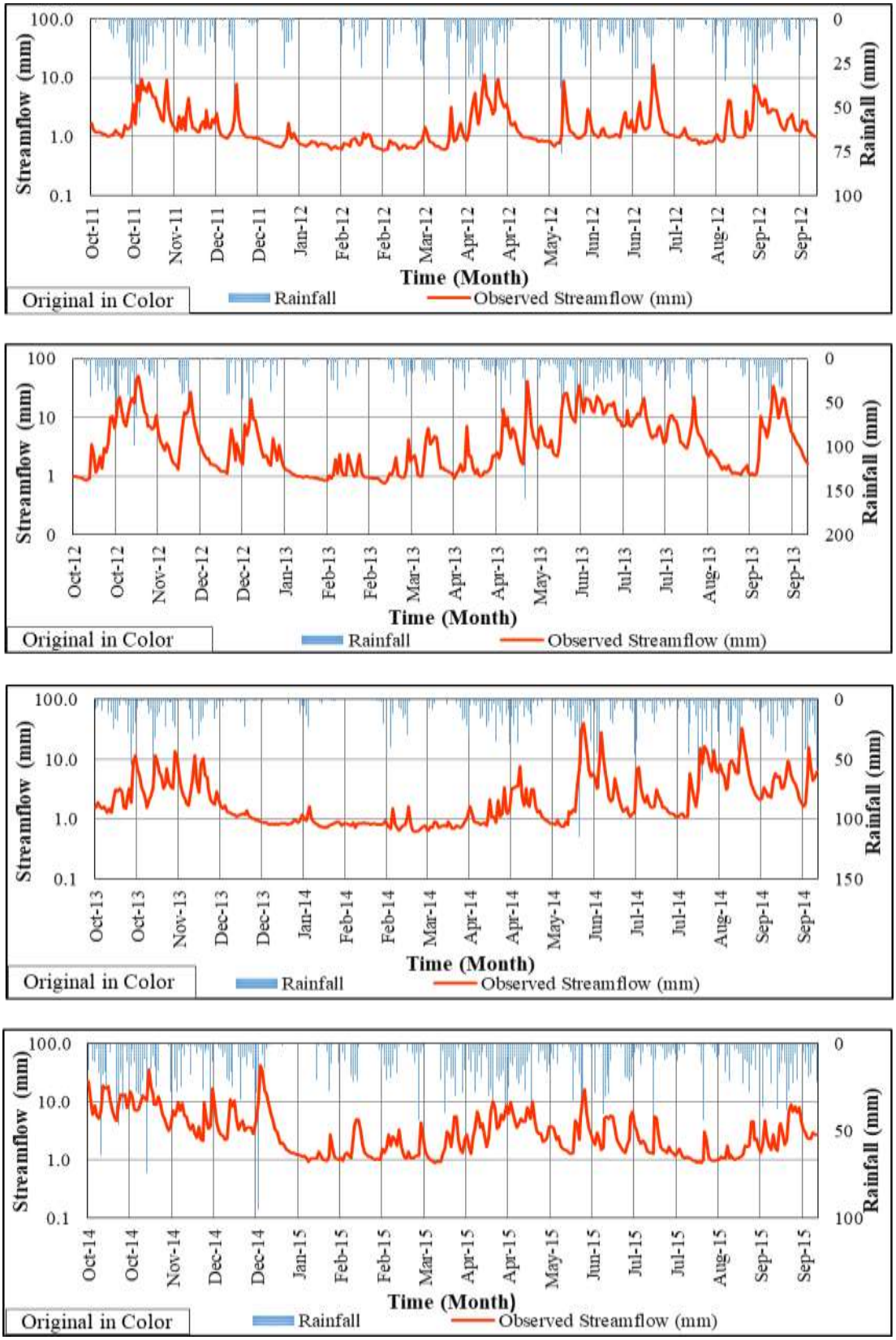

Figure A-25: Streamflow response of Hanwella with Thiessen rainfall for year 2011-2015

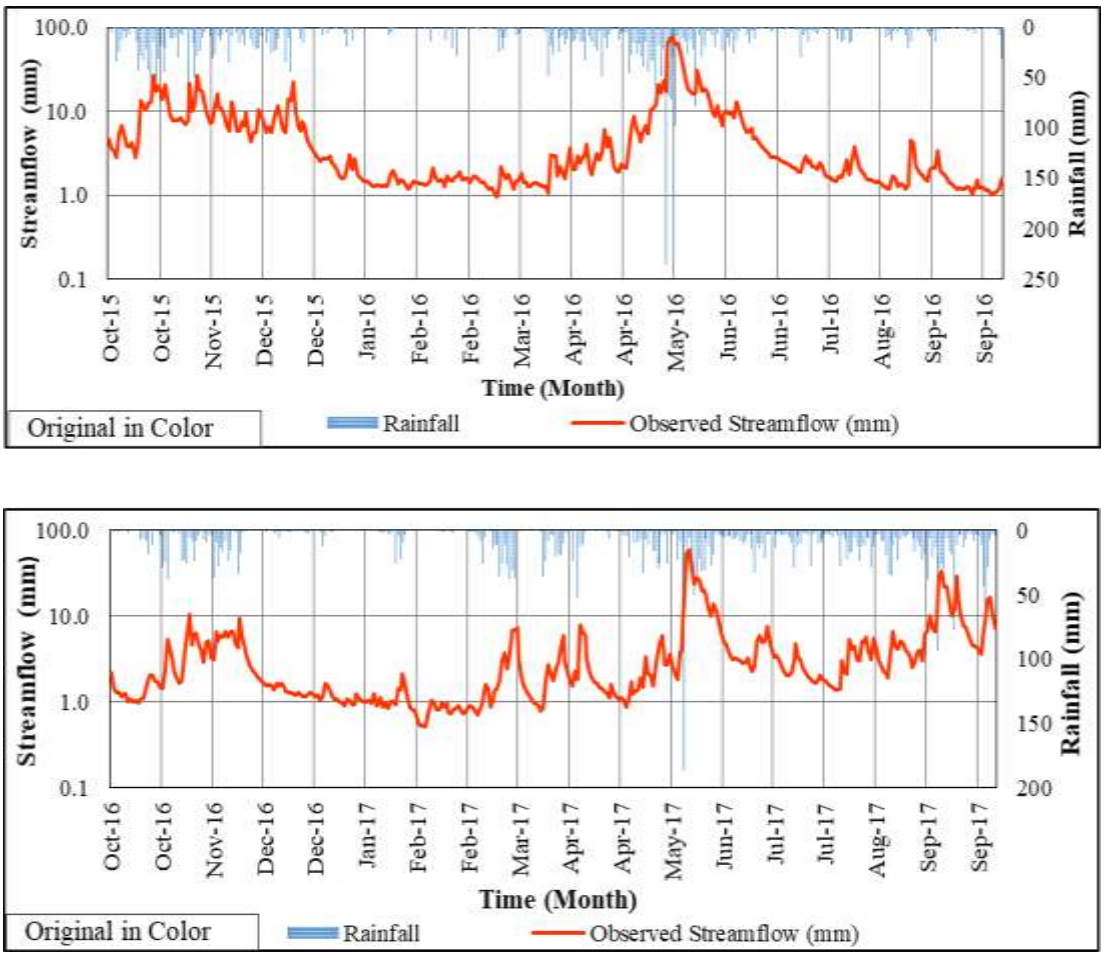

Figure A-26: Streamflow response of Hanwella with Thiessen rainfall for year 2015-2017

Appendix B: Parameter estimation

Table 1-B Canopy storage parameters

Lumped							
Object ID	**Count**	**Area**	**Min**	**Max**	**Range**	**Mean**	**Std**
W440	2,026,486.0	1,824.6	0	2.54	2.54	1.87	0.54
Three-subdivision							
Object ID	**Count**	**Area**	**Min**	**Max**	**Range**	**Mean**	**Std**
W480	771,761	694.6	0	2.54	2.54	1.79	0.49
W700	797,211	717.5	0	2.54	2.54	1.82	0.51
W760	457,514	411.8	0	2.54	2.54	2.07	0.62
Five-subdivision							
Object ID	**Count**	**Area**	**Min**	**Max**	**Range**	**Mean**	**Std**
W450	369,225	332.3	0	2.54	2.54	1.70	0.50
W480	402,536	362.3	0	2.54	2.54	1.88	0.48
W490	292,254	263.0	0	2.54	2.54	1.68	0.51
W710	504,957	454.5	0	2.54	2.54	1.90	0.50
W780	457,514	411.8	0	2.54	2.54	2.07	0.62
Eight-subdivision							
Object ID	**Count**	**Area**	**Min**	**Max**	**Range**	**Mean**	**Std**
W440	170,793	153.7	0	2.54	2.54	1.63	0.52
W450	198,432	178.6	0	2.54	2.54	1.75	0.46
W460	288,000	259.2	0	2.54	2.54	1.90	0.50
W480	114,536	103.1	0	2.54	2.54	1.83	0.41
W490	292,254	263.0	0	2.54	2.54	1.68	0.51
W590	171,536	154.4	0	2.54	2.54	1.81	0.42
W710	333,421	300.1	0	2.54	2.54	1.95	0.52
W780	457,514	411.8	0	2.54	2.54	2.07	0.62
12-Subdivision							
Object ID	**Count**	**Area**	**Min**	**Max**	**Range**	**Mean**	**Std**
W440	170,793	153.7	0	2.54	2.54	1.63	0.52
W450	198,432	178.6	0	2.54	2.54	1.75	0.46
W460	288,000	259.2	0	2.54	2.54	1.90	0.50
W480	114,536	103.1	0	2.54	2.54	1.83	0.41
W490	121,407	109.3	0	2.54	2.54	1.62	0.45
W490	171,536	154.4	0	2.54	2.54	1.81	0.42
W610	69,723	62.8	0	2.03	2.03	1.48	0.40
W670	163,107	146.8	0	2.54	2.54	1.91	0.38
W700	101,097	91.0	0	2.54	2.54	1.88	0.57
W710	170,314	153.3	0	2.54	2.54	2.00	0.63
W770	221,695	199.5	0	2.54	2.54	2.08	0.67
W780	235,819	212.2	0	2.54	2.54	2.07	0.57

Note: The unit of area is in km^2 and all other unit are in meter.

Table 2 -B Surface storage parameters

Lumped												
Object ID	**Count**	**Area**	**Min**	**Max**	**Range**	**Mean**	**Std**	**Sum**	**Variety**	**Majority**	**Minority**	**Median**
W440	225,265	1,824.6	1	50	49	11.8	14.7	2,660,025	3	9	50	9
Three-subdivision												
Object ID	**Count**	**Area**	**Min**	**Max**	**Range**	**Mean**	**Std**	**Sum**	**Variety**	**Majority**	**Minority**	**Median**
W480	85,769	694.7	1	50	49	9.9	12.6	850,636	3	9	50	9
W700	88,648	718.0	1	50	49	15.7	17.7	1,393,329	3	9	50	9
W760	50,848	411.9	1	50	49	8.2	10.2	416,060	3	9	50	9
Five-subdivision												
Object ID	**Count**	**Area**	**Min**	**Max**	**Range**	**Mean**	**Std**	**Sum**	**Variety**	**Majority**	**Minority**	**Median**
W450	41,025	332.3	1	50	49	10.3	12.5	422,560	3	9	50	9
W480	44,744	362.4	1	50	49	9.6	12.6	428,076	3	9	50	9
W490	32,473	263.0	1	50	49	25.2	20.5	817,519	3	9	1	9
W710	56,175	455.0	1	50	49	10.3	13.0	575,810	3	9	50	9
W780	50,848	411.9	1	50	49	8.2	10.2	416,060	3	9	50	9
Eight-subdivision												
Object ID	**Count**	**Area**	**Min**	**Max**	**Range**	**Mean**	**Std**	**Sum**	**Variety**	**Majority**	**Minority**	**Median**
W440	18,977	153.7	1	50	49	10.3	12.3	195,780	3	9	50	9
W450	22,048	178.6	1	50	49	10.3	12.8	226,780	3	9	50	9
W460	32,000	259.2	1	50	49	7.4	9.7	237,417	3	9	50	9
W480	12,744	103.2	1	50	49	15.0	16.7	190,659	3	9	1	9
W490	32,473	263.0	1	50	49	25.2	20.5	817,519	3	9	1	9
W590	19,072	154.5	1	50	49	14.7	16.2	279,800	3	9	1	9

W710	37,103	300.5	1	50	49	8.0	10.4	296,010	3	9	50	9
W780	50,848	411.9	1	50	49	8.2	10.2	416,060	3	9	50	9
12-subdivision												
Object ID	**Count**	**Area**	**Min**	**Max**	**Range**	**Mean**	**Std**	**Sum**	**Variety**	**Majority**	**Minority**	**Median**
W440	18,977	153.7	1	50	49	10.3	12.3	195,780	3	9	50	9
W450	22,048	178.6	1	50	49	10.3	12.8	226,780	3	9	50	9
W460	32,000	259.2	1	50	49	7.4	9.7	237,417	3	9	50	9
W480	12,744	103.2	1	50	49	15.0	16.7	190,659	3	9	1	9
W490	13,490	109.3	1	50	49	27.2	20.5	367,006	3	9	1	9
W490	19,072	154.5	1	50	49	14.7	16.2	279,800	3	9	1	9
W610	7,747	62.8	1	50	49	32.1	20.4	248,320	3	50	1	50
W670	18,160	147.1	1	50	49	9.8	11.8	177,442	3	9	50	9
W700	11,233	91.0	1	50	49	18.0	18.1	202,043	3	9	1	9
W710	18,943	153.4	1	50	49	6.3	8.4	118,568	3	1	50	9
W770	24,639	199.6	1	50	49	7.8	10.2	191,673	3	9	50	9
W780	26,209	212.3	1	50	49	8.6	10.2	224,387	3	9	50	9

Note: All units are in the SI system only the area unit is in km^2 and all other units are in meter (m).

Table 3-B Land cover and landuse coefficient

LULC Category	Impervious surface coefficient
Commercial/Industrial/Paved	33.87
Residential & commercial	25.97
Turf & tree complex	13.64
Rural residential	12.48
Pasture & hay & grass	6.87
Deciduous forest	3.48
Coniferous forest	1.87
Exposed soil	34.61
Pasture & hay / exposed soil	11.08
Forest / clear cut	9.62
Deciduous shrub wetland	12.65
Exposed soil / cropland	2.92
Turf & grass	2.40
Nursery stock	NA
Exposed ground & sand	NA
Shallow water & mud flats	2.91
Coniferous forested wetland	NA
Deciduous forested wetland	2.18
Non-forested wetland	2.52
Scrub & shrub	1.35
Mixed forest	0.37
Deciduous forest & Mt Laurel	0.25
Dead & dying hemlock	0.00
High coastal marsh	0.00
Deep water	0.86

Table 4 –B Impervious percentage parameters

Lumped												
Object ID	**Count**	**Area**	**Min**	**Max**	**Range**	**Mean**	**Std**	**Sum**	**Variety**	**Majority**	**Minority**	**Median**
W440	2,026,486	1,824.6	1	85	84	12.9	11.3	26,165,028	12	11	16	11
Three-subdivision												
Object ID	**Count**	**Area**	**Min**	**Max**	**Range**	**Mean**	**Std**	**Sum**	**Variety**	**Majority**	**Minority**	**Median**
W480	771,761	694.7	1	85	84	14.4	10.9	11,122,658	11	11	16	11
W700	797,211	718	1	85	84	13.7	10.9	10,952,833	11	11	16	11
W760	457,514	411.9	1	85	84	8.9	11.7	4,089,537	10	7	68	7
Five-subdivision												
Object ID	**Count**	**Area**	**Min**	**Max**	**Range**	**Mean**	**Std**	**Sum**	**Variety**	**Majority**	**Minority**	**Median**
W450	369,225	332.3	1	85	84	15.5	10.7	5,715,737	9	11	85	11
W480	402,536	362.4	1	85	84	13.4	11.1	5,406,921	11	11	16	11
W490	292,254	263	1	85	84	15.6	10.1	4,549,949	10	30	68	11
W710	504,957	455	1	85	84	12.7	11.2	6,402,884	10	11	16	11
W780	457,514	411.9	1	85	84	8.9	11.7	4,089,537	10	7	68	7
Eight-subdivision												
Object ID	**Count**	**Area**	**Min**	**Max**	**Range**	**Mean**	**Std**	**Sum**	**Variety**	**Majority**	**Minority**	**Median**
W440	170,793	153.7	1	85	84	15.6	10.8	2,669,722	9	11	85	11
W450	198,432	178.6	1	85	84	15.4	10.5	3,046,015	9	11	85	11
W460	288,000	259.2	1	85	84	13.2	11.8	3,810,930	11	11	16	11
W480	114,536	103.2	1	85	84	13.9	9	1,595,991	9	11	10	11
W490	292,254	263	1	85	84	15.6	10.1	4,549,949	10	30	68	11
W590	171,536	154.5	1	85	84	14.1	8.1	2,417,119	8	11	14	11
W710	333,421	300.5	1	85	84	12	12.5	3,985,765	10	11	16	11

W780	457,514	411.9	1	85	84	8.9	11.7	4,089,537	10	7	68	7
12- subdivision												
Object ID	**Count**	**Area**	**Min**	**Max**	**Range**	**Mean**	**STD**	**Sum**	**Variety**	**Majority**	**Minority**	**Median**
W440	170,793	153.7	1	85	84	15.6	10.8	2,669,722	9	11	85	11
W450	198,432	178.6	1	85	84	15.4	10.5	3,046,015	9	11	85	11
W460	288,000	259.2	1	85	84	13.2	11.8	3,810,930	11	11	16	11
W480	114,536	103.2	1	85	84	13.9	9	1,595,991	9	11	10	11
W490	121,407	109.3	1	85	84	15.7	9.4	1,910,468	10	14	68	14
W490	171,536	154.5	1	85	84	14.1	8.1	2,417,119	8	11	14	11
W610	69,723	62.8	1	68	67	19.8	10.6	1,382,485	7	30	68	14
W670	163,107	147.1	1	85	84	12.7	7.5	2,063,530	9	11	16	11
W700	101,097	91	1	68	67	12.4	9.5	1,256,186	8	11	68	11
W710	170,314	153.4	1	85	84	11.3	15.8	1,922,235	9	3	16	7
W770	221,695	199.6	1	85	84	9.3	13.7	2,062,723	10	7	68	7
W780	235,819	212.3	1	85	84	8.6	9.5	2,026,814	9	7	68	7

Note: All units are in the SI system that area unit is in km^2 and the min, max, range, mean and STD are in %.

Table 5 –B CN grid parameters for lumped and distributed models

Lumped												
Object ID	**Count**	**Area**	**Min**	**Max**	**Range**	**Mean**	**Std**	**Sum**	**Variety**	**Majority**	**Minority**	**Median**
W440	2,026,486	1,824.6	71	98	27	81.5	4.1	182,464,650	10	82	90	82
Three-subdivision												
Object ID	**Count**	**Area**	**Min**	**Max**	**Range**	**Mean**	**Std**	**Sum**	**Variety**	**Majority**	**Minority**	**Median**
W480	771,761	694.7	71	98	27	82.2	3.5	63,411,609	9	82	90	82
W700	797,211	718	71	98	27	81.6	4.3	65,035,991	9	82	90	82
W760	457,514	411.9	71	98	27	80.4	4.5	36,781,078	9	79	96	79
Five-subdivision												
Object ID	**Count**	**Area**	**Min**	**Max**	**Range**	**Mean**	**Std**	**Sum**	**Variety**	**Majority**	**Minority**	**Median**
W450	369,225	332.3	71	98	27	82.4	3.1	30,441,358	7	82	71	82
W480	402,536	362.4	71	98	27	81.9	3.8	32,970,251	9	82	90	82
W490	292,254	263	71	98	27	80.6	5.5	23,554,325	8	85	96	82
W710	504,957	455	71	98	27	82.1	3.3	41,481,666	8	82	90	82
W780	457,514	411.9	71	98	27	80.39	4.5	36,781,078	9	79	96	79
Eight-subdivision												
Object ID	**Count**	**Area**	**Min**	**Max**	**Range**	**Mean**	**Std**	**Sum**	**Variety**	**Majority**	**Minority**	**Median**
W440	170,793	153.7	71	98	27	82.5	2.9	14,097,103	7	82	80	82
W450	198,432	178.6	71	98	27	82.4	3.2	16,344,255	7	82	71	82
W460	288,000	259.2	71	98	27	82.0	3.6	23,627,590	9	82	90	82
W480	114,536	103.2	71	98	27	81.6	4.2	9,342,661	7	82	80	82
W490	292,254	263	71	98	27	80.6	5.5	23,554,325	8	85	96	82
W590	171,536	154.5	71	98	27	82.7	2.3	14,177,454	6	82	71	82
W710	333,421	300.5	71	98	27	81.9	3.6	27,304,212	8	82	90	82
W780	457,514	411.9	71	98	27	80.4	4.5	36,781,078	9	79	96	79

12-subdivision												
Object ID	**Count**	**Area**	**Min**	**Max**	**Range**	**Mean**	**Std**	**Sum**	**Variety**	**Majority**	**Minority**	**Median**
W440	170,793	153.7	71	98	27	82.5	2.9	14,097,103	7	82	80	82
W450	198,432	178.6	71	98	27	82.4	3.2	16,344,255	7	82	71	82
W460	288,000	259.2	71	98	27	82.0	3.6	23,627,590	9	82	90	82
W480	114,536	103.2	71	98	27	81.6	4.2	9,342,661	7	82	80	82
W490	121,407	109.3	71	98	27	78.9	6.2	9,583,735	8	71	96	79
W490	171,536	154.5	71	98	27	82.7	2.3	14,177,454	6	82	71	82
W610	69,723	62.8	71	98	27	81.8	5.1	5,705,150	6	85	96	85
W670	163,107	147.1	71	98	27	82.3	2.5	13,429,096	7	82	90	82
W700	101,097	91	71	98	27	81.7	4.1	8,263,145	7	82	96	82
W710	170,314	153.4	78	98	20	81.5	4.4	13,875,116	7	78	90	82
W770	221,695	199.6	71	98	27	80.7	5.1	17,881,244	9	79	96	79
W780	235,819	212.3	71	98	27	80.1	3.7	18,899,834	9	79	76	79

Note: All the units are in the SI system that area unit is in km^2 and the min, max, range, mean, variety, majority, minority and median units are dimensionless.

Table 6 –B Slope, TC, SC and length parameter for lumped and distributed models

Lumped									
Object ID	**Area (mi^2)**	**Area (m^2)**	**CN**	**Slope %**	**River length (m)**	**River length (mi)**	**River length (Ft)**	**Time of concentration (Hr)**	**Storage coefficient (Hr)**
W440	704.5	1,824,646,500	81.53	24.38	100,916.68	62.71	331,091.47	10.6	10.34
Three- subdivision									
Object ID	**Area (mi^2)**	**Area (m^2)**	**CN**	**Slope %**	**River length (m)**	**River length (mi)**	**River length (Ft)**	**Time of concentration (Hr)**	**Storage coefficient (Hr)**
W480	268.24	694,728,900	82.16	24.47	56,923.64	35.37	186,757.34	6.56	6.92
W700	277.26	718,097,400	81.58	18.9	66,793.62	41.5	219,139.19	8.64	7.96
W760	159.02	411,868,800	80.39	25.73	52,636.71	32.71	172,692.64	6.36	5.57
Five-subdivision									
Object ID	**Area (mi^2)**	**Area (m^2)**	**CN**	**Slope %**	**River length (m)**	**River length (mi)**	**River length (Ft)**	**Time of concentration (Hr)**	**Storage coefficient (Hr)**
W450	128.3	332,302,500	82.45	22.71	44,302.25	27.53	145,348.60	5.52	5.23
W480	139.93	362,426,400	81.91	26.07	43,376.21	26.95	142,310.42	5.15	5.2
W490	101.58	263,079,900	80.6	9.91	26,308.88	16.35	86,315.21	5.84	7.2
W710	175.68	455,017,500	82.15	24.11	50,468.12	31.36	165,577.84	6	5.85
W780	159.02	411,868,800	80.39	25.73	52,636.71	32.71	172,692.64	6.36	5.57
Eight-subdivision									
Object ID	**Area (mi^2)**	**Area (m^2)**	**CN**	**Slope %**	**River length (m)**	**River length (mi)**	**River length (Ft)**	**Time of concentration (Hr)**	**Storage coefficient (Hr)**
W440	59.35	153,713,700	82.54	21.97	27,743.26	17.24	91,021.19	3.85	3.94
W450	68.95	178,588,800	82.37	23.35	26,328.84	16.36	86,380.71	3.6	4.04

W460	100.08	259,200,000	82.04	29.14	33,294.02	20.69	109,232.35	3.93	4.28
W480	39.86	103,226,400	81.57	18.38	25,218.51	15.67	82,737.88	4.02	3.72
W490	101.56	263,031,300	80.6	9.91	26,181.60	16.27	85,897.63	5.82	7.18
W590	59.65	154,483,200	82.65	18.1	24,866.45	15.45	81,582.86	3.87	4.3
W710	116.04	300,534,300	81.89	27.19	34,933.21	21.71	114,610.27	4.25	4.7
W780	159.02	411,868,800	80.39	25.73	52,636.71	32.71	172,692.64	6.36	5.57
12-subdivision									
Object ID	**Area (mi^2)**	**Area (m^2)**	**CN**	**Slope %**	**River length (m)**	**River length (mi)**	**River length (Ft)**	**Time of concentration (Hr)**	**Storage coefficient (Hr)**
W440	59.35	153,713,700	82.54	21.97	27,743.26	17.24	91,021.19	3.85	3.94
W450	68.95	178,588,800	82.37	23.35	26,328.84	16.36	86,380.71	3.6	4.04
W460	100.08	259,200,000	82.04	29.14	33,294.02	20.69	109,232.35	3.93	4.28
W480	39.86	103,226,400	81.57	18.38	25,218.51	15.67	82,737.88	4.02	3.72
W490	42.19	109,269,000	78.94	7.93	16,733.93	10.4	54,901.33	4.79	5.93
W590	59.65	154,483,200	82.65	18.1	24,866.45	15.45	81,582.86	3.87	4.3
W610	24.23	62,750,700	81.83	6.8	18,010.46	11.19	59,089.45	5.01	5.07
W670	56.79	147,096,000	82.33	22.95	22,451.90	13.95	73,661.08	3.2	3.72
W690	35.13	90,987,300	81.73	14.43	24,124.62	14.99	79,149.01	4.36	3.94
W700	0.03	72,900	85	1.72	307.28	0.19	1,008.13	0.34	0.46
W710	59.24	153,438,300	81.47	31.26	21,369.25	13.28	70,109.08	2.71	3.26
W770	77.06	199,575,900	80.66	28.07	42,942.20	26.68	140,886.50	5.13	3.38
W780	81.97	212,292,900	80.15	23.53	52,636.71	32.71	172,692.64	6.7	2.2

Note: All the units are in the SI system that area unit is in km^2 and the min, max, range, mean, variety, majority, minority and median units are dimensionless.

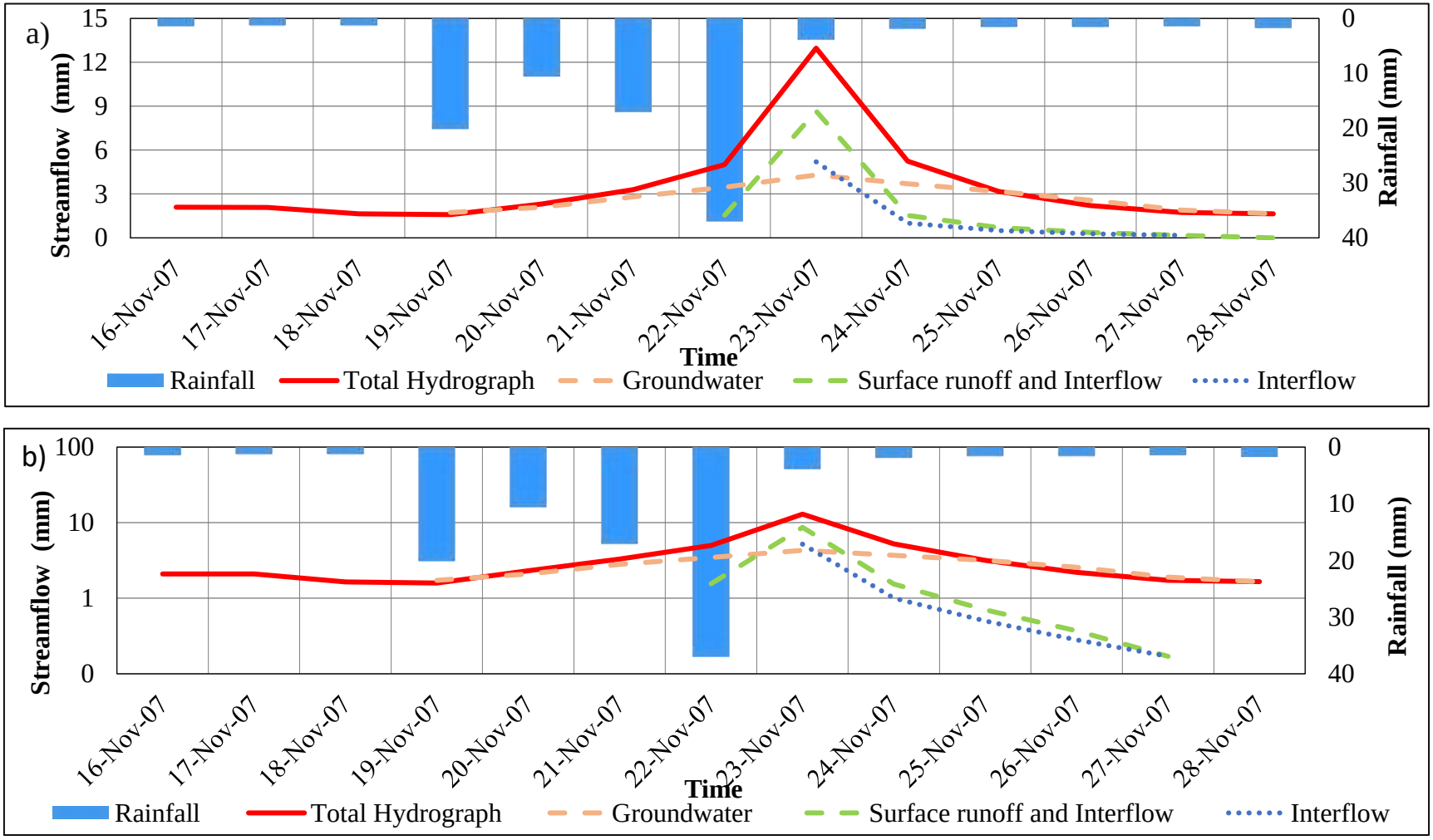

Figure 1- B Selected event from year 2007 for streamflow recession analysis (a,b)

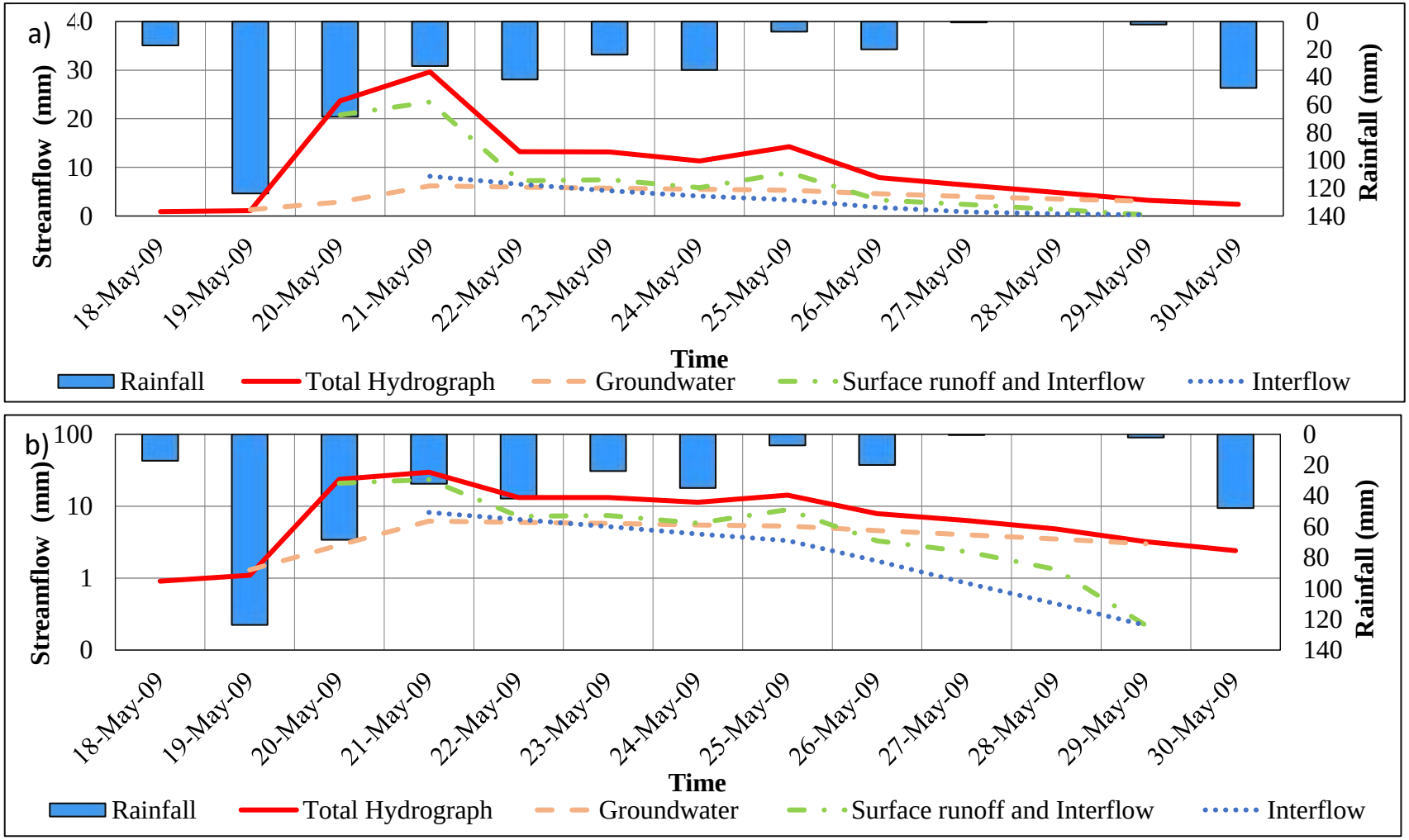

Figure 2- B Selected event from year 2009 for streamflow recession analysis (a,b)

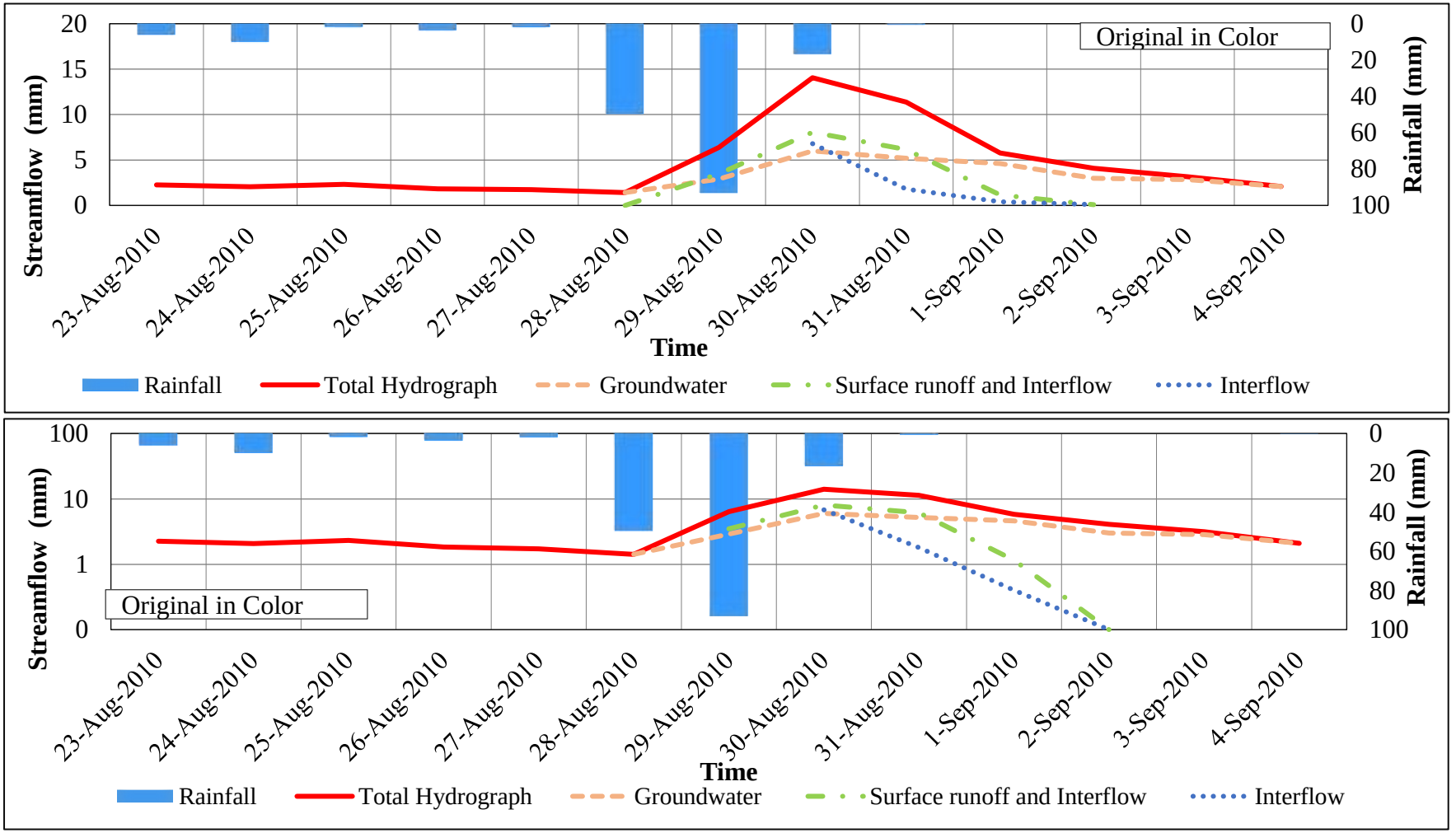

Figure 3- B Selected event from year 2010 for streamflow recession analysis (a,b)

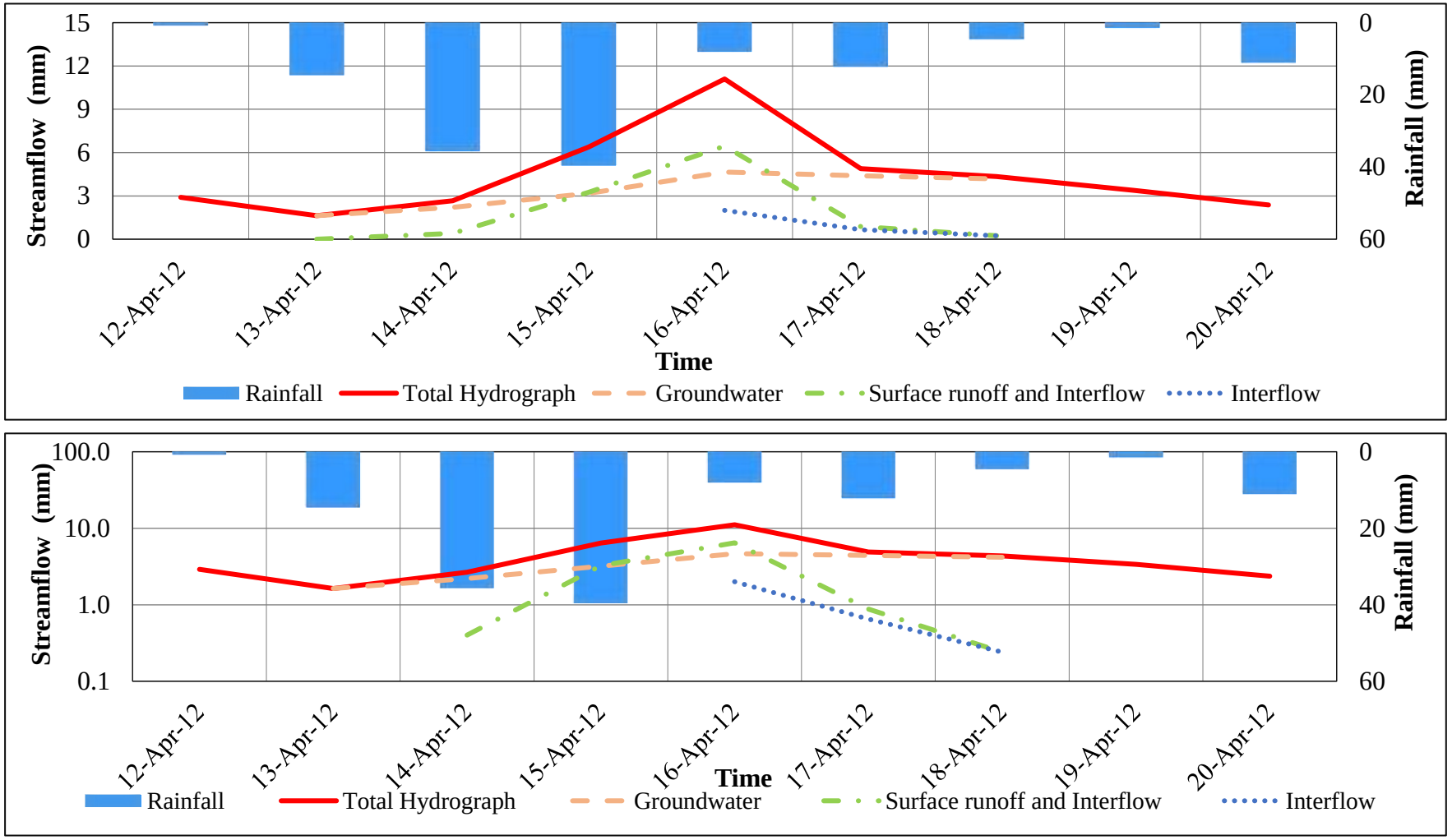

Figure 4- B Selected event from year 2012 for streamflow recession analysis (a,b)

Appendix C: Results

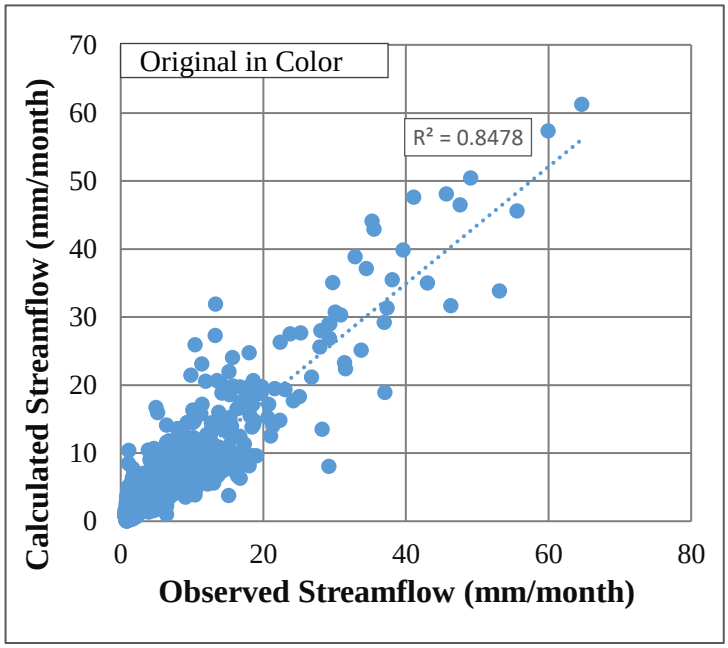

Figure 1- C Relationship between observed and simulated streamflow in scatter plot for the lumped model during calibration period

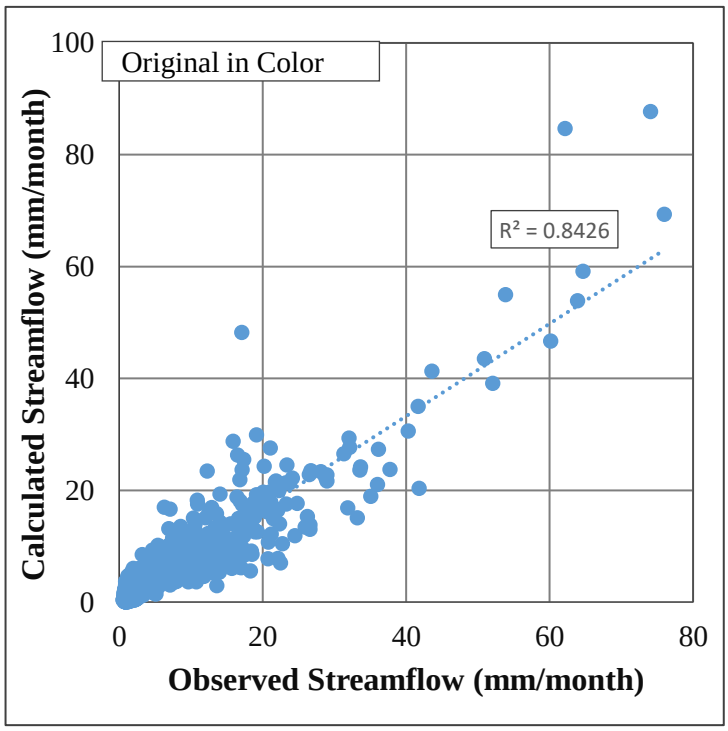

Figure 2-C Relationship between observed and simulated streamflow in scatter plot for the lumped model during verification period

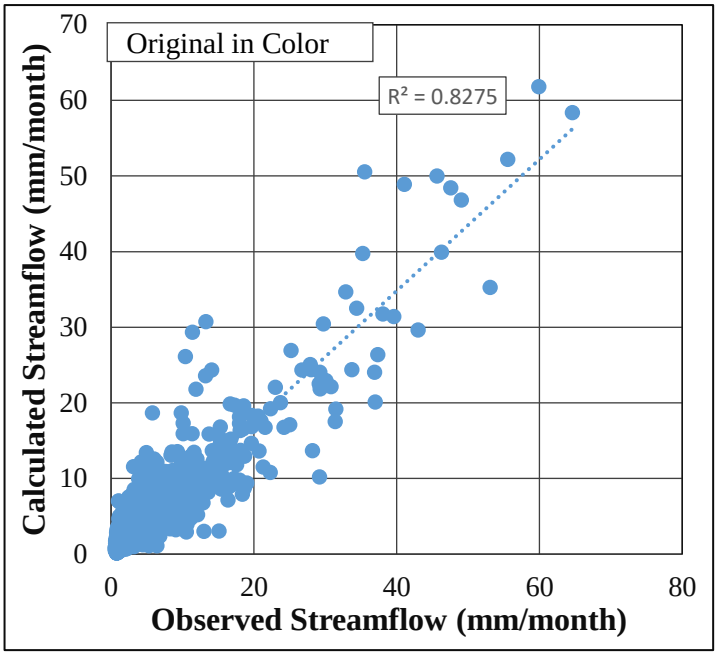

Figure 3-C Relation between observed and simulated streamflow in scatter plot for the three-subdivision model during calibration period

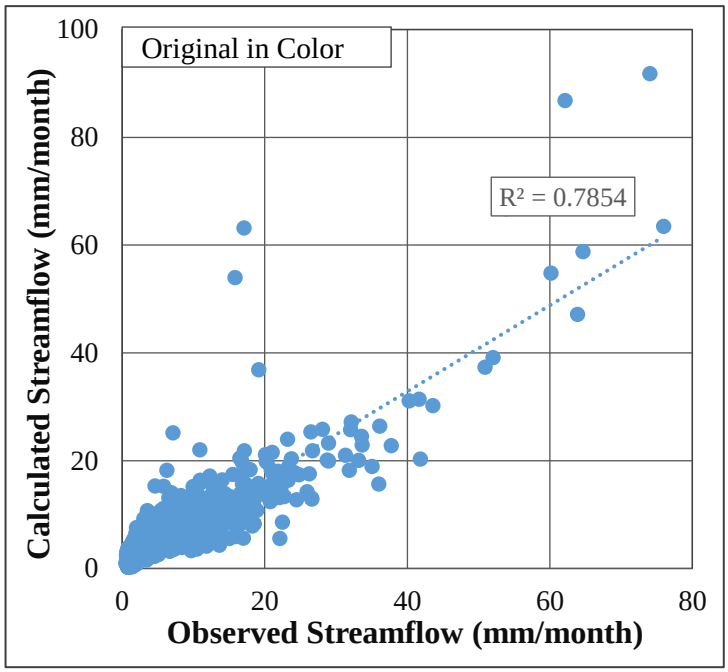

Figure 4-C Relationship between observed and simulated streamflow in scatter plot for the three-subdivision model during verification period

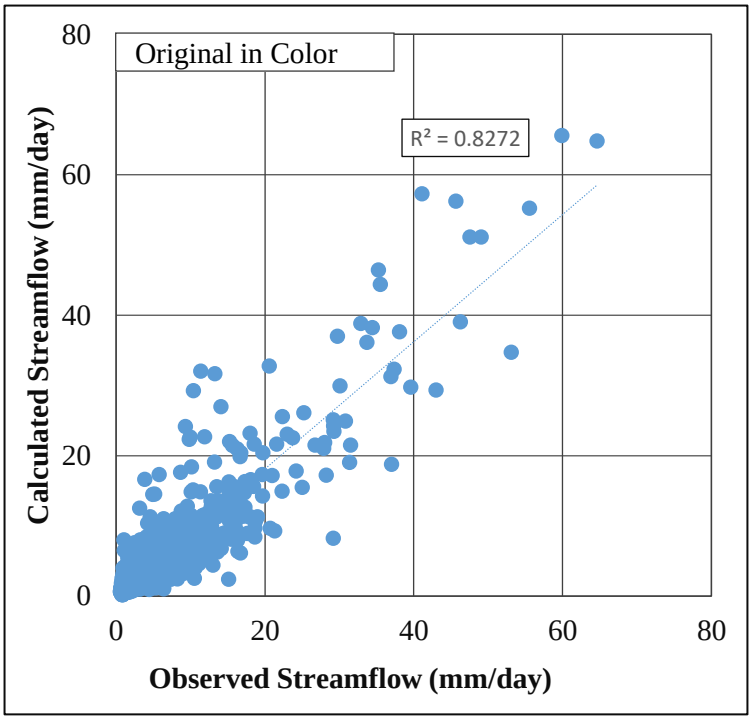

Figure 5-C Relationship between observed and simulated streamflow in scatter plot for the five-subdivision model during calibration period

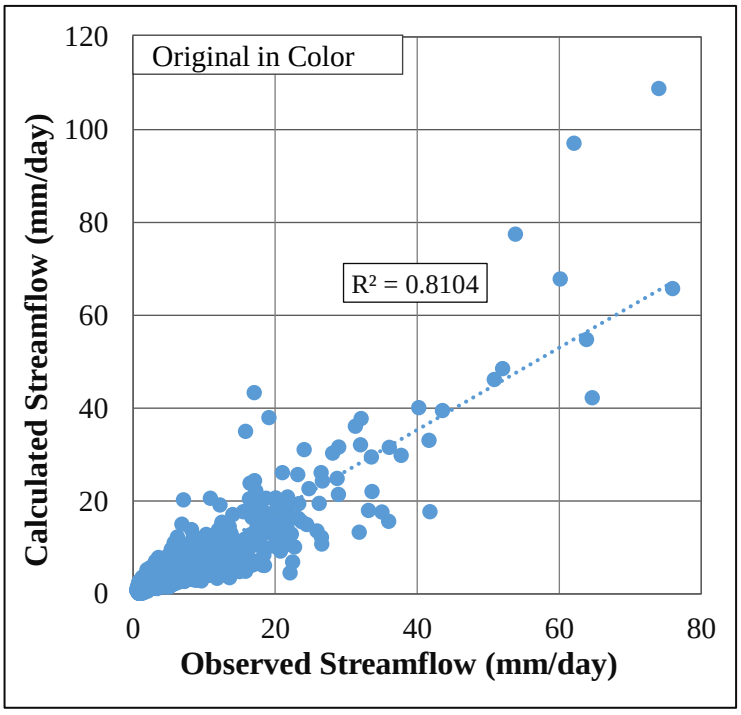

Figure 6-C Relationship between observed and simulated streamflow in scatter plot for the Five-subdivision model during verification period

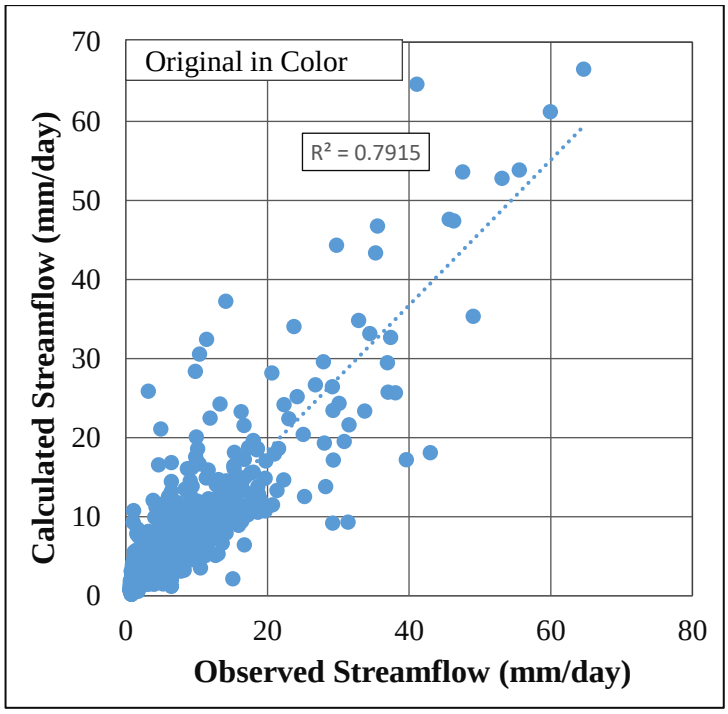

Figure 7-C Relation between observed and simulated streamflow in scatter plot for the eight-subdivision model during the calibration period

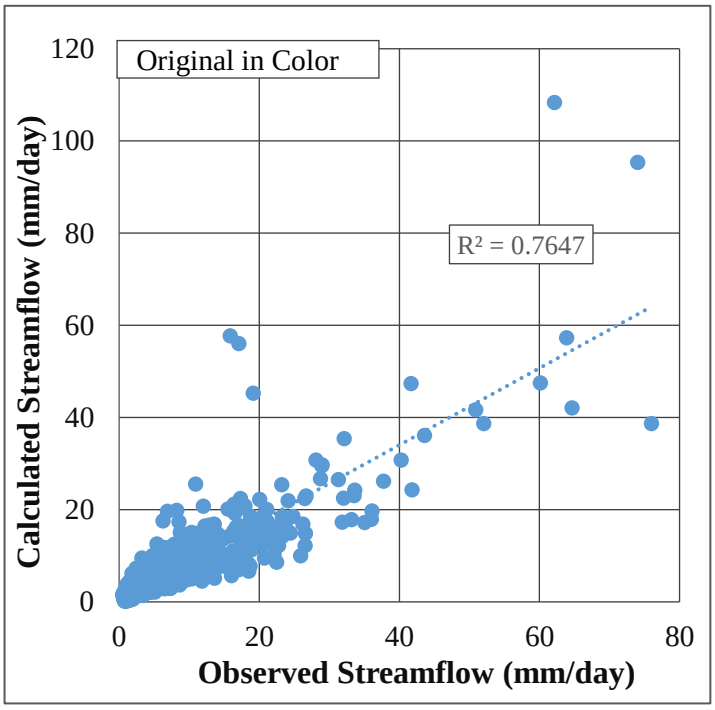

Figure 8-C Relationship between observed and simulated streamflow in scatter plot for the eight-subdivision model during verification period

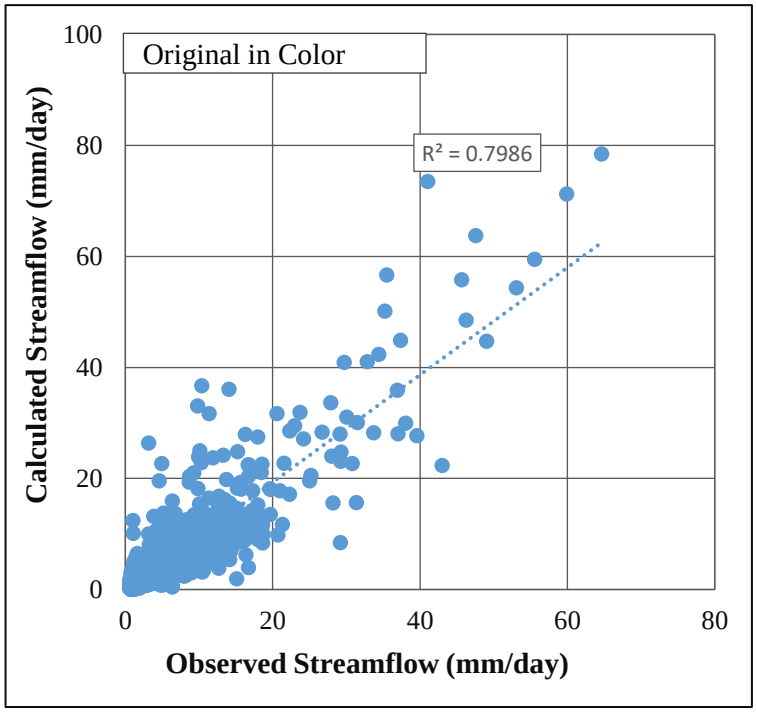

Figure 9-C Relationship between observed and simulated streamflow in scatter plot for the 12-subdivision model during calibration period

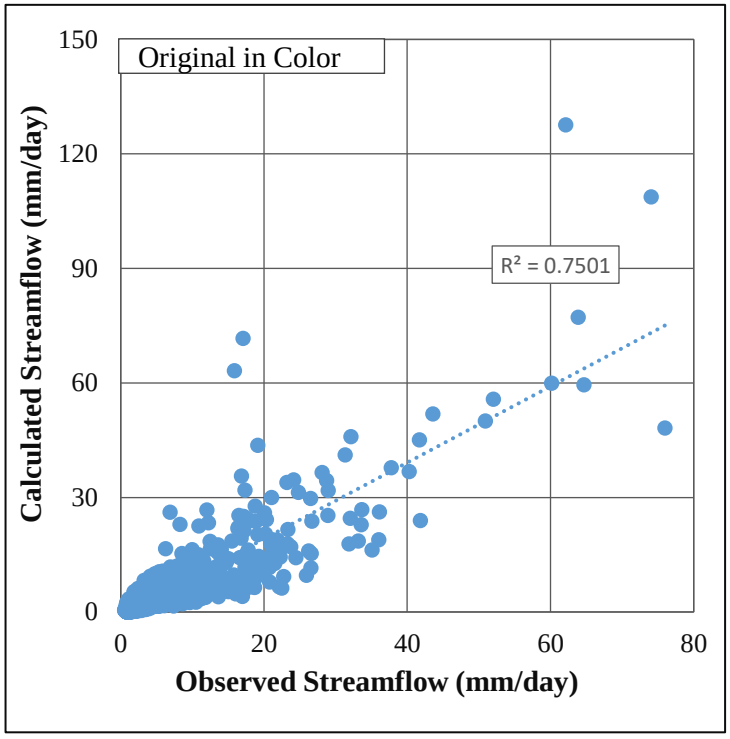

Figure 10-C Relation between observed and simulated streamflow in scatter plot for the 12-subdivision model during verification period